Precision Calculations Of Long-Range Interactions Among Three Atomic Systems

by

Pei-Gen Yan

Bachelor of Science, Ludong University, China, 2010
Master of Science, Jilin University, China, 2013

A DISSERTATION SUBMITTED IN PARTIAL FULFILLMENT OF THE REQUIREMENTS FOR THE DEGREE OF

DOCTOR OF PHILOSOPHY

In the Graduate Academic Unit of Physics Department

Supervisor(s):	Zong-Chao Yan, PhD, Dept. of Physics
Examining Board:	William Ward, PhD, Dept. of Physics
	Li-Hong Xu, PhD, Dept. of Physics,UNBSJ
	Guohua Yan, PhD, Dept. of Mathematics and Statistics
External Examiner:	Robin Côté, PhD, Dept. of Physics
	University of Connecticut

This dissertation is accepted by the

Dean of Graduate Studies

THE UNIVERSITY OF NEW BRUNSWICK

May, 2018

Abstract

Using perturbation theory for energies, we evaluate the coefficients C_3 of the first order dipolar interactions and the coefficients C_6 and C_8 of the second order additive and nonadditive interactions for Li(2^2S)- Li(2^2S)- Li(2^2P), He($1\,^1S$)-He($1\,^1S$)-He($2\,^1P$), He($2\,^1S$)-He($2\,^1S$)-He($2\,^1P$), He($2\,^3S$)-He($2\,^3S$)-He($2\,^3P$) systems. Both the dipolar and dispersion interaction coefficients show dependences on the geometrical configurations of the three atoms. The nonadditive interactions start to appear in second-order. We evaluate the coefficients C_6 and C_8 of the second order additive interactions for He(1^1S)- He(1^1S)- He(2^1S) system. These coefficients also show dependences on the geometrical configurations of the three atoms. We also evaluate the coefficients C_4, C_6 and C_8 of the second order additive interactions and the coefficients C_7 and C_9 of the third-order additive and nonadditive interactions for Li($2\,^2S$)-Li($2\,^2S$)-Li$^+$($1\,^1S$) system. The nonadditive interaction coefficients depend on the geometrical configurations of this three-body system and on the different positions of the ion for each configuration. The obtained coefficients C_n are evaluated with highly accurate variationally-generated nonrelativistic wave functions in Hylleraas coordinates. The present dipolar coefficients and additive and nonadditive interaction coefficients may be useful in constructing precise potential energy surfaces for the corresponding three-body system.

Dedication

To my parents.

Acknowledgements

I sincerely thank my thesis advisor Prof. Zong-Chao Yan for his supervision and financial support through his NSERC grant in carrying out this work.

I would like to thank the Physics Department and the School of Graduate Studies of the University of New Brunswick for providing me with graduate teaching and research assistantships.

I wish to thank Dr. James F. Babb, from Harvard-Smithsonian Center for Astrophysics, and Dr. Li-Yan Tang, from Wuhan Institute of Physics and Mathematics (WIPM), for many insightful discussions, guidance, and collaboration. I also wish to thank Dr. Li-Yan Tang and Dr. Ting-Yun Shi of WIPM for their hospitality during my summer visits.

Finally, and most of all, I wish to express my sincere gratitude to my parents for their encouragement and support throughout my PhD studies and my life.

Table of Contents

List of Tables

List of Figures

Chapter 1

Introduction

Over the past few years, impressive advances in manipulating ultracold atoms and laser-cooled ions have opened a new chapter in quantum physics research [1, 2, 3, 4, 5]. At ultralow temperatures, the quantum nature of the world can be investigated macroscopically, and research on such systems gives new insights into quantum theory of matter-matter and matter-light interactions, which is crucial for many areas of physics and for future quantum technologies [6]. In general, for a cold or ultracold system, the internuclear distances could be much larger than the size of an atom. In a dense system, however, collisions among cold atoms may lead to a collapse of the system. Due to the relative large internuclear distances, the long-range part of interaction plays a very important role in cold and ultracold studies, such as the formation of a long-range molecule [7, 8] via photoassociation, ultracold ion-atom elastic and charge-transfer collisions [1, 4, 5], and the creation of ultralong-range Rydberg trimers [9, 10, 11].

1.1 Status of Long-Range Interaction Studies

1.1.1 Two-Body Neutral Atom-Atom Interaction

In general, the long-range interaction potential between two identical neutral atoms of separation R can be expressed as a power series in $1/R$ [12]. For two spherically symmetric S-state atoms, the long-range interaction can be written in the form [13, 14]:

$$V(R) = -\frac{C_6}{R^6} - \frac{C_8}{R^8} - \frac{C_{10}}{R^{10}} - \cdots \tag{1.1}$$

where C_n are the van der Waals dispersion coefficients that have been widely calculated for various systems with well-separated atoms (sufficiently far apart that the electron exchange can be ignored). Thus, in this thesis, we don't consider the exchange energy of the form $\pm AR^{\alpha}e^{-\beta R}$, which would decay extremely rapidly due to the large separations among atoms.

For two identical atoms with one being in an excited nonzero angular momentum L state, one needs to consider the exchange symmetry of these two atoms, where the zeroth-order wave function of this system becomes a linear combination of the two degenerate eigenstates. The leading term of the long-range interaction becomes $-C_{2L+1}/R^{2L+1}$, as a first-order energy correction. The simplest example of such an interaction is $-C_3/R^3$ [15, 16] that appears when one atom is in an S state and the other is in a P state.

The long-range interactions between two neutral atoms find many applications, such as in formation of long-range excited diatomic helium molecules via a photoassociation process, where the potential well is purely long-range and bound states have inner turning points at internuclear distances larger than 150 a_0 [17]. Also the long-range interaction has been proven to be very important in the calculation of binding energies of rare gases. For example, with the inclusion of only two-body pairwise

additive interactions, the binding energies of rare gases were predicted to be about 4% for Ne to 9% for Xe lower than the experimental values [18]. For some ultracold three-body or many-body systems, many properties are also determined by this two-body long-range additive interaction. As an example, the van der Waals length in the studies of Efimov state is connected to the leading term of long-range interaction $-C_6/R^6$ [19, 20].

1.1.2 Two-Body Ion-Neutral Atom Interaction

The long-range interaction between an S-state ion and an S-state neutral atom can be written as [1, 4, 5, 6]

$$V(R) = -\frac{C_4^{\rm ind}}{R^4} - \frac{C_6^{\rm ind}}{R^6} - \frac{C_8^{\rm ind}}{R^8} - \frac{C_6^{\rm disp}}{R^6} - \frac{C_8^{\rm disp}}{R^8} - \cdots \tag{1.2}$$

In the above, the leading long-range induction coefficient $C_4^{\rm ind}$ is caused by an induced atomic dipole due to the electric field of the ion [2, 3], which is related to the static dipole polarizability α of the neutral atom by

$$C_4^{\rm ind} = \frac{Q^2\alpha}{2} \tag{1.3}$$

with Q being the charge of the ion. Similarly,

$$C_6^{\rm ind} = \frac{Q^2\beta}{2} \tag{1.4}$$

$$C_8^{\rm ind} = \frac{Q^2\gamma}{2} \tag{1.5}$$

where β and γ are, respectively, the static quadrupole and octupole polarizability. These two terms can be interpreted as the interaction between the charge of the ion and the induced quadrupole and octupole moment of the atom. The coefficients

$C_6^{\rm disp}$ and $C_8^{\rm disp}$ in (1.2) are the dispersion interaction coefficients.

When the neutral atom is in an excited state with nonzero angular momentum L, the long-range interaction between this excited-state atom and the S-state ion becomes [6]:

$$V(R) = -\frac{C_3^{\rm elst}}{R^3} - \frac{C_4^{\rm ind}}{R^4} - \frac{C_5^{\rm elst}}{R^5} - \frac{C_6^{\rm ind}}{R^6} - \frac{C_8^{\rm ind}}{R^8} - \frac{C_6^{\rm disp}}{R^6} - \frac{C_8^{\rm disp}}{R^8} - \cdots \tag{1.6}$$

where C_3^{elst}/R^3 and C_5^{elst}/R^5 describe, respectively, the electrostatic interaction between the charge of the ion and the quadrupole and hexadecapole moments of the atom.

With recent developments of controllable laser-cooled ion techniques, the precise knowledge of long-range interaction between a laser-cooled ion and a neutral atom becomes more and more important in studies of three-body recombination [21], photoionization [22], Coulomb explosion [23], and ultracold plasma [24].

1.1.3 Interaction Among Three Neutral S-State Atoms

Considerable attention has been given to the study of long-range interactions between three S-state atoms, for which the leading nonadditive (not expressible as a sum of pairs) term in the mutual potential energy occurs in third-order perturbation theory and contains a geometrical factor depending on relative orientation of the three atoms [25, 26, 27, 28]. This nonadditive interaction term can be written as

$$\Delta E^{(3)} = \frac{C_{123}}{R_{12}^{L_s+L_t+1} R_{23}^{L_t+L_u+1} R_{31}^{L_u+L_s+1}} \tag{1.7}$$

which can be interpreted as the interaction arising from 2^{L_s}-, 2^{L_t}- and 2^{L_u}-pole moments, induced in the charge distributions of atoms 1, 2 and 3. The coefficient C_{123} depends on the relative position of the three atoms.

Recently, there is a growing interest in calculating long-range three-body interac-

tions [30, 31, 32]. Reliable determinations of long-range interactions have many applications in cold collisions [33, 34, 35, 36, 37, 38, 39], three-body recombination [7, 8, 18], study in Pfaffian states [40], color superfluids [41], and Efimov effects [19, 20, 42]. Typically, in most of these studies, only the leading additive two-body interactions [7, 18, 19, 20, 42] might be used, but the importance of higher-order nonadditive three-body interactions has also been underlined, for the construction of precise potential energy surfaces [14, 43, 44]. As mentioned earlier, only the two-body additive pairwise interactions are included, the binding energies of the rare gases were predicted to be between 4% and 9% lower than the experimental values for Ne and Xe, respectively. With the three-body nonadditive interactions included, the discrepancies in binding energies can be reduced to about 1% [18]. Experimentally, the multi-body interactions have been observed as inelastic loss resonances in three- and four-body recombinations of atom-atom and atom-molecule collisions [45, 46].

1.2 Importance of Long-Range Three-Body Interaction Involving An Excited Atom

Recently, some interesting theoretical investigations on the Efimov effect in higher partial waves (P-waves) have been reported [42]. However, long-range three-body interactions for three atoms with one atom in an excited state are less studied, though we expect that they might be a consideration for characterizing excited trimers in photoassociation [47, 48, 49], in implementing quantum information processing with blockade mechanisms [50, 51], and in spectroscopic studies of highly excited bound trimer states [10, 11, 52]. In particular, a theoretical description on the creation of ultracold excited triatomic molecules through photoassociation has been proposed [33]. There are, of course, many studies on the ground and excited potential energy surfaces of three like alkali-metal atoms for spectroscopy and for chemical

dynamics. We believe long-range interactions in these trimers would be needed to analyze the molecular spectroscopy [34, 35, 36, 53, 54, 55] and to study chemical dynamics between atoms and diatomic molecules [15, 47, 48, 49]. We will refer to the case of the homonuclear bound molecule as a trimer and to the case of an atom and a bound homonuclear dimer (such as for scattering) as an atom-dimer. A "global" potential energy surface would encompass both of these regimes, but a global potential energy surface might not be necessary for describing a particular physical process. For example, in a recent theoretical study of the photoassociation of a $Cs(6^2S)$ atom and a $Cs_2(X^1\Sigma_g^+, v = 0)$ dimer [33], where two $Cs(6^2S)$ atoms are already bound together as a diatomic molecule with vibrational quantum number $v = 0$, the long-range interaction potential energies [56, 57] of the atom-dimer system $Cs(6^2P)$–$Cs_2(X^1\Sigma_g^+, v = 0)$ were used.

1.2.1 Homonuclear Three-Lithium System With One in An Excited State

Studies on lithium system potential energy surfaces include the trimer system [34, 35, 36] and treatments of atom-dimer configuration within the context of a global trimer potential energy surface [58, 59, 60]. Motivated by ultracold science, some recent studies on lithium focused on improving global potential energy surfaces for the trimer [53, 55] and also addressing the atom-dimer configuration in further detail [37, 38, 39]. Calculations of ultracold collisions between a $Li(2^2S)$ atom and a $Li_2(a^3\Sigma_u^+, v = 0 - 7)$ dimer were carried out [37]. Recent efforts on long-range interactions for a three-lithium system focus on atom-dimer scattering and atom-dimer photoassociation in the ultracold domain [38, 39, 55]. We are aware of the work by Cvitaš et al [61]. For the case of three well-separated spin-polarized lithium atoms, they made a connection between the long-range interactions for atom-dimer and for atom-atom-atom potential energy surfaces. Here we consider the case of three

well-separated lithium atoms with one being in the 2^2P excited state.

1.2.2 Homonuclear Three-Helium System With One in An Excited State

Rare gas metastable helium atoms have been widely used in many studies involving photoassociation spectroscopy [62], metastable loss in magneto-optical traps [63], penning ionization [64, 65, 66, 67], associative ionization [63], and production of He_3^+ molecular ion [68]. If the excited atom is in a P state, the first-order resonant dipole-dipole interaction produces an interatomic potential varying as $-C_3/R^3$, where the coefficient C_3 for weakly bound dimers of helium has been calculated in many syudies [15, 16]. However, due to the degeneracy, these coefficients may not be used directly in studies of helium clusters or atom-molecule and molecule-molecule collisions involving a P state. This is because, when an excited helium dimer turns into an excited trimer or a cluster involving that excited atom, the interaction between atoms has been totally changed due to the quantum many-body effect. Thus one needs to proceed to calculate molecular He_n^* excimer potential energy surfaces, where the long-range multi-body interactions for this degenerate system are warranted.

1.3 Importance of Long-Range Three-Body Interactions Involving An Ion

With recent experimental advances in manipulating ultracold atoms and ions, there is a growing interest in studying such a few-body hybrid system containing an ion [1, 4]. The long-range part of ion-atom interaction is especially important for cold and ultracold physics and chemistry because quantum reflection and tunneling take place at relatively large internuclear distances in the quantum regime [4, 5, 43]. The

highly successful use of a single ion in three-body reaction in an ultracold atomic gas has renewed theoretical interest in studying long-range interactions of many-body systems with cold trapped ions [21].

1.4 Brief Introduction To Long-Range Three-Body Interaction Involving An Excited Atom

1.4.1 Studies on Li($2\,^2S$)-Li($2\,^2S$)-Li($2\,^2P$)

In this thesis, we use perturbation theory up to second order to derive general formulas for calculating the long-range interaction coefficients for three like atoms with two atoms in identical S states and the other atom in an excited P state. For this system, we find that the *first order* (dipolar) interaction coefficients depend on the geometrical configurations of the three atoms and that in *second order* nonadditive dispersion interactions appear. The formalism is demonstrated by the calculation of various dispersion coefficients for the Li($2\,^2S$)-Li($2\,^2S$)-Li($2\,^2P$) system using variationally generated atomic lithium wave functions in Hylleraas coordinates. In addition, the coefficients are given explicitly and evaluated numerically for the three basic geometrical configurations of an equilateral triangle, of an isosceles triangle, and of the atoms equally spaced co-linearly, corresponding, respectively, to D_{3h}, C_{2v}, and $D_{\infty h}$ symmetries.

1.4.2 Studies on He($n_0\,^\lambda S$)-He($n_0\,^\lambda S$)-He($n_0'\,^\lambda L$)

In this thesis, we also present our research on long-range interactions for three like helium atoms involving one in an excited state. Using variationally generated atomic helium wave functions in Hylleraas coordinate, we present our theoretical calculations of long-range interaction coefficients for the He($n_0\,^\lambda S$)-He($n_0\,^\lambda S$)-He($n_0'\,^\lambda L$) with the

energetically lowest five states: He($1\,^1S$), He($2\,^3S$), He($2\,^1S$), He($2\,^3P$) and He($2\,^1P$). We present the additive "dipolar" interactions coefficients C_3 and additive dispersion interactions coefficients C_6 and C_8 that enter, respectively, in first- and second-order perturbation theory. We also evaluate the second-order nonadditive dispersion interactions coefficients C_6 and C_8 that contain a dependence on the geometrical configuration of the three atoms. In addition, the coefficients are given explicitly and evaluated numerically for the three basic geometrical configurations of the nuclei in an equilateral triangle, in an isosceles right triangle or equally spaced collinearly. Finally, long-range potentials in the sum of first and second order energies for these three geometrical configurations are shown graphically.

1.5 Brief Introduction To Long-Range Three-Body Interaction Involving An Ion

Using perturbation theory up to third-order, we derive the formulas for the long-range interaction coefficients for Li($2\,^2S$)-Li($2\,^2S$)-Li$^+$($1\,^1S$) and evaluate these coefficients using highly accurate, variationally determined wave functions in Hylleraas coordinate. Firstly, we exhibit the additive interaction coefficients C_4, C_6, and C_8 that enter in second-order perturbation theory, where "additive" means pairwise amongst the three particles. Then we present additive interaction coefficients C_7 and C_9 and nonadditive interaction coefficients $C_7^{(12,23)}$, $C_9^{(12,23)}$, $C_7^{(31,12)}$, $C_9^{(31,12)}$, $C_7^{(12,23,31)}$, and $C_9^{(12,23,31)}$ that enter in third order, where nonadditive means that these terms appear collectively amongst these three particles. Due to their dependence on the geometrical structure of the three atoms, these coefficients are calculated numerically for four specific geometrical configurations: equilateral triangle, isosceles right triangle, isosceles triangle with 120-degree angle, and the one with three atoms equally spaced collinearly. In addition, we find that, for some configurations, these

nonadditive interaction coefficients also depend on the position of the ion.

Chapter 2

Energy Eigenvalue Problems for Coulomb Systems

In this chapter, we will first review the procedure of deriving the Hamiltonian for an $(N+1)$-body Coulomb system in the center of mass frame. The Rayleigh-Ritz variational method for solving the energy eigenvalue problem is then introduced. We then focus on constructing variational basis sets in Hylleraas coordinates by taking lithium as an example. We will then discuss the Newton's method for optimizing the energy eigenvalues, as well as the basic integrals that are needed. Atomic units are used throughout this work, where $\hbar = e = m_e = 1$, the unit of length is $a_0 = \hbar^2/(m_e e^2)$, and the unit of energy is $E = e^2/a_0$.

2.1 The Hamiltonian in Center of Mass Frame

For an isolated $(N+1)$-body Coulomb system, the nonrelativistic Hamiltonian in laboratory frame is [69],

$$H_0 = -\frac{1}{2m_0}\nabla^2_{R_0} - \sum_{i=1}^{N}\frac{1}{2m_i}\nabla^2_{R_i} + \sum_{i>j\geq 0}^{N}\frac{Q_i Q_j}{|\mathbf{R}_i - \mathbf{R}_j|}, \tag{2.1}$$

where m_i, Q_i, and $\mathbf{R}_i$ are, respectively, the mass, the charge, and the position vector of the ith particle. The first two terms on the right hand side are, respectively, the kinetic energy for the nucleus and the electrons. The third term is the Coulomb potential energy of the system. The total angular momentum of the system

$$\mathbf{L} = -i \sum_{i=0}^{N} \mathbf{R}_i \times \nabla_{R_i}, \tag{2.2}$$

commutes with the Hamiltonian and it is thus a good quantum number. Since the system is isolated, we may first eliminate the center of mass motion from the Hamiltonian so that the resulting Hamiltonian reflects the internal structure of the system only. For this purpose, we introduce the following coordinate transformations

$$\mathbf{r}_i = \mathbf{R}_i - \mathbf{R}_0, \tag{2.3}$$

with $i = 1, 2, 3, 4, \cdots, N$

$$\mathbf{X} = \frac{1}{M_T} \sum_{j=0}^{N} m_j \mathbf{R}_j \tag{2.4}$$

where $M_T = \sum_{i=0}^{N} m_i$ is the total mass of the system and $\mathbf{X}$ is the position vector for the center of mass of the system. In the above, we take particle 0 as a reference and thus $\mathbf{r}_i$ are the internal coordinates of the system. The corresponding inverse transformation is,

$$\mathbf{R}_0 = \mathbf{X} - \frac{1}{M_T} \sum_{j=1}^{N} m_j \mathbf{R}_j, \tag{2.5}$$

$$\mathbf{R}_i = \mathbf{X} + (1 - \frac{m_i}{M_T})\mathbf{r}_i - \sum_{\substack{j \neq i \\ j \geq 1}}^{N} \frac{m_j}{M_T} \mathbf{r}_j. \tag{2.6}$$

Using the new set of coordinates $(\mathbf{X}, r_1, r_2, \cdots)$, ∇_{R_0} becomes

$$\begin{aligned} \nabla_{R_0} &= \frac{\partial \mathbf{X}}{\partial \mathbf{R}_0}\frac{\partial}{\partial \mathbf{X}} + \frac{\partial \mathbf{r}_j}{\partial \mathbf{R}_0}\frac{\partial}{\partial \mathbf{r}_j} \\ &= \frac{m_0}{M_T}\nabla_X - \sum_{j=1}^{N}\nabla_{r_j} \end{aligned} \tag{2.7}$$

and $\nabla^2_{R_0}$ becomes

$$\begin{aligned} \nabla^2_{R_0} &= \{\frac{m_0}{M_T}\nabla_X - \sum_{i=1}^{N}\nabla_{r_i}\}\cdot\{\frac{m_0}{M_T}\nabla_X - \sum_{j=1}^{N}\nabla_{r_j}\} \\ &= (\frac{m_0}{M_T})^2\nabla^2_X + \sum_{j=1}^{N}\nabla^2_{r_j} + 2\sum_{j>i\geq 1}^{N}\nabla_{r_i}\cdot\nabla_{r_j} \\ &\quad -\frac{2m_0}{M_T}\sum_{j=1}^{N}\nabla_{r_j}\cdot\nabla_X\,. \end{aligned} \tag{2.8}$$

Similarly we can obtain

$$\nabla_{R_i} = \nabla_{r_i} + \frac{m_i}{M_T}\nabla_X\,. \tag{2.9}$$

$$\nabla^2_{R_i} = \nabla^2_{r_i} + \left(\frac{m_i}{M_T}\right)^2\nabla^2_X + 2\frac{m_i}{M_T}\nabla_{r_i}\cdot\nabla_X\,. \tag{2.10}$$

With these preparations, the original Hamiltonian now becomes

$$H = -\sum_{i=1}^{N}\frac{1}{2\mu_i}\nabla^2_i - \frac{1}{m_0}\sum_{i>j\geq 1}^{N}\nabla_i\cdot\nabla_j + Q_0\sum_{i=1}^{N}\frac{Q_i}{r_i} + \sum_{i>j\geq 1}^{N}\frac{Q_iQ_j}{r_{ij}} - \frac{1}{2M_T}\nabla^2_X\,, \tag{2.11}$$

where $r_{ij} = |\mathbf{r}_i - \mathbf{r}_j|$ and $\mu_i = m_i m_0/(m_i + m_0)$ is the reduced mass for particle i relative to particle 0. It is clear that the center of mass coordinate $\mathbf{X}$ appears only in ∇_X^2; thus its motion can be separated completely from the Hamiltonian and the remaining part of the Hamiltonian involves only the internal coordinates of the system. In other words, if we take the center of mass as our coordinate system, the ∇_X^2 term can be safely neglected. The Hamiltonian responsible for the internal structure of the system is thus

$$H = -\sum_{i=1}^{N} \frac{1}{2\mu_i}\nabla_i^2 - \frac{1}{m_0}\sum_{i>j\geq 1}^{N} \nabla_i \cdot \nabla_j + Q_0 \sum_{i=1}^{N} \frac{Q_i}{r_i} + \sum_{i>j\geq 1}^{N} \frac{Q_i Q_j}{r_{ij}}\,, \tag{2.12}$$

Similarly, in the new coordinates, the total angular momentum $\mathbf{L}$ is reduced to

$$\mathbf{L} = -i\sum_{i=1}^{N} \mathbf{r}_i \times \nabla_i\,, \tag{2.13}$$

Since H, $\mathbf{L}^2$, L_z, and Π mutually commute, where Π is the space inversion parity operator, we may seek common eigenfunctions of these four operators.

Next thing is to express the transition operators in terms of the new coordinates. The 2^l-pole transition operator is defined as

$$T_l = \sum_{i=0}^{n} q_i R_i^l Y_{l0}(\hat{\mathbf{R}}_i)\,, \tag{2.14}$$

According to Eqs. (2.5) and (2.7), we can recast $\mathbf{R}_i$ in the form

$$\mathbf{R}_i = \sum_{j=1}^{n} \epsilon_{ij}\mathbf{r}_j\,, \tag{2.15}$$

where $\epsilon_i = \delta_{ij} - m_j/M_T$, $i = 0, 1, 2, \ldots, N$, and $j = 0, 1, 2, \ldots, N$. By applying the

expansion for the spherical harmonics

$$Y_{lm}(\hat{\mathbf{r}}) = \sqrt{\frac{3}{4\pi}} \prod_{i=1}^{l-1} \left(\sqrt{\frac{2i+3}{i+1}} \right) (\underbrace{\hat{\mathbf{r}} \otimes \hat{\mathbf{r}} \otimes \cdots \hat{\mathbf{r}}}_{l})_m^{(l)} , \tag{2.16}$$

where $\otimes$ means the tensorial product, and inserting Eqs. (2.15) and (2.16) into Eq. (2.14), we obtain

$$T_l = \sqrt{\frac{3}{4\pi}} \prod_{m=1}^{l-1} \left(\sqrt{\frac{2m+3}{m+1}} \right) \sum_{j_1,\cdots,j_l} \left(\sum_{i=0}^{n} q_i \epsilon_{ij_1} \epsilon_{ij_2} \cdots \epsilon_{ij_l} \right) (\hat{\mathbf{r}}_{j_1} \otimes \hat{\mathbf{r}}_{j_1} \otimes \cdots \hat{\mathbf{r}}_{j_l})_0^{(l)} , \tag{2.17}$$

with $\prod_{m=1}^{l-1} \sqrt{\frac{2m+3}{m+1}} = 1$ for the case of $l = 1$.

2.2 Rayleigh-Ritz Variational Method

For a few-body atomic or molecular system, the eigenvalue problem for the Hamiltonian can not be solved analytically. It is thus necessary to find some approximate solutions. The Rayleigh-Ritz variational method is one of the most powerful tools for finding these solutions, although numerically. The systems that have been tackled by the Rayleigh-Ritz variational method to a sufficiently high precision include helium, lithium, and hydrogen molecular ions. As the size of variational basis set increases progressively, the variational upper bounds for the ground and excited state move down correspondingly toward their true values. The converged numbers of digits in the energy eigenvalues can thus be estimated reliably.

Suppose we choose a basis set $\{\Phi_i, i = 1, 2, \ldots, N\}$, where the basis members may not be orthogonal. We use this basis set to expand our trial wave function

$$\Psi_t = \sum_{i=1}^{N} c_i \Phi_i , \tag{2.18}$$

where $\{\ c_i\ \}$ are linear variational parameters. The expectation value of the Hamiltonian is then

$$\mathcal{E} = \langle H \rangle \ = \ \frac{A}{B} = \frac{\langle \Psi_t | H | \Psi_t \rangle}{\langle \Psi_t | \Psi_t \rangle} = \frac{\sum_{ij} c_i^* c_j H_{ij}}{\sum_{ij} c_i^* c_j S_{ij}} \,, \tag{2.19}$$

where $H_{ij} = \langle \Phi_i | H | \Phi_j \rangle$ are the Hamiltonian matrix elements and $S_{ij} = \langle \Phi_i | \Phi_j \rangle$ are the overlap matrix elements. Performing partial differentiation of (2.19) with respect to the variational parameters c_k yields

$$\frac{\partial \mathcal{E}}{\partial c_k^*} \ = \ \frac{1}{B^2} \left[\frac{\partial A}{\partial c_k^*} B - A \frac{\partial B}{\partial c_k^*} \right] , \tag{2.20}$$

where

$$\frac{\partial A}{\partial c_k^*} \ = \ \sum_{ij} \frac{\partial c_i^*}{\partial c_k^*} c_j H_{ij} = \sum_{ij} \delta_{ik} c_j H_{ij} = \sum_j c_j H_{kj} \,, \tag{2.21}$$

$$\frac{\partial B}{\partial c_k^*} \ = \ \sum_{ij} \frac{\partial c_i^*}{\partial c_k^*} c_j S_{ij} = \sum_{ij} \delta_{ik} c_j S_{ij} = \sum_j c_j S_{kj} \,. \tag{2.22}$$

The equation (2.20) thus becomes

$$\begin{aligned} \frac{\partial \mathcal{E}}{\partial c_k^*} \ &= \ \frac{1}{B^2} \left[\sum_j c_j H_{kj} B - A \sum_j c_j S_{kj} \right] \\ &= \ \frac{1}{B} \left[\sum_j c_j H_{kj} - \mathcal{E} \sum_j c_j S_{kj} \right] \\ &= \ 0 \,. \end{aligned} \tag{2.23}$$

We thus have

$$\sum_j c_j H_{kj} - \mathcal{E} \sum_j c_j S_{kj} \ = \ \sum_j c_j \Big(H_{kj} - \mathcal{E} S_{kj} \Big) = 0 \,, \tag{2.24}$$

where $k = 1, 2, 3, \ldots, N$. For a nonzero vector $(c_1, c_2, \cdots, c_N)$, we must have

$$\det(\mathcal{H} - \mathcal{E}\mathcal{S}) = 0\,, \tag{2.25}$$

which determines the solutions to the generalized eigenvalue problem

$$\mathcal{H}\mathcal{C} = \mathcal{E}\mathcal{S}\mathcal{C}\,. \tag{2.26}$$

In the above, $\mathcal{H}$ is the Hamiltonian matrix

$$\mathcal{H} = \begin{bmatrix} H_{11} & H_{12} & \cdots & H_{1N} \\ H_{21} & H_{22} & \cdots & H_{2N} \\ \cdots & \cdots & \cdots & \cdots \\ H_{N1} & H_{N2} & \cdots & H_{NN} \end{bmatrix}, \tag{2.27}$$

$\mathcal{S}$ is the overlap matrix

$$\mathcal{S} = \begin{bmatrix} S_{11} & S_{12} & \cdots & S_{1N} \\ S_{21} & S_{22} & \cdots & S_{2N} \\ \cdots & \cdots & \cdots & \cdots \\ S_{N1} & S_{N2} & \cdots & S_{NN} \end{bmatrix}, \tag{2.28}$$

and $\mathcal{C}$ is a column matrix formed by the expansion coefficients c_i

$$\mathcal{C} = \begin{pmatrix} c_1 \\ c_2 \\ \vdots \\ c_N \end{pmatrix}. \tag{2.29}$$

Suppose we have N roots in order of increasing value

$$\mathcal{E}_1 \leq \mathcal{E}_2 \leq \cdots \leq \mathcal{E}_N \,. \tag{2.30}$$

If we arrange the true eigenvalues of H in the following order

$$E_1 \leq E_2 \leq \cdots \leq E_N \tag{2.31}$$

then the Hylleraas-MacDonald theorem [71] says that

$$\mathcal{E}_1 \geq E_1, \mathcal{E}_2 \geq E_2, \cdots, \mathcal{E}_N \geq E_N \,. \tag{2.32}$$

It is thus seen that the Rayleigh-Ritz method has a power of providing the upper bounds to the lowest N true eigenvalues. When an extra column and row are added to an $N \times N$ matrix, the N old eigenvalues fall between the $N+1$ new ones. Consequently, all eigenvalues numbered from the bottom up must move inexorably downward to the exact eigenvalues as N is increased progressively.

The Rayleigh-Ritz procedure can be considered as an optimization of the linear variational parameters. However, in the Hylleraas basis set there are some nonlinear parameters, in addition to the linear parameters. All nonlinear parameters are optimized using the Newton's method by calculating analytically the first-order derivatives of the variation energy with respect to these parameters

$$\frac{\partial \mathcal{E}}{\partial \tau} = -2\langle \Psi | H | \frac{\partial \psi}{\partial \tau} \rangle - 2\mathcal{E}\langle \Psi | \frac{\partial \psi}{\partial \tau} \rangle \,, \tag{2.33}$$

where τ can be one of the nonlinear parameters. The second-order derivatives could be estimated by taking differentials. Newton's method tells us how to locate the zeros of the first derivatives. In the next loop of calculation, we could use these newly located nonlinear parameters as inputs to start with. After several iterations, we

could obtain a set of optimized nonlinear parameters for the final energy calculation.

2.3 The Four-Body System and The Hylleraas Basis Set

Consider the Hamiltonian for the atomic lithium, a four-body atomic system

$$H_0 = -\frac{1}{2\mu}\sum_{i=1}^{3}\nabla_i^2 - \frac{1}{m_0}\sum_{i>j\geq 1}\nabla_i\cdot\nabla_j + \sum_{i=1}^{3}\frac{Z}{r_i} + \sum_{i>j\geq 1}^{3}\frac{1}{r_{ij}}\,, \tag{2.34}$$

where Z is the charge of the nucleus. The Hylleraas-type basis function ϕ_{t,μ_t} can be written as

$$\phi_{t,\mu_t}(\mathbf{r}_1,\mathbf{r}_2,\mathbf{r}_3) = r_1^{j_1}r_2^{j_2}r_3^{j_3}r_{12}^{j_{12}}r_{23}^{j_{23}}r_{31}^{j_{31}}e^{-\alpha r_1-\beta r_2-\gamma r_3}\mathcal{Y}^{L,M_L}_{(l_1,l_2)l_{12},l_3}(\hat{r}_1,\hat{r}_2,\hat{r}_3)\mathcal{X}(1,2,3)\,, \tag{2.35}$$

where $r_{ij}=|\mathbf{r}_i-\mathbf{r}_j|$ is the distance between electrons i and j, $r_{12}^{j_{12}}$, $r_{23}^{j_{23}}$, $r_{31}^{j_{31}}$ represent the correlations for three pairs of electrons, and $\mathcal{X}(1,2,3)$ is for the spin 1/2 function. Also in the above, $\mathcal{Y}^{L,M_L}_{(l_1,l_2)l_{12},l_3}(\hat{r}_1,\hat{r}_2,\hat{r}_3)$ is a coupled spherical harmonic, which is the common eigenstate of operators L^2, L_z, and Π with the corresponding eigenvalues $L(L+1)$, M_L, and $(-1)^{l_1+l_2+l_3}$, respectively

$$\begin{aligned}\mathcal{Y}^{L,M_L}_{(l_1,l_2)l_{12},l_3}(\hat{r}_1,\hat{r}_2,\hat{r}_3) &= \sum_{m_i}\langle l_1m_1,l_2m_2|l_1l_2;l_{12}m_{12}\rangle \\ \times\ \langle l_{12}m_{12},l_3m_3|l_{12}l_3;LM_L\rangle &Y_{l_1m_1}(\hat{r}_1)Y_{l_2m_2}(\hat{r}_2)Y_{l_3m_3}(\hat{r}_3)\,,\end{aligned} \tag{2.36}$$

where $\langle l_1 m_1, l_2 m_2 | l_1 l_2; l_{12} m_{12} \rangle$ and $\langle l_{12} m_{12}, l_3 m_3 | l_{12} l_3; L M_L \rangle$ are two Clebsch-Gordan coefficients. The variational wavefunction is expanded in terms of the Hylleraas basis functions

$$\Psi(\mathbf{r}_1, \mathbf{r}_2, \mathbf{r}_3) \;=\; \mathcal{A} \sum_t \sum_{\mu_t} a_{t,\mu_t} \Phi_{t,\mu_t}(\mathbf{r}_1, \mathbf{r}_2, \mathbf{r}_3)\,, \tag{2.37}$$

where $\mathcal{A}$ is the anti-symmetrization operator, the index μ_t stands for the six integers j_1, j_2, j_3, j_{12}, j_{23}, and j_{31}, index t stands for a block of nonlinear parameters α, β. The basis set includes all combinations of j_1, j_2, j_3, j_{12}, j_{23}, and j_{31} with $j_1 + j_2 + j_3 + j_{12} + j_{23} + j_{31} \leq \Omega$, where Ω is an integer that controls the size of the basis set. Of course, terms that may potentially cause near linear dependencies should be excluded from the basis set. More details about partitioning the basis set into different blocks, as well as into different angular configurations, can be found in [70]. For this three-electron system, in the center of mass frame, T_l $(l = 1, 2, 3)$ can be reduced to

$$T_1 \;=\; \sum_{j=1}^{3} \left(\sum_{i=0}^{3} Q_i \epsilon_{ij} \right) r_j Y_{10}(\hat{\mathbf{r}}_j)\,, \tag{2.38}$$

$$T_2 \;=\; \sum_{j=1}^{3} \left(\sum_{i=0}^{3} Q_i \epsilon_{ij}^2 \right) r_j^2 Y_{20}(\hat{\mathbf{r}}_j) + \sqrt{\frac{15}{2\pi}} \sum_{\{j,k\}} \left(\sum_{i=0}^{3} Q_i \epsilon_{ij} \epsilon_{ik} \right) r_j r_k (\hat{\mathbf{r}}_j \otimes \hat{\mathbf{r}}_k)_0^{(2)}\,, \tag{2.39}$$

where { j,k } = (1,2), (2,3), (3,1),

$$\begin{aligned} T_3 &= \sum_{j=1}^{3}\left(\sum_{i=0}^{3} Q_i \epsilon_{ij}^3\right) r_j^3 Y_{30}(\hat{\mathbf{r}}_j) \\ &+ 3\sqrt{\frac{35}{8\pi}} \sum_{\substack{j,k=1,2,3 \\ j\neq k}} \left(\sum_{i=0}^{3} Q_i \epsilon_{ij}^2 \epsilon_{ik}\right) r_j^2 r_k ((\hat{\mathbf{r}}_j \otimes \hat{\mathbf{r}}_k)^{(2)} \otimes \hat{\mathbf{r}}_k)_0^{(3)} \\ &+ 6\sqrt{\frac{35}{8\pi}}\left(\sum_{i=0}^{3} Q_i \epsilon_{i1}\epsilon_{i2}\epsilon_{i3}\right) r_1 r_2 r_3 ((\hat{\mathbf{r}}_1 \otimes \hat{\mathbf{r}}_2)^{(2)} \otimes \hat{\mathbf{r}}_3)_0^{(3)}\,, \end{aligned} \tag{2.40}$$

where the effect of the finite nuclear mass is reflected in the transition operator T_l by an l-th order polynomial in m_i/M_T. For example, in T_3

$$\sum_{i=0}^{3} Q_i \epsilon_{ij}^3 = Q_j - 3Q_j\left(\frac{m_j}{M_T}\right) + 3Q_j\left(\frac{m_j}{M_T}\right)^2, \tag{2.41}$$

$$\sum_{i=0}^{3} Q_i \epsilon_{ij}^2 \epsilon_{ik} = -Q_j\left(\frac{m_k}{M_T}\right) + 2Q_j\left(\frac{m_j}{M_T}\right)\left(\frac{m_k}{M_T}\right) + Q_k\left(\frac{m_j}{M_T}\right)^2, \tag{2.42}$$

$$\sum_{i=0}^{3} Q_i \epsilon_{i1}\epsilon_{i2}\epsilon_{i3} = Q_1\left(\frac{m_2}{M_T}\right)\left(\frac{m_3}{M_T}\right) + Q_2\left(\frac{m_3}{M_T}\right)\left(\frac{m_1}{M_T}\right) + Q_3\left(\frac{m_1}{M_T}\right)\left(\frac{m_2}{M_T}\right). \tag{2.43}$$

2.4 Basic Integrals

In forming the Hamiltonian matrix and overlap matrix, one needs to deal with two types of integrals. The first one is the overlap integral between two Hylleraas-type

basis functions

$$
\begin{aligned}
& I(l_1', m_1', l_2', m_2', l_3', m_3', l_1, m_1, l_2, m_2, l_3, m_3; j_1, j_2, j_3, j_{12}, j_{23}, j_{31}; \alpha, \beta, \gamma) \\
= & \int d\mathbf{r}_1 d\mathbf{r}_2 d\mathbf{r}_3 r_1^{j_1} r_2^{j_2} r_3^{j_3} r_{12}^{j_{12}} r_{23}^{j_{23}} r_{31}^{j_{31}} e^{-\alpha r_1 - \beta r_2 - \gamma r_3} \\
\times & Y^*_{l_1', m_1'}(\hat{r}_1) Y^*_{l_2', m_2'}(\hat{r}_2) Y^*_{l_3', m_3'}(\hat{r}_3) Y_{l_1, m_1}(\hat{r}_1) Y_{l_2, m_2}(\hat{r}_2) Y_{l_3, m_3}(\hat{r}_3) \\
= & \sum_{\{q_{\mu\nu}=0\}}^{\{M_{\mu\nu}\}} \sum_{\{k_{\mu\nu}=0\}}^{\{L_{\mu\nu}\}} I_{\mathrm{ang}}(l_1', m_1', l_2', m_2', l_3', m_3', l_1, m_1, l_2, m_2, l_3, m_3; q_{12}, q_{23}, q_{31}) \\
\times & I_R(q_{12}, q_{23}, q_{31}, k_{12}, k_{23}, k_{31}; j_1, j_2, j_3, j_{12}, j_{23}, j_{31}; \alpha, \beta, \gamma)\,, \qquad (2.44)
\end{aligned}
$$

where $k_{\mu\nu}$ stands for k_{12}, k_{23}, k_{31}; $q_{\mu\nu}$ stands for q_{12}, q_{23}, q_{31}; $L_{\mu\nu}$ stands for L_{12}, L_{23}, L_{31}; $M_{\mu\nu}$ stands for M_{12}, M_{23}, M_{31}. And I_R is the radial integral and I_{ang} the angular integral. The second one is the integral of the Laplacian operator and gradient operator, for example

$$
\begin{aligned}
& \int d\mathbf{r}_1 d\mathbf{r}_2 d\mathbf{r}_3 r_1^{j_1'} r_2^{j_2'} r_3^{j_3'} r_{12}^{j_{12}'} r_{23}^{j_{23}'} r_{31}^{j_{31}'} e^{-\alpha' r_1 - \beta' r_2 - \gamma' r_3} Y^*_{l_1', m_1'}(\hat{r}_1) Y^*_{l_2', m_2'}(\hat{r}_2) Y^*_{l_3', m_3'}(\hat{r}_3) \\
\times & \nabla_1^2 \left(r_1^{j_1} r_2^{j_2} r_3^{j_3} r_{12}^{j_{12}} r_{23}^{j_{23}} r_{31}^{j_{31}} e^{-\alpha r_1 - \beta r_2 - \gamma r_3} Y_{l_1, m_1}(\hat{r}_1) Y_{l_2, m_2}(\hat{r}_2) Y_{l_3, m_3}(\hat{r}_3) \right) \\
= & \alpha^2 F_0 + [j_1(j_1+1) - l_1(l_1+1)] F_1 + j_{12}(j_{12}+1) F_2 + j_{31}(j_{31}+1) F_3 - 2\alpha(j_1+1) F_4 \\
+ & 2 j_{12} j_1 F_5 - 2 j_{12} \alpha F_6 + 2 j_{31} j_1 F_7 - 2 j_{31} \alpha F_8 + 2 j_{12} j_{31} F_9 - 2 j_{12} g_1 - 2 j_{31} g_2\,. \qquad (2.45)
\end{aligned}
$$

where F_n, g_n are some subsidiary integrals. The further details about these two types of integrals can be found in [72].

Chapter 3

Calculations of Long-Range Three-Body Interaction for Li($2\,^2S$)-Li($2\,^2S$)-Li($2\,^2P$)

3.1 Theoretical Formulation

Consider three well-separated lithium atoms where the overlap of their wave functions can be neglected. The Hamiltonian for this system can be written as

$$H = H^{(0)} + H' \,, \tag{3.1}$$

where

$$H^{(0)} = H_1^{(0)} + H_2^{(0)} + H_3^{(0)} \,, \tag{3.2}$$

$$H' \equiv V_{123} = V_{12} + V_{23} + V_{31} \,, \tag{3.3}$$

with $H_1^{(0)}$, $H_2^{(0)}$, and $H_3^{(0)}$ being the unperturbed Hamiltonian of, respectively, atom 1, 2, and 3, and V_{12}, V_{23}, and V_{31} their mutual electrostatic interactions. We label

the atoms by I, J, and K, with, respectively, internal coordinates $\boldsymbol{\sigma}$, $\boldsymbol{\rho}$, and $\boldsymbol{\varsigma}$. When the labels I, J, or K appear, it is understood that cyclic permutation can be used. V_{IJ} can be expanded according to Ref. [26]

$$V_{IJ} = \sum_{l_I l_J} \sum_{m_I m_J} T_{l_I\, -\, m_I}(\boldsymbol{\sigma}) T_{l_J m_J}(\boldsymbol{\rho}) W_{l_I l_J}^{m_I - m_J}(IJ)\,. \tag{3.4}$$

In Eq.(3.4), the multipole transition operators are

$$T_{l_I - m_I}(\boldsymbol{\sigma}) = \sum_i Q_i \sigma_i^{l_I} Y_{l_I - m_I}(\hat{\boldsymbol{\sigma}}_i)\,, \tag{3.5}$$

$$T_{l_J m_J}(\boldsymbol{\rho}) = \sum_j q_j \rho_j^{l_J} Y_{l_J m_J}(\hat{\boldsymbol{\rho}}_j)\,, \tag{3.6}$$

and the geometry factor is

$$\begin{aligned} W_{l_I l_J}^{m_I - m_J}(IJ) &= \frac{4\pi(-1)^{l_J}}{R_{IJ}^{l_I + l_J + 1}} \frac{(l_I + l_J - m_I + m_J)!(l_I, l_J)^{-1/2}}{[(l_I + m_I)!(l_I - m_I)!(l_J + m_J)!(l_J - m_J)!]^{1/2}} \\ &\times P_{l_I + l_J}^{m_I - m_J}(\cos\theta_{IJ}) \exp[i(m_I - m_J)\Phi_{IJ}]\,, \end{aligned} \tag{3.7}$$

where $\mathbf{R}_{IJ} = \mathbf{R}_J - \mathbf{R}_I$ is the relative position vector from atom I to atom J, the notation $(a, b, \ldots) = (2a+1)(2b+1)\ldots$, and $P_{l_I + l_J}^{m_I - m_J}(\cos\theta_{IJ})$ is the associated Legendre function with θ_{IJ} representing the angle between $\mathbf{R}_{IJ}$ and the z-axis. Similar expressions exist for V_{JK} and V_{KI}. The choice of the z-axis is discussed below.

3.1.1 The Zeroth-Order Wave Functions

For the Li(n_0S)-Li(n_0S)-Li($n_0'L$) system, where the angular momentum of one atom is L and the associated magnetic quantum number is M, there are three orthogonal eigenvectors for the unperturbed Hamiltonian corresponding to the same energy

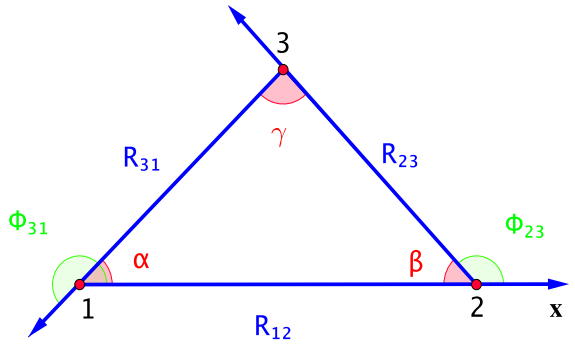

Figure 3.1: Coordinate system for the three atoms: the z-axis is perpendicular to the plane of the three atoms and the x-axis is parallel to $\mathbf{R}_{12}$. The angles satisfy $\Phi_{12} = 0$, $\Phi_{23} = \pi - \beta$, $\Phi_{31} = \pi + \alpha$.

eigenvalue $E^{(0)}_{n_0 n_0 n'_0} = 2E^{(0)}_{n_0 S} + E^{(0)}_{n'_0 L}$,

$$|\phi_1\rangle = |\varphi_{n'_0}(LM;\boldsymbol{\sigma})\varphi_{n_0}(0;\boldsymbol{\rho})\varphi_{n_0}(0;\boldsymbol{\varsigma})\rangle\,, \tag{3.8}$$

$$|\phi_2\rangle = |\varphi_{n_0}(0;\boldsymbol{\sigma})\varphi_{n'_0}(LM;\boldsymbol{\rho})\varphi_{n_0}(0;\boldsymbol{\varsigma})\rangle\,, \tag{3.9}$$

$$|\phi_3\rangle = |\varphi_{n_0}(0;\boldsymbol{\sigma})\varphi_{n_0}(0;\boldsymbol{\rho})\varphi_{n'_0}(LM;\boldsymbol{\varsigma})\rangle\,. \tag{3.10}$$

According to degenerate perturbation theory, the zeroth-order wave function is a linear combination of the eigenvectors given in Eqs. (3.8), (3.9), and (3.10),

$$|\Psi^{(0)}\rangle = a|\phi_1\rangle + b|\phi_2\rangle + c|\phi_3\rangle\,. \tag{3.11}$$

The expansion coefficients a, b, and c are determined by diagonalizing the perturbation V_{123} in the basis set $\{\phi_1, \phi_2, \phi_3\}$, which depends on the geometrical configuration formed by the three atoms.

3.1.2 Choice of Coordinates for Three Atoms

In this work, we set the coordinates for the three atoms as shown in Fig. 3.1. Specifically, we choose the nucleus of atom 1 as the origin of our coordinate system and the x-y plane as the plane formed by the three atomic nuclei. Furthermore, we set the x-axis to be $\mathbf{R}_{12}$ and the z-axis perpendicular to the x-y plane by the right-hand convention. The interior angles of the triangle formed by the three atoms are denoted as α, β, γ. Noting that [26] $\theta_{12} = \theta_{23} = \theta_{31} = \pi/2$, the associated Legendre functions can be simplified according to

$$P_l^m(0) = \frac{1}{2^{l+1}}[1+(-1)^{l+m}](-1)^{\frac{l+m}{2}}(l+m)!\left[\left(\frac{l+m}{2}\right)!\right]^{-1}\left[\left(\frac{l-m}{2}\right)!\right]^{-1}. \tag{3.12}$$

The angles Φ_{12}, Φ_{23}, and Φ_{31} satisfy $\Phi_{12} = 0$, $\Phi_{23} = \pi - \beta$, and $\Phi_{31} = \pi + \alpha$, which can be used to simplify the exponential function $\exp[i(m_I - m_J)\Phi_{IJ}]$ in the geometry factor.

3.1.3 The Connection With Other Studies

With these eigenvectors and zero-order wave function, we can easily find the connection between this work and preceding studies of long-range interactions. For example, if we eliminate the terms involving particle 3 (with angular momentum L), our formulae describe the long-range interactions for the two-body $n_0S - n_0S$ system. If we set $a = \frac{1}{\sqrt{2}}$, $b = \pm\frac{1}{\sqrt{2}}$, $c = 0$ and remove the terms involving particle 3 (with angular momentum 0), our expressions describe the long-range interactions for the two-body $n_0S - n_0'L$ system. If we set $a = 1$, $b = c = 0$ and $L = 0$, the long-range three-body $n_0S - n_0S - n_0'S$ interaction is described.

We noted that Cvitaš et al. [61] considered the connection between the long-range interactions for atom-dimer and atom-atom-atom potential energy surfaces, which

corresponds to the *ground state* for the three *spin-aligned* atoms. They rewrote the atom-atom distances in terms of Jacobi coordinates R, r, and θ and expanded the corresponding results as a power series in r/R for $r \ll R$. The contributions of atom-atom coefficients to the atom-diatom coefficients have been shown in their studies. They can do this approximation because, in the $n_0S - n_0S - n_0S$ system, the atom-atom coefficients are constants. However, for the $n_0S - n_0S - n_0'L$ system, we find that the atom-atom coefficients depend on the geometrical configuration of the three atoms because of the quantum superposition principle. Hence we cannot use their method directly to achieve the transition from the well-separated system to the atom-diatom system in the $n_0S - n_0S - n_0'L$ system. However we can make it by adjusting the state of this system. For example, if we set $a = b = 0$, $c = 1$, our formulae reduce to the long-range interactions between an atom $n_0'L$ and a diatom $n_0S - n_0S$. This situation can be related to a heteronuclear system, such as He($n_0'P$)-Li(n_0S)-Li(n_0S). This situation plays a particular role in the heteronuclear system and the asymptotic region. We note it here for future reference. In this thesis, we will focus on the long-range interactions for the homonuclear atom-atom-atom lithium system.

In Appendix A, we give the general expressions of the interaction coefficients for $n_0S - n_0S - n_0'L$ up to second order in perturbation theory. To be specific, here we focus on the case of $n_0 = 2$, $n_0' = 2$, and $L = 1$ for the Li($2\,^2S$)-Li($2\,^2S$)-Li($2\,^2P$) system.

3.1.4 The First-Order Energy

According to perturbation theory, the first-order energy correction for the Li($2\,^2S$)-Li($2\,^2S$)-Li($2\,^2P$) system is

$$\Delta E^{(1)} = -\frac{C_3^{(12)}(1,M)}{R_{12}^3} - \frac{C_3^{(23)}(1,M)}{R_{23}^3} - \frac{C_3^{(31)}(1,M)}{R_{31}^3}\,, \tag{3.13}$$

where

$$C_3^{(IJ)}(1,M) \;=\; (A_I^* A_J + A_J^* A_I)\mathbb{D}_0(M)\,, \tag{3.14}$$

$$A_1 = a, A_2 = b, A_3 = c\,, \tag{3.15}$$

and

$$\mathbb{D}_0(M) \;=\; \frac{4\pi(-1)^{1+M}}{9(1-M)!(1+M)!}|\langle\varphi_{n_0}(0;\boldsymbol{\sigma})\|T_1(\boldsymbol{\sigma})\|\varphi_{n_0'}(1;\boldsymbol{\sigma})\rangle|^2\,. \tag{3.16}$$

Where a, b, c are defined in Eq. (3.11). It should be mentioned that there exist only additive long-range interaction terms at this order of perturbation.

3.1.5 The Second-Order Energy

The second-order energy correction for the Li($2\,^2S$)-Li($2\,^2S$)-Li($2\,^2P$) system can be written as

$$\begin{aligned}\Delta E^{(2)} \;=\; & -\sum_{n\geq 3}\left(\frac{C_{2n}^{(12)}(1,M)}{R_{12}^{2n}} + \frac{C_{2n}^{(23)}(1,M)}{R_{23}^{2n}} + \frac{C_{2n}^{(31)}(1,M)}{R_{31}^{2n}}\right. \\ & + \left.\frac{C_{2n}^{(12,23)}(1,M)}{R_{12}^{n}R_{23}^{n}} + \frac{C_{2n}^{(23,31)}(1,M)}{R_{23}^{n}R_{31}^{n}} + \frac{C_{2n}^{(31,12)}(1,M)}{R_{31}^{n}R_{12}^{n}}\right),\end{aligned} \tag{3.17}$$

where the $C_{2n}^{(12)}(1,M)$, $C_{2n}^{(23)}(1,M)$, and $C_{2n}^{(31)}(1,M)$ are the additive dispersion coefficients, and $C_{2n}^{(12,23)}(1,M)$, $C_{2n}^{(23,31)}(1,M)$, and $C_{2n}^{(31,12)}(1,M)$ are the nonadditive dispersion ones. The derivation of these coefficients is given in Appendix A. In this work we are only concerned with $n = 3$ and 4 in Eq. (3.17). The corresponding dispersion coefficients are

$$C_6^{(IJ)}(1,M) \;=\; (|A_I|^2 + |A_J|^2)\mathbb{D}_1(M) + |A_K|^2\mathbb{D}_2\,, \tag{3.18}$$

$$C_8^{(IJ)}(1,M) \;=\; (|A_I|^2+|A_J|^2)\mathbb{Q}_1(M)+|A_K|^2\mathbb{Q}_2+(A_I^*A_J+A_J^*A_I)\mathbb{Q}_3(M)\,, \tag{3.19}$$

$$C_6^{(IJ,JK)}(1,M) \;=\; \mathbb{Q}_4(A_K,A_I,1,M,\eta_J)\,, \tag{3.20}$$

$$C_8^{(IJ,JK)}(1,M) \;=\; \mathbb{Q}_4(A_K,A_I,2,M,\eta_J)\,, \tag{3.21}$$

with

$$A_1=a, A_2=b, A_3=c, \eta_1=\alpha, \eta_2=\beta, \eta_3=\gamma\,, \tag{3.22}$$

where a, b, and c are defined in Eq. (3.11), α, β, and γ are the interior angles, and the other terms in Eqs. (3.18)-(3.21) are given by

$$\mathbb{D}_1(M) \;=\; \sum_{n_s n_t L_s} F_1(n_s,n_t,L_s,1;1,1;1,M)\,, \tag{3.23}$$

$$\mathbb{D}_2 \;=\; \sum_{n_s n_t} F_2(n_s,n_t,1,1)\,, \tag{3.24}$$

$$\begin{aligned}\mathbb{Q}_1(M) \;=\; &\sum_{n_s n_t L_s} [F_1(n_s,n_t,L_s,1;1,3;1,M)+F_1(n_s,n_t,L_s,1;2,2;1,M)\\ &+\; F_1(n_s,n_t,L_s,1;3,1;1,M)+F_1(n_s,n_t,L_s,2;1,1;1,M)]\,,\end{aligned} \tag{3.25}$$

$$\mathbb{Q}_2 \;=\; \sum_{n_s n_t} [F_2(n_s,n_t,1,2)+F_2(n_s,n_t,2,1)]\,, \tag{3.26}$$

$$\begin{aligned}\mathbb{Q}_3(M) \;=\; &\sum_{n_s n_t} [F_3(n_s,n_t,1,1;2,2;1,M)+F_3(n_s,n_t,1,2;2,1;1,M)\\ &+\; F_3(n_s,n_t,2,1;1,2;1,M)+F_3(n_s,n_t,2,2;1,1;1,M)]\,,\end{aligned} \tag{3.27}$$

and

$$\mathbb{Q}_4(A_K, A_I, \lambda, M, \eta_J) \;=\; 2\sum_{n_t M_t} \mathrm{Re}[A_K^* A_I\, e^{i(M_t - M)\eta_J}] F_4(n_t, \lambda, M_t; 1, M)\,. \tag{3.28}$$

In the above (I, J, K) forms a permutation of (1,2,3) and the F_i-functions are defined by Eqs. (A.20), (A.21), (A.22), and (A.23) in Appendix A.

3.1.6 Three Special Geometrical Configurations

In this work, three special geometrical configurations formed by the three atoms are considered. The first configuration is the equilateral triangle, where the interatomic separations are the same: $R_{12} = R_{23} = R_{31} = R$, corresponding to D_{3h} symmetry. With this configuration, all the diagonal perturbation matrix elements are zero and all the off diagonal matrix elements are the same. The perturbation matrix with respect to $\{\phi_1, \phi_2, \phi_3\}$ thus becomes

$$H' = H'_{12} \begin{pmatrix} 0 & 1 & 1 \\ 1 & 0 & 1 \\ 1 & 1 & 0 \end{pmatrix}, \tag{3.29}$$

where

$$H'_{12} \;=\; \frac{4\pi}{R^{2L+1}} \frac{(-1)^M [(2L-1)!!]^2}{(2L+1)^2 (L-M)!(L+M)!} |\langle \varphi_{n_0}(0; \boldsymbol{\sigma}) \| T_L(\boldsymbol{\sigma}) \| \varphi_{n'_0}(L; \boldsymbol{\sigma}) \rangle|^2\,.$$

Solving the eigenvalue problem of the above matrix, one obtains the eigenvalues: $2H'_{12}$, $-H'_{12}$, $-H'_{12}$, and the corresponding orthonormalized zeroth-order wave func-

tions:

$$\Psi^{(0)}_{1,\Delta} = \frac{1}{\sqrt{3}}|\phi_1\rangle + \frac{1}{\sqrt{3}}|\phi_2\rangle + \frac{1}{\sqrt{3}}|\phi_3\rangle\,, \tag{3.30}$$

$$\Psi^{(0)}_{2,\Delta} = \frac{1}{\sqrt{2}}|\phi_1\rangle - \frac{1}{\sqrt{2}}|\phi_3\rangle\,, \tag{3.31}$$

$$\Psi^{(0)}_{3,\Delta} = \frac{1}{\sqrt{6}}|\phi_1\rangle - \sqrt{\frac{2}{3}}|\phi_2\rangle + \frac{1}{\sqrt{6}}|\phi_3\rangle\,, \tag{3.32}$$

where the symbol Δ denotes the equilateral triangle.

The second special geometrical configuration is the isosceles right triangle such that $R_{12} = \frac{1}{\sqrt{2}}R_{23} = R_{31} = R$, corresponding to C_{2v} symmetry. With this configuration, the perturbation matrix has the form

$$H' = H'_{12}\begin{pmatrix} 0 & 1 & 1 \\ 1 & 0 & \frac{1}{2\sqrt{2}} \\ 1 & \frac{1}{2\sqrt{2}} & 0 \end{pmatrix}. \tag{3.33}$$

The eigenvalues are $\frac{H'_{12}}{8}\left(\sqrt{2}+\sqrt{130}\right), \frac{H'_{12}}{8}\left(\sqrt{2}-\sqrt{130}\right), -\frac{H'_{12}}{2\sqrt{2}}$, and the corresponding orthonormalized zeroth-order wave functions are

$$\Psi^{(0)}_{1,\perp} = \frac{\sqrt{130}-\sqrt{2}}{2\sqrt{65-\sqrt{65}}}|\phi_1\rangle + \frac{4}{\sqrt{65-\sqrt{65}}}|\phi_2\rangle + \frac{4}{\sqrt{65-\sqrt{65}}}|\phi_3\rangle\,, \tag{3.34}$$

$$\Psi^{(0)}_{2,\perp} = \frac{-(\sqrt{130}+\sqrt{2})}{2\sqrt{65+\sqrt{65}}}|\phi_1\rangle + \frac{4}{\sqrt{65+\sqrt{65}}}|\phi_2\rangle + \frac{4}{\sqrt{65+\sqrt{65}}}|\phi_3\rangle\,, \tag{3.35}$$

$$\Psi^{(0)}_{3,\perp} = -\frac{1}{\sqrt{2}}|\phi_2\rangle + \frac{1}{\sqrt{2}}|\phi_3\rangle\,, \tag{3.36}$$

where the symbol $\perp$ denotes the isosceles right triangle.

The third special geometrical configuration is that the three atoms are in a straight

line such that $R_{12} = \frac{1}{2}R_{23} = R_{31} = R$, corresponding to $D_{\infty h}$ symmetry. With this configuration, the perturbation matrix is

$$H' = H'_{12} \begin{pmatrix} 0 & 1 & 1 \\ 1 & 0 & \frac{1}{8} \\ 1 & \frac{1}{8} & 0 \end{pmatrix} . \tag{3.37}$$

The eigenvalues are $\frac{H'_{12}}{16}\left(1+3\sqrt{57}\right), \frac{H'_{12}}{16}\left(1-3\sqrt{57}\right), -\frac{H'_{12}}{8}$, and the corresponding orthonormalized zeroth-order wave functions are

$$\Psi^{(0)}_{1,-} = \frac{3\sqrt{57}-1}{\sqrt{1026-6\sqrt{57}}}|\phi_1\rangle + \frac{16}{\sqrt{1026-6\sqrt{57}}}|\phi_2\rangle + \frac{16}{\sqrt{1026-6\sqrt{57}}}|\phi_3\rangle\,, \tag{3.38}$$

$$\Psi^{(0)}_{2,-} = \frac{-(3\sqrt{57}+1)}{\sqrt{1026+6\sqrt{57}}}|\phi_1\rangle + \frac{16}{\sqrt{1026+6\sqrt{57}}}|\phi_2\rangle + \frac{16}{\sqrt{1026+6\sqrt{57}}}|\phi_3\rangle\,, \tag{3.39}$$

$$\Psi^{(0)}_{3,-} = -\frac{1}{\sqrt{2}}|\phi_2\rangle + \frac{1}{\sqrt{2}}|\phi_3\rangle\,, \tag{3.40}$$

where the symbol – denotes the geometrical configuration of a straight line.

3.2 Results and Discussion

In our calculations, the atomic wave functions of lithium were constructed variationally using Hylleraas basis sets, and the intermediate states were generated by diagonalizing the lithium Hamiltonian, as described in Ref. [73]. All the relevant matrix elements for the multipole transition operators were thus evaluated, including the finite nuclear mass corrections. With these, the first and second order long-range coefficients for Li($2\,^2S$)-Li($2\,^2S$)-Li($2\,^2P$) were obtained.

Table 3.1 lists the values of $\mathbb{D}_0(M=0)$, $\mathbb{D}_0(M=\pm1)$, $\mathbb{D}_1(M=0)$, $\mathbb{D}_1(M=\pm1)$, $\mathbb{D}_2$,

Table 3.1: Values of $\mathbb{D}_0(M=0)$, $\mathbb{D}_0(M=\pm1)$, $\mathbb{D}_1(M=0)$, $\mathbb{D}_1(M=\pm1)$, $\mathbb{D}_2$, $\mathbb{Q}_1(M=0)$, $\mathbb{Q}_1(M=\pm1)$, $\mathbb{Q}_2$, $\mathbb{Q}_3(M=0)$, and $\mathbb{Q}_3(M=\pm1)$ for the Li($2\,^2S$)-Li($2\,^2S$)-Li($2\,^2P$) system, in atomic units. All these quantities are independent of the geometrical configuration formed by the three atoms. The numbers in parentheses represent the computational uncertainties.

Atom	$\mathbb{D}_0(M=0)$ $\mathbb{Q}_1(M=0)$	$\mathbb{D}_0(M=\pm1)$ $\mathbb{Q}_1(M=\pm1)$	$\mathbb{D}_1(M=0)$ $\mathbb{Q}_2$	$\mathbb{D}_1(M=\pm1)$ $\mathbb{Q}_3(M=0)$	$\mathbb{D}_2$ $\mathbb{Q}_3(M=\pm1)$
$^{\infty}$Li	−5.500111(1) 75804.1(5)	2.750054(1) 354147(4)	1406.68(3) 83429(1)	1741.06(5) 27239.28(1)	1393.42(5) −165583.70(1)
^{7}Li	−5.500926(1) 75809.6(5)	2.750462(1) 354206(4)	1407.15(5) 83456(5)	1741.59(4) 27242.91(2)	1394.05(5) −165615.09(1)
^{6}Li	−5.501062(1) 75810.5(5)	2.750530(1) 354216(4)	1407.20(2) 83460(5)	1741.68(4) 27243.52(2)	1394.16(5) −165620.32(1)

$\mathbb{Q}_1(M=0)$, $\mathbb{Q}_1(M=\pm1)$, $\mathbb{Q}_2$, $\mathbb{Q}_3(M=0)$, and $\mathbb{Q}_3(M=\pm1)$ for lithium isotopes, all of which are independent of the geometrical configuration of the three lithium atoms. However, the quantity $\mathbb{Q}_4$, not listed in Table 3.1, is related to the nonadditive dispersion coefficients and is geometrical configuration dependent. $\mathbb{D}_0(M=0)$ and $\mathbb{D}_0(M=\pm1)$ are connected with the first-order additive coefficient $C_3^{(IJ)}(L,M)$. $\mathbb{D}_1(M=0)$, $\mathbb{D}_1(M=\pm1)$, and $\mathbb{D}_2$ are connected with the second-order additive dispersion coefficient $C_6^{(IJ)}(L,M)$, and $\mathbb{Q}_1(M=0)$, $\mathbb{Q}_1(M=\pm1)$, $\mathbb{Q}_2$, $\mathbb{Q}_3(M=0)$, and $\mathbb{Q}_3(M=\pm1)$ are connected with the second-order additive dispersion coefficient $C_8^{(IJ)}(L,M)$.

With the values in Table 3.1, we can obtain the long-range interaction coefficients for geometrical configurations specified by R_{12}, R_{23}, R_{31}, α, β, and γ as follows: Initially, we obtain the geometric parameters for the configuration under consideration by the method as described in Sec. 3.1.6. Then, the long-range interaction coefficients for that configuration are given by the Eqs. (3.13)-(3.28). In the following, we will discuss the long-range coefficients by explicitly evaluating the coefficients for the three elementary geometrical configurations of an equilateral triangle, an isosceles triangle,

and equally spaced co-linear atoms, representing, respectively, the symmetries D_{3h}, C_{2v}, and $D_{\infty h}$.

3.2.1 Dispersion Coefficients for An Equilateral Triangle

Using the coefficients a, b, c of the zeroth-order wave functions Eqs. (3.30)-(3.32), for the case where the three atoms form an equilateral triangle, the first-order additive coefficients are listed in Table 3.2 and the second-order additive and nonadditive dispersion coefficients are listed in Tables 3.3-3.4.

From Table 3.2, we can see that for the zeroth-order wave function $\Psi^{(0)}_{1,\Delta}$, $C_3^{(12)}(1, M = 0)$, $C_3^{(23)}(1, M = 0)$, and $C_3^{(31)}(1, M = 0)$ are all the same because of $a = b = c = 1/\sqrt{3}$; similarly $C_3^{(12)}(1, M = \pm 1)$, $C_3^{(23)}(1, M = \pm 1)$, and $C_3^{(31)}(1, M = \pm 1)$ are all the same. For the zeroth-order wave function $\Psi^{(0)}_{2,\Delta}$, $C_3^{(12)}(1, M)$ and $C_3^{(23)}(1, M)$, whenever $M = 0$ or $M = \pm 1$, are zero because of $b = 0$. For the zeroth-order wave function $\Psi^{(0)}_{3,\Delta}$, $C_3^{(12)}(1, M)$ and $C_3^{(23)}(1, M)$ are the same because of $a = c = 1/\sqrt{6}$. The coefficients between $M = 0$ and $M = \pm 1$ satisfy the relationship $C_3^{(IJ)}(1, M = 0) = -2C_3^{(IJ)}(1, M = \pm 1)$. Also listed in Table 3.2 are the values for ^{7}Li and ^{6}Li by taking the finite nuclear mass into consideration.

For the leading terms of the second-order long-range interaction, there exist both additive and nonadditive terms as shown in Table 3.3 for $C_6^{(IJ)}(1, M = 0)$, $C_6^{(IJ,JK)}(1, M = 0)$, $C_6^{(IJ)}(1, M = \pm 1)$, and $C_6^{(IJ,JK)}(1, M = \pm 1)$, for the Li($2\,^2S$)-Li($2\,^2S$)-Li($2\,^2P$) system. For the second zeroth-order wave function $\Psi^{(0)}_{2,\Delta}$, the nonadditive coefficients $C_6^{(23,31)}(1, M)$ and $C_6^{(31,12)}(1, M)$ are zero for $M = 0$ or $M = \pm 1$ because of $\mathbb{Q}_4(a, b, 1, M, \gamma) = 0$ and $b = 0$. For $\Psi^{(0)}_{2,\Delta}$ and $\Psi^{(0)}_{3,\Delta}$, we have $C_6^{(12)}(1, M) = C_6^{(23)}(1, M)$ and $C_6^{(23,31)}(1, M) = C_6^{(31,12)}(1, M)$ for $M = 0$ or $M = \pm 1$ due to $a = c$. The long-range dispersion coefficients $C_8^{(IJ)}(1, M)$ and $C_8^{(IJ,JK)}(1, M)$ are listed in Table 3.4 for the Li($2\,^2S$)-Li($2\,^2S$)-Li($2\,^2P$) system. These coefficients have very similar characteristic as $C_6^{(IJ)}(1, M)$ and $C_6^{(IJ,JK)}(1, M)$. For example, for fixed

Table 3.2: The additive long-range coefficients $C_3^{(IJ)}(1, M)$ of the Li($2\,^2S$)-Li($2\,^2S$)-Li($2\,^2P$) system for three different types of the zeroth-order wave functions, where the three atoms form an equilateral triangle, in atomic units. The numbers in parentheses represent the computational uncertainties.

Atom	State	$C_3^{(12)}(1, M=0)$	$C_3^{(23)}(1, M=0)$	$C_3^{(31)}(1, M=0)$	$C_3^{(12)}(1, M=\pm1)$	$C_3^{(23)}(1, M=\pm1)$	$C_3^{(31)}(1, M=\pm1)$
$^{\infty}$Li	$\Psi_{1,\Delta}^{(0)}$	−3.6667415(5)	−3.6667415(5)	−3.6667415(5)	1.8333702(3)	1.8333702(3)	1.8333702(3)
	$\Psi_{2,\Delta}^{(0)}$	0	0	5.500110(1)	0	0	−2.750054(1)
	$\Psi_{3,\Delta}^{(0)}$	3.6667415(5)	3.6667415(5)	−1.8333702(3)	−1.8333702(3)	−1.8333702(3)	0.9166850(2)
^{7}Li	$\Psi_{1,\Delta}^{(0)}$	−3.667284(1)	−3.667284(1)	−3.667284(1)	1.8336420(5)	1.8336420(5)	1.8336420(5)
	$\Psi_{2,\Delta}^{(0)}$	0	0	5.500925(2)	0	0	−2.750462(1)
	$\Psi_{3,\Delta}^{(0)}$	3.667284(1)	3.667284(1)	−1.8336420(5)	−1.8336420(5)	−1.8336420(5)	0.9168210(2)
^{6}Li	$\Psi_{1,\Delta}^{(0)}$	−3.667374(1)	−3.667374(1)	−3.667374(1)	1.833686(1)	1.833686(1)	1.833686(1)
	$\Psi_{2,\Delta}^{(0)}$	0	0	5.501062(1)	0	0	−2.750530(1)
	$\Psi_{3,\Delta}^{(0)}$	3.667374(1)	3.667374(1)	−1.833686(1)	−1.833686(1)	−1.833686(1)	0.9168437(2)

Table 3.3: The additive and nonadditive dispersion coefficients $C_6^{(IJ)}(1,M)$ and $C_6^{(IJ,JK)}(1,M)$ of the Li($2\,^2S$)-Li($2\,^2S$)-Li($2\,^2P$) system for three different types of the zeroth-order wave functions, where the three atoms form an equilateral triangle, in atomic units. The numbers in parentheses represent the computational uncertainties.

Atom	State	$C_6^{(12)}(1,M=0)$	$C_6^{(23)}(1,M=0)$	$C_6^{(31)}(1,M=0)$	$C_6^{(12,23)}(1,M=0)$	$C_6^{(23,31)}(1,M=0)$	$C_6^{(31,12)}(1,M=0)$
$^{\infty}$Li	$\Psi_{1,\Delta}^{(0)}$	1402.26(4)	1402.26(4)	1402.26(4)	157.059(5)	157.059(5)	157.059(5)
	$\Psi_{2,\Delta}^{(0)}$	1400.05(4)	1400.05(4)	1406.69(4)	−235.588(7)	0	0
	$\Psi_{3,\Delta}^{(0)}$	1404.46(3)	1404.46(3)	1397.85(5)	78.530(3)	−157.059(5)	−157.059(5)
^{7}Li	$\Psi_{1,\Delta}^{(0)}$	1402.77(4)	1402.77(4)	1402.77(4)	157.132(5)	157.132(5)	157.132(5)
	$\Psi_{2,\Delta}^{(0)}$	1400.59(4)	1400.59(4)	1407.14(4)	−235.697(7)	0	0
	$\Psi_{3,\Delta}^{(0)}$	1404.95(4)	1404.95(4)	1398.41(4)	78.565(2)	−157.132(5)	−157.132(5)
^{6}Li	$\Psi_{1,\Delta}^{(0)}$	1402.86(4)	1402.86(4)	1402.86(4)	157.144(5)	157.144(5)	157.144(5)
	$\Psi_{2,\Delta}^{(0)}$	1400.68(4)	1400.68(4)	1407.20(3)	−235.715(7)	0	0
	$\Psi_{3,\Delta}^{(0)}$	1405.02(3)	1405.02(3)	1398.50(4)	78.571(2)	−157.144(5)	−157.144(5)

Atom	State	$C_6^{(12)}(1,M=\pm1)$	$C_6^{(23)}(1,M=\pm1)$	$C_6^{(31)}(1,M=\pm1)$	$C_6^{(12,23)}(1,M=\pm1)$	$C_6^{(23,31)}(1,M=\pm1)$	$C_6^{(31,12)}(1,M=\pm1)$
$^{\infty}$Li	$\Psi_{1,\Delta}^{(0)}$	1625.18(5)	1625.18(5)	1625.18(5)	−137.426(4)	−137.426(4)	−137.426(4)
	$\Psi_{2,\Delta}^{(0)}$	1567.24(5)	1567.24(5)	1741.06(5)	206.141(7)	0	0
	$\Psi_{3,\Delta}^{(0)}$	1683.12(5)	1683.12(5)	1509.30(5)	−68.713(2)	137.426(4)	137.426(4)
^{7}Li	$\Psi_{1,\Delta}^{(0)}$	1625.74(4)	1625.74(4)	1625.74(4)	−137.490(4)	−137.490(4)	−137.490(4)
	$\Psi_{2,\Delta}^{(0)}$	1567.82(4)	1567.82(4)	1741.59(4)	206.235(6)	0	0
	$\Psi_{3,\Delta}^{(0)}$	1683.67(4)	1683.67(4)	1509.89(4)	−68.745(2)	137.490(4)	137.490(4)
^{6}Li	$\Psi_{1,\Delta}^{(0)}$	1625.84(4)	1625.84(4)	1625.84(4)	−137.500(4)	−137.500(4)	−137.500(4)
	$\Psi_{2,\Delta}^{(0)}$	1567.92(4)	1567.92(4)	1741.68(4)	206.252(7)	0	0
	$\Psi_{3,\Delta}^{(0)}$	1683.76(4)	1683.76(4)	1509.99(4)	−68.750(2)	137.500(4)	137.500(4)

Table 3.4: The additive and nonadditive dispersion coefficients $C_8^{(IJ)}(1,M)$ and $C_8^{(IJ,JK)}(1,M)$ of the Li($2\,^2S$)-Li($2\,^2S$)-Li($2\,^2P$) system for three different types of the zeroth-order wave functions, where the three atoms form an equilateral triangle, in atomic units. The numbers in parentheses represent the computational uncertainties.

Atom	State	$C_8^{(12)}(1,M=0)$	$C_8^{(23)}(1,M=0)$	$C_8^{(31)}(1,M=0)$	$C_8^{(12,23)}(1,M=0)$	$C_8^{(23,31)}(1,M=0)$	$C_8^{(31,12)}(1,M=0)$
$^\infty$Li	$\Psi_{1,\Delta}^{(0)}$	96505.6(9)	96505.6(9)	96505.6(9)	9858.985(6)	9858.985(6)	9858.985(6)
	$\Psi_{2,\Delta}^{(0)}$	79616.8(9)	79616.8(9)	48564.8(5)	−14788.47(1)	0	0
	$\Psi_{3,\Delta}^{(0)}$	58915.7(8)	58915.7(8)	89968(2)	4929.492(3)	−9858.985(6)	−9858.985(6)
^{7}Li	$\Psi_{1,\Delta}^{(0)}$	96519.5(9)	96519.5(9)	96519.5(9)	9861.200(6)	9861.200(6)	9861.200(6)
	$\Psi_{2,\Delta}^{(0)}$	79631.3(9)	79631.3(9)	48566.4(2)	−14791.80(1)	0	0
	$\Psi_{3,\Delta}^{(0)}$	58921.7(8)	58921.7(8)	89987(2)	4930.600(3)	−9861.200(6)	−9861.200(6)
^{6}Li	$\Psi_{1,\Delta}^{(0)}$	96521.8(9)	96521.8(9)	96521.8(9)	9861.567(5)	9861.567(5)	9861.567(5)
	$\Psi_{2,\Delta}^{(0)}$	79633.7(9)	79633.7(9)	48566.9(4)	−14792.35(1)	0	0
	$\Psi_{3,\Delta}^{(0)}$	58922.7(8)	58922.7(8)	89990(2)	4930.784(3)	−9861.567(5)	−9861.567(5)

Atom	State	$C_8^{(12)}(1,M=\pm1)$	$C_8^{(23)}(1,M=\pm1)$	$C_8^{(31)}(1,M=\pm1)$	$C_8^{(12,23)}(1,M=\pm1)$	$C_8^{(23,31)}(1,M=\pm1)$	$C_8^{(31,12)}(1,M=\pm1)$
$^\infty$Li	$\Psi_{1,\Delta}^{(0)}$	153520(4)	153520(4)	153520(4)	−26496.02(2)	−26496.02(2)	−26496.02(2)
	$\Psi_{2,\Delta}^{(0)}$	218790(4)	218790(4)	519731(4)	39744.04(3)	0	0
	$\Psi_{3,\Delta}^{(0)}$	419417(4)	419417(4)	118475(3)	−13248.01(1)	26496.02(2)	26496.02(2)
^{7}Li	$\Psi_{1,\Delta}^{(0)}$	153546(4)	153546(4)	153546(4)	−26501.97(2)	−26501.97(2)	−26501.97(2)
	$\Psi_{2,\Delta}^{(0)}$	218830(3)	218830(3)	519821(4)	39752.95(2)	0	0
	$\Psi_{3,\Delta}^{(0)}$	419491(4)	419491(4)	118500(3)	−13250.98(1)	26501.97(2)	26501.97(2)
^{6}Li	$\Psi_{1,\Delta}^{(0)}$	153549(3)	153549(3)	153549(3)	−26502.97(2)	−26502.97(2)	−26502.97(2)
	$\Psi_{2,\Delta}^{(0)}$	218838(4)	218838(4)	519838(5)	39754.44(2)	0	0
	$\Psi_{3,\Delta}^{(0)}$	419504(4)	419504(4)	118504(3)	−13251.48(1)	26502.97(2)	26502.97(2)

Table 3.5: The total long-range interaction coefficients of the Li($2\,^2S$)-Li($2\,^2S$)-Li($2\,^2P$) system for three different types of the zeroth-order wave functions, where the three atoms form an equilateral triangle, in atomic units. The numbers in parentheses represent the computational uncertainties.

Atom	State	$C_3(1, M = 0)$	$C_3(1, M = \pm 1)$	$C_6(1, M = 0)$	$C_6(1, M = \pm 1)$	$C_8(1, M = 0)$	$C_8(1, M = \pm 1)$
$^{\infty}$Li	$\Psi^{(0)}_{1,\Delta}$	−11.0002245(15)	5.5001106(9)	4677.957(135)	4463.262(162)	319093.8(27)	381071(12)
	$\Psi^{(0)}_{2,\Delta}$	5.500110(1)	−2.750054(1)	3971.202(127)	5081.681(157)	193009.9(23)	997055(12)
	$\Psi^{(0)}_{3,\Delta}$	5.5001128(13)	−2.7500554(8)	3971.182(123)	5081.679(160)	193010.9(18)	997053(11)

M, $C_8^{(IJ)}(1,M)$ are all the same for the zeroth-order wave function $\Psi_{1,\Delta}^{(0)}$; similarly for $C_8^{(IJ,JK)}(1,M)$, they are all the same for $\Psi_{1,\Delta}^{(0)}$. For $\Psi_{2,\Delta}^{(0)}$, $C_8^{(23,31)}(1,M)$ and $C_8^{(31,12)}(1,M)$ are zero because $\mathbb{Q}_4(a,b,2,M,\gamma)=0$ and $b=0$. We also have $C_8^{(12)}(1,M) = C_8^{(23)}(1,M)$ and $C_8^{(23,31)}(1,M) = C_8^{(31,12)}(1,M)$ for both $\Psi_{2,\Delta}^{(0)}$ and $\Psi_{3,\Delta}^{(0)}$.

From Tables 3.3-3.4, we can also see that the dispersion coefficients for the additive terms are always positive, but the dispersion coefficients for the nonadditive terms can be positive or negative. Furthermore, the absolute values of the non-zero nonadditive dispersion coefficients are less than the additive dispersion coefficients by one to two orders of the magnitude. However, the nonadditive terms may not be neglected in constructing an accurate potential surface for Li($2\,^2S$)-Li($2\,^2S$)-Li($2\,^2P$). For example, for the case of $\Psi_{2,\Delta}^{(0)}$, the ratio of $(\frac{C_8^{(12,23)}(1,M=\pm1)}{R_{12}^4 R_{23}^4})/(\frac{C_8^{(12)}(1,M=\pm1)}{R_{12}^8})$ IS 18%. The sums of $\Delta E^{(1)}$ and $\Delta E^{(2)}$, given by, respectively, Eqs. (3.13) and (3.17), for this configuration are listed in Table 3.5. Long-range potentials times R^3 for three different types of the zeroth-order wave functions are plotted in Figure 3.2. For each curve labeled by a wave function, the plotted curve is the sum of $\Delta E^{(1)}$ and $\Delta E^{(2)}$.

3.2.2 Dispersion Coefficients for An Isosceles Right Triangle

For the configuration of isosceles right triangle, the first-order additive coefficients are listed in Table 3.6 and the second-order additive and nonadditive dispersion coefficients are listed in Tables 3.7-3.8.

For this configuration, we have $b=c$ for the first two zeroth-order wave functions $\Psi_{1,\perp}^{(0)}$ and $\Psi_{2,\perp}^{(0)}$, and $b=-c$ and $a=0$ for the third zeroth-order wave function $\Psi_{3,\perp}^{(0)}$. We can clearly see that $C_3^{(12)}(1,M)$ equals $C_3^{(31)}(1,M)$ for $\Psi_{1,\perp}^{(0)}$ and $\Psi_{2,\perp}^{(0)}$, and $C_3^{(12)}(1,M) = C_3^{(31)}(1,M) = 0$ for $\Psi_{3,\perp}^{(0)}$, as shown in Table 3.6. Compared to the values in Table 3.2, we can conclude that a change in geometric configuration will influence the long-range coefficients.

Table 3.6: The additive long-range coefficients $C_3^{(IJ)}(1, M)$ of the Li($2\,^2S$)-Li($2\,^2S$)-Li($2\,^2P$) system for three different types of the zeroth-order wave functions, where the three atoms form an isosceles right triangle, in atomic units. The numbers in parentheses represent the computational uncertainties.

Atom	State	$C_3^{(12)}(1, M=0)$	$C_3^{(23)}(1, M=0)$	$C_3^{(31)}(1, M=0)$	$C_3^{(12)}(1, M=\pm1)$	$C_3^{(23)}(1, M=\pm1)$	$C_3^{(31)}(1, M=\pm1)$
$^{\infty}$Li	$\Psi_{1,\perp}^{(0)}$	−3.8591328(7)	−3.0911576(6)	−3.8591328(7)	1.9295663(4)	1.5455789(3)	1.9295663(4)
	$\Psi_{2,\perp}^{(0)}$	3.8591328(7)	−2.4089529(4)	3.8591328(7)	−1.9295663(4)	1.2044764(2)	−1.9295663(4)
	$\Psi_{3,\perp}^{(0)}$	0	5.500111(1)	0	0	−2.7500551(6)	0
^{7}Li	$\Psi_{1,\perp}^{(0)}$	−3.8597053(9)	−3.0916162(7)	−3.8597053(9)	1.9298527(4)	1.5458080(4)	1.9298527(4)
	$\Psi_{2,\perp}^{(0)}$	3.8597053(9)	−2.4093103(5)	3.8597053(9)	−1.9298527(4)	1.2046552(2)	−1.9298527(4)
	$\Psi_{3,\perp}^{(0)}$	0	5.500926(1)	0	0	−2.7504631(7)	0
^{6}Li	$\Psi_{1,\perp}^{(0)}$	−3.8598006(9)	−3.0916924(8)	−3.8598006(9)	1.9299002(5)	1.5458460(6)	1.9299002(5)
	$\Psi_{2,\perp}^{(0)}$	3.8598006(9)	−2.4093697(6)	3.8598006(9)	−1.9299002(5)	1.2046848(3)	−1.9299002(5)
	$\Psi_{3,\perp}^{(0)}$	0	5.501062(1)	0	0	−2.7505310(7)	0

Table 3.7: The additive and nonadditive dispersion coefficients $C_6^{(IJ)}(1,M)$ and $C_6^{(IJ,JK)}(1,M)$ of the Li($2\,^2S$)-Li($2\,^2S$)-Li($2\,^2P$) system for three different types of the zeroth-order wave functions, where the three atoms form an isosceles right triangle, in atomic units. The numbers in parentheses represent the computational uncertainties.

Atom	State	$C_6^{(12)}(1,M=0)$	$C_6^{(23)}(1,M=0)$	$C_6^{(31)}(1,M=0)$	$C_6^{(12,23)}(1,M=0)$	$C_6^{(23,31)}(1,M=0)$	$C_6^{(31,12)}(1,M=0)$
$^\infty$Li	$\Psi_{1,\perp}^{(0)}$	1402.96(4)	1400.87(4)	1402.96(4)	165.300(5)	165.300(5)	132.405(4)
	$\Psi_{2,\perp}^{(0)}$	1403.78(4)	1399.22(4)	1403.78(4)	−165.300(5)	−165.300(5)	103.183(3)
	$\Psi_{3,\perp}^{(0)}$	1400.05(4)	1406.69(4)	1400.05(4)	0	0	−235.588(7)
^{7}Li	$\Psi_{1,\perp}^{(0)}$	1403.46(4)	1401.40(4)	1403.46(4)	165.376(5)	165.376(5)	132.466(4)
	$\Psi_{2,\perp}^{(0)}$	1404.27(4)	1399.78(4)	1404.27(4)	−165.376(5)	−165.376(5)	103.231(3)
	$\Psi_{3,\perp}^{(0)}$	1400.59(4)	1407.14(4)	1400.59(4)	0	0	−235.697(7)
^{6}Li	$\Psi_{1,\perp}^{(0)}$	1403.54(4)	1401.49(4)	1403.54(4)	165.389(5)	165.389(5)	132.476(4)
	$\Psi_{2,\perp}^{(0)}$	1404.35(4)	1399.87(4)	1404.35(4)	−165.389(5)	−165.389(5)	103.239(3)
	$\Psi_{3,\perp}^{(0)}$	1400.68(4)	1407.20(3)	1400.68(4)	0	0	−235.715(7)

Atom	State	$C_6^{(12)}(1,M=\pm1)$	$C_6^{(23)}(1,M=\pm1)$	$C_6^{(31)}(1,M=\pm1)$	$C_6^{(12,23)}(1,M=\pm1)$	$C_6^{(23,31)}(1,M=\pm1)$	$C_6^{(31,12)}(1,M=\pm1)$
$^\infty$Li	$\Psi_{1,\perp}^{(0)}$	1643.37(5)	1588.80(5)	1643.37(5)	41.324(1)	41.324(1)	−264.810(8)
	$\Psi_{2,\perp}^{(0)}$	1664.93(5)	1545.68(5)	1664.93(5)	−41.324(1)	−41.324(1)	−206.367(6)
	$\Psi_{3,\perp}^{(0)}$	1567.24(5)	1741.06(5)	1567.24(5)	0	0	471.18(2)
^{7}Li	$\Psi_{1,\perp}^{(0)}$	1643.94(5)	1589.37(4)	1643.94(5)	41.344(2)	41.344(2)	−264.932(8)
	$\Psi_{2,\perp}^{(0)}$	1665.48(4)	1546.26(4)	1665.48(4)	−41.344(2)	−41.344(2)	−206.462(6)
	$\Psi_{3,\perp}^{(0)}$	1567.83(5)	1741.59(4)	1567.83(5)	0	0	471.40(2)
^{6}Li	$\Psi_{1,\perp}^{(0)}$	1644.02(4)	1589.48(5)	1644.02(4)	41.348(2)	41.348(2)	−264.954(9)
	$\Psi_{2,\perp}^{(0)}$	1665.59(5)	1546.36(4)	1665.59(5)	−41.348(2)	−41.348(2)	−206.478(6)
	$\Psi_{3,\perp}^{(0)}$	1567.93(5)	1741.68(4)	1567.93(5)	0	0	471.42(1)

Table 3.8: The additive and nonadditive dispersion coefficients $C_8^{(IJ)}(1,M)$ and $C_8^{(IJ,JK)}(1,M)$ of the Li($2\,^2S$)-Li($2\,^2S$)-Li($2\,^2P$) system for three different types of the zeroth-order wave functions, where the three atoms form an isosceles right triangle, in atomic units. The numbers in parentheses represent the computational uncertainties.

Atom	State	$C_8^{(12)}(1,M=0)$	$C_8^{(23)}(1,M=0)$	$C_8^{(31)}(1,M=0)$	$C_8^{(12,23)}(1,M=0)$	$C_8^{(23,31)}(1,M=0)$	$C_8^{(31,12)}(1,M=0)$
$^{\infty}$Li	$\Psi_{1,\perp}^{(0)}$	97059.4(9)	94454(2)	97059.4(9)	14674.28(1)	14674.28(1)	0
	$\Psi_{2,\perp}^{(0)}$	58361.9(9)	92021(2)	58361.9(9)	−14674.28(1)	−14674.28(1)	0
	$\Psi_{3,\perp}^{(0)}$	79617(2)	48564.8(5)	79617(2)	0	0	0
^{7}Li	$\Psi_{1,\perp}^{(0)}$	97072(1)	94468(1)	97072(1)	14677.57(1)	14677.57(1)	0
	$\Psi_{2,\perp}^{(0)}$	58368.8(9)	92038(2)	58368.8(9)	−14677.57(1)	−14677.57(1)	0
	$\Psi_{3,\perp}^{(0)}$	79631(1)	48566.7(5)	79631(1)	0	0	0
^{6}Li	$\Psi_{1,\perp}^{(0)}$	97074(1)	94472(2)	97074(1)	14678.12(1)	14678.12(1)	0
	$\Psi_{2,\perp}^{(0)}$	58370(1)	92041(2)	58370(1)	−14678.12(1)	−14678.12(1)	0
	$\Psi_{3,\perp}^{(0)}$	79633(1)	48567.0(5)	79633(1)	0	0	0

Atom	State	$C_8^{(12)}(1,M=\pm1)$	$C_8^{(23)}(1,M=\pm1)$	$C_8^{(31)}(1,M=\pm1)$	$C_8^{(12,23)}(1,M=\pm1)$	$C_8^{(23,31)}(1,M=\pm1)$	$C_8^{(31,12)}(1,M=\pm1)$
$^{\infty}$Li	$\Psi_{1,\perp}^{(0)}$	161893(4)	142518(4)	161893(4)	−16508.56(1)	−16508.56(1)	0
	$\Psi_{2,\perp}^{(0)}$	411044(4)	129477(3)	411044(4)	16508.56(1)	16508.56(1)	0
	$\Psi_{3,\perp}^{(0)}$	218790(4)	519731(4)	218790(4)	0	0	0
^{7}Li	$\Psi_{1,\perp}^{(0)}$	161920(4)	142544(4)	161920(4)	−16512.27(1)	−16512.27(1)	0
	$\Psi_{2,\perp}^{(0)}$	411116(3)	129502(3)	411116(3)	16512.27(1)	16512.27(1)	0
	$\Psi_{3,\perp}^{(0)}$	218830(3)	519821(4)	218830(3)	0	0	0
^{6}Li	$\Psi_{1,\perp}^{(0)}$	161924(4)	142548(4)	161924(4)	−16512.89(1)	−16512.89(1)	0
	$\Psi_{2,\perp}^{(0)}$	411130(4)	129506(3)	411130(4)	16512.89(1)	16512.89(1)	0
	$\Psi_{3,\perp}^{(0)}$	218838(4)	519838(5)	218838(4)	0	0	0

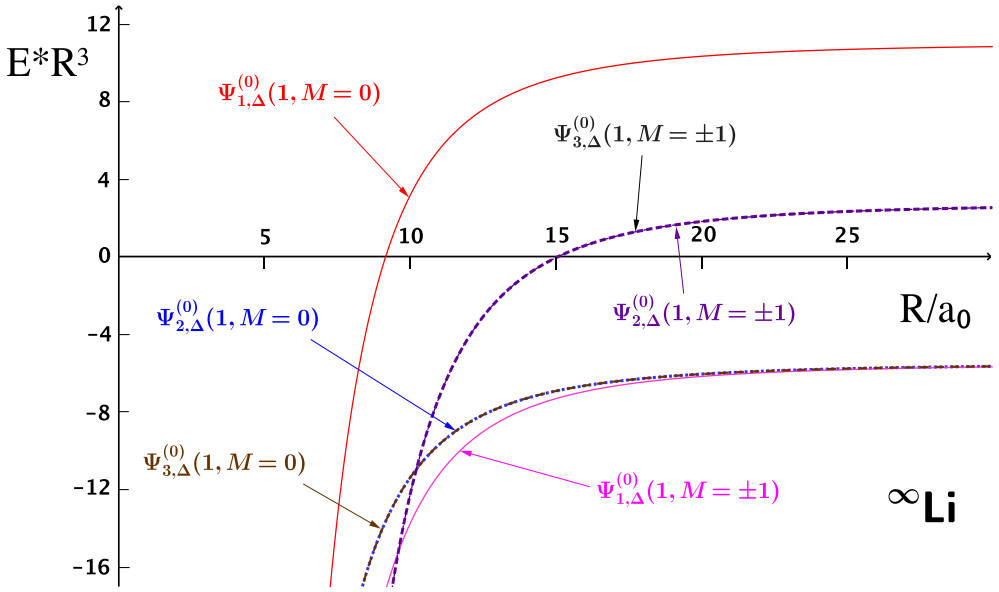

Figure 3.2: Long-range potentials times R^3 for the Li($2\,^2S$)-Li($2\,^2S$)-Li($2\,^2P$) system for three different types of the zeroth-order wave functions, where the three atoms form an equilateral triangle, in atomic units. For each curve labeled by a wave function, the plotted curve is the sum of $\Delta E^{(1)}$ and $\Delta E^{(2)}$.

The second-order dispersion coefficients $C_6^{(IJ)}$, $C_6^{(IJ,JK)}$, $C_8^{(IJ)}$, and $C_8^{(IJ,JK)}$ are listed in Tables 3.7-3.8. One can see that $C_6^{(12)}(1, M) = C_6^{(31)}(1, M)$, $C_6^{(12,23)}(1, M) = C_6^{(23,31)}(1, M)$, $C_8^{(12)}(1, M) = C_8^{(31)}(1, M)$, and $C_8^{(12,23)}(1, M) = C_8^{(23,31)}(1, M)$ due to $b = \pm c$, $a = 0$, and $\beta = \gamma$. Also $C_8^{(31,12)}(1, M) = 0$, $C_6^{(31,12)}(1, M) \neq 0$; this is because $\alpha = \pi/2$ and the odd or even nature of $M_t - M$ in Eq. (3.28). In Tables 3.7-3.8, we also find that the finite nuclear mass increases the additive dispersion coefficients. Similarly, the nonadditive terms may not be neglected in constructing a three-body potential surface for Li($2\,^2S$)-Li($2\,^2S$)-Li($2\,^2P$). Long-range potentials times R^3 for three different types of the zeroth-order wave functions are plotted in Figure 3.3. For each curve labeled by a wave function, the plotted curve is the sum of $\Delta E^{(1)}$ and $\Delta E^{(2)}$.

Table 3.9: The additive long-range coefficients $C_3^{(IJ)}(1, M)$ of the Li($2\,^2S$)-Li($2\,^2S$)-Li($2\,^2P$) system for three different types of the zeroth-order wave functions, where the three atoms form a straight line, in atomic units. The numbers in parentheses represent the computational uncertainties.

Atom	State	$C_3^{(12)}(1, M=0)$	$C_3^{(23)}(1, M=0)$	$C_3^{(31)}(1, M=0)$	$C_3^{(12)}(1, M=\pm1)$	$C_3^{(23)}(1, M=\pm1)$	$C_3^{(31)}(1, M=\pm1)$
$^{\infty}$Li	$\Psi_{1,-}^{(0)}$	−3.8853730(7)	−2.8714730(6)	−3.8853730(7)	1.9426864(4)	1.4357365(3)	1.9426864(4)
	$\Psi_{2,-}^{(0)}$	3.8853730(7)	−2.6286373(5)	3.8853730(7)	−1.9426864(4)	1.3143187(2)	−1.9426864(4)
	$\Psi_{3,-}^{(0)}$	0	5.500111(1)	0	0	−2.7500551(6)	0
^{7}Li	$\Psi_{1,-}^{(0)}$	−3.885949(1)	−2.8718991(7)	−3.885949(1)	1.9429746(5)	1.4359496(3)	1.9429746(5)
	$\Psi_{2,-}^{(0)}$	3.885949(1)	−2.6290273(6)	3.885949(1)	−1.9429746(5)	1.3145136(3)	−1.9429746(5)
	$\Psi_{3,-}^{(0)}$	0	5.500926(1)	0	0	−2.7504631(7)	0
^{6}Li	$\Psi_{1,-}^{(0)}$	−3.886045(1)	−2.8719700(7)	−3.886045(1)	1.9430227(4)	1.4359849(4)	1.9430227(4)
	$\Psi_{2,-}^{(0)}$	3.886045(1)	−2.6290922(6)	3.886045(1)	−1.9430227(4)	1.3145461(3)	−1.9430227(4)
	$\Psi_{3,-}^{(0)}$	0	5.501062(1)	0	0	−2.7505310(7)	0

Table 3.10: The additive and nonadditive dispersion coefficients $C_6^{(IJ)}(1,M)$ and $C_6^{(IJ,JK)}(1,M)$ of the Li($2\,^2S$)-Li($2\,^2S$)-Li($2\,^2P$) system for three different types of the zeroth-order wave functions, where the three atoms form a straight line, in atomic units. The numbers in parentheses represent the computational uncertainties.

Atom	State	$C_6^{(12)}(1,M=0)$	$C_6^{(23)}(1,M=0)$	$C_6^{(31)}(1,M=0)$	$C_6^{(12,23)}(1,M=0)$	$C_6^{(23,31)}(1,M=0)$	$C_6^{(31,12)}(1,M=0)$
$^\infty$Li	$\Psi_{1,-}^{(0)}$	1403.22(4)	1400.34(4)	1403.22(4)	166.425(6)	166.425(6)	122.995(4)
	$\Psi_{2,-}^{(0)}$	1403.50(3)	1399.76(4)	1403.50(3)	−166.425(6)	−166.425(6)	112.594(4)
	$\Psi_{3,-}^{(0)}$	1400.05(4)	1406.69(4)	1400.05(4)	0	0	−235.588(7)
^{7}Li	$\Psi_{1,-}^{(0)}$	1403.72(4)	1400.88(4)	1403.72(4)	166.502(6)	166.502(6)	123.052(4)
	$\Psi_{2,-}^{(0)}$	1404.01(4)	1400.30(4)	1404.01(4)	−166.502(6)	−166.502(6)	112.646(4)
	$\Psi_{3,-}^{(0)}$	1400.59(4)	1407.14(4)	1400.59(4)	0	0	−235.697(7)
^{6}Li	$\Psi_{1,-}^{(0)}$	1403.80(4)	1400.97(4)	1403.80(4)	166.513(5)	166.513(5)	123.060(3)
	$\Psi_{2,-}^{(0)}$	1404.09(4)	1400.39(4)	1404.09(4)	−166.513(5)	−166.513(5)	112.655(4)
	$\Psi_{3,-}^{(0)}$	1400.68(4)	1407.20(3)	1400.68(4)	0	0	−235.715(7)

Atom	State	$C_6^{(12)}(1,M=\pm1)$	$C_6^{(23)}(1,M=\pm1)$	$C_6^{(31)}(1,M=\pm1)$	$C_6^{(12,23)}(1,M=\pm1)$	$C_6^{(23,31)}(1,M=\pm1)$	$C_6^{(31,12)}(1,M=\pm1)$
$^\infty$Li	$\Psi_{1,-}^{(0)}$	1650.30(4)	1574.90(4)	1650.30(4)	416.06(2)	416.06(2)	307.487(9)
	$\Psi_{2,-}^{(0)}$	1657.99(5)	1559.55(4)	1657.99(5)	−416.06(2)	−416.06(2)	281.483(8)
	$\Psi_{3,-}^{(0)}$	1567.24(5)	1741.06(5)	1567.24(5)	0	0	−588.97(2)
^{7}Li	$\Psi_{1,-}^{(0)}$	1650.88(5)	1575.49(4)	1650.88(5)	416.25(1)	416.25(1)	307.63(1)
	$\Psi_{2,-}^{(0)}$	1658.54(4)	1560.16(5)	1658.54(4)	−416.25(1)	−416.25(1)	281.615(9)
	$\Psi_{3,-}^{(0)}$	1567.83(5)	1741.59(4)	1567.83(5)	0	0	−589.24(2)
^{6}Li	$\Psi_{1,-}^{(0)}$	1650.96(4)	1575.60(5)	1650.96(4)	416.29(2)	416.29(2)	307.653(9)
	$\Psi_{2,-}^{(0)}$	1658.65(5)	1560.24(4)	1658.65(5)	−416.29(2)	−416.29(2)	281.636(9)
	$\Psi_{3,-}^{(0)}$	1567.93(5)	1741.68(4)	1567.93(5)	0	0	−589.29(2)

Table 3.11: The additive and nonadditive dispersion coefficients $C_8^{(IJ)}(1,M)$ and $C_8^{(IJ,JK)}(1,M)$ of the Li($2\,^2S$)-Li($2\,^2S$)-Li($2\,^2P$) system for three different types of the zeroth-order wave functions, where the three atoms form a straight line, in atomic units. The numbers in parentheses represent the computational uncertainties.

Atom	State	$C_8^{(12)}(1,M=0)$	$C_8^{(23)}(1,M=0)$	$C_8^{(31)}(1,M=0)$	$C_8^{(12,23)}(1,M=0)$	$C_8^{(23,31)}(1,M=0)$	$C_8^{(31,12)}(1,M=0)$
$^\infty$Li	$\Psi_{1,-}^{(0)}$	97037.1(9)	93669(1)	97037.1(9)	20893.68(2)	20893.68(2)	−15441.40(1)
	$\Psi_{2,-}^{(0)}$	58384.2(9)	92803(1)	58384.2(9)	−20893.68(2)	−20893.68(2)	−14135.55(1)
	$\Psi_{3,-}^{(0)}$	79617(1)	48564.8(5)	79617(1)	0	0	29576.95(2)
^{7}Li	$\Psi_{1,-}^{(0)}$	97049.9(9)	93685(1)	97049.9(9)	20898.36(1)	20898.36(1)	−15444.87(1)
	$\Psi_{2,-}^{(0)}$	58391.4(9)	92821(2)	58391.4(9)	−20898.36(1)	−20898.36(1)	−14138.73(2)
	$\Psi_{3,-}^{(0)}$	79631(1)	48566.7(5)	79631(1)	0	0	29583.60(2)
^{6}Li	$\Psi_{1,-}^{(0)}$	97052(1)	93689(2)	97052(1)	20899.14(1)	20899.14(1)	−15445.45(1)
	$\Psi_{2,-}^{(0)}$	58392.6(9)	92822(1)	58392.6(9)	−20899.14(1)	−20899.14(1)	−14139.26(2)
	$\Psi_{3,-}^{(0)}$	79633(1)	48567.0(5)	79633(1)	0	0	29584.70(2)

Atom	State	$C_8^{(12)}(1,M=\pm1)$	$C_8^{(23)}(1,M=\pm1)$	$C_8^{(31)}(1,M=\pm1)$	$C_8^{(12,23)}(1,M=\pm1)$	$C_8^{(23,31)}(1,M=\pm1)$	$C_8^{(31,12)}(1,M=\pm1)$
$^\infty$Li	$\Psi_{1,-}^{(0)}$	166509(4)	138319(4)	166509(4)	41787.35(3)	41787.35(3)	−30882.81(2)
	$\Psi_{2,-}^{(0)}$	406428(4)	133676(3)	406428(4)	−41787.35(3)	−41787.35(3)	−28271.10(2)
	$\Psi_{3,-}^{(0)}$	218790(4)	519731(4)	218790(4)	0	0	59153.90(3)
^{7}Li	$\Psi_{1,-}^{(0)}$	166537(4)	138343(3)	166537(4)	41796.72(2)	41796.72(2)	−30889.75(2)
	$\Psi_{2,-}^{(0)}$	406499(3)	133701(3)	406499(3)	−41796.72(2)	−41796.72(2)	−28277.45(2)
	$\Psi_{3,-}^{(0)}$	218830(3)	519821(4)	218830(3)	0	0	59167.19(3)
^{6}Li	$\Psi_{1,-}^{(0)}$	166540(3)	138347(3)	166540(3)	41798.29(2)	41798.29(2)	−30890.90(2)
	$\Psi_{2,-}^{(0)}$	406513(4)	133707(4)	406513(4)	−41798.29(2)	−41798.29(2)	−28278.51(2)
	$\Psi_{3,-}^{(0)}$	218838(4)	519838(5)	218838(4)	0	0	59169.40(3)

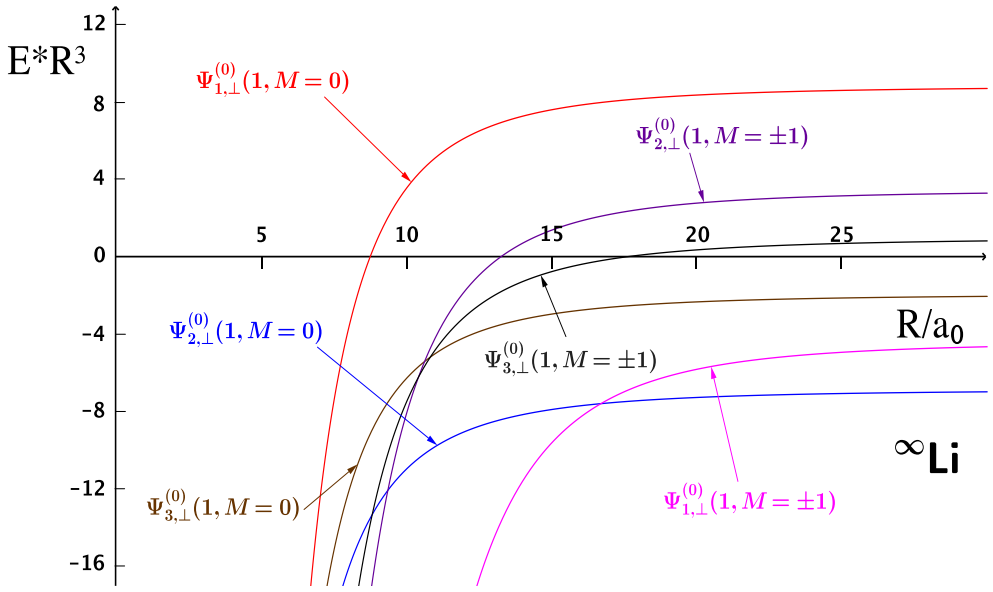

Figure 3.3: Long-range potentials times R^3 for the Li($2\,^2S$)-Li($2\,^2S$)-Li($2\,^2P$) system for three different types of the zeroth-order wave functions, where the three atoms form an isosceles right triangle, in atomic units. For each curve labeled by a wave function, the plotted curve is the sum of $\Delta E^{(1)}$ and $\Delta E^{(2)}$.

3.2.3 Dispersion Coefficients for a Linear Configuration

For the configuration of three atoms forming a straight line, the long-range dispersion coefficients are listed in Tables 3.9-3.11. Since the zeroth-order wave function coefficients have $b = c$ in Eqs. (3.38) and (3.39), and $a = 0$ and $b = -c$ in Eq. (3.40), which are similar to the isosceles right triangle, the dispersion coefficients have similar characteristic to the case of the isosceles right triangle. The only differences are the values of three interior angles: $\beta = \gamma = 0$ and $\alpha = 2\pi$, which leads to the relatively larger nonzero dispersion coefficients $C_8^{(31,12)}(1, M = 0)$ and $C_8^{(31,12)}(1, M = \pm 1)$. Long-range potentials times R^3 for three different types of the zeroth-order wave functions are plotted in Figure 3.4. For each curve labeled by a wave function, the plotted curve is the sum of $\Delta E^{(1)}$ and $\Delta E^{(2)}$.

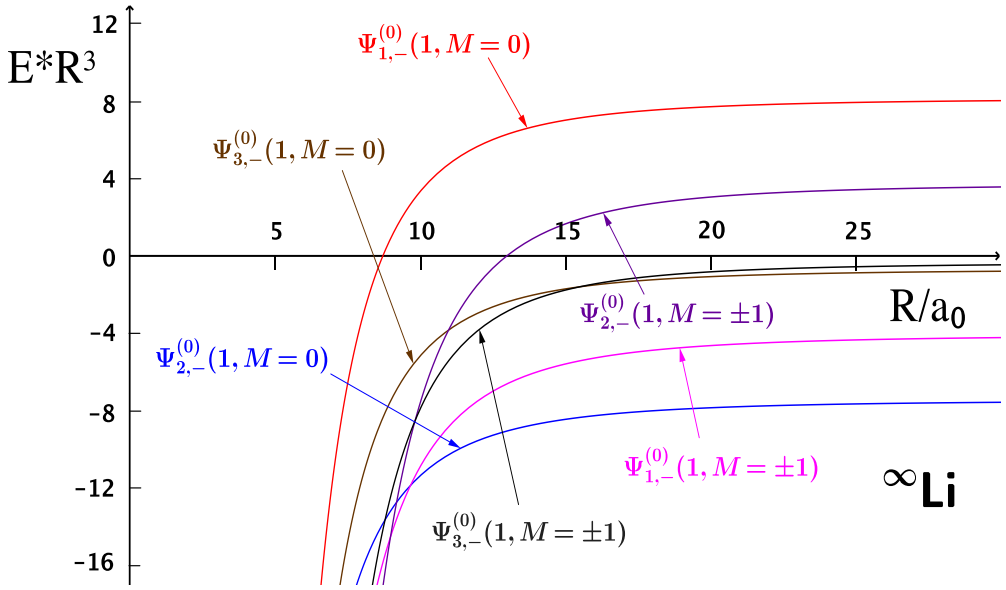

Figure 3.4: Long-range potentials times R^3 for the Li($2\,^2S$)-Li($2\,^2S$)-Li($2\,^2P$) system for three different types of the zeroth-order wave functions, where the three atoms form a straight line, in atomic units. For each curve labeled by a wave function, the plotted curve is the sum of $\Delta E^{(1)}$ and $\Delta E^{(2)}$.

Chapter 4

Calculations of Long-Range Three-Body Interactions for He($n_0\,^\lambda S$)-He($n_0\,^\lambda S$)-He($n_0'\,^\lambda L$)

4.1 Theoretical Formulation for He($1\,^1S$)-He($1\,^1S$)-He($2\,^1S$)

In Chapter 3 and Appendix A, we have given the general formulas for the Li($2\,^2S$)-Li($2\,^2S$)-Li($2\,^2P$) system, which are also applicable to the He($n_0\,^\lambda S$)-He($n_0\,^\lambda S$)-He($n_0'\,^\lambda P$) system. In this section, however, we will focus on the He($n_0\,^\lambda S$)-He($n_0\,^\lambda S$)-He($n_0'\,^\lambda S$) system.

4.1.1 The Zeroth-Order Wave Function

According to the degenerate perturbation theory, the zero-order wave function of the unperturbed system can also be written as

$$|\Psi^{(0)}\rangle = a|\phi_1\rangle + b|\phi_2\rangle + c|\phi_3\rangle\,, \tag{4.1}$$

where ϕ_1, ϕ_2, ϕ_3 are three orthonormalized eigenfunctions corresponding to the same energy eigenvalue $E^{(0)}_{n_0 n_0 n_0'} = 2E^{(0)}_{n_0 S} + E^{(0)}_{n_0' S}$

$$|\phi_1\rangle = |\varphi_{n_0'}(0;\boldsymbol{\sigma})\varphi_{n_0}(0;\boldsymbol{\rho})\varphi_{n_0}(0;\boldsymbol{\varsigma})\rangle\,, \tag{4.2}$$

$$|\phi_2\rangle = |\varphi_{n_0}(0;\boldsymbol{\sigma})\varphi_{n_0'}(0;\boldsymbol{\rho})\varphi_{n_0}(0;\boldsymbol{\varsigma})\rangle\,, \tag{4.3}$$

$$|\phi_3\rangle = |\varphi_{n_0}(0;\boldsymbol{\sigma})\varphi_{n_0}(0;\boldsymbol{\rho})\varphi_{n_0'}(0;\boldsymbol{\varsigma})\rangle\,. \tag{4.4}$$

The expansion coefficients a, b, and c are determined by diagonalizing the perturbation in the basis set $\{\phi_1, \phi_2, \phi_3\}$, which depends on the geometrical configuration formed by the three atoms. The expansions of V_{IJ} are shown in Eqs. (3.4)-(3.7).

4.1.2 The Second-Order Energy

For the He($1\,^1S$)-He($1\,^1S$)-He($2\,^1S$) system, the first-order energy corrections are zero. The leading terms start from the second-order, which can be written as

$$\begin{aligned}\Delta E^{(2)} &= -\sum_{n_s n_t n_u}\sum_{L_s L_t L_u}\sum_{M_s M_t M_u}\frac{|\langle\Psi^{(0)}|V_{123}|\chi_{n_s}(L_s M_s;\boldsymbol{\sigma})\chi_{n_t}(L_t M_t;\boldsymbol{\rho})\chi_{n_u}(L_u M_u;\boldsymbol{\varsigma})\rangle|^2}{E_{n_s L_s;n_t L_t;n_u L_u} - E^{(0)}_{n_0 S;n_0 S;n_0' S}} \\ &= -\sum_{n\geq 3}\left(\frac{C^{(12)}_{2n}}{R^{2n}_{12}} + \frac{C^{(23)}_{2n}}{R^{2n}_{23}} + \frac{C^{(31)}_{2n}}{R^{2n}_{31}}\right), \end{aligned} \tag{4.5}$$

where $\chi_{n_s}(L_s M_s;\boldsymbol{\sigma})\chi_{n_t}(L_t M_t;\boldsymbol{\rho})\chi_{n_u}(L_u M_u;\boldsymbol{\varsigma})$ are the intermediate states of the system with the energy eigenvalues $E_{n_s L_s;n_t L_t;n_u L_u} = E_{n_s L_s} + E_{n_t L_t} + E_{n_u L_u}$. It is noted that the above summations should exclude terms with $E_{n_s L_s;n_t L_t;n_u L_u} = E^{(0)}_{n_0 S;n_0 S;n_0' S}$. The coefficients $C^{(12)}_{2n}$, $C^{(23)}_{2n}$ and $C^{(31)}_{2n}$ are the additive dispersion coefficients. In this work, we are only concerned with $n = 3$ and 4 in Eq. (4.5), with the corresponding dispersion coefficients being

$$C^{(IJ)}_6 = (|A_I|^2 + |A_J|^2)\mathbb{T}_1 + |A_K|^2\mathbb{T}_2 + (A^*_I A_J + A^*_J A_I)\mathbb{T}_3\,, \tag{4.6}$$

$$C_8^{(IJ)} = (|A_I|^2 + |A_J|^2)\mathbb{R}_1 + |A_K|^2\mathbb{R}_2 + (A_I^* A_J + A_J^* A_I)\mathbb{R}_3\,, \tag{4.7}$$

$$A_1 = a, A_2 = b, A_3 = c\,, \tag{4.8}$$

where a, b, and c are defined in Eq. (4.1). The other terms in Eqs. (4.6) and (4.7) are given by

$$\mathbb{T}_1 = \sum_{n_s n_t} K_1(n_s, n_t, 1, 1) \tag{4.9}$$

$$\mathbb{T}_2 = \sum_{n_s n_t} K_2(n_s, n_t, 1, 1) \tag{4.10}$$

$$\mathbb{T}_3 = \sum_{n_s n_t} K_3(n_s, n_t, 1, 1) \tag{4.11}$$

$$\mathbb{R}_1 = \sum_{n_s n_t} [K_1(n_s, n_t, 1, 2) + K_1(n_s, n_t, 2, 1)] \tag{4.12}$$

$$\mathbb{R}_2 = \sum_{n_s n_t} [K_2(n_s, n_t, 1, 2) + K_2(n_s, n_t, 2, 1)] \tag{4.13}$$

$$\mathbb{R}_3 = \sum_{n_s n_t} [K_3(n_s, n_t, 1, 2) + K_3(n_s, n_t, 2, 1)] \tag{4.14}$$

The K_i-Functions are defined by Eqs. (B.16)-(B.18) in Appendix B.

The formulas for the He($n_0\,^\lambda S$)-He($n_0\,^\lambda S$)-He($n_0'\,^\lambda P$) system are the same as those for the Li($2\,^2S$)-Li($2\,^2S$)-Li($2\,^2P$) system, which have been shown in Sections 3.1.4 and 3.1.5 of Chapter 3.

4.1.3 The Interaction Constants

Now, let us reconsider the formulas of additive dispersion coefficients that are shown in Eqs. (4.6), (4.7), (3.14), (3.18), and (3.19). Since these coefficients do not contain the interior angles α, β, γ, we can easily separate them into the geometric parameters a, b, and c multiplying the geometrical-configuration independent interaction *constants* $\mathbb{T}_1$, $\mathbb{T}_2$, $\mathbb{T}_3$, $\mathbb{R}_1$, $\mathbb{R}_2$, $\mathbb{R}_3$, $\mathbb{D}_0(M=0)$, $\mathbb{D}_0(M=\pm1)$, $\mathbb{D}_1(M=0)$, $\mathbb{D}_1(M=\pm1)$, $\mathbb{D}_2$, $\mathbb{Q}_1(M=0)$, $\mathbb{Q}_1(M=\pm1)$, $\mathbb{Q}_2$, $\mathbb{Q}_3(M=0)$, and $\mathbb{Q}_3(M=\pm1)$. For the He($1\,^1S$)-He($1\,^1S$)-He($2\,^1S$) system, $\mathbb{T}_1$, $\mathbb{T}_2$, $\mathbb{T}_3$ are connected to the second-order additive dispersion coefficient $C_6^{(IJ)}$. $\mathbb{R}_1$, $\mathbb{R}_2$, $\mathbb{R}_3$ are connected to the second-order additive dispersion coefficient $C_8^{(IJ)}$. For the He($n_0\,^\lambda S$)-He($n_0\,^\lambda S$)-He($n_0'\,^\lambda P$) system, $\mathbb{D}_0(M=0)$ and $\mathbb{D}_0(M=\pm1)$ are connected to the first-order additive coefficient $C_3^{(IJ)}(L,M)$. $\mathbb{D}_1(M=0)$, $\mathbb{D}_1(M=\pm1)$, and $\mathbb{D}_2$ are connected to the second-order additive dispersion coefficient $C_6^{(IJ)}(L,M)$, and $\mathbb{Q}_1(M=0)$, $\mathbb{Q}_1(M=\pm1)$, $\mathbb{Q}_2$, $\mathbb{Q}_3(M=0)$, and $\mathbb{Q}_3(M=\pm1)$ are connected to the second-order additive dispersion coefficient $C_8^{(IJ)}(L,M)$. The values of these interaction constants for two helium isotopes are listed in Tables 4.1 and 4.2, respectively. As shown in Eqs. (3.20) and (3.21), the nonadditive interaction coefficients are inseparable, because they contain both the expansion coefficients a, b, c and the interior angles α, β, γ.

4.1.4 The Connection With Other Studies

Actually, with these interaction constants, we can easily find the connection between this work and previous studies of long-range interactions for two-body system. For example, If we set $a=\frac{1}{\sqrt{2}}$, $b=\pm\frac{1}{\sqrt{2}}$, $c=0$, our expressions describe the long-range interactions for the two-body $n_0S-n_0'L$ system. For the He($n_0\,^\lambda S$)-He($n_0\,^\lambda S$)-He($n_0'\,^\lambda P$) system, the first-order dispersion interaction coefficient $C_3(M)=\mathbb{D}_0(M)$, and the second-order dispersion coefficients $C_6(M)=\mathbb{D}_1(M)$ and $C_8(M)=\mathbb{Q}_1(M)+\mathbb{Q}_3(M)$. Similarly, If we set $a=b=0$, $c=1$, our expressions describe the long-range

Table 4.1: Values of $\mathbb{T}_1$, $\mathbb{T}_2$, $\mathbb{T}_3$, $\mathbb{R}_1$, $\mathbb{R}_2$, $\mathbb{R}_3$ for the He($1\,^1S$)-He($1\,^1S$)-He($2\,^1S$) system, in atomic units. All these quantities are independent of the geometrical configuration formed by the three atoms. The numbers in parentheses represent the computational uncertainties.

Atom	$\mathbb{T}_1$	$\mathbb{T}_2$	$\mathbb{T}_3$	$\mathbb{R}_1$	$\mathbb{R}_2$	$\mathbb{R}_3$
$^{\infty}$He	41.8413161(1)	1.4609778377(1)	2.90911603(1)	3310.4418(1)	14.11785735(1)	96.090681(2)
^{4}He	41.8723173(1)	1.4621228531(1)	2.91128666(1)	3312.0535(1)	14.12578804(1)	96.141508(2)
^{3}He	41.8824647(1)	1.4624976699(1)	2.91199719(1)	3312.5809(1)	14.12838381(1)	96.158143(2)

Table 4.2: Values of $\mathbb{D}_0(M=0)$, $\mathbb{D}_0(M=\pm1)$, $\mathbb{D}_1(M=0)$, $\mathbb{D}_1(M=\pm1)$, $\mathbb{D}_2$, $\mathbb{Q}_1(M=0)$, $\mathbb{Q}_1(M=\pm1)$, $\mathbb{Q}_2$, $\mathbb{Q}_3(M=0)$, and $\mathbb{Q}_3(M=\pm1)$ for the He($n_0\,^\lambda S$)-He($n_0\,^\lambda S$)-He($n_0'\,^\lambda P$) system, in atomic units. All these quantities are independent of the geometrical configuration formed by the three atoms. The numbers in parentheses represent the computational uncertainties.

Atom	$\mathbb{D}_0(M=0)$ $\mathbb{Q}_1(M=0)$	$\mathbb{D}_0(M=\pm1)$ $\mathbb{Q}_1(M=\pm1)$	$\mathbb{D}_1(M=0)$ $\mathbb{Q}_2$	$\mathbb{D}_1(M=\pm1)$ $\mathbb{Q}_3(M=0)$	$\mathbb{D}_2$ $\mathbb{Q}_3(M=\pm1)$
		He($1\,^1S$)-He($1\,^1S$)-He($2\,^1P$)			
$^\infty$He	−0.17705560274(4) 377.01369(9)	0.08852780137(2) 5123.8556(1)	32.6430764067(3) 14.1178573524(3)	45.7581833555(1) 19.5357464(2)	1.46097783774(1) −78.9244427(5)
^{4}He	−0.17707653057(4) 376.95084(9)	0.08853826528(2) 5127.4835(1)	32.6709827359(1) 14.12578804150(1)	45.797120320(1) 19.5451867(2)	1.46212285318930(3) −78.9606567(6)
^{3}He	−0.17708338005(4) 376.9301(1)	0.08854169002(2) 5128.6709(1)	32.6801176662(2) 14.1283838158(2)	45.8098660234(2) 19.5482763(2)	1.46249766997352(3) −78.9725084(6)
		He($2\,^1S$)-He($2\,^1S$)-He($2\,^1P$)			
$^\infty$He	−8.504834302621(5) 456379(2)	4.252417151311(3) 1547973(4)	4068.2(1) 817250.251(2)	4849.0(2) 36573.750187(6)	11241.0468363(8) −962005.75122(2)
^{4}He	−8.507870788593(2) 456573(2)	4.2539353942961(6) 1548946(5)	4071.8(1) 817626.242(2)	4853.3(2) 36641.828992(6)	11247.7393032(8) −962545.95034(1)
^{3}He	−8.50886435820(3) 456635(3)	4.254432179120(1) 1549265(5)	4073.0(1) 817749.274(2)	4854.7(2) 36664.109324(7)	11249.9297473(7) −962722.73142(1)
		He($2\,^3S$)-He($2\,^3S$)-He($2\,^3P$)			
$^\infty$He	−6.4077465538656(1) 135961.610(2)	3.20387327693284(7) 531453.96(2)	1862.5727(2) 210566.55(2)	2251.4034(2) 32944.521865(3)	3276.6801(3) −291050.42846(1)
^{4}He	−6.4090875602043(2) 135980.281(2)	3.2045437801021(1) 531566.81(2)	1863.4728(2) 210667.81(2)	2252.4905(1) 32941.0762590(3)	3279.4590(3) −291128.593759(1)
^{3}He	−6.4095263009351(2) 135986.388(2)	3.20476315046753(8) 531603.71(1)	1863.7672(1) 210700.95(2)	2252.8465(2) 32939.9454728(3)	3280.3686(2) −291154.170393(1)

interactions for the two-body $n_0S - n_0S$ system, where $C_6 = \mathbb{D}_2$ and $C_8 = \mathbb{Q}_2$.

4.2 Results and Discussion for He$(1\,^1S)$-He$(1\,^1S)$-He$(2\,^1S)$

Here we first construct atomic wave functions of helium variationally using Hylleraas basis sets and then we generate the intermediate states by diagonalizing the helium Hamiltonian [15].

4.2.1 The Zeroth-Order Wave Function

In this thesis, we are only concerned with the geometrical configuration of the equilateral triangle with $R_{12} = R_{23} = R_{31} = R$. The perturbation matrix with respect to $\{\phi_1, \phi_2, \phi_3\}$ thus becomes

$$H' = \begin{pmatrix} A & D & D \\ D & A & D \\ D & D & A \end{pmatrix}, \tag{4.15}$$

where

$$A = \Delta_{11} = \Delta_{22} = \Delta_{33}\,, \tag{4.16}$$

$$D = \Delta_{12} = \Delta_{13} = \Delta_{21} = \Delta_{23} = \Delta_{31} = \Delta_{32}\,. \tag{4.17}$$

Solving the eigenvalue problem of the above matrix yields the eigenvalues $A+2D$, $A-D$, and $A-D$, and the corresponding zeroth-order wave functions

$$\Psi^{(0)}_{1,\Delta} = \frac{1}{\sqrt{3}}|\phi_1\rangle + \frac{1}{\sqrt{3}}|\phi_2\rangle + \frac{1}{\sqrt{3}}|\phi_3\rangle\,, \tag{4.18}$$

$$\Psi^{(0)}_{2,\Delta} = \frac{1}{\sqrt{2}}|\phi_1\rangle - \frac{1}{\sqrt{2}}|\phi_3\rangle\,, \tag{4.19}$$

$$\Psi^{(0)}_{3,\Delta} = \frac{1}{\sqrt{6}}|\phi_1\rangle - \sqrt{\frac{2}{3}}|\phi_2\rangle + \frac{1}{\sqrt{6}}|\phi_3\rangle\,. \tag{4.20}$$

4.2.2 Dispersion Coefficients for An Equilateral Triangle

With these zeroth-order wave functions Eqs. (4.18)-(4.20), the corresponding long-range interaction coefficients $C_6^{(IJ)}$ and $C_8^{(IJ)}$ for the He($1\,^1S$)-He($1\,^1S$)-He($2\,^1S$) systems are listed in Table 4.3. We note that these coefficients are all the same and positive for $\Psi^{(0)}_{1,\Delta}$ with the geometric parameter $a=b=c=1/\sqrt{3}$. For $\Psi^{(0)}_{2,\Delta}$ with the geometric parameter $b=0$, $a=-c=1/\sqrt{2}$, $C_6^{(12)}=C_6^{(23)}$ and $C_8^{(12)}=C_8^{(23)}$. For $\Psi^{(0)}_{3,\Delta}$ with the geometric parameter $b=-\sqrt{\frac{2}{3}}$, $a=c=1/\sqrt{6}$, we also have $C_6^{(12)}$= $C_6^{(23)}$ and $C_8^{(12)}$= $C_8^{(23)}$.

The curves of potential energy for the He($1\,^1S$)-He($1\,^1S$)-He($2\,^1S$) system, corresponding to different zeroth-order wave functions, are plotted in Fig. 4.1.

4.3 Results and Discussion for He($n_0\,^\lambda S$)-He($n_0\,^\lambda S$)-He($n_0'\,^\lambda P$)

4.3.1 The Zeroth-Order Wave Function

In this work, we need to obtain the values of these geometric parameters for specific configurations by using degenerate perturbation theory. Here, we can set a universal configuration with R_{12}= λ_1 R_{23} = λ_2 R_{31} =R. The perturbation matrix with respect

Table 4.3: The additive dispersion coefficients $C_6^{(IJ)}$ and $C_8^{(IJ)}$ of the He($1\,^1S$)-He($1\,^1S$)-He($2\,^1S$) system for three different types of the zeroth-order wave functions, where the three atoms form an equilateral triangle, in atomic units. The numbers in parentheses represent the computational uncertainties.

Atom	State	$C_6^{(12)}$	$C_6^{(23)}$	$C_6^{(31)}$	$C_8^{(12)}$	$C_8^{(23)}$	$C_8^{(31)}$
$^{\infty}$He	$\Psi_{1,\Delta}^{(0)}$	30.3206140(1)	30.3206140(1)	30.3206140(1)	2275.727(1)	2275.727(1)	2275.727(1)
	$\Psi_{2,\Delta}^{(0)}$	21.6511469(1)	21.6511469(1)	38.932200(1)	1662.2798(1)	1662.2798(1)	3214.351(1)
	$\Psi_{3,\Delta}^{(0)}$	33.1718490(1)	33.1718490(1)	15.8907959(1)	2696.9940(1)	2696.9940(1)	1144.9227(1)
^{4}He	$\Psi_{1,\Delta}^{(0)}$	30.3431102(1)	30.3431102(1)	30.3206140(1)	2276.83865(4)	2276.83865(4)	2276.83865(4)
	$\Psi_{2,\Delta}^{(0)}$	21.6672200(1)	21.6672200(1)	38.9610306(1)	1663.08968(3)	1663.08968(3)	3215.91205(5)
	$\Psi_{3,\Delta}^{(0)}$	33.1964271(1)	33.1964271(1)	15.9026165(1)	2698.30459(4)	2698.30459(4)	1145.48222(2)
^{3}He	$\Psi_{1,\Delta}^{(0)}$	30.3504738(1)	30.3504738(1)	30.3504738(1)	2277.20221(3)	2277.20221(3)	2277.20221(3)
	$\Psi_{2,\Delta}^{(0)}$	21.6724812(1)	21.6724812(1)	38.9704675(1)	1663.35469(3)	1663.35469(3)	3216.42285(5)
	$\Psi_{3,\Delta}^{(0)}$	33.204472(1)	33.204472(1)	15.9064857(1)	2698.73347(5)	2698.73347(5)	1145.66530(2)

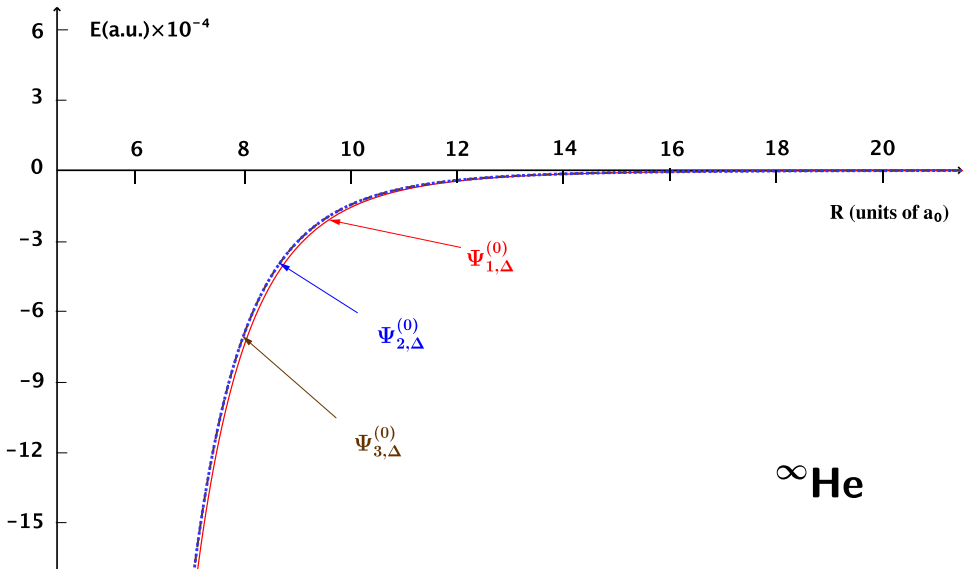

Figure 4.1: Long-range potentials for the He($1\,^1S$)-He($1\,^1S$)-He($2\,^1S$) system for three different types of the zeroth-order wave functions, where the three atoms form an equilateral triangle, in atomic units. For each curve labeled by a wave function, the plotted curve is the sum of $\Delta E^{(1)}$ and $\Delta E^{(2)}$, where $\Delta E^{(1)}$=0.

to $\{\phi_1, \phi_2, \phi_3\}$ thus becomes

$$H' = H'_{12} \begin{pmatrix} 0 & 1 & \lambda_2^3 \\ 1 & 0 & \lambda_1^3 \\ \lambda_2^3 & \lambda_1^3 & 0 \end{pmatrix}, \tag{4.21}$$

where

$$H'_{12} = \frac{4\pi}{R^{2L+1}} \frac{(-1)^M[(2L-1)!!]^2}{(2L+1)^2(L-M)!(L+M)!} |\langle \varphi_{n_0}(0;\boldsymbol{\sigma}) \| T_L(\boldsymbol{\sigma}) \| \varphi_{n'_0}(L;\boldsymbol{\sigma}) \rangle|^2 . \tag{4.22}$$

Solving the eigenvalue problem of the above matrix, we can obtain the eigenvalues and the corresponding orthonormalized zero-order wave functions. In the following, we will discuss the long-range interaction coefficients by explicitly evaluating coefficients for the three elementary geometrical configurations of the three-body system

in an equilateral triangle, an isosceles triangle, and equally-spaced collinearly, representing, respectively, the symmetries D_{3h}, C_{2v} and $D_{\infty h}$.

4.3.2 Dispersion Coefficients for an Equilateral Triangle

For $\lambda_1 = \lambda_2 = 1$, solving the eigenvalue problem of the above matrix (Eq. (4.21)) for the equilateral triangle, one obtains the eigenvalues: $2H'_{12}$, $-H'_{12}$, $-H'_{12}$, and the corresponding orthonormalized zeroth-order wave functions:

$$\Psi^{(0)}_{1,\Delta} = \frac{1}{\sqrt{3}}|\phi_1\rangle + \frac{1}{\sqrt{3}}|\phi_2\rangle + \frac{1}{\sqrt{3}}|\phi_3\rangle\,, \tag{4.23}$$

$$\Psi^{(0)}_{2,\Delta} = \frac{1}{\sqrt{2}}|\phi_1\rangle - \frac{1}{\sqrt{2}}|\phi_3\rangle\,, \tag{4.24}$$

$$\Psi^{(0)}_{3,\Delta} = \frac{1}{\sqrt{6}}|\phi_1\rangle - \sqrt{\frac{2}{3}}|\phi_2\rangle + \frac{1}{\sqrt{6}}|\phi_3\rangle\,. \tag{4.25}$$

With these zeroth-order wave functions Eqs. (4.23)-(4.25), the long-range interaction coefficients for the He($1\,^1S$)-He($1\,^1S$)-He($2\,^1P$), He($2\,^1S$)-He($2\,^1S$)-He($2\,^1P$), and He($2\,^3S$)-He($2\,^3S$)-He($2\,^3P$) systems are listed in Tables 4.4-4.13.

Tables 4.4-4.5 list the first-order dipolar coefficients $C_3^{(IJ)}$(1,M) for the equilateral triangle. We note that these coefficients all satisfy $C_3^{(IJ)}(1, M = 0) = -2C_3^{(IJ)}(1, M = \pm 1)$. For $\Psi^{(0)}_{1,\Delta}$ with the geometric parameter $a = b = c = 1/\sqrt{3}$, $C_3^{(IJ)}(1, M = 0)$ are all the same and negative and $C_3^{(IJ)}(1, M = \pm 1)$ are all the same and positive. For $\Psi^{(0)}_{2,\Delta}$ with the geometric parameter $b = 0$, $a = -c = 1/\sqrt{2}$, $C_3^{(12)}(1, M) = C_3^{(23)}(1, M) = 0$, $C_3^{(31)}(1, M = 0)$ appears to be positive and $C_3^{(31)}(1, M = \pm 1)$ appears to be negative. For $\Psi^{(0)}_{3,\Delta}$ with the geometric parameter $b = -\sqrt{\frac{2}{3}}$, $a = c = 1/\sqrt{6}$, $C_3^{(12)}(1, M = 0)$ and $C_3^{(23)}(1, M = 0)$ are the same and positive, and $C_3^{(12)}(1, M = \pm 1)$ and $C_3^{(23)}(1, M = \pm 1)$ are the same and negative; also $C_3^{(31)}(1, M = 0)$ appears to be negative and $C_3^{(31)}(1, M = \pm 1)$ positive. These positive or negative signs indicate that different states of a system may lead to different types of interactions: attractive or repulsive.

Table 4.4: The additive long-range coefficients $C_3^{(IJ)}(1, M = 0)$ of the He($n_0\,^\lambda S$)-He($n_0\,^\lambda S$)-He($n_0'\,^\lambda P$) system for three different types of the zeroth-order wave functions, where the three atoms form an equilateral triangle, in atomic units. The numbers in parentheses represent the computational uncertainties.

Atom	State	$C_3^{(12)}(1, M = 0)$	$C_3^{(23)}(1, M = 0)$	$C_3^{(31)}(1, M = 0)$
		He($1\,^1S$)-He($1\,^1S$)-He($2\,^1P$)		
$^\infty$He	$\Psi_{1,\Delta}^{(0)}$	−0.11803706848(2)	−0.11803706848(2)	−0.11803706848(2)
	$\Psi_{2,\Delta}^{(0)}$	0	0	0.17705560274(4)
	$\Psi_{3,\Delta}^{(0)}$	0.11803706848(2)	0.11803706848(2)	−0.05901853424(1)
^{4}He	$\Psi_{1,\Delta}^{(0)}$	−0.11805102037(2)	−0.11805102037(2)	−0.11805102037(2)
	$\Psi_{2,\Delta}^{(0)}$	0	0	0.17707653057(4)
	$\Psi_{3,\Delta}^{(0)}$	0.11805102037(2)	0.11805102037(2)	−0.05902551019(2)
^{3}He	$\Psi_{1,\Delta}^{(0)}$	−0.11805558670(3)	−0.11805558670(3)	−0.11805558670(3)
	$\Psi_{2,\Delta}^{(0)}$	0	0	0.17708338005(4)
	$\Psi_{3,\Delta}^{(0)}$	0.11805558670(3)	0.11805558670(3)	−0.05902779334(1)
		He($2\,^1S$)-He($2\,^1S$)-He($2\,^1P$)		
$^\infty$He	$\Psi_{1,\Delta}^{(0)}$	−5.669889535080(3)	−5.669889535080(3)	−5.669889535080(3)
	$\Psi_{2,\Delta}^{(0)}$	0	0	8.504834302621(5)
	$\Psi_{3,\Delta}^{(0)}$	5.669889535080(3)	5.669889535080(3)	−2.834944767539(1)
^{4}He	$\Psi_{1,\Delta}^{(0)}$	−5.671913859061(1)	−5.671913859061(1)	−5.671913859061(1)
	$\Psi_{2,\Delta}^{(0)}$	0	0	8.507870788593(2)
	$\Psi_{3,\Delta}^{(0)}$	5.671913859061(1)	5.671913859061(1)	−2.835956929531(1)
^{3}He	$\Psi_{1,\Delta}^{(0)}$	−5.672576238826(1)	−5.672576238826(1)	−5.672576238826(1)
	$\Psi_{2,\Delta}^{(0)}$	0	0	8.508864358240(2)
	$\Psi_{3,\Delta}^{(0)}$	5.672576238826(1)	5.672576238826(1)	−2.8362881194133(5)
		He($2\,^3S$)-He($2\,^3S$)-He($2\,^3P$)		
$^\infty$He	$\Psi_{1,\Delta}^{(0)}$	−4.2718310359104(1)	−4.2718310359104(1)	−4.2718310359104(1)
	$\Psi_{2,\Delta}^{(0)}$	0	0	6.4077465538656(1)
	$\Psi_{3,\Delta}^{(0)}$	4.2718310359104(1)	4.2718310359104(1)	−2.13591551795523(5)
^{4}He	$\Psi_{1,\Delta}^{(0)}$	−4.2727250401361(1)	−4.2727250401361(1)	−4.2727250401361(1)
	$\Psi_{2,\Delta}^{(0)}$	0	0	6.4090875602043(2)
	$\Psi_{3,\Delta}^{(0)}$	4.2727250401361(1)	4.2727250401361(1)	−2.13636252006809(5)
^{3}He	$\Psi_{1,\Delta}^{(0)}$	−4.2730175339568(2)	−4.2730175339568(2)	−4.2730175339568(2)
	$\Psi_{2,\Delta}^{(0)}$	0	0	6.4095263009351(2)
	$\Psi_{3,\Delta}^{(0)}$	4.2730175339568(2)	4.2730175339568(2)	−2.13650876697836(6)

Table 4.5: The additive long-range coefficients $C_3^{(IJ)}(1, M = \pm 1)$ of the He($n_0\,^\lambda S$)-He($n_0\,^\lambda S$)-He($n_0'\,^\lambda P$) system for three different types of the zeroth-order wave functions, where the three atoms form an equilateral triangle, in atomic units. The numbers in parentheses represent the computational uncertainties.

Atom	State	$C_3^{(12)}(1, M = \pm 1)$	$C_3^{(23)}(1, M = \pm 1)$	$C_3^{(31)}(1, M = \pm 1)$
		He($1\,^1S$)-He($1\,^1S$)-He($2\,^1P$)		
$^\infty$He	$\Psi_{1,\Delta}^{(0)}$	0.05901853424(1)	0.05901853424(1)	0.05901853424(1)
	$\Psi_{2,\Delta}^{(0)}$	0	0	−0.08852780137(2)
	$\Psi_{3,\Delta}^{(0)}$	−0.05901853424(1)	−0.05901853424(1)	0.029509267124(7)
^{4}He	$\Psi_{1,\Delta}^{(0)}$	0.05902551019(2)	0.05902551019(2)	0.05902551019(2)
	$\Psi_{2,\Delta}^{(0)}$	0	0	−0.08853826528(2)
	$\Psi_{3,\Delta}^{(0)}$	−0.05902551019(2)	−0.05902551019(2)	0.029512755096(7)
^{3}He	$\Psi_{1,\Delta}^{(0)}$	0.05902779334(1)	0.05902779334(1)	0.05902779334(1)
	$\Psi_{2,\Delta}^{(0)}$	0	0	−0.08854169002(2)
	$\Psi_{3,\Delta}^{(0)}$	−0.05902779334(1)	−0.05902779334(1)	0.029513896674(6)
		He($2\,^1S$)-He($2\,^1S$)-He($2\,^1P$)		
$^\infty$He	$\Psi_{1,\Delta}^{(0)}$	2.834944767539(1)	2.834944767539(1)	2.834944767539(1)
	$\Psi_{2,\Delta}^{(0)}$	0	0	−4.252417151311(3)
	$\Psi_{3,\Delta}^{(0)}$	−2.834944767539(1)	−2.834944767539(1)	1.417472383770(1)
^{4}He	$\Psi_{1,\Delta}^{(0)}$	2.835956929531(1)	2.835956929531(1)	2.835956929531(1)
	$\Psi_{2,\Delta}^{(0)}$	0	0	−4.253935394296(1)
	$\Psi_{3,\Delta}^{(0)}$	−2.835956929531(1)	−2.835956929531(1)	1.4179784647653(2)
^{3}He	$\Psi_{1,\Delta}^{(0)}$	2.8362881194133(5)	2.8362881194133(5)	2.8362881194133(5)
	$\Psi_{2,\Delta}^{(0)}$	0	0	−4.254432179120(1)
	$\Psi_{3,\Delta}^{(0)}$	−2.8362881194133(5)	−2.8362881194133(5)	1.4181440597067(3)
		He($2\,^3S$)-He($2\,^3S$)-He($2\,^3P$)		
$^\infty$He	$\Psi_{1,\Delta}^{(0)}$	2.13591551795523(5)	2.13591551795523(5)	2.13591551795523(5)
	$\Psi_{2,\Delta}^{(0)}$	0	0	−3.20387327693284(7)
	$\Psi_{3,\Delta}^{(0)}$	−2.13591551795523(5)	−2.13591551795523(5)	1.06795775897762(3)
^{4}He	$\Psi_{1,\Delta}^{(0)}$	2.13636252006809(5)	2.13636252006809(5)	2.13636252006809(5)
	$\Psi_{2,\Delta}^{(0)}$	0	0	−3.2045437801021(1)
	$\Psi_{3,\Delta}^{(0)}$	−2.13636252006809(5)	−2.13636252006809(5)	1.06818126003405(3)
^{3}He	$\Psi_{1,\Delta}^{(0)}$	2.13650876697836(6)	2.13650876697836(6)	2.13650876697836(6)
	$\Psi_{2,\Delta}^{(0)}$	0	0	−3.2047631504675(1)
	$\Psi_{3,\Delta}^{(0)}$	−2.13650876697836(6)	−2.13650876697836(6)	1.06825438348918(3)

Table 4.6: The additive and nonadditive dispersion coefficients $C_6^{(IJ)}(1, M = 0)$ of the He($n_0\,^\lambda S$)-He($n_0\,^\lambda S$)-He($n_0'\,^\lambda P$) system for three different types of the zeroth-order wave functions, where the three atoms form an equilateral triangle, in atomic units. The numbers in parentheses represent the computational uncertainties.

Atom	State	$C_6^{(12)}(1, M = 0)$	$C_6^{(23)}(1, M = 0)$	$C_6^{(31)}(1, M = 0)$
		He($1\,^1S$)-He($1\,^1S$)-He($2\,^1P$)		
$^\infty$He	$\Psi_{1,\Delta}^{(0)}$	22.2490435504(2)	22.2490435504(2)	22.2490435504(2)
	$\Psi_{2,\Delta}^{(0)}$	17.0520271221(1)	17.0520271221(1)	32.6430764067(3)
	$\Psi_{3,\Delta}^{(0)}$	27.4460599786(3)	27.4460599786(3)	11.8550106940(1)
^{4}He	$\Psi_{1,\Delta}^{(0)}$	22.26802944166(5)	22.26802944166(5)	22.26802944166(5)
	$\Psi_{2,\Delta}^{(0)}$	17.06655279456(5)	17.06655279456(5)	32.6709827359(1)
	$\Psi_{3,\Delta}^{(0)}$	27.4695060888(1)	27.4695060888(1)	11.86507614743(3)
^{3}He	$\Psi_{1,\Delta}^{(0)}$	22.2742443341(1)	22.2742443341(1)	22.2742443341(1)
	$\Psi_{2,\Delta}^{(0)}$	17.0713076681(1)	17.0713076681(1)	32.6801176662(2)
	$\Psi_{3,\Delta}^{(0)}$	27.4771810002(2)	27.4771810002(2)	11.8683710021(1)
		He($2\,^1S$)-He($2\,^1S$)-He($2\,^1P$)		
$^\infty$He	$\Psi_{1,\Delta}^{(0)}$	6459.14(5)	6459.14(5)	6459.14(5)
	$\Psi_{2,\Delta}^{(0)}$	7654.62(4)	7654.62(4)	4068.2(1)
	$\Psi_{3,\Delta}^{(0)}$	5263.7(1)	5263.7(1)	8850.10(3)
^{4}He	$\Psi_{1,\Delta}^{(0)}$	6463.79(6)	6463.79(6)	6463.79(6)
	$\Psi_{2,\Delta}^{(0)}$	7659.77(4)	7659.77(4)	4071.8(1)
	$\Psi_{3,\Delta}^{(0)}$	5267.8(1)	5267.8(1)	8855.76(3)
^{3}He	$\Psi_{1,\Delta}^{(0)}$	6465.31(6)	6465.31(6)	6465.31(6)
	$\Psi_{2,\Delta}^{(0)}$	7661.47(5)	7661.47(5)	4073.0(1)
	$\Psi_{3,\Delta}^{(0)}$	5269.15(7)	5269.15(7)	8857.62(3)
		He($2\,^3S$)-He($2\,^3S$)-He($2\,^3P$)		
$^\infty$He	$\Psi_{1,\Delta}^{(0)}$	2333.9418(2)	2333.9418(2)	2333.9418(2)
	$\Psi_{2,\Delta}^{(0)}$	2569.6263(2)	2569.6263(2)	1862.5727(2)
	$\Psi_{3,\Delta}^{(0)}$	2098.2571(1)	2098.2571(1)	2805.3109(2)
^{4}He	$\Psi_{1,\Delta}^{(0)}$	2335.4680(1)	2335.4680(1)	2335.4680(1)
	$\Psi_{2,\Delta}^{(0)}$	2571.4658(2)	2571.4658(2)	1863.4728(2)
	$\Psi_{3,\Delta}^{(0)}$	2099.4703(1)	2099.4703(1)	2807.4635(2)
^{3}He	$\Psi_{1,\Delta}^{(0)}$	2335.9678(2)	2335.9678(2)	2335.9678(2)
	$\Psi_{2,\Delta}^{(0)}$	2572.0680(2)	2572.0680(2)	1863.7672(1)
	$\Psi_{3,\Delta}^{(0)}$	2099.8674(1)	2099.8674(1)	2808.1682(2)

Table 4.7: The additive and nonadditive dispersion coefficients $C_6^{(IJ,JK)}(1, M = 0)$ of the He($n_0\,^\lambda S$)-He($n_0\,^\lambda S$)-He($n_0'\,^\lambda P$) system for three different types of the zeroth-order wave functions, where the three atoms form an equilateral triangle, in atomic units. The numbers in parentheses represent the computational uncertainties.

Atom	State	$C_6^{(12,23)}(1, M = 0)$	$C_6^{(23,31)}(1, M = 0)$	$C_6^{(31,12)}(1, M = 0)$
		He($1\,^1S$)-He($1\,^1S$)-He($2\,^1P$)		
$^\infty$He	$\Psi_{1,\Delta}^{(0)}$	0.3183512641(1)	0.3183512641(1)	0.3183512641(1)
	$\Psi_{2,\Delta}^{(0)}$	−0.4775268962(1)	0	0
	$\Psi_{3,\Delta}^{(0)}$	0.15917563204(6)	−0.3183512641(1)	−0.3183512641(1)
^{4}He	$\Psi_{1,\Delta}^{(0)}$	0.3185403283(1)	0.3185403283(1)	0.3185403283(1)
	$\Psi_{2,\Delta}^{(0)}$	−0.4778104925(1)	0	0
	$\Psi_{3,\Delta}^{(0)}$	0.15927016414(6)	−0.3185403283(1)	−0.3185403283(1)
^{3}He	$\Psi_{1,\Delta}^{(0)}$	0.3186022100(1)	0.3186022100(1)	0.3186022100(1)
	$\Psi_{2,\Delta}^{(0)}$	−0.4779033149(2)	0	0
	$\Psi_{3,\Delta}^{(0)}$	0.15930110500(5)	−0.3186022100(1)	−0.3186022100(1)
		He($2\,^1S$)-He($2\,^1S$)-He($2\,^1P$)		
$^\infty$He	$\Psi_{1,\Delta}^{(0)}$	1277.73986528(7)	1277.73986528(7)	1277.73986528(7)
	$\Psi_{2,\Delta}^{(0)}$	−1916.6097979(1)	0	0
	$\Psi_{3,\Delta}^{(0)}$	638.86993263(3)	−1277.73986528(7)	−1277.73986528(7)
^{4}He	$\Psi_{1,\Delta}^{(0)}$	1278.50761033(6)	1278.50761033(6)	1278.50761033(6)
	$\Psi_{2,\Delta}^{(0)}$	−1917.7614155(1)	0	0
	$\Psi_{3,\Delta}^{(0)}$	639.25380516(3)	−1278.50761033(6)	−1278.50761033(6)
^{3}He	$\Psi_{1,\Delta}^{(0)}$	1278.75889180(6)	1278.75889180(6)	1278.75889180(6)
	$\Psi_{2,\Delta}^{(0)}$	−1918.1383377(1)	0	0
	$\Psi_{3,\Delta}^{(0)}$	639.37944590(3)	−1278.75889180(6)	−1278.75889180(6)
		He($2\,^3S$)-He($2\,^3S$)-He($2\,^3P$)		
$^\infty$He	$\Psi_{1,\Delta}^{(0)}$	376.62601(3)	376.62601(3)	376.62601(3)
	$\Psi_{2,\Delta}^{(0)}$	−564.93901(4)	0	0
	$\Psi_{3,\Delta}^{(0)}$	188.31301(2)	−376.62601(3)	−376.62601(3)
^{4}He	$\Psi_{1,\Delta}^{(0)}$	376.94770(2)	376.94770(2)	376.94770(2)
	$\Psi_{2,\Delta}^{(0)}$	−565.42155(3)	0	0
	$\Psi_{3,\Delta}^{(0)}$	188.47385(1)	−376.94770(2)	−376.94770(2)
^{3}He	$\Psi_{1,\Delta}^{(0)}$	377.05302(2)	377.05302(2)	377.05302(2)
	$\Psi_{2,\Delta}^{(0)}$	−565.57955(4)	0	0
	$\Psi_{3,\Delta}^{(0)}$	188.52651(1)	−377.05302(2)	−377.05302(2)

Table 4.8: The additive and nonadditive dispersion coefficients $C_6^{(IJ)}(1, M = \pm 1)$ of the He($n_0\,^\lambda S$)-He($n_0\,^\lambda S$)-He($n_0'\,^\lambda P$) system for three different types of the zeroth-order wave functions, where the three atoms form an equilateral triangle, in atomic units. The numbers in parentheses represent the computational uncertainties.

Atom	State	$C_6^{(12)}(1, M = \pm 1)$	$C_6^{(23)}(1, M = \pm 1)$	$C_6^{(31)}(1, M = \pm 1)$
		He($1\,^1S$)-He($1\,^1S$)-He($2\,^1P$)		
$^\infty$He	$\Psi_{1,\Delta}^{(0)}$	30.99244818295(4)	30.99244818295(4)	30.99244818295(4)
	$\Psi_{2,\Delta}^{(0)}$	23.60958059665(2)	23.60958059665(2)	45.7581833555(1)
	$\Psi_{3,\Delta}^{(0)}$	38.3753157692(1)	38.3753157692(1)	16.22671301034(1)
^{4}He	$\Psi_{1,\Delta}^{(0)}$	31.0187878317(2)	31.0187878317(2)	31.0187878317(2)
	$\Psi_{2,\Delta}^{(0)}$	23.6296215870(2)	23.6296215870(2)	45.797120320(1)
	$\Psi_{3,\Delta}^{(0)}$	38.4079540763(3)	38.4079540763(3)	16.2404553424(1)
^{3}He	$\Psi_{1,\Delta}^{(0)}$	31.0274099057(1)	31.0274099057(1)	31.0274099057(1)
	$\Psi_{2,\Delta}^{(0)}$	23.6361818467(2)	23.6361818467(2)	45.8098660236(2)
	$\Psi_{3,\Delta}^{(0)}$	38.4186379646(2)	38.4186379646(2)	16.2449537878(1)
		He($2\,^1S$)-He($2\,^1S$)-He($2\,^1P$)		
$^\infty$He	$\Psi_{1,\Delta}^{(0)}$	6979.8(2)	6979.8(2)	6979.8(2)
	$\Psi_{2,\Delta}^{(0)}$	8045.0(1)	8045.0(1)	4849.0(2)
	$\Psi_{3,\Delta}^{(0)}$	5914.4(2)	5914.4(2)	9110.4(1)
^{4}He	$\Psi_{1,\Delta}^{(0)}$	6984.7(1)	6984.7(1)	6984.7(1)
	$\Psi_{2,\Delta}^{(0)}$	8050.5(1)	8050.5(1)	4853.3(2)
	$\Psi_{3,\Delta}^{(0)}$	5919.0(2)	5919.0(2)	9116.27(7)
^{3}He	$\Psi_{1,\Delta}^{(0)}$	6986.5(2)	6986.5(2)	6986.5(2)
	$\Psi_{2,\Delta}^{(0)}$	8052.3(1)	8052.3(1)	4854.7(2)
	$\Psi_{3,\Delta}^{(0)}$	5920.6(2)	5920.6(2)	9118.19(7)
		He($2\,^3S$)-He($2\,^3S$)-He($2\,^3P$)		
$^\infty$He	$\Psi_{1,\Delta}^{(0)}$	2593.1622(2)	2593.1622(2)	2593.1622(2)
	$\Psi_{2,\Delta}^{(0)}$	2764.0417(2)	2764.0417(2)	2251.4034(2)
	$\Psi_{3,\Delta}^{(0)}$	2422.2828(2)	2422.2828(2)	2934.9211(2)
^{4}He	$\Psi_{1,\Delta}^{(0)}$	2594.8134(2)	2594.8134(2)	2594.8134(2)
	$\Psi_{2,\Delta}^{(0)}$	2765.9749(3)	2765.9749(3)	2252.4905(1)
	$\Psi_{3,\Delta}^{(0)}$	2423.6520(2)	2423.6520(2)	2937.1361(2)
^{3}He	$\Psi_{1,\Delta}^{(0)}$	2595.3540(3)	2595.3540(3)	2595.3540(3)
	$\Psi_{2,\Delta}^{(0)}$	2766.6075(2)	2766.6075(2)	2252.8465(2)
	$\Psi_{3,\Delta}^{(0)}$	2424.1002(2)	2424.1002(2)	2937.8612(2)

Table 4.9: The additive and nonadditive dispersion coefficients $C_6^{(IJ,JK)}(1, M = \pm 1)$ of the He($n_0\,^\lambda S$)-He($n_0\,^\lambda S$)-He($n_0'\,^\lambda P$) system for three different types of the zeroth-order wave functions, where the three atoms form an equilateral triangle, in atomic units. The numbers in parentheses represent the computational uncertainties.

Atom	State	$C_6^{(12,23)}(1, M = \pm 1)$	$C_6^{(23,31)}(1, M = \pm 1)$	$C_6^{(31,12)}(1, M = \pm 1)$
		He($1\,^1S$)-He($1\,^1S$)-He($2\,^1P$)		
$^\infty$He	$\Psi_{1,\Delta}^{(0)}$	−0.2785573560(1)	−0.2785573560(1)	−0.2785573560(1)
	$\Psi_{2,\Delta}^{(0)}$	0.4178360340(2)	0	0
	$\Psi_{3,\Delta}^{(0)}$	−0.13927867804(5)	0.2785573560(1)	0.2785573560(1)
^{4}He	$\Psi_{1,\Delta}^{(0)}$	−0.2787227872(1)	−0.2787227872(1)	−0.2787227872(1)
	$\Psi_{2,\Delta}^{(0)}$	0.4180841809(1)	0	0
	$\Psi_{3,\Delta}^{(0)}$	−0.13936139363(5)	0.2787227872(1)	0.2787227872(1)
^{3}He	$\Psi_{1,\Delta}^{(0)}$	−0.2787769337(1)	−0.2787769337(1)	−0.2787769337(1)
	$\Psi_{2,\Delta}^{(0)}$	0.4181654005(2)	0	0
	$\Psi_{3,\Delta}^{(0)}$	−0.13938846686(5)	0.2787769337(1)	0.2787769337(1)
		He($2\,^1S$)-He($2\,^1S$)-He($2\,^1P$)		
$^\infty$He	$\Psi_{1,\Delta}^{(0)}$	−1118.02238212(6)	−1118.02238212(6)	−1118.02238212(6)
	$\Psi_{2,\Delta}^{(0)}$	1677.0335732(1)	0	0
	$\Psi_{3,\Delta}^{(0)}$	−559.01119106(3)	1118.02238212(6)	1118.02238212(6)
^{4}He	$\Psi_{1,\Delta}^{(0)}$	−1118.69415903(5)	−1118.69415903(5)	−1118.69415903(5)
	$\Psi_{2,\Delta}^{(0)}$	1678.04123856(8)	0	0
	$\Psi_{3,\Delta}^{(0)}$	−559.34707952(3)	1118.694159003(5)	1118.694159003(5)
^{3}He	$\Psi_{1,\Delta}^{(0)}$	−1118.91403032(5)	−1118.91403032(5)	−1118.91403032(5)
	$\Psi_{2,\Delta}^{(0)}$	1678.37104549(8)	0	0
	$\Psi_{3,\Delta}^{(0)}$	−559.45701515(2)	1118.91403032(5)	1118.91403032(5)
		He($2\,^3S$)-He($2\,^3S$)-He($2\,^3P$)		
$^\infty$He	$\Psi_{1,\Delta}^{(0)}$	−329.54775(2)	−329.54775(2)	−329.54775(2)
	$\Psi_{2,\Delta}^{(0)}$	494.32164(4)	0	0
	$\Psi_{3,\Delta}^{(0)}$	−164.77387(1)	329.54775(2)	329.54775(2)
^{4}He	$\Psi_{1,\Delta}^{(0)}$	−329.82924(2)	−329.82924(2)	−329.82924(2)
	$\Psi_{2,\Delta}^{(0)}$	494.74386(3)	0	0
	$\Psi_{3,\Delta}^{(0)}$	−164.91462(1)	329.82924(2)	329.82924(2)
^{3}He	$\Psi_{1,\Delta}^{(0)}$	−329.92141(3)	−329.92141(3)	−329.92141(3)
	$\Psi_{2,\Delta}^{(0)}$	494.88211(4)	0	0
	$\Psi_{3,\Delta}^{(0)}$	−164.96071(2)	329.92141(3)	329.92141(3)

Table 4.10: The additive and nonadditive dispersion coefficients $C_8^{(IJ)}(1, M = 0)$ of the He($n_0\,^\lambda S$)-He($n_0\,^\lambda S$)-He($n_0'\,^\lambda P$) system for three different types of the zeroth-order wave functions, where the three atoms form an equilateral triangle, in atomic units. The numbers in parentheses represent the computational uncertainties.

Atom	State	$C_8^{(12)}(1, M = 0)$	$C_8^{(23)}(1, M = 0)$	$C_8^{(31)}(1, M = 0)$
		He($1\,^1S$)-He($1\,^1S$)-He($2\,^1P$)		
$^\infty$He	$\Psi_{1,\Delta}^{(0)}$	269.07224(6)	269.07224(6)	269.07224(6)
	$\Psi_{2,\Delta}^{(0)}$	195.56578(5)	195.56578(5)	357.47794(9)
	$\Psi_{3,\Delta}^{(0)}$	303.50721(7)	303.50721(7)	141.59505(3)
^{4}He	$\Psi_{1,\Delta}^{(0)}$	269.03928(6)	269.03928(6)	269.03928(6)
	$\Psi_{2,\Delta}^{(0)}$	195.53832(5)	195.53832(5)	357.40565(9)
	$\Psi_{3,\Delta}^{(0)}$	303.44988(8)	303.44988(8)	141.58253(3)
^{3}He	$\Psi_{1,\Delta}^{(0)}$	269.02843(6)	269.02843(6)	269.02843(6)
	$\Psi_{2,\Delta}^{(0)}$	195.52927(4)	195.52927(4)	357.38190(9)
	$\Psi_{3,\Delta}^{(0)}$	303.4310(1)	303.4310(1)	141.57840(3)
		He($2\,^1S$)-He($2\,^1S$)-He($2\,^1P$)		
$^\infty$He	$\Psi_{1,\Delta}^{(0)}$	601051(2)	601051(2)	601051(2)
	$\Psi_{2,\Delta}^{(0)}$	636815(1)	636815(1)	419806(2)
	$\Psi_{3,\Delta}^{(0)}$	492143(1)	492143(1)	709151.3(7)
^{4}He	$\Psi_{1,\Delta}^{(0)}$	601351(6)	601351(6)	601351(2)
	$\Psi_{2,\Delta}^{(0)}$	637098(2)	637098(2)	419931(2)
	$\Psi_{3,\Delta}^{(0)}$	492320(2)	492320(2)	709488(1)
^{3}He	$\Psi_{1,\Delta}^{(0)}$	601449(2)	601449(2)	601449(2)
	$\Psi_{2,\Delta}^{(0)}$	637193(1)	637193(1)	419971(3)
	$\Psi_{3,\Delta}^{(0)}$	492379(2)	492379(2)	709599(1)
		He($2\,^3S$)-He($2\,^3S$)-He($2\,^3P$)		
$^\infty$He	$\Psi_{1,\Delta}^{(0)}$	182792.939(7)	182792.939(7)	182792.939(7)
	$\Psi_{2,\Delta}^{(0)}$	173264.08(1)	173264.08(1)	103017.090(3)
	$\Psi_{3,\Delta}^{(0)}$	126432.753(5)	126432.753(5)	196679.74(1)
^{4}He	$\Psi_{1,\Delta}^{(0)}$	182836.841(7)	182836.841(7)	182836.841(7)
	$\Psi_{2,\Delta}^{(0)}$	173324.043(8)	173324.043(8)	103039.204(2)
	$\Psi_{3,\Delta}^{(0)}$	126467.484(4)	126467.484(4)	196752.32(1)
^{3}He	$\Psi_{1,\Delta}^{(0)}$	182851.205(6)	182851.205(6)	182851.205(6)
	$\Psi_{2,\Delta}^{(0)}$	173343.67(1)	173343.67(1)	103046.443(2)
	$\Psi_{3,\Delta}^{(0)}$	126478.851(4)	126478.851(4)	196776.07(1)

Table 4.11: The additive and nonadditive dispersion coefficients $C_8^{(IJ,JK)}(1, M = 0)$ of the He($n_0\,^\lambda S$)-He($n_0\,^\lambda S$)-He($n_0'\,^\lambda P$) system for three different types of the zeroth-order wave functions, where the three atoms form an equilateral triangle, in atomic units. The numbers in parentheses represent the computational uncertainties.

Atom	State	$C_8^{(12,23)}(1, M = 0)$	$C_8^{(23,31)}(1, M = 0)$	$C_8^{(31,12)}(1, M = 0)$
		He($1\,^1S$)-He($1\,^1S$)-He($2\,^1P$)		
$^\infty$He	$\Psi_{1,\Delta}^{(0)}$	1.007423570(1)	1.007423570(1)	1.007423570(1)
	$\Psi_{2,\Delta}^{(0)}$	−1.511135354(1)	0	0
	$\Psi_{3,\Delta}^{(0)}$	0.5037117851(5)	−1.007423570(1)	−1.007423570(1)
^{4}He	$\Psi_{1,\Delta}^{(0)}$	1.007830781(1)	1.007830781(1)	1.007830781(1)
	$\Psi_{2,\Delta}^{(0)}$	−1.511746172(2)	0	0
	$\Psi_{3,\Delta}^{(0)}$	0.5039153905(5)	−1.007830781(1)	−1.007830781(1)
^{3}He	$\Psi_{1,\Delta}^{(0)}$	1.007964062(1)	1.007964062(1)	1.007964062(1)
	$\Psi_{2,\Delta}^{(0)}$	−1.511946094(2)	0	0
	$\Psi_{3,\Delta}^{(0)}$	0.5039820312(5)	−1.007964062(1)	−1.007964062(1)
		He($2\,^1S$)-He($2\,^1S$)-He($2\,^1P$)		
$^\infty$He	$\Psi_{1,\Delta}^{(0)}$	64166.8492(1)	64166.8492(1)	64166.8492(1)
	$\Psi_{2,\Delta}^{(0)}$	−96250.2737(1)	0	0
	$\Psi_{3,\Delta}^{(0)}$	32083.42460(5)	−64166.8492(1)	−64166.8492(1)
^{4}He	$\Psi_{1,\Delta}^{(0)}$	64203.6588(1)	64203.6588(1)	64203.6588(1)
	$\Psi_{2,\Delta}^{(0)}$	−96305.4883(2)	0	0
	$\Psi_{3,\Delta}^{(0)}$	32101.82942(5)	−64203.6588(1)	−64203.6588(1)
^{3}He	$\Psi_{1,\Delta}^{(0)}$	64215.7044(1)	64215.7044(1)	64215.7044(1)
	$\Psi_{2,\Delta}^{(0)}$	−96323.5566(1)	0	0
	$\Psi_{3,\Delta}^{(0)}$	32107.85225(6)	−64215.7044(1)	−64215.7044(1)
		He($2\,^3S$)-He($2\,^3S$)-He($2\,^3P$)		
$^\infty$He	$\Psi_{1,\Delta}^{(0)}$	19616.970942(4)	19616.970942(4)	19616.970942(4)
	$\Psi_{2,\Delta}^{(0)}$	−29425.456413(6)	0	0
	$\Psi_{3,\Delta}^{(0)}$	9808.485471(2)	−19616.970942(4)	−19616.970942(4)
^{4}He	$\Psi_{1,\Delta}^{(0)}$	19623.233157(4)	19623.233157(4)	19623.233157(4)
	$\Psi_{2,\Delta}^{(0)}$	−29434.849735(6)	0	0
	$\Psi_{3,\Delta}^{(0)}$	9811.616578(2)	−19623.233157(4)	−19623.233157(4)
^{3}He	$\Psi_{1,\Delta}^{(0)}$	19625.282308(4)	19625.282308(4)	19625.282308(4)
	$\Psi_{2,\Delta}^{(0)}$	−29437.923462(6)	0	0
	$\Psi_{3,\Delta}^{(0)}$	9812.641154(2)	−19625.282308(4)	−19625.282308(4)

Table 4.12: The additive and nonadditive dispersion coefficients $C_8^{(IJ)}(1, M = \pm 1)$ of the He($n_0\,^\lambda S$)-He($n_0\,^\lambda S$)-He($n_0'\,^\lambda P$) system for three different types of the zeroth-order wave functions, where the three atoms form an equilateral triangle, in atomic units. The numbers in parentheses represent the computational uncertainties.

Atom	State	$C_8^{(12)}(1, M = \pm 1)$	$C_8^{(23)}(1, M = \pm 1)$	$C_8^{(31)}(1, M = \pm 1)$
		He($1\,^1S$)-He($1\,^1S$)-He($2\,^1P$)		
$^\infty$He	$\Psi_{1,\Delta}^{(0)}$	3367.99345(8)	3367.99345(8)	3367.99345(8)
	$\Psi_{2,\Delta}^{(0)}$	2568.98677(6)	2568.98677(6)	5202.7801(1)
	$\Psi_{3,\Delta}^{(0)}$	4324.8490(1)	4324.8490(1)	1691.05565(4)
^{4}He	$\Psi_{1,\Delta}^{(0)}$	3370.39056(8)	3370.39056(8)	3370.39056(8)
	$\Psi_{2,\Delta}^{(0)}$	2570.80469(6)	2570.80469(6)	5206.4442(1)
	$\Psi_{3,\Delta}^{(0)}$	4327.8977(1)	4327.8977(1)	1692.25817(4)
^{3}He	$\Psi_{1,\Delta}^{(0)}$	3371.17511(7)	3371.17511(7)	3371.17511(7)
	$\Psi_{2,\Delta}^{(0)}$	2571.39969(6)	2571.39969(6)	5207.6434(1)
	$\Psi_{3,\Delta}^{(0)}$	4328.8955(1)	4328.8955(1)	1692.65175(4)
		He($2\,^1S$)-He($2\,^1S$)-He($2\,^1P$)		
$^\infty$He	$\Psi_{1,\Delta}^{(0)}$	663061(3)	663061(3)	663061(3)
	$\Psi_{2,\Delta}^{(0)}$	1182611(2)	1182611(2)	2509977(5)
	$\Psi_{3,\Delta}^{(0)}$	2067523(3)	2067523(3)	740156(1)
^{4}He	$\Psi_{1,\Delta}^{(0)}$	663476(3)	663476(3)	663476(3)
	$\Psi_{2,\Delta}^{(0)}$	1183287(2)	1183287(2)	2511492(5)
	$\Psi_{3,\Delta}^{(0)}$	2068757(4)	2068757(4)	740550(2)
^{3}He	$\Psi_{1,\Delta}^{(0)}$	663612(3)	663612(3)	663612(3)
	$\Psi_{2,\Delta}^{(0)}$	1183508(2)	1183508(2)	2511988(5)
	$\Psi_{3,\Delta}^{(0)}$	2069161(4)	2069161(4)	740681(1)
		He($2\,^3S$)-He($2\,^3S$)-He($2\,^3P$)		
$^\infty$He	$\Psi_{1,\Delta}^{(0)}$	230457.87(2)	230457.87(2)	230457.87(2)
	$\Psi_{2,\Delta}^{(0)}$	371010.24(1)	371010.24(1)	822504.39(2)
	$\Psi_{3,\Delta}^{(0)}$	672006.34(2)	672006.34(2)	220512.21(2)
^{4}He	$\Psi_{1,\Delta}^{(0)}$	230514.73(1)	230514.73(1)	230514.73(1)
	$\Psi_{2,\Delta}^{(0)}$	371117.31(2)	371117.31(2)	822695.40(2)
	$\Psi_{3,\Delta}^{(0)}$	672169.37(2)	672169.37(2)	220591.28(2)
^{3}He	$\Psi_{1,\Delta}^{(0)}$	230533.34(1)	230533.34(1)	230533.34(1)
	$\Psi_{2,\Delta}^{(0)}$	371152.34(2)	371152.34(2)	822757.90(2)
	$\Psi_{3,\Delta}^{(0)}$	672222.71(2)	672222.71(2)	220617.15(2)

Table 4.13: The additive and nonadditive dispersion coefficients $C_8^{(IJ,JK)}(1, M = \pm 1)$ of the He($n_0\,^\lambda S$)-He($n_0\,^\lambda S$)-He($n_0'\,^\lambda P$) system for three different types of the zeroth-order wave functions, where the three atoms form an equilateral triangle, in atomic units. The numbers in parentheses represent the computational uncertainties.

Atom	State	$C_8^{(12,23)}(1, M = \pm 1)$	$C_8^{(23,31)}(1, M = \pm 1)$	$C_8^{(31,12)}(1, M = \pm 1)$
		He($1\,^1S$)-He($1\,^1S$)-He($2\,^1P$)		
$^\infty$He	$\Psi_{1,\Delta}^{(0)}$	−2.707450845(3)	−2.707450845(3)	−2.707450845(3)
	$\Psi_{2,\Delta}^{(0)}$	4.061176267(4)	0	0
	$\Psi_{3,\Delta}^{(0)}$	−1.353725423(2)	2.707450845(3)	2.707450845(3)
^{4}He	$\Psi_{1,\Delta}^{(0)}$	−2.708545224(3)	−2.708545224(3)	−2.708545224(3)
	$\Psi_{2,\Delta}^{(0)}$	4.062817836(4)	0	0
	$\Psi_{3,\Delta}^{(0)}$	−1.354272611(1)	2.708545224(3)	2.708545224(3)
^{3}He	$\Psi_{1,\Delta}^{(0)}$	−2.708903418(3)	−2.708903418(3)	−2.708903418(3)
	$\Psi_{2,\Delta}^{(0)}$	4.063355127(4)	0	0
	$\Psi_{3,\Delta}^{(0)}$	−1.354451708(1)	2.708903418(3)	2.708903418(3)
		He($2\,^1S$)-He($2\,^1S$)-He($2\,^1P$)		
$^\infty$He	$\Psi_{1,\Delta}^{(0)}$	−172448.4071(2)	−172448.4071(2)	−172448.4071(2)
	$\Psi_{2,\Delta}^{(0)}$	258672.6108(4)	0	0
	$\Psi_{3,\Delta}^{(0)}$	−86224.2035(1)	172448.4071(2)	172448.4071(2)
^{4}He	$\Psi_{1,\Delta}^{(0)}$	−172547.3332(3)	−172547.3332(3)	−172547.3332(3)
	$\Psi_{2,\Delta}^{(0)}$	258820.9997(4)	0	0
	$\Psi_{3,\Delta}^{(0)}$	−86273.6665(1)	172547.3332(3)	172547.3332(3)
^{3}He	$\Psi_{1,\Delta}^{(0)}$	−172579.7058(3)	−172579.7058(3)	−172579.7058(3)
	$\Psi_{2,\Delta}^{(0)}$	258869.5588(5)	0	0
	$\Psi_{3,\Delta}^{(0)}$	−86289.8528(1)	172579.7058(3)	172579.7058(3)
		He($2\,^3S$)-He($2\,^3S$)-He($2\,^3P$)		
$^\infty$He	$\Psi_{1,\Delta}^{(0)}$	−52720.60940(1)	−52720.60940(1)	−52720.60940(1)
	$\Psi_{2,\Delta}^{(0)}$	79080.91411(2)	0	0
	$\Psi_{3,\Delta}^{(0)}$	−26360.304704(6)	52720.60940(1)	52720.60940(1)
^{4}He	$\Psi_{1,\Delta}^{(0)}$	−52737.43910(1)	−52737.43910(1)	−52737.43910(1)
	$\Psi_{2,\Delta}^{(0)}$	79106.15865(1)	0	0
	$\Psi_{3,\Delta}^{(0)}$	−26368.719554(5)	52737.43910(1)	52737.43910(1)
^{3}He	$\Psi_{1,\Delta}^{(0)}$	−52742.94620(1)	−52742.94620(1)	−52742.94620(1)
	$\Psi_{2,\Delta}^{(0)}$	79114.41929(1)	0	0
	$\Psi_{3,\Delta}^{(0)}$	−26371.473102(6)	52742.94620(1)	52742.94620(1)

Tables 4.6-4.7 list the leading terms of the second-order long-range interaction $C_6^{(IJ)}(1, M = 0)$ and $C_6^{(IJ,JK)}(1, M = 0)$ for the equilateral triangle. Tables 4.8-4.9 list $C_6^{(IJ)}(1, M = \pm 1)$ and $C_6^{(IJ,JK)}(1, M = \pm 1)$. We note that the absolute values of $C_6^{(IJ)}(1, M = 0)$ and $C_6^{(IJ,JK)}(1, M = 0)$ are always a bit larger than those of $C_6^{(IJ)}(1, M = \pm 1)$ and $C_6^{(IJ,JK)}(1, M = \pm 1)$, respectively. The additive interaction coefficients $C_6^{(IJ)}(1, M)$ are always positive, and the nonadditive interaction coefficients $C_6^{(IJ,JK)}(1, M)$ can be either positive or negative or zero, due to different signs of $\mathbb{Q}_4(a, b, 1, M, \gamma)$ and geometric parameters. For example, for $\Psi_{2,\Delta}^{(0)}$, the nonadditive coefficients $C_6^{(12,23)}(1, M = 0)$ is negative because $\mathbb{Q}_4(a, b, 1, M, \gamma) > 0$ and $a = -c = 1/\sqrt{2}$, and the nonadditive coefficients $C_6^{(23,31)}(1, M)$ and $C_6^{(31,12)}(1, M)$ are zero because $\mathbb{Q}_4(a, b, 1, M, \gamma) = 0$ and $b = 0$. Tables 4.10-4.13 list the second-order long-range interaction coefficients $C_8^{(IJ)}(1, M)$ and $C_8^{(IJ,JK)}(1, M)$.

From Tables 4.6-4.13, we can see that the dispersion coefficients for the additive terms are always positive, but the dispersion coefficients for the nonadditive terms can be either positive or negative or zero. Furthermore, the absolute values of the nonzero nonadditive dispersion coefficients are less than the additive dispersion coefficients by one to two orders of magnitude. However, the nonadditive terms may not be neglected in constructing an accurate potential surface. For example, the ratios of $(\frac{C_8^{(12,23)}(1,M=\pm1)}{R_{12}^4 R_{23}^4})/(\frac{C_8^{(12)}(1,M=\pm1)}{R_{12}^8})$ for the $\Psi_{1,\Delta}^{(0)}$ of He($1\,^1S$)-He($1\,^1S$)-He($2\,^1P$), He($2\,^1S$)-He($2\,^1S$)-He($2\,^1P$), and He($2\,^3S$)-He($2\,^3S$)-He($2\,^3P$) are 0.08%, 26%, and 24%, respectively. The curves of potential energy for the He($1\,^1S$)-He($1\,^1S$)-He($2\,^1P$), He($2\,^1S$)-He($2\,^1S$)-He($2\,^1P$), and He($2\,^3S$)-He($2\,^3S$)-He($2\,^3P$), corresponding to the different zeroth-order wave functions, are plotted in Figs. 4.2-4.4.

4.3.3 Dispersion Coefficients for an Isosceles Right Triangle

For $\lambda_1 = \frac{1}{\sqrt{2}}$ and $\lambda_2 = 1$, solving the eigenvalue problem of the above matrix (Eq.(4.21)) for the isosceles right triangle, one obtains the eigenvalues: $\frac{H'_{12}}{8}\left(\sqrt{2} + \sqrt{130}\right)$, $\frac{H'_{12}}{8}\left(\sqrt{2} -$

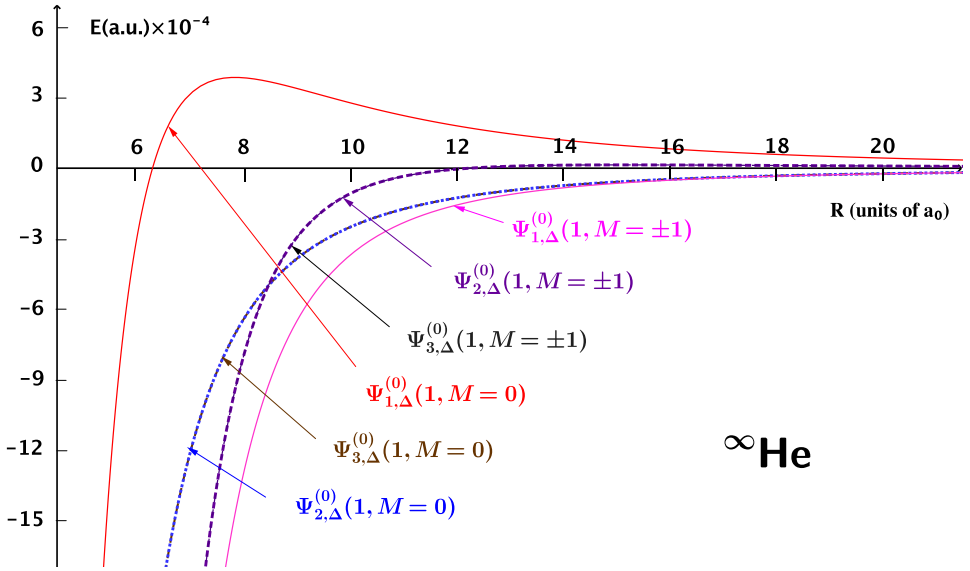

Figure 4.2: Long-range potentials for the He($1\,^1S$)-He($1\,^1S$)-He($2\,^1P$) system for three different types of the zeroth-order wave functions, where the three atoms form an equilateral triangle, in atomic units. For each curve labeled by a wave function, the plotted curve is the sum of $\Delta E^{(1)}$ and $\Delta E^{(2)}$.

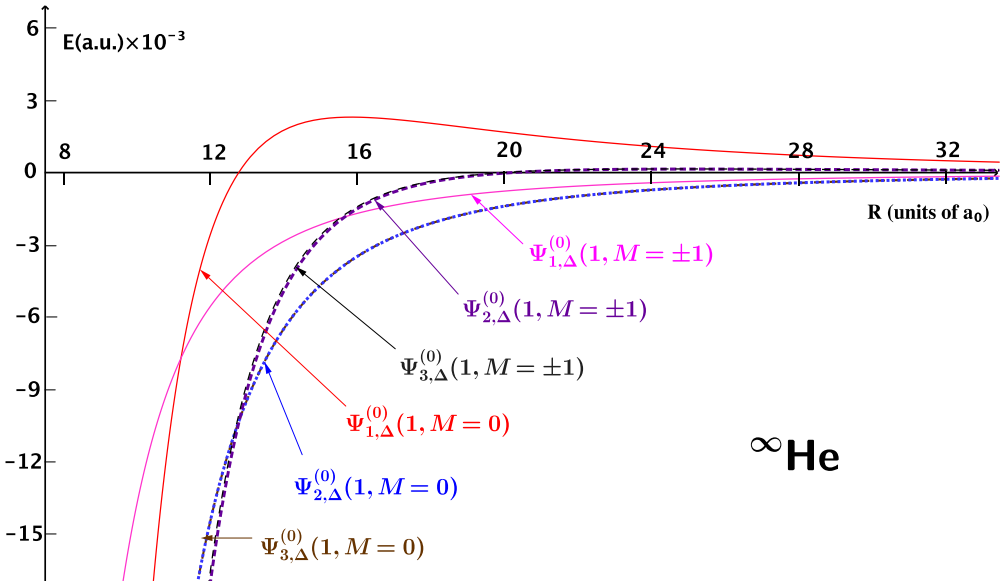

Figure 4.3: Long-range potentials for the He($2\,^1S$)-He($2\,^1S$)-He($2\,^1P$) system for three different types of the zeroth-order wave functions, where the three atoms form an equilateral triangle, in atomic units. For each curve labeled by a wave function, the plotted curve is the sum of $\Delta E^{(1)}$ and $\Delta E^{(2)}$.

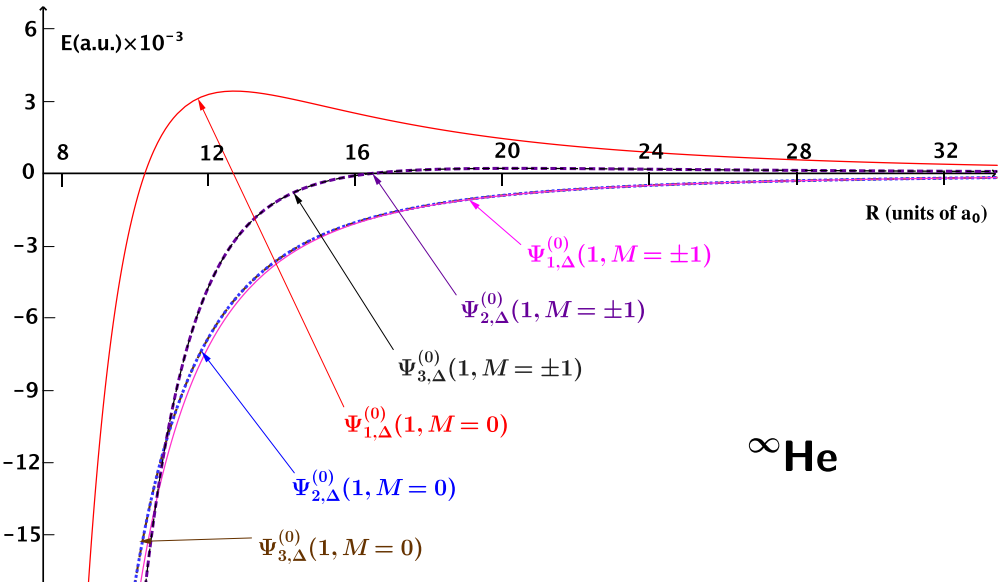

Figure 4.4: Long-range potentials for the He($2\,^3S$)-He($2\,^3S$)-He($2\,^3P$) system for three different types of the zeroth-order wave functions, where the three atoms form an equilateral triangle, in atomic units. For each curve labeled by a wave function, the plotted curve is the sum of $\Delta E^{(1)}$ and $\Delta E^{(2)}$.

and the corresponding orthonormalized zeroth-order wave functions:

$$\Psi^{(0)}_{1,\perp} = \frac{\sqrt{130}-\sqrt{2}}{2\sqrt{65-\sqrt{65}}}|\phi_1\rangle + \frac{4}{\sqrt{65-\sqrt{65}}}|\phi_2\rangle + \frac{4}{\sqrt{65-\sqrt{65}}}|\phi_3\rangle\,, \tag{4.26}$$

$$\Psi^{(0)}_{2,\perp} = \frac{-(\sqrt{130}+\sqrt{2})}{2\sqrt{65+\sqrt{65}}}|\phi_1\rangle + \frac{4}{\sqrt{65+\sqrt{65}}}|\phi_2\rangle + \frac{4}{\sqrt{65+\sqrt{65}}}|\phi_3\rangle\,, \tag{4.27}$$

$$\Psi^{(0)}_{3,\perp} = -\frac{1}{\sqrt{2}}|\phi_2\rangle + \frac{1}{\sqrt{2}}|\phi_3\rangle\,, \tag{4.28}$$

With these zeroth-order wave functions, the long-range interaction coefficients are calculated and the results are listed in Tables 4.14-4.23, for the systems of He($1\,^1S$)-He($1\,^1S$)-He($2\,^1P$), He($2\,^1S$)-He($2\,^1S$)-He($2\,^1P$), and He($2\,^3S$)-He($2\,^3S$)-He($2\,^3P$). Tables 4.14-4.15 are the first-order dipolar coefficients $C_3^{(31)}(1, M)$. We note that $C_3^{(12)}(1, M) = C_3^{(31)}(1, M)$ for all the three zeroth-order wave functions $\Psi^{(0)}_{1,\perp}$, $\Psi^{(0)}_{2,\perp}$

with the geometric parameters $b = c$, as well as $\Psi^{(0)}_{3,\perp}$ with the geometric parameter $a = 0$ that explains why $C_3^{(12)}(1, M) = C_3^{(31)}(1, M) = 0$ for this wave function. Similar to the coefficients shown in Tables 4.4-4.5, these coefficients also satisfy the relation $C_3^{(IJ)}(1, M = 0) = -2C_3^{(IJ)}(1, M = \pm 1)$.

Tables 4.16-4.23 contain the second-order dispersion coefficients $C_6^{(IJ)}(1, M)$ and $C_6^{(IJ,JK)}(1, M)$, $C_8^{(IJ)}(1, M)$, and $C_8^{(IJ,JK)}(1, M)$ for the the isosceles right triangle. We note that $C_6^{(12)}(1, M) = C_6^{(31)}(1, M)$, $C_6^{(12,23)}(1, M) = C_6^{(23,31)}(1, M)$, $C_8^{(12)}(1, M) = C_8^{(31)}(1, M)$, and $C_8^{(12,23)}(1, M) = C_8^{(23,31)}(1, M)$ due to the conditions of $b = \pm c$, $a = 0$, and $\beta = \gamma$. We also have $C_8^{(31,12)}(1, M) = 0$ and $C_6^{(31,12)}(1, M) \neq 0$ because $\alpha = \pi/2$ and $M_t - M$ can be either even or odd in Eq. (3.28). We find that, for the case of finite nuclear mass, the additive dispersion coefficients increase, as shown in Tables 4.16-4.23. The nonadditive terms may still be important in constructing the three-body potential surface for He($n_0\,^\lambda S$)-He($n_0\,^\lambda S$)-Li($n_0'\,^\lambda P$). The potential energy curves of the He($1\,^1S$)-He($1\,^1S$)-He($2\,^1P$), He($2\,^1S$)-He($2\,^1S$)-He($2\,^1P$), and He($2\,^3S$)-He($2\,^3S$)-He($2\,^3P$) systems, resulting from $\Delta E^{(1)}$ and $\Delta E^{(2)}$ for this geometrical structure, are shown in Figs. 4.5-4.7.

4.3.4 Dispersion Coefficients for a Straight Line Configuration

For $\lambda_1 = \frac{1}{2}$ and $\lambda_2 = 1$, solving the eigenvalue problem of the above matrix (Eq.(4.21)) for a straight line, one obtains the eigenvalues: $\frac{H'_{12}}{16}\left(1 + 3\sqrt{57}\right)$, $\frac{H'_{12}}{16}\left(1 - 3\sqrt{57}\right)$, $-\frac{H'_{12}}{8}$, and the corresponding orthonormalized zeroth-order wave functions:

Table 4.14: The additive long-range coefficients $C_3^{(IJ)}(1, M = 0)$ of the He($n_0\,^\lambda S$)-He($n_0\,^\lambda S$)-He($n_0'\,^\lambda P$) system for three different types of the zeroth-order wave functions, where the three atoms form an isosceles right triangle, in atomic units. The numbers in parentheses represent the computational uncertainties.

Atom	State	$C_3^{(12)}(1, M = 0)$	$C_3^{(23)}(1, M = 0)$	$C_3^{(31)}(1, M = 0)$
			He($1\,^1S$)-He($1\,^1S$)-He($2\,^1P$)	
$^\infty$He	$\Psi_{1,\perp}^{(0)}$	−0.12423042900(3)	−0.09950832371(2)	−0.12423042900(3)
	$\Psi_{2,\perp}^{(0)}$	0.12423042900(3)	−0.07754727902(2)	0.12423042900(3)
	$\Psi_{3,\perp}^{(0)}$	0	0.17705560274(4)	0
^{4}He	$\Psi_{1,\perp}^{(0)}$	−0.12424511294(3)	−0.09952008553(3)	−0.12424511294(3)
	$\Psi_{2,\perp}^{(0)}$	0.12424511294(3)	−0.07755644505(2)	0.12424511294(3)
	$\Psi_{3,\perp}^{(0)}$	0	0.17707653057(4)	0
^{3}He	$\Psi_{1,\perp}^{(0)}$	−0.12424991885(3)	−0.09952393504(2)	−0.12424991885(3)
	$\Psi_{2,\perp}^{(0)}$	0.12424991885(3)	−0.07755944500(2)	0.12424991885(3)
	$\Psi_{3,\perp}^{(0)}$	0	0.17708338005(4)	0
			He($2\,^1S$)-He($2\,^1S$)-He($2\,^1P$)	
$^\infty$He	$\Psi_{1,\perp}^{(0)}$	−5.967386502392(3)	−4.779864584036(3)	−5.967386502392(3)
	$\Psi_{2,\perp}^{(0)}$	5.967386502392(3)	−3.724969718586(3)	5.967386502392(3)
	$\Psi_{3,\perp}^{(0)}$	0	8.504834302621(5)	0
^{4}He	$\Psi_{1,\perp}^{(0)}$	−5.969517041890(1)	−4.781571141887(1)	−5.969517041890(1)
	$\Psi_{2,\perp}^{(0)}$	5.969517041890(1)	−3.7262996467049(5)	5.969517041890(1)
	$\Psi_{3,\perp}^{(0)}$	0	8.507870788594(3)	0
^{3}He	$\Psi_{1,\perp}^{(0)}$	−5.970214176471(1)	−4.782129545285(1)	−5.970214176471(1)
	$\Psi_{2,\perp}^{(0)}$	5.970214176471(1)	−3.7267348129549(6)	5.970214176471(1)
	$\Psi_{3,\perp}^{(0)}$	0	8.508864358240(2)	0
			He($2\,^3S$)-He($2\,^3S$)-He($2\,^3P$)	
$^\infty$He	$\Psi_{1,\perp}^{(0)}$	−4.4959724006039(1)	− 3.60126484849465(7)	−4.4959724006039(1)
	$\Psi_{2,\perp}^{(0)}$	4.4959724006039(1)	−2.80648170537100(5)	4.4959724006039(1)
	$\Psi_{3,\perp}^{(0)}$	0	6.4077465538656(1)	0
^{4}He	$\Psi_{1,\perp}^{(0)}$	−4.4969133128944(1)	−3.6020185173466(1)	−4.4969133128944(1)
	$\Psi_{2,\perp}^{(0)}$	4.4969133128944(1)	−2.8070690428577(1)	4.4969133128944(1)
	$\Psi_{3,\perp}^{(0)}$	0	6.4090875602043(2)	0
^{3}He	$\Psi_{1,\perp}^{(0)}$	−4.4972211537555(1)	−3.6022650972570(1)	−4.4972211537555(1)
	$\Psi_{2,\perp}^{(0)}$	4.4972211537555(1)	−2.8072612036780(1)	4.4972211537555(1)
	$\Psi_{3,\perp}^{(0)}$	0	6.4095263009351(2)	0

Table 4.15: The additive long-range coefficients $C_3^{(IJ)}(1, M = \pm 1)$ of the He($n_0\,^\lambda S$)-He($n_0\,^\lambda S$)-He($n_0'\,^\lambda P$) system for three different types of the zeroth-order wave functions, where the three atoms form an isosceles right triangle, in atomic units. The numbers in parentheses represent the computational uncertainties.

Atom	State	$C_3^{(12)}(1, M = \pm 1)$	$C_3^{(23)}(1, M = \pm 1)$	$C_3^{(31)}(1, M = \pm 1)$
			He($1\,^1S$)-He($1\,^1S$)-He($2\,^1P$)	
$^\infty$He	$\Psi_{1,\perp}^{(0)}$	0.06211521449(1)	0.04975416185(1)	0.06211521449(1)
	$\Psi_{2,\perp}^{(0)}$	−0.06211521449(1)	0.03877363951(1)	−0.06211521449(1)
	$\Psi_{3,\perp}^{(0)}$	0	−0.08852780137(2)	0
^{4}He	$\Psi_{1,\perp}^{(0)}$	0.06212255646(1)	0.04976004277(2)	0.06212255646(1)
	$\Psi_{2,\perp}^{(0)}$	−0.06212255646(1)	0.03877822252(1)	−0.06212255646(1)
	$\Psi_{3,\perp}^{(0)}$	0	−0.08853826528(2)	0
^{3}He	$\Psi_{1,\perp}^{(0)}$	0.06212495943(2)	0.04976196752(1)	0.06212495943(2)
	$\Psi_{2,\perp}^{(0)}$	−0.06212495943(2)	0.03877972250(1)	−0.06212495943(2)
	$\Psi_{3,\perp}^{(0)}$	0	−0.08854169002(2)	0
			He($2\,^1S$)-He($2\,^1S$)-He($2\,^1P$)	
$^\infty$He	$\Psi_{1,\perp}^{(0)}$	2.983693251196(1)	2.389932292017(1)	2.983693251196(1)
	$\Psi_{2,\perp}^{(0)}$	−2.983693251196(1)	1.862484859292(1)	−2.983693251196(1)
	$\Psi_{3,\perp}^{(0)}$	0	−4.252417151311(3)	0
^{4}He	$\Psi_{1,\perp}^{(0)}$	2.9847585209452(5)	2.3907855709437(4)	2.9847585209452(5)
	$\Psi_{2,\perp}^{(0)}$	−2.9847585209452(5)	1.8631498233525(3)	−2.9847585209452(5)
	$\Psi_{3,\perp}^{(0)}$	0	−4.2539353942961(5)	0
^{3}He	$\Psi_{1,\perp}^{(0)}$	2.9851070882359(5)	2.3910647726425(5)	2.9851070882359(5)
	$\Psi_{2,\perp}^{(0)}$	−2.9851070882359(5)	1.8633674064774(3)	−2.9851070882359(5)
	$\Psi_{3,\perp}^{(0)}$	0	−4.254432179120(1)	0
			He($2\,^3S$)-He($2\,^3S$)-He($2\,^3P$)	
$^\infty$He	$\Psi_{1,\perp}^{(0)}$	2.24798620030195(5)	1.80063242424733(4)	2.24798620030195(5)
	$\Psi_{2,\perp}^{(0)}$	−2.24798620030195(5)	1.40324085268549(2)	−2.24798620030195(5)
	$\Psi_{3,\perp}^{(0)}$	0	−3.20387327693284(7)	0
^{4}He	$\Psi_{1,\perp}^{(0)}$	2.24845665644723(5)	1.80100925867330(4)	2.24845665644723(5)
	$\Psi_{2,\perp}^{(0)}$	−2.24845665644723(5)	1.40353452142883(3)	−2.24845665644723(5)
	$\Psi_{3,\perp}^{(0)}$	0	−3.2045437801021(1)	0
^{3}He	$\Psi_{1,\perp}^{(0)}$	2.24861057687777(6)	1.80113254862853(5)	2.24861057687777(6)
	$\Psi_{2,\perp}^{(0)}$	−2.24861057687777(6)	1.40363060183901(4)	−2.24861057687777(6)
	$\Psi_{3,\perp}^{(0)}$	0	−3.2047631504675(1)	0

Table 4.16: The additive and nonadditive dispersion coefficients $C_6^{(IJ)}(1, M = 0)$ of the He($n_0\,^\lambda S$)-He($n_0\,^\lambda S$)-He($n_0'\,^\lambda P$) system for three different types of the zeroth-order wave functions, where the three atoms form an isosceles right triangle, in atomic units. The numbers in parentheses represent the computational uncertainties.

Atom	State	$C_6^{(12)}(1, M = 0)$	$C_6^{(23)}(1, M = 0)$	$C_6^{(31)}(1, M = 0)$
		He($1\,^1S$)-He($1\,^1S$)-He($2\,^1P$)		
$^\infty$He	$\Psi_{1,\perp}^{(0)}$	23.8806359344(2)	18.9858587822(2)	23.8806359344(2)
	$\Psi_{2,\perp}^{(0)}$	25.8144675944(2)	15.1181954622(1)	25.8144675944(2)
	$\Psi_{3,\perp}^{(0)}$	17.0520271221(1)	32.6430764067(3)	17.0520271221(1)
^{4}He	$\Psi_{1,\perp}^{(0)}$	23.90102210213(6)	19.00204412073(4)	23.90102210213(6)
	$\Psi_{2,\perp}^{(0)}$	25.83651342833(7)	15.13106146836(4)	25.83651342833(7)
	$\Psi_{3,\perp}^{(0)}$	17.0665527946(1)	32.6709827359(1)	17.0665527946(1)
^{3}He	$\Psi_{1,\perp}^{(0)}$	23.9076953644(1)	19.0073422734(1)	23.9076953644(1)
	$\Psi_{2,\perp}^{(0)}$	25.8437299699(2)	15.1352730627(1)	25.8437299699(2)
	$\Psi_{3,\perp}^{(0)}$	17.0713076681(1)	32.6801176662(2)	17.0713076681(1)
		He($2\,^1S$)-He($2\,^1S$)-He($2\,^1P$)		
$^\infty$He	$\Psi_{1,\perp}^{(0)}$	6083.83(6)	7209.77(4)	6083.83(6)
	$\Psi_{2,\perp}^{(0)}$	5639.00(7)	8099.47(4)	5639.00(7)
	$\Psi_{3,\perp}^{(0)}$	7654.62(4)	4068.2(1)	7654.62(4)
^{4}He	$\Psi_{1,\perp}^{(0)}$	6088.31(6)	7214.73(4)	6088.31(6)
	$\Psi_{2,\perp}^{(0)}$	5643.28(7)	8104.81(4)	5643.28(7)
	$\Psi_{3,\perp}^{(0)}$	7659.77(4)	4071.8(1)	7659.77(4)
^{3}He	$\Psi_{1,\perp}^{(0)}$	6089.77(6)	7216.37(5)	6089.77(6)
	$\Psi_{2,\perp}^{(0)}$	5644.67(6)	8106.56(4)	5644.67(6)
	$\Psi_{3,\perp}^{(0)}$	7661.47(5)	4073.0(1)	7661.47(5)
		He($2\,^3S$)-He($2\,^3S$)-He($2\,^3P$)		
$^\infty$He	$\Psi_{1,\perp}^{(0)}$	2259.9491(2)	2481.9271(2)	2259.9491(2)
	$\Psi_{2,\perp}^{(0)}$	2172.2499(2)	2657.3257(3)	2172.2499(2)
	$\Psi_{3,\perp}^{(0)}$	2569.6263(2)	1862.5727(2)	2569.6263(2)
^{4}He	$\Psi_{1,\perp}^{(0)}$	2261.3772(2)	2483.6501(2)	2261.3772(2)
	$\Psi_{2,\perp}^{(0)}$	2173.5613(1)	2659.2815(2)	2173.5613(1)
	$\Psi_{3,\perp}^{(0)}$	2571.4658(2)	1863.4728(2)	2571.4658(2)
^{3}He	$\Psi_{1,\perp}^{(0)}$	2261.8446(2)	2484.2141(2)	2261.8446(2)
	$\Psi_{2,\perp}^{(0)}$	2173.9907(2)	2659.9219(2)	2173.9907(2)
	$\Psi_{3,\perp}^{(0)}$	2572.0680(2)	1863.7672(1)	2572.0680(2)

Table 4.17: The additive and nonadditive dispersion coefficients $C_6^{(IJ,JK)}(1, M = 0)$ of the He($n_0\,^\lambda S$)-He($n_0\,^\lambda S$)-He($n_0'\,^\lambda P$) system for three different types of the zeroth-order wave functions, where the three atoms form an isosceles right triangle, in atomic units. The numbers in parentheses represent the computational uncertainties.

Atom	State	$C_6^{(12,23)}(1, M = 0)$	$C_6^{(23,31)}(1, M = 0)$	$C_6^{(31,12)}(1, M = 0)$
		He($1\,^1S$)-He($1\,^1S$)-He($2\,^1P$)		
$^\infty$He	$\Psi_{1,\perp}^{(0)}$	0.3350550348(2)	0.3350550348(2)	0.2683784091(1)
	$\Psi_{2,\perp}^{(0)}$	−0.3350550348(2)	−0.3350550348(2)	0.2091484871(1)
	$\Psi_{3,\perp}^{(0)}$	0	0	−0.4775268962(1)
^{4}He	$\Psi_{1,\perp}^{(0)}$	0.3352540193(1)	0.3352540193(1)	0.2685377950(1)
	$\Psi_{2,\perp}^{(0)}$	−0.3352540193(1)	−0.3352540193(1)	0.20927269742(7)
	$\Psi_{3,\perp}^{(0)}$	0	0	−0.4778104925(1)
^{3}He	$\Psi_{1,\perp}^{(0)}$	0.3353191479(1)	0.3353191479(1)	0.2685899629(1)
	$\Psi_{2,\perp}^{(0)}$	−0.3353191479(1)	−0.3353191479(1)	0.2093133520(1)
	$\Psi_{3,\perp}^{(0)}$	0	0	−0.4779033149(2)
		He($2\,^1S$)-He($2\,^1S$)-He($2\,^1P$)		
$^\infty$He	$\Psi_{1,\perp}^{(0)}$	1344.78239450(6)	1344.78239450(6)	1077.16799276(6)
	$\Psi_{2,\perp}^{(0)}$	−1344.78239450(6)	−1344.78239450(6)	839.44180515(4)
	$\Psi_{3,\perp}^{(0)}$	0	0	−1916.6097979(1)
^{4}He	$\Psi_{1,\perp}^{(0)}$	1345.59042287(7)	1345.59042287(7)	1077.81522183(5)
	$\Psi_{2,\perp}^{(0)}$	−1345.59042287(7)	−1345.59042287(7)	839.94619366(4)
	$\Psi_{3,\perp}^{(0)}$	0	0	−1917.7614155(1)
^{3}He	$\Psi_{1,\perp}^{(0)}$	1345.85488897(6)	1345.85488897(6)	1078.02705866(5)
	$\Psi_{2,\perp}^{(0)}$	−1345.85488897(6)	−1345.85488897(6)	840.11127904(4)
	$\Psi_{3,\perp}^{(0)}$	0	0	−1918.1383377(1)
		He($2\,^3S$)-He($2\,^3S$)-He($2\,^3P$)		
$^\infty$He	$\Psi_{1,\perp}^{(0)}$	396.38743(3)	396.38743(3)	317.50553(2)
	$\Psi_{2,\perp}^{(0)}$	−396.38743(3)	−396.38743(3)	247.43346(1)
	$\Psi_{3,\perp}^{(0)}$	0	0	−564.93901(4)
^{4}He	$\Psi_{1,\perp}^{(0)}$	396.72600(2)	396.72600(2)	317.77673(2)
	$\Psi_{2,\perp}^{(0)}$	−396.72600(2)	−396.72600(2)	247.64483(2)
	$\Psi_{3,\perp}^{(0)}$	0	0	−565.42155(3)
^{3}He	$\Psi_{1,\perp}^{(0)}$	396.83685(2)	396.83685(2)	317.86552(2)
	$\Psi_{2,\perp}^{(0)}$	−396.83685(2)	−396.83685(2)	247.71402(2)
	$\Psi_{3,\perp}^{(0)}$	0	0	−565.57955(4)

Table 4.18: The additive and nonadditive dispersion coefficients $C_6^{(IJ)}(1, M = \pm 1)$ of the He($n_0\,^\lambda S$)-He($n_0\,^\lambda S$)-He($n_0'\,^\lambda P$) system for three different types of the zeroth-order wave functions, where the three atoms form an isosceles right triangle, in atomic units. The numbers in parentheses represent the computational uncertainties.

Atom	State	$C_6^{(12)}(1, M = \pm 1)$	$C_6^{(23)}(1, M = \pm 1)$	$C_6^{(31)}(1, M = \pm 1)$
		He($1\,^1S$)-He($1\,^1S$)-He($2\,^1P$)		
$^\infty$He	$\Psi_{1,\perp}^{(0)}$	33.31028394374(4)	26.35677666137(3)	33.31028394374(4)
	$\Psi_{2,\perp}^{(0)}$	36.0574800084(1)	20.86238453192(2)	36.0574800084(1)
	$\Psi_{3,\perp}^{(0)}$	23.60958059665(2)	45.7581833555(1)	23.60958059665(2)
^{4}He	$\Psi_{1,\perp}^{(0)}$	33.3386010430(2)	26.3791614090(2)	33.3386010430(2)
	$\Psi_{2,\perp}^{(0)}$	36.0881408650(2)	20.8800817651(1)	36.0881408650(2)
	$\Psi_{3,\perp}^{(0)}$	23.6296215870(2)	45.797120320(1)	23.6296215870(2)
^{3}He	$\Psi_{1,\perp}^{(0)}$	33.34787043(2)	26.3864888785(1)	33.34787043(2)
	$\Psi_{2,\perp}^{(0)}$	36.0981774510(2)	20.8858748150(1)	36.0981774510(2)
	$\Psi_{3,\perp}^{(0)}$	23.6361818467(2)	45.8098660236(2)	23.6361818467(2)
		He($2\,^1S$)-He($2\,^1S$)-He($2\,^1P$)		
$^\infty$He	$\Psi_{1,\perp}^{(0)}$	6645.3(2)	7648.6(1)	6645.3(2)
	$\Psi_{2,\perp}^{(0)}$	6248.8(1)	8441.5(2)	6248.8(1)
	$\Psi_{3,\perp}^{(0)}$	8045.0(1)	4849.0(2)	8045.0(1)
^{4}He	$\Psi_{1,\perp}^{(0)}$	6650.1(1)	7653.9(1)	6650.1(1)
	$\Psi_{2,\perp}^{(0)}$	6253.7(2)	8447.1(1)	6253.7(2)
	$\Psi_{3,\perp}^{(0)}$	8050.5(1)	4853.3(2)	8050.5(1)
^{3}He	$\Psi_{1,\perp}^{(0)}$	6651.9(2)	7655.7(1)	6651.9(2)
	$\Psi_{2,\perp}^{(0)}$	6255.1(1)	8448.9(1)	6255.1(1)
	$\Psi_{3,\perp}^{(0)}$	8052.3(1)	4854.7(2)	8052.3(1)
		He($2\,^3S$)-He($2\,^3S$)-He($2\,^3P$)		
$^\infty$He	$\Psi_{1,\perp}^{(0)}$	2539.5150(2)	2700.4567(2)	2539.5150(2)
	$\Psi_{2,\perp}^{(0)}$	2475.9300(2)	2827.6266(2)	2475.9300(2)
	$\Psi_{3,\perp}^{(0)}$	2764.0417(2)	2251.4034(2)	2764.0417(2)
^{4}He	$\Psi_{1,\perp}^{(0)}$	2541.0776(2)	2702.2849(2)	2541.0776(2)
	$\Psi_{2,\perp}^{(0)}$	2477.3878(2)	2829.6646(2)	2477.3878(2)
	$\Psi_{3,\perp}^{(0)}$	2765.9749(3)	2252.4906(2)	2765.9749(3)
^{3}He	$\Psi_{1,\perp}^{(0)}$	2541.5891(2)	2702.8833(2)	2541.5891(2)
	$\Psi_{2,\perp}^{(0)}$	2477.8649(2)	2830.3319(3)	2477.8649(2)
	$\Psi_{3,\perp}^{(0)}$	2766.6075(2)	2252.8465(2)	2766.6075(2)

Table 4.19: The additive and nonadditive dispersion coefficients $C_6^{(IJ,JK)}(1, M = \pm 1)$ of the He($n_0\,^\lambda S$)-He($n_0\,^\lambda S$)-He($n_0'\,^\lambda P$) system for three different types of the zeroth-order wave functions, where the three atoms form an isosceles right triangle, in atomic units. The numbers in parentheses represent the computational uncertainties.

Atom	State	$C_6^{(12,23)}(1, M = \pm 1)$	$C_6^{(23,31)}(1, M = \pm 1)$	$C_6^{(31,12)}(1, M = \pm 1)$
		He($1\,^1S$)-He($1\,^1S$)-He($2\,^1P$)		
$^\infty$He	$\Psi_{1,\perp}^{(0)}$	0.08376375874(3)	0.08376375874(3)	−0.5367568179(2)
	$\Psi_{2,\perp}^{(0)}$	−0.08376375874(3)	−0.08376375874(3)	−0.4182969742(2)
	$\Psi_{3,\perp}^{(0)}$	0	0	0.9550537923(3)
^{4}He	$\Psi_{1,\perp}^{(0)}$	0.08381350482(3)	0.08381350482(3)	−0.5370755900(2)
	$\Psi_{2,\perp}^{(0)}$	−0.08381350482(3)	−0.08381350482(3)	−0.4185453947(2)
	$\Psi_{3,\perp}^{(0)}$	0	0	0.9556209849(3)
^{3}He	$\Psi_{1,\perp}^{(0)}$	0.08382978697(3)	0.08382978697(3)	−0.5371799259(1)
	$\Psi_{2,\perp}^{(0)}$	−0.08382978697(3)	−0.08382978697(3)	−0.4186267040(2)
	$\Psi_{3,\perp}^{(0)}$	0	0	0.9558066300(3)
		He($2\,^1S$)-He($2\,^1S$)-He($2\,^1P$)		
$^\infty$He	$\Psi_{1,\perp}^{(0)}$	336.19559863(2)	336.19559863(2)	−2154.3359856(2)
	$\Psi_{2,\perp}^{(0)}$	−336.19559863(2)	−336.19559863(2)	−1678.88361031(8)
	$\Psi_{3,\perp}^{(0)}$	0	0	3833.2195958(2)
^{4}He	$\Psi_{1,\perp}^{(0)}$	336.39760572(2)	336.39760572(2)	−2155.6304436(1)
	$\Psi_{2,\perp}^{(0)}$	−336.39760572(2)	−336.39760572(2)	−1679.89238732(8)
	$\Psi_{3,\perp}^{(0)}$	0	0	3835.5228310(2)
^{3}He	$\Psi_{1,\perp}^{(0)}$	336.46372223(1)	336.46372223(1)	−2156.0541173(1)
	$\Psi_{2,\perp}^{(0)}$	−336.46372223(1)	−336.46372223(1)	−1680.22255808(8)
	$\Psi_{3,\perp}^{(0)}$	0	0	3836.2766754(2)
		He($2\,^3S$)-He($2\,^3S$)-He($2\,^3P$)		
$^\infty$He	$\Psi_{1,\perp}^{(0)}$	99.096858(7)	99.096858(7)	−635.01108(5)
	$\Psi_{2,\perp}^{(0)}$	−99.096858(7)	−99.096858(7)	−494.86694(3)
	$\Psi_{3,\perp}^{(0)}$	0	0	1129.87803(8)
^{4}He	$\Psi_{1,\perp}^{(0)}$	99.181504(7)	99.181504(7)	−635.55347(4)
	$\Psi_{2,\perp}^{(0)}$	−99.181504(7)	−99.181504(7)	−495.28966(4)
	$\Psi_{3,\perp}^{(0)}$	0	0	1130.84312(7)
^{3}He	$\Psi_{1,\perp}^{(0)}$	99.209216(7)	99.209216(7)	−635.73105(4)
	$\Psi_{2,\perp}^{(0)}$	−99.209216(7)	−99.209216(7)	−495.42803(3)
	$\Psi_{3,\perp}^{(0)}$	0	0	1131.1591(1)

Table 4.20: The additive and nonadditive dispersion coefficients $C_8^{(IJ)}(1, M = 0)$ of the He($n_0\,^\lambda S$)-He($n_0\,^\lambda S$)-He($n_0'\,^\lambda P$) system for three different types of the zeroth-order wave functions, where the three atoms form an isosceles right triangle, in atomic units. The numbers in parentheses represent the computational uncertainties.

Atom	State	$C_8^{(12)}(1, M = 0)$	$C_8^{(23)}(1, M = 0)$	$C_8^{(31)}(1, M = 0)$
		He($1\,^1S$)-He($1\,^1S$)-He($2\,^1P$)		
$^\infty$He	$\Psi_{1,\perp}^{(0)}$	288.74400(7)	229.05104(5)	288.74400(7)
	$\Psi_{2,\perp}^{(0)}$	283.83548(8)	181.61624(4)	283.83548(8)
	$\Psi_{3,\perp}^{(0)}$	195.56578(5)	357.4779(1)	195.56578(5)
^{4}He	$\Psi_{1,\perp}^{(0)}$	288.70765(6)	229.02450(5)	288.70765(6)
	$\Psi_{2,\perp}^{(0)}$	283.78149(7)	181.59731(4)	283.78149(7)
	$\Psi_{3,\perp}^{(0)}$	195.53832(5)	357.4056(1)	195.53832(5)
^{3}He	$\Psi_{1,\perp}^{(0)}$	288.69571(7)	229.01576(5)	288.69571(7)
	$\Psi_{2,\perp}^{(0)}$	283.76377(8)	181.59107(4)	283.76377(8)
	$\Psi_{3,\perp}^{(0)}$	195.52927(4)	357.3819(1)	195.52927(4)
		He($2\,^1S$)-He($2\,^1S$)-He($2\,^1P$)		
$^\infty$He	$\Psi_{1,\perp}^{(0)}$	583448(2)	634990(1)	583448(2)
	$\Psi_{2,\perp}^{(0)}$	509746(1)	675213(1)	509746(1)
	$\Psi_{3,\perp}^{(0)}$	636815(1)	419806(2)	636815(1)
^{4}He	$\Psi_{1,\perp}^{(0)}$	583741(2)	635300(2)	583741(2)
	$\Psi_{2,\perp}^{(0)}$	509930(2)	675539(1)	509930(2)
	$\Psi_{3,\perp}^{(0)}$	637098(2)	419931(1)	637098(2)
^{3}He	$\Psi_{1,\perp}^{(0)}$	583838(1)	635402(2)	583838(1)
	$\Psi_{2,\perp}^{(0)}$	509991(2)	675646(1)	509991(2)
	$\Psi_{3,\perp}^{(0)}$	637193(1)	419971(3)	637193(1)
		He($2\,^3S$)-He($2\,^3S$)-He($2\,^3P$)		
$^\infty$He	$\Psi_{1,\perp}^{(0)}$	180041.652(6)	187152.67(1)	180041.652(6)
	$\Psi_{2,\perp}^{(0)}$	129184.040(6)	192320.01(1)	129184.040(6)
	$\Psi_{3,\perp}^{(0)}$	173264.08(1)	103017.090(3)	173264.08(1)
^{4}He	$\Psi_{1,\perp}^{(0)}$	180081.111(5)	187205.577(8)	180081.111(5)
	$\Psi_{2,\perp}^{(0)}$	129223.211(4)	192383.58(1)	129223.211(4)
	$\Psi_{3,\perp}^{(0)}$	173324.043(8)	103039.204(2)	173324.043(8)
^{3}He	$\Psi_{1,\perp}^{(0)}$	180094.022(5)	187222.890(8)	180094.022(5)
	$\Psi_{2,\perp}^{(0)}$	129236.034(5)	192404.39(1)	129236.034(5)
	$\Psi_{3,\perp}^{(0)}$	173343.67(1)	103046.443(2)	173343.67(1)

Table 4.21: The additive and nonadditive dispersion coefficients $C_8^{(IJ,JK)}(1, M = 0)$ of the He($n_0\,^\lambda S$)-He($n_0\,^\lambda S$)-He($n_0'\,^\lambda P$) system for three different types of the zeroth-order wave functions, where the three atoms form an isosceles right triangle, in atomic units. The numbers in parentheses represent the computational uncertainties.

Atom	State	$C_8^{(12,23)}(1, M = 0)$	$C_8^{(23,31)}(1, M = 0)$	$C_8^{(31,12)}(1, M = 0)$
		He($1\,^1S$)-He($1\,^1S$)-He($2\,^1P$)		
$^\infty$He	$\Psi_{1,\perp}^{(0)}$	1.499466182(2)	1.499466182(2)	0
	$\Psi_{2,\perp}^{(0)}$	−1.499466182(2)	−1.499466182(2)	0
	$\Psi_{3,\perp}^{(0)}$	0	0	0
^{4}He	$\Psi_{1,\perp}^{(0)}$	1.500072280(1)	1.500072280(1)	0
	$\Psi_{2,\perp}^{(0)}$	−1.500072280(1)	−1.500072280(1)	0
	$\Psi_{3,\perp}^{(0)}$	0	0	0
^{3}He	$\Psi_{1,\perp}^{(0)}$	1.500270660(2)	1.500270660(2)	0
	$\Psi_{2,\perp}^{(0)}$	−1.500270660(2)	−1.500270660(2)	0
	$\Psi_{3,\perp}^{(0)}$	0	0	0
		He($2\,^1S$)-He($2\,^1S$)-He($2\,^1P$)		
$^\infty$He	$\Psi_{1,\perp}^{(0)}$	95507.0172(1)	95507.0172(1)	0
	$\Psi_{2,\perp}^{(0)}$	−95507.0172(1)	−95507.0172(1)	0
	$\Psi_{3,\perp}^{(0)}$	0	0	0
^{4}He	$\Psi_{1,\perp}^{(0)}$	95561.8053(1)	95561.8053(1)	0
	$\Psi_{2,\perp}^{(0)}$	−95561.8053(1)	−95561.8053(1)	0
	$\Psi_{3,\perp}^{(0)}$	0	0	0
^{3}He	$\Psi_{1,\perp}^{(0)}$	95579.7342(1)	95579.7342(1)	0
	$\Psi_{2,\perp}^{(0)}$	−95579.7342(1)	−95579.7342(1)	0
	$\Psi_{3,\perp}^{(0)}$	0	0	0
		He($2\,^3S$)-He($2\,^3S$)-He($2\,^3P$)		
$^\infty$He	$\Psi_{1,\perp}^{(0)}$	29198.229411(6)	29198.229411(6)	0
	$\Psi_{2,\perp}^{(0)}$	−29198.229411(6)	−29198.229411(6)	0
	$\Psi_{3,\perp}^{(0)}$	0	0	0
^{4}He	$\Psi_{1,\perp}^{(0)}$	29207.550197(6)	29207.550197(6)	0
	$\Psi_{2,\perp}^{(0)}$	−29207.550197(6)	−29207.550197(6)	0
	$\Psi_{3,\perp}^{(0)}$	0	0	0
^{3}He	$\Psi_{1,\perp}^{(0)}$	29210.600188(6)	29210.600188(6)	0
	$\Psi_{2,\perp}^{(0)}$	−29210.600188(6)	−29210.600188(6)	0
	$\Psi_{3,\perp}^{(0)}$	0	0	0

Table 4.22: The additive and nonadditive dispersion coefficients $C_8^{(IJ)}(1, M = \pm 1)$ of the He($n_0\,^\lambda S$)-He($n_0\,^\lambda S$)-He($n_0'\,^\lambda P$) system for three different types of the zeroth-order wave functions, where the three atoms form an isosceles right, in atomic units. The numbers in parentheses represent the computational uncertainties.

Atom	State	$C_8^{(12)}(1, M = \pm 1)$	$C_8^{(23)}(1, M = \pm 1)$	$C_8^{(31)}(1, M = \pm 1)$
		He($1\,^1S$)-He($1\,^1S$)-He($2\,^1P$)		
$^\infty$He	$\Psi_{1,\perp}^{(0)}$	3632.59793(8)	2841.52234(6)	3632.59793(8)
	$\Psi_{2,\perp}^{(0)}$	4060.2445(1)	2217.52675(5)	4060.2445(1)
	$\Psi_{3,\perp}^{(0)}$	2568.98676(5)	5202.7801(1)	2568.98676(5)
^{4}He	$\Psi_{1,\perp}^{(0)}$	3635.18318(8)	2843.54441(6)	3635.18318(8)
	$\Psi_{2,\perp}^{(0)}$	4063.1051(1)	2219.10430(5)	4063.1051(1)
	$\Psi_{3,\perp}^{(0)}$	2570.80469(6)	5206.4442(1)	2570.80469(6)
^{3}He	$\Psi_{1,\perp}^{(0)}$	3636.02933(8)	2844.20623(6)	3636.02933(8)
	$\Psi_{2,\perp}^{(0)}$	4064.04135(9)	2219.62063(5)	4064.04135(9)
	$\Psi_{3,\perp}^{(0)}$	2571.3997(1)	5207.6434(1)	2571.3997(1)
		He($2\,^1S$)-He($2\,^1S$)-He($2\,^1P$)		
$^\infty$He	$\Psi_{1,\perp}^{(0)}$	667645(3)	687265(2)	667645(3)
	$\Psi_{2,\perp}^{(0)}$	2062939(3)	715953(1)	2062939(3)
	$\Psi_{3,\perp}^{(0)}$	1182611(2)	2509977(5)	1182611(2)
^{4}He	$\Psi_{1,\perp}^{(0)}$	668073(3)	687674(2)	668073(3)
	$\Psi_{2,\perp}^{(0)}$	2064160(4)	716353(2)	2064160(4)
	$\Psi_{3,\perp}^{(0)}$	1183287(2)	2511492(5)	1183287(2)
^{3}He	$\Psi_{1,\perp}^{(0)}$	668211(4)	687808(2)	668211(4)
	$\Psi_{2,\perp}^{(0)}$	2064560(4)	716485(2)	2064560(4)
	$\Psi_{3,\perp}^{(0)}$	1183508(2)	2511988(5)	1183508(2)
		He($2\,^3S$)-He($2\,^3S$)-He($2\,^3P$)		
$^\infty$He	$\Psi_{1,\perp}^{(0)}$	237067.32(2)	227335.45(2)	237067.32(2)
	$\Psi_{2,\perp}^{(0)}$	665396.89(2)	223634.63(2)	665396.89(2)
	$\Psi_{3,\perp}^{(0)}$	371010.24(1)	822504.39(2)	371010.24(1)
^{4}He	$\Psi_{1,\perp}^{(0)}$	237122.07(2)	227399.29(2)	237122.07(2)
	$\Psi_{2,\perp}^{(0)}$	665562.05(2)	223706.73(2)	665562.05(2)
	$\Psi_{3,\perp}^{(0)}$	371117.31(2)	822695.40(2)	371117.31(2)
^{3}He	$\Psi_{1,\perp}^{(0)}$	237139.98(2)	227420.17(1)	237139.98(2)
	$\Psi_{2,\perp}^{(0)}$	665616.07(1)	223730.31(1)	665616.07(1)
	$\Psi_{3,\perp}^{(0)}$	371152.34(2)	822757.90(2)	371152.34(2)

Table 4.23: The additive and nonadditive dispersion coefficients $C_8^{(IJ,JK)}(1, M = \pm 1)$ of the He($n_0\,^\lambda S$)-He($n_0\,^\lambda S$)-He($n_0'\,^\lambda P$) system for three different types of the zeroth-order wave functions, where the three atoms form an isosceles right, in atomic units. The numbers in parentheses represent the computational uncertainties.

Atom	State	$C_8^{(12,23)}(1, M = \pm 1)$	$C_8^{(23,31)}(1, M = \pm 1)$	$C_8^{(31,12)}(1, M = \pm 1)$
		He($1\,^1S$)-He($1\,^1S$)-He($2\,^1P$)		
$^\infty$He	$\Psi_{1,\perp}^{(0)}$	−1.686899453(1)	−1.686899453(1)	0
	$\Psi_{2,\perp}^{(0)}$	1.686899453(1)	1.686899453(1)	0
	$\Psi_{3,\perp}^{(0)}$	0	0	0
^{4}He	$\Psi_{1,\perp}^{(0)}$	−1.687581315(1)	−1.687581315(1)	0
	$\Psi_{2,\perp}^{(0)}$	1.687581315(1)	1.687581315(1)	0
	$\Psi_{3,\perp}^{(0)}$	0	0	0
^{3}He	$\Psi_{1,\perp}^{(0)}$	−1.687804492(2)	−1.687804492(2)	0
	$\Psi_{2,\perp}^{(0)}$	1.687804492(2)	1.687804492(2)	0
	$\Psi_{3,\perp}^{(0)}$	0	0	0
		He($2\,^1S$)-He($2\,^1S$)-He($2\,^1P$)		
$^\infty$He	$\Psi_{1,\perp}^{(0)}$	−107445.3945(2)	−107445.3945(2)	0
	$\Psi_{2,\perp}^{(0)}$	107445.3945(2)	107445.3945(2)	0
	$\Psi_{3,\perp}^{(0)}$	0	0	0
^{4}He	$\Psi_{1,\perp}^{(0)}$	−107507.0311(2)	−107507.0311(2)	0
	$\Psi_{2,\perp}^{(0)}$	107507.0311(2)	107507.0311(2)	0
	$\Psi_{3,\perp}^{(0)}$	0	0	0
^{3}He	$\Psi_{1,\perp}^{(0)}$	−107527.2011(2)	−107527.2011(2)	0
	$\Psi_{2,\perp}^{(0)}$	107527.2011(2)	107527.2011(2)	0
	$\Psi_{3,\perp}^{(0)}$	0	0	0
		He($2\,^3S$)-He($2\,^3S$)-He($2\,^3P$)		
$^\infty$He	$\Psi_{1,\perp}^{(0)}$	−32848.008087(7)	−32848.008087(7)	0
	$\Psi_{2,\perp}^{(0)}$	32848.008087(7)	32848.008087(7)	0
	$\Psi_{3,\perp}^{(0)}$	0	0	0
^{4}He	$\Psi_{1,\perp}^{(0)}$	−32858.493972(7)	−32858.493972(7)	0
	$\Psi_{2,\perp}^{(0)}$	32858.493972(7)	32858.493972(7)	0
	$\Psi_{3,\perp}^{(0)}$	0	0	0
^{3}He	$\Psi_{1,\perp}^{(0)}$	−32861.925212(7)	−32861.925212(7)	0
	$\Psi_{2,\perp}^{(0)}$	32861.925212(7)	32861.925212(7)	0
	$\Psi_{3,\perp}^{(0)}$	0	0	0

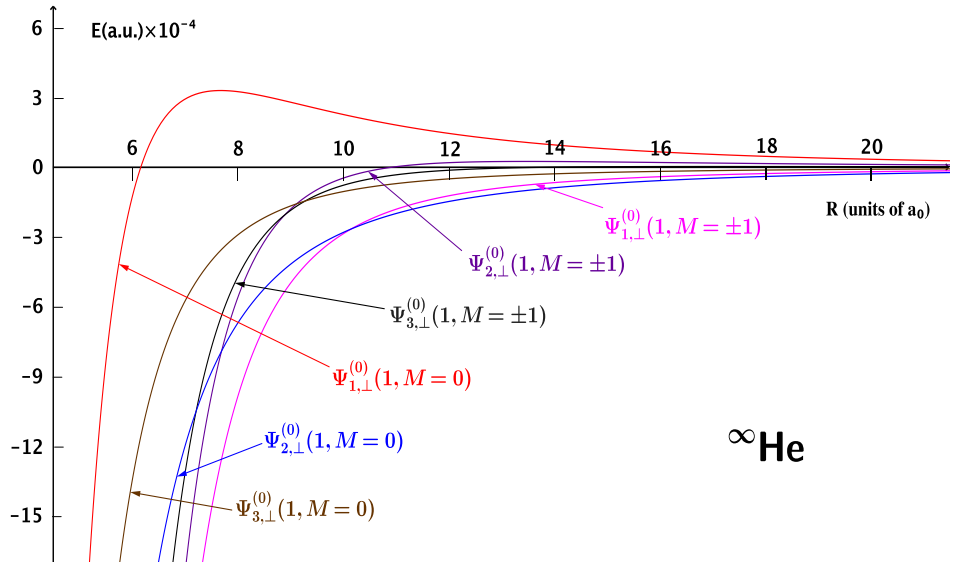

Figure 4.5: Long-range potentials for the He($1\,^1S$)-He($1\,^1S$)-He($2\,^1P$) system for three different types of the zeroth-order wave functions, where the three atoms form an isosceles right triangle, in atomic units. For each curve labeled by a wave function, the plotted curve is the sum of $\Delta E^{(1)}$ and $\Delta E^{(2)}$.

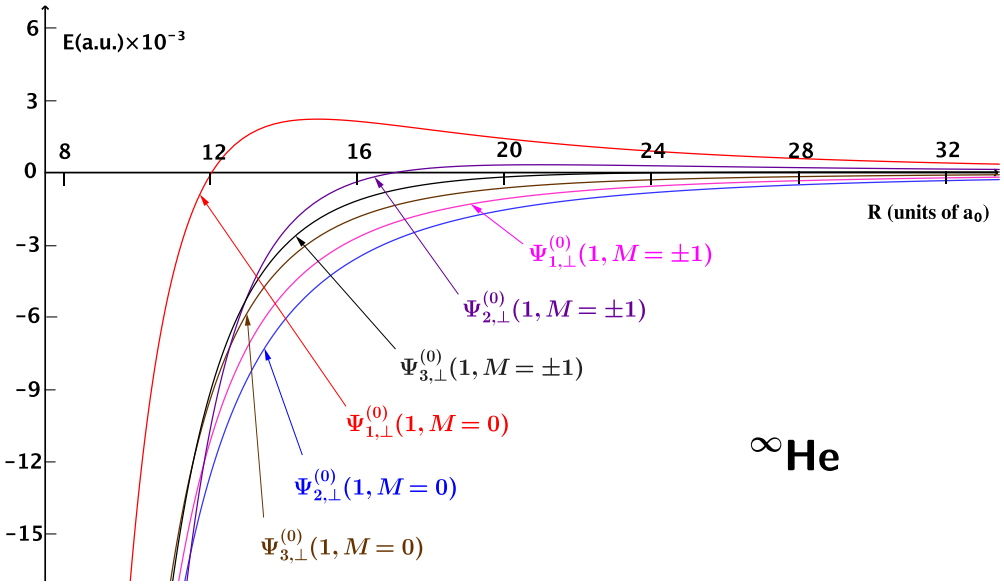

Figure 4.6: Long-range potentials for the He($2\,^1S$)-He($2\,^1S$)-He($2\,^1P$) system for three different types of the zeroth-order wave functions, where the three atoms form an isosceles right triangle, in atomic units. For each curve labeled by a wave function, the plotted curve is the sum of $\Delta E^{(1)}$ and $\Delta E^{(2)}$.

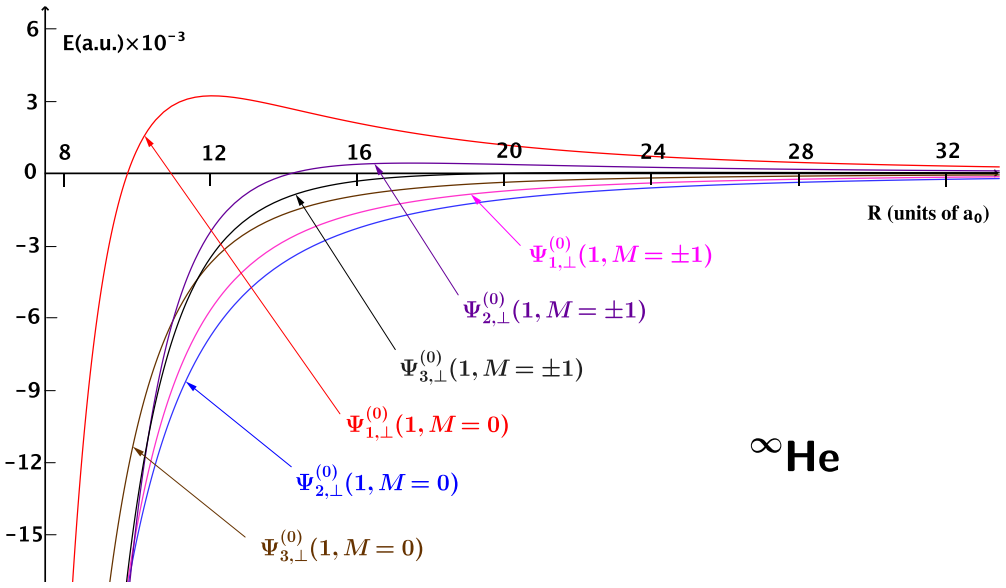

Figure 4.7: Long-range potentials for the He($2\,^3S$)-He($2\,^3S$)-He($2\,^3P$) system for three different types of the zeroth-order wave functions, where the three atoms form an isosceles right triangle, in atomic units. For each curve labeled by a wave function, the plotted curve is the sum of $\Delta E^{(1)}$ and $\Delta E^{(2)}$.

$$\Psi^{(0)}_{1,-} = \frac{3\sqrt{57}-1}{\sqrt{1026-6\sqrt{57}}}|\phi_1\rangle + \frac{16}{\sqrt{1026-6\sqrt{57}}}|\phi_2\rangle + \frac{16}{\sqrt{1026-6\sqrt{57}}}|\phi_3\rangle\,, \tag{4.29}$$

$$\Psi^{(0)}_{2,-} = \frac{-(3\sqrt{57}+1)}{\sqrt{1026+6\sqrt{57}}}|\phi_1\rangle + \frac{16}{\sqrt{1026+6\sqrt{57}}}|\phi_2\rangle + \frac{16}{\sqrt{1026+6\sqrt{57}}}|\phi_3\rangle\,, \tag{4.30}$$

$$\Psi^{(0)}_{3,-} = -\frac{1}{\sqrt{2}}|\phi_2\rangle + \frac{1}{\sqrt{2}}|\phi_3\rangle\,, \tag{4.31}$$

With these zeroth-order wave functions, the long-range interaction coefficients are calculated for the systems of He($1\,^1S$)-He($1\,^1S$)-He($2\,^1P$), He($2\,^1S$)-He($2\,^1S$)-He($2\,^1P$), and He($2\,^3S$)-He($2\,^3S$)-He($2\,^3P$) and their values are listed in Tables 4.24-4.33. Since the zeroth-order wave function coefficients have $b = c$ in Eqs. (4.29) and

Table 4.24: The additive long-range coefficients $C_3^{(IJ)}(1, M = 0)$ of the He($n_0\,^\lambda S$)-He($n_0\,^\lambda S$)-He($n_0'\,^\lambda P$) system for three different types of the zeroth-order wave functions, where the three atoms form a straight line, in atomic units. The numbers in parentheses represent the computational uncertainties.

Atom	State	$C_3^{(12)}(1, M = 0)$	$C_3^{(23)}(1, M = 0)$	$C_3^{(31)}(1, M = 0)$
		He($1\,^1S$)-He($1\,^1S$)-He($2\,^1P$)		
$^\infty$He	$\Psi_{1,-}^{(0)}$	−0.12507513324(3)	−0.09243639928(2)	−0.12507513324(3)
	$\Psi_{2,-}^{(0)}$	0.12507513324(3)	−0.08461920345(2)	0.12507513324(3)
	$\Psi_{3,-}^{(0)}$	0	0.17705560274(4)	0
^{4}He	$\Psi_{1,-}^{(0)}$	−0.12508991701(2)	−0.09244732519(2)	−0.12508991701(2)
	$\Psi_{2,-}^{(0)}$	0.12508991701(2)	−0.08462920538(2)	0.12508991701(2)
	$\Psi_{3,-}^{(0)}$	0	0.17707653057(4)	0
^{3}He	$\Psi_{1,-}^{(0)}$	−0.12509475561(3)	−0.09245090113(2)	−0.12509475561(3)
	$\Psi_{2,-}^{(0)}$	0.12509475561(3)	−0.08463247891(2)	0.12509475561(3)
	$\Psi_{3,-}^{(0)}$	0	0.17708338005(4)	0
		He($2\,^1S$)-He($2\,^1S$)-He($2\,^1P$)		
$^\infty$He	$\Psi_{1,-}^{(0)}$	−6.007961720158(3)	−4.440165955066(3)	−6.007961720158(3)
	$\Psi_{2,-}^{(0)}$	6.007961720158(3)	−4.064668347556(3)	6.007961720158(3)
	$\Psi_{3,-}^{(0)}$	0	8.504834302621(5)	0
^{4}He	$\Psi_{1,-}^{(0)}$	−6.010106746250(1)	−4.4417512301165(7)	−6.010106746250(1)
	$\Psi_{2,-}^{(0)}$	6.010106746250(1)	−4.0661195584758(6)	6.010106746250(1)
	$\Psi_{3,-}^{(0)}$	0	8.507870788593(2)	0
^{3}He	$\Psi_{1,-}^{(0)}$	−6.010808620995(1)	−4.442269948526(1)	−6.010808620995(1)
	$\Psi_{2,-}^{(0)}$	6.010808620995(1)	−4.066594409714(1)	6.010808620995(1)
	$\Psi_{3,-}^{(0)}$	0	8.508864358240(2)	0
		He($2\,^3S$)-He($2\,^3S$)-He($2\,^3P$)		
$^\infty$He	$\Psi_{1,-}^{(0)}$	−4.52654274478244(8)	−3.34532773770729(7)	−4.52654274478244(8)
	$\Psi_{2,-}^{(0)}$	4.52654274478244(8)	−3.06241881615838(6)	4.52654274478244(8)
	$\Psi_{3,-}^{(0)}$	0	6.4077465538656(1)	0
^{4}He	$\Psi_{1,-}^{(0)}$	−4.5274900548019(1)	−3.34602784431470(8)	−4.5274900548019(1)
	$\Psi_{2,-}^{(0)}$	4.5274900548019(1)	−3.0630597158896(1)	4.5274900548019(1)
	$\Psi_{3,-}^{(0)}$	0	6.4090875602043(2)	0
^{3}He	$\Psi_{1,-}^{(0)}$	−4.5277999888255(1)	−3.3462569001183(1)	−4.5277999888255(1)
	$\Psi_{2,-}^{(0)}$	4.5277999888255(1)	−3.0632694008167(1)	4.5277999888255(1)
	$\Psi_{3,-}^{(0)}$	0	6.4095263009351(2)	0

Table 4.25: The additive long-range coefficients $C_3^{(IJ)}(1, M = \pm 1)$ of the He($n_0\,^\lambda S$)-He($n_0\,^\lambda S$)-He($n_0'\,^\lambda P$) system for three different types of the zeroth-order wave functions, where the three atoms form a straight line, in atomic units. The numbers in parentheses represent the computational uncertainties.

Atom	State	$C_3^{(12)}(1, M = \pm 1)$	$C_3^{(23)}(1, M = \pm 1)$	$C_3^{(31)}(1, M = \pm 1)$
		He($1\,^1S$)-He($1\,^1S$)-He($2\,^1P$)		
$^\infty$He	$\Psi_{1,-}^{(0)}$	0.06253756661(1)	0.04621819964(1)	0.06253756661(1)
	$\Psi_{2,-}^{(0)}$	−0.06253756661(1)	0.04230960172(1)	−0.06253756661(1)
	$\Psi_{3,-}^{(0)}$	0	−0.08852780137(2)	0
^{4}He	$\Psi_{1,-}^{(0)}$	0.06254495850(1)	0.04622366259(1)	0.06254495850(1)
	$\Psi_{2,-}^{(0)}$	−0.06254495850(1)	0.04231460269(1)	−0.06254495850(1)
	$\Psi_{3,-}^{(0)}$	0	−0.08853826528(2)	0
^{3}He	$\Psi_{1,-}^{(0)}$	0.06254737781(2)	0.04622545056(1)	0.06254737781(2)
	$\Psi_{2,-}^{(0)}$	−0.06254737781(2)	0.04231623945(1)	−0.06254737781(2)
	$\Psi_{3,-}^{(0)}$	0	−0.08854169002(2)	0
		He($2\,^1S$)-He($2\,^1S$)-He($2\,^1P$)		
$^\infty$He	$\Psi_{1,-}^{(0)}$	3.003980860078(1)	2.220082977532(1)	3.003980860078(1)
	$\Psi_{2,-}^{(0)}$	−3.003980860078(1)	2.032334173777(1)	−3.003980860078(1)
	$\Psi_{3,-}^{(0)}$	0	−4.252417151311(3)	0
^{4}He	$\Psi_{1,-}^{(0)}$	3.0050533731251(5)	2.2208756150583(4)	3.0050533731251(5)
	$\Psi_{2,-}^{(0)}$	−3.0050533731251(5)	2.0330597792379(3)	−3.0050533731251(5)
	$\Psi_{3,-}^{(0)}$	0	−4.2539353942961(6)	0
^{3}He	$\Psi_{1,-}^{(0)}$	3.0054043104976(5)	2.2211349742630(4)	3.0054043104976(5)
	$\Psi_{2,-}^{(0)}$	−3.0054043104976(5)	2.0332972048568(3)	−3.0054043104976(5)
	$\Psi_{3,-}^{(0)}$	0	−4.2544321791200(8)	0
		He($2\,^3S$)-He($2\,^3S$)-He($2\,^3P$)		
$^\infty$He	$\Psi_{1,-}^{(0)}$	2.26327137239122(4)	1.67266386885365(4)	2.26327137239122(4)
	$\Psi_{2,-}^{(0)}$	−2.26327137239122(4)	1.53120940807919(3)	−2.26327137239122(4)
	$\Psi_{3,-}^{(0)}$	0	−3.20387327693284(7)	0
^{4}He	$\Psi_{1,-}^{(0)}$	2.26374502740096(5)	1.67301392215735(4)	2.26374502740096(5)
	$\Psi_{2,-}^{(0)}$	−2.26374502740096(5)	1.53152985794479(4)	−2.26374502740096(5)
	$\Psi_{3,-}^{(0)}$	0	−3.20454378010215(8)	0
^{3}He	$\Psi_{1,-}^{(0)}$	2.26389999441278(6)	1.67312845005916(4)	2.26389999441278(6)
	$\Psi_{2,-}^{(0)}$	−2.26389999441278(6)	1.53163470040838(5)	−2.26389999441278(6)
	$\Psi_{3,-}^{(0)}$	0	−3.2047631504675(1)	0

Table 4.26: The additive and nonadditive dispersion coefficients $C_6^{(IJ)}(1, M = 0)$ of the He($n_0\,^\lambda S$)-He($n_0\,^\lambda S$)-He($n_0'\,^\lambda P$) system for three different types of the zeroth-order wave functions, where the three atoms form a straight line, in atomic units. The numbers in parentheses represent the computational uncertainties.

Atom	State	$C_6^{(12)}(1, M = 0)$	$C_6^{(23)}(1, M = 0)$	$C_6^{(31)}(1, M = 0)$
		He($1\,^1S$)-He($1\,^1S$)-He($2\,^1P$)		
$^\infty$He	$\Psi_{1,-}^{(0)}$	24.5033709436(3)	17.7403887642(2)	24.5033709436(3)
	$\Psi_{2,-}^{(0)}$	25.1917325854(2)	16.3636654802(1)	25.1917325854(2)
	$\Psi_{3,-}^{(0)}$	17.0520271221(1)	32.6430764067(3)	17.0520271221(1)
^{4}He	$\Psi_{1,-}^{(0)}$	24.5242915590(1)	17.75550520692(5)	24.5242915590(1)
	$\Psi_{2,-}^{(0)}$	25.21324397142(7)	16.37760038218(4)	25.21324397142(7)
	$\Psi_{3,-}^{(0)}$	17.0665527946(1)	32.6709827359(1)	17.0665527946(1)
^{3}He	$\Psi_{1,-}^{(0)}$	24.5311397688(1)	17.7604534647(1)	24.5311397688(1)
	$\Psi_{2,-}^{(0)}$	25.2202855655(2)	16.3821618715(1)	25.2202855655(2)
	$\Psi_{3,-}^{(0)}$	17.0713076681(1)	32.6801176662(2)	17.0713076681(1)
		He($2\,^1S$)-He($2\,^1S$)-He($2\,^1P$)		
$^\infty$He	$\Psi_{1,-}^{(0)}$	5940.58(6)	7496.27(4)	5940.58(6)
	$\Psi_{2,-}^{(0)}$	5782.25(7)	7812.97(4)	5782.25(7)
	$\Psi_{3,-}^{(0)}$	7654.62(4)	4068.2(1)	7654.62(4)
^{4}He	$\Psi_{1,-}^{(0)}$	5945.01(7)	7501.37(5)	5945.01(7)
	$\Psi_{2,-}^{(0)}$	5786.58(6)	7818.18(4)	5786.58(6)
	$\Psi_{3,-}^{(0)}$	7659.77(4)	4071.8(1)	7659.77(4)
^{3}He	$\Psi_{1,-}^{(0)}$	5946.44(6)	7503.02(4)	5946.44(6)
	$\Psi_{2,-}^{(0)}$	5788.00(6)	7819.89(4)	5788.00(6)
	$\Psi_{3,-}^{(0)}$	7661.47(5)	4073.0(1)	7661.47(5)
		He($2\,^3S$)-He($2\,^3S$)-He($2\,^3P$)		
$^\infty$He	$\Psi_{1,-}^{(0)}$	2231.7081(2)	2538.4092(2)	2231.7081(2)
	$\Psi_{2,-}^{(0)}$	2200.4909(2)	2600.8435(2)	2200.4909(2)
	$\Psi_{3,-}^{(0)}$	2569.6263(2)	1862.5727(2)	2569.6263(2)
^{4}He	$\Psi_{1,-}^{(0)}$	2233.0985(1)	2540.2072(2)	2233.0985(1)
	$\Psi_{2,-}^{(0)}$	2201.8400(2)	2602.7245(2)	2201.8400(2)
	$\Psi_{3,-}^{(0)}$	2571.4658(2)	1863.4728(2)	2571.4658(2)
^{3}He	$\Psi_{1,-}^{(0)}$	2233.5538(2)	2540.7957(2)	2233.5538(2)
	$\Psi_{2,-}^{(0)}$	2202.2814(1)	2603.3402(2)	2202.2814(1)
	$\Psi_{3,-}^{(0)}$	2572.0680(2)	1863.7672(1)	2572.0680(2)

Table 4.27: The additive and nonadditive dispersion coefficients $C_6^{(IJ,JK)}(1, M = 0)$ of the He($n_0\,^\lambda S$)-He($n_0\,^\lambda S$)-He($n_0'\,^\lambda P$) system for three different types of the zeroth-order wave functions, where the three atoms form a straight line, in atomic units. The numbers in parentheses represent the computational uncertainties.

Atom	State	$C_6^{(12,23)}(1, M = 0)$	$C_6^{(23,31)}(1, M = 0)$	$C_6^{(31,12)}(1, M = 0)$
		He($1\,^1S$)-He($1\,^1S$)-He($2\,^1P$)		
$^\infty$He	$\Psi_{1,-}^{(0)}$	0.3373332400(2)	0.3373332400(2)	0.2493051118(1)
	$\Psi_{2,-}^{(0)}$	−0.3373332400(2)	−0.3373332400(2)	0.2282217843(1)
	$\Psi_{3,-}^{(0)}$	0	0	−0.4775268962(1)
^{4}He	$\Psi_{1,-}^{(0)}$	0.3375335775(1)	0.3375335775(1)	0.2494531705(1)
	$\Psi_{2,-}^{(0)}$	−0.3375335775(1)	−0.3375335775(1)	0.22835732191(9)
	$\Psi_{3,-}^{(0)}$	0	0	−0.4778104925(1)
^{3}He	$\Psi_{1,-}^{(0)}$	0.3375991489(1)	0.3375991489(1)	0.249501629(1)
	$\Psi_{2,-}^{(0)}$	−0.3375991489(1)	−0.3375991489(1)	0.228401683(1)
	$\Psi_{3,-}^{(0)}$	0	0	−0.4779033149(2)
		He($2\,^1S$)-He($2\,^1S$)-He($2\,^1P$)		
$^\infty$He	$\Psi_{1,-}^{(0)}$	1353.92623636(6)	1353.92623636(6)	1000.61509384(5)
	$\Psi_{2,-}^{(0)}$	−1353.92623636(6)	−1353.92623636(6)	915.99470407(5)
	$\Psi_{3,-}^{(0)}$	0	0	−1916.6097979(1)
^{4}He	$\Psi_{1,-}^{(0)}$	1354.73975890(6)	1354.73975890(6)	1001.21632520(4)
	$\Psi_{2,-}^{(0)}$	−1354.73975890(6)	−1354.73975890(6)	916.54509029(5)
	$\Psi_{3,-}^{(0)}$	0	0	−1917.7614155(1)
^{3}He	$\Psi_{1,-}^{(0)}$	1355.00602327(7)	1355.00602327(7)	1001.41310708(5)
	$\Psi_{2,-}^{(0)}$	−1355.00602327(7)	−1355.00602327(7)	916.72523063(5)
	$\Psi_{3,-}^{(0)}$	0	0	−1918.1383377(1)
		He($2\,^3S$)-He($2\,^3S$)-He($2\,^3P$)		
$^\infty$He	$\Psi_{1,-}^{(0)}$	399.08267(3)	399.08267(3)	294.94085(3)
	$\Psi_{2,-}^{(0)}$	−399.08267(3)	−399.08267(3)	269.99817(2)
	$\Psi_{3,-}^{(0)}$	0	0	−564.93901(4)
^{4}He	$\Psi_{1,-}^{(0)}$	399.42355(3)	399.42355(3)	295.19278(3)
	$\Psi_{2,-}^{(0)}$	−399.42355(3)	−399.42355(3)	270.22878(1)
	$\Psi_{3,-}^{(0)}$	0	0	−565.42155(3)
^{3}He	$\Psi_{1,-}^{(0)}$	399.53514(2)	399.53514(2)	295.27524(2)
	$\Psi_{2,-}^{(0)}$	−399.53514(2)	−399.53514(2)	270.30430(2)
	$\Psi_{3,-}^{(0)}$	0	0	−565.57955(4)

Table 4.28: The additive and nonadditive dispersion coefficients $C_6^{(IJ)}(1, M = \pm 1)$ of the He($n_0\,^\lambda S$)-He($n_0\,^\lambda S$)-He($n_0'\,^\lambda P$) system for three different types of the zeroth-order wave functions, where the three atoms form a straight line, in atomic units. The numbers in parentheses represent the computational uncertainties.

Atom	State	$C_6^{(12)}(1, M = \pm 1)$	$C_6^{(23)}(1, M = \pm 1)$	$C_6^{(31)}(1, M = \pm 1)$
		He($1\,^1S$)-He($1\,^1S$)-He($2\,^1P$)		
$^\infty$He	$\Psi_{1,-}^{(0)}$	34.19493962581(4)	24.58746529725(2)	34.19493962581(4)
	$\Psi_{2,-}^{(0)}$	35.17282432641(4)	22.63169589605(2)	35.17282432641(4)
	$\Psi_{3,-}^{(0)}$	23.60958059665(2)	45.7581833555(1)	23.60958059665(2)
^{4}He	$\Psi_{1,-}^{(0)}$	34.2240114649(2)	24.6083405653(2)	34.2240114649(2)
	$\Psi_{2,-}^{(0)}$	35.2027304431(3)	22.6509026088(1)	35.2027304431(3)
	$\Psi_{3,-}^{(0)}$	23.6296215870(2)	45.797120320(1)	23.6296215870(2)
^{3}He	$\Psi_{1,-}^{(0)}$	34.2335278990(2)	24.6151739190(1)	34.2335278990(2)
	$\Psi_{2,-}^{(0)}$	35.2125199713(2)	22.6571897745(1)	35.2125199713(2)
	$\Psi_{3,-}^{(0)}$	23.6361818467(2)	45.8098660236(2)	23.6361818467(2)
		He($2\,^1S$)-He($2\,^1S$)-He($2\,^1P$)		
$^\infty$He	$\Psi_{1,-}^{(0)}$	6517.6(2)	7903.9(1)	6517.6(2)
	$\Psi_{2,-}^{(0)}$	6376.5(2)	8186.1(1)	6376.5(2)
	$\Psi_{3,-}^{(0)}$	8045.0(1)	4849.0(1)	8045.0(1)
^{4}He	$\Psi_{1,-}^{(0)}$	6522.5(2)	7909.3(1)	6522.5(2)
	$\Psi_{2,-}^{(0)}$	6381.4(2)	8191.6(1)	6381.4(2)
	$\Psi_{3,-}^{(0)}$	8050.5(1)	4853.3(2)	8050.5(1)
^{3}He	$\Psi_{1,-}^{(0)}$	6524.0(1)	7911.1(1)	6524.0(1)
	$\Psi_{2,-}^{(0)}$	6382.9(2)	8193.5(1)	6382.9(2)
	$\Psi_{3,-}^{(0)}$	8052.3(1)	4854.7(2)	8052.3(1)
		He($2\,^3S$)-He($2\,^3S$)-He($2\,^3P$)		
$^\infty$He	$\Psi_{1,-}^{(0)}$	2519.0393(2)	2741.4083(3)	2519.0393(2)
	$\Psi_{2,-}^{(0)}$	2496.4058(2)	2786.6752(2)	2496.4058(2)
	$\Psi_{3,-}^{(0)}$	2764.0417(2)	2251.4034(2)	2764.0417(2)
^{4}He	$\Psi_{1,-}^{(0)}$	2520.5681(2)	2743.3039(2)	2520.5681(2)
	$\Psi_{2,-}^{(0)}$	2497.8973(2)	2788.6456(2)	2497.8973(2)
	$\Psi_{3,-}^{(0)}$	2765.9749(3)	2252.4905(1)	2765.9749(3)
^{3}He	$\Psi_{1,-}^{(0)}$	2521.0686(2)	2743.9244(2)	2521.0686(2)
	$\Psi_{2,-}^{(0)}$	2498.3853(1)	2789.2908(3)	2498.3853(1)
	$\Psi_{3,-}^{(0)}$	2766.6075(2)	2252.8465(2)	2766.6075(2)

Table 4.29: The additive and nonadditive dispersion coefficients $C_6^{(IJ,JK)}(1, M = \pm 1)$ of the He($n_0\,^\lambda S$)-He($n_0\,^\lambda S$)-He($n_0'\,^\lambda P$) system for three different types of the zeroth-order wave functions, where the three atoms form a straight line, in atomic units. The numbers in parentheses represent the computational uncertainties.

Atom	State	$C_6^{(12,23)}(1, M = \pm 1)$	$C_6^{(23,31)}(1, M = \pm 1)$	$C_6^{(31,12)}(1, M = \pm 1)$
		He($1\,^1S$)-He($1\,^1S$)-He($2\,^1P$)		
$^\infty$He	$\Psi_{1,-}^{(0)}$	0.8433331004(3)	0.8433331004(3)	0.6232627794(3)
	$\Psi_{2,-}^{(0)}$	−0.8433331004(3)	−0.8433331004(3)	0.5705544608(2)
	$\Psi_{3,-}^{(0)}$	0	0	−1.1938172404(4)
^{4}He	$\Psi_{1,-}^{(0)}$	0.8438339437(3)	0.8438339437(3)	0.6236329263(2)
	$\Psi_{2,-}^{(0)}$	−0.8438339437(3)	−0.8438339437(3)	0.5708933048(2)
	$\Psi_{3,-}^{(0)}$	0	0	−1.1945262311(4)
^{3}He	$\Psi_{1,-}^{(0)}$	0.8439978723(3)	0.8439978723(3)	0.6237540772(1)
	$\Psi_{2,-}^{(0)}$	−0.8439978723(3)	−0.8439978723(3)	0.571004208(2)
	$\Psi_{3,-}^{(0)}$	0	0	−1.1947582873(5)
		He($2\,^1S$)-He($2\,^1S$)-He($2\,^1P$)		
$^\infty$He	$\Psi_{1,-}^{(0)}$	3384.8155908(1)	3384.8155908(1)	2501.5377345(1)
	$\Psi_{2,-}^{(0)}$	−3384.8155908(1)	−3384.8155908(1)	2289.9867601(1)
	$\Psi_{3,-}^{(0)}$	0	0	−4791.5244947(2)
^{4}He	$\Psi_{1,-}^{(0)}$	3386.8493973(2)	3386.8493973(2)	2503.0408130(1)
	$\Psi_{2,-}^{(0)}$	−3386.8493973(2)	−3386.8493973(2)	2291.3627258(2)
	$\Psi_{3,-}^{(0)}$	0	0	−4794.4035388(3)
^{3}He	$\Psi_{1,-}^{(0)}$	3387.5150582(2)	3387.5150582(2)	2503.5327676(1)
	$\Psi_{2,-}^{(0)}$	−3387.5150582(2)	−3387.5150582(2)	2291.81308(1)
	$\Psi_{3,-}^{(0)}$	0	0	−4795.3458442(2)
		He($2\,^3S$)-He($2\,^3S$)-He($2\,^3P$)		
$^\infty$He	$\Psi_{1,-}^{(0)}$	997.70667(7)	997.70667(7)	737.35211(6)
	$\Psi_{2,-}^{(0)}$	−997.70667(7)	−997.70667(7)	674.99542(4)
	$\Psi_{3,-}^{(0)}$	0	0	−1412.34752(9)
^{4}He	$\Psi_{1,-}^{(0)}$	998.55888(7)	998.55888(7)	737.98192(5)
	$\Psi_{2,-}^{(0)}$	−998.55888(7)	−998.55888(7)	675.57198(4)
	$\Psi_{3,-}^{(0)}$	0	0	−1413.5539(1)
^{3}He	$\Psi_{1,-}^{(0)}$	998.8379(1)	998.8379(1)	738.18812(5)
	$\Psi_{2,-}^{(0)}$	−998.8379(1)	−998.8379(1)	675.76074(4)
	$\Psi_{3,-}^{(0)}$	0	0	−1413.9488(1)

Table 4.30: The additive and nonadditive dispersion coefficients $C_8^{(IJ)}(1, M = 0)$ of the He($n_0\,^\lambda S$)-He($n_0\,^\lambda S$)-He($n_0'\,^\lambda P$) system for three different types of the zeroth-order wave functions, where the three atoms form a straight line, in atomic units. The numbers in parentheses represent the computational uncertainties.

Atom	State	$C_8^{(12)}(1, M = 0)$	$C_8^{(23)}(1, M = 0)$	$C_8^{(31)}(1, M = 0)$
		He($1\,^1S$)-He($1\,^1S$)-He($2\,^1P$)		
$^\infty$He	$\Psi_{1,-}^{(0)}$	296.0844962(1)	213.77603(5)	296.0844962(1)
	$\Psi_{2,-}^{(0)}$	276.49490(7)	196.8912(1)	276.49490(7)
	$\Psi_{3,-}^{(0)}$	195.56578(5)	357.4779(1)	195.56578(5)
^{4}He	$\Psi_{1,-}^{(0)}$	296.04686(7)	213.75195(5)	296.04686(7)
	$\Psi_{2,-}^{(0)}$	276.44230(7)	196.86987(4)	276.44230(7)
	$\Psi_{3,-}^{(0)}$	195.53832(5)	357.4056(1)	195.53832(5)
^{3}He	$\Psi_{1,-}^{(0)}$	296.03445(7)	213.74400(5)	296.03445(7)
	$\Psi_{2,-}^{(0)}$	276.42501(7)	196.86284(5)	276.42501(7)
	$\Psi_{3,-}^{(0)}$	195.52927(4)	357.3819(1)	195.52927(4)
		He($2\,^1S$)-He($2\,^1S$)-He($2\,^1P$)		
$^\infty$He	$\Psi_{1,-}^{(0)}$	576416(2)	647941(2)	576416(2)
	$\Psi_{2,-}^{(0)}$	516777(2)	662260(1)	516777(2)
	$\Psi_{3,-}^{(0)}$	636815(1)	419806(2)	636815(1)
^{4}He	$\Psi_{1,-}^{(0)}$	576705(2)	648259(1)	576705(2)
	$\Psi_{2,-}^{(0)}$	516966(2)	662582(1)	516966(2)
	$\Psi_{3,-}^{(0)}$	637098(2)	419931(2)	637098(2)
^{3}He	$\Psi_{1,-}^{(0)}$	576800(2)	648361(2)	576800(2)
	$\Psi_{2,-}^{(0)}$	517028(2)	662687(1)	517028(2)
	$\Psi_{3,-}^{(0)}$	637193(1)	419971(3)	637193(1)
		He($2\,^3S$)-He($2\,^3S$)-He($2\,^3P$)		
$^\infty$He	$\Psi_{1,-}^{(0)}$	178708.897(6)	188816.664(8)	178708.897(6)
	$\Psi_{2,-}^{(0)}$	130516.795(6)	190656.01(1)	130516.795(6)
	$\Psi_{3,-}^{(0)}$	173264.08(1)	103017.090(3)	173264.08(1)
^{4}He	$\Psi_{1,-}^{(0)}$	178746.690(5)	188873.006(8)	178746.690(5)
	$\Psi_{2,-}^{(0)}$	130557.634(5)	190716.156(8)	130557.634(5)
	$\Psi_{3,-}^{(0)}$	173324.043(8)	103039.204(2)	173324.043(8)
^{3}He	$\Psi_{1,-}^{(0)}$	178759.057(6)	188891.445(9)	178759.057(6)
	$\Psi_{2,-}^{(0)}$	130571.000(5)	190735.837(8)	130571.000(5)
	$\Psi_{3,-}^{(0)}$	173343.669(9)	103046.443(2)	173343.669(9)

Table 4.31: The additive and nonadditive dispersion coefficients $C_8^{(IJ,JK)}(1, M = 0)$ of the He($n_0\,^\lambda S$)-He($n_0\,^\lambda S$)-He($n_0'\,^\lambda P$) system for three different types of the zeroth-order wave functions, where the three atoms form a straight line, in atomic units. The numbers in parentheses represent the computational uncertainties.

Atom	State	$C_8^{(12,23)}(1, M = 0)$	$C_8^{(23,31)}(1, M = 0)$	$C_8^{(31,12)}(1, M = 0)$
		He($1\,^1S$)-He($1\,^1S$)-He($2\,^1P$)		
$^\infty$He	$\Psi_{1,-}^{(0)}$	2.134984185(2)	2.134984185(2)	−1.577853610(1)
	$\Psi_{2,-}^{(0)}$	−2.134984185(2)	−2.134984185(2)	−1.444417100(2)
	$\Psi_{3,-}^{(0)}$	0	0	3.022270710(3)
^{4}He	$\Psi_{1,-}^{(0)}$	2.135847167(2)	2.135847167(2)	−1.578491396(2)
	$\Psi_{2,-}^{(0)}$	−2.135847167(2)	−2.135847167(2)	−1.445000948(2)
	$\Psi_{3,-}^{(0)}$	0	0	3.023492343(3)
^{3}He	$\Psi_{1,-}^{(0)}$	2.136129624(2)	2.136129624(2)	−1.578700145(2)
	$\Psi_{2,-}^{(0)}$	−2.136129624(2)	−2.136129624(2)	−1.445192042(1)
	$\Psi_{3,-}^{(0)}$	0	0	3.023892187(3)
		He($2\,^1S$)-He($2\,^1S$)-He($2\,^1P$)		
$^\infty$He	$\Psi_{1,-}^{(0)}$	135985.7088(2)	135985.7088(2)	−100499.8272(2)
	$\Psi_{2,-}^{(0)}$	−135985.7088(2)	−135985.7088(2)	−92000.7203(1)
	$\Psi_{3,-}^{(0)}$	0	0	192500.5476(3)
^{4}He	$\Psi_{1,-}^{(0)}$	136063.7177(2)	136063.7177(2)	−100557.4795(2)
	$\Psi_{2,-}^{(0)}$	−136063.7177(2)	−136063.7177(2)	−92053.50(1)
	$\Psi_{3,-}^{(0)}$	0	0	192610.9765(3)
^{3}He	$\Psi_{1,-}^{(0)}$	136089.2454(2)	136089.2454(2)	−100576.3455(1)
	$\Psi_{2,-}^{(0)}$	−136089.2454(2)	−136089.2454(2)	−92070.7677(1)
	$\Psi_{3,-}^{(0)}$	0	0	192647.1134(3)
		He($2\,^3S$)-He($2\,^3S$)-He($2\,^3P$)		
$^\infty$He	$\Psi_{1,-}^{(0)}$	41573.30041(1)	41573.30041(1)	−30724.622050(6)
	$\Psi_{2,-}^{(0)}$	−41573.30041(1)	−41573.30041(1)	−28126.290775(6)
	$\Psi_{3,-}^{(0)}$	0	0	58850.91282(1)
^{4}He	$\Psi_{1,-}^{(0)}$	41586.57162(1)	41586.57162(1)	−30734.430098(6)
	$\Psi_{2,-}^{(0)}$	−41586.57162(1)	−41586.57162(1)	−28135.269372(6)
	$\Psi_{3,-}^{(0)}$	0	0	58869.69946(1)
^{3}He	$\Psi_{1,-}^{(0)}$	41590.914293(8)	41590.914293(8)	−30737.639533(6)
	$\Psi_{2,-}^{(0)}$	−41590.914293(8)	−41590.914293(8)	−28138.207391(6)
	$\Psi_{3,-}^{(0)}$	0	0	58875.84692(1)

Table 4.32: The additive and nonadditive dispersion coefficients $C_8^{(IJ)}(1, M = \pm 1)$ of the He($1\,^1S$)-He($1\,^1S$)-He($2\,^1P$) system for three different types of the zeroth-order wave functions, where the three atoms form a straight line, in atomic units. The numbers in parentheses represent the computational uncertainties.

Atom	State	$C_8^{(12)}(1, M = \pm 1)$	$C_8^{(23)}(1, M = \pm 1)$	$C_8^{(31)}(1, M = \pm 1)$
		He($1\,^1S$)-He($1\,^1S$)-He($2\,^1P$)		
$^{\infty}$He	$\Psi_{1,-}^{(0)}$	3734.26752(8)	2640.58247(6)	3734.26752(8)
	$\Psi_{2,-}^{(0)}$	3958.5749(1)	2418.46662(5)	3958.5749(1)
	$\Psi_{3,-}^{(0)}$	2568.98676(5)	5202.7801(1)	2568.98676(5)
^{4}He	$\Psi_{1,-}^{(0)}$	3736.92490(8)	2642.46139(6)	3736.92490(8)
	$\Psi_{2,-}^{(0)}$	3961.3633(1)	2420.18732(5)	3961.3633(1)
	$\Psi_{3,-}^{(0)}$	2570.80469(6)	5206.4442(1)	2570.80469(6)
^{3}He	$\Psi_{1,-}^{(0)}$	3737.79465(8)	2643.07636(6)	3737.79465(8)
	$\Psi_{2,-}^{(0)}$	3962.27603(9)	2420.75050(5)	3962.27603(9)
	$\Psi_{3,-}^{(0)}$	2571.3997(1)	5207.6434(1)	2571.3997(1)
		He($2\,^1S$)-He($2\,^1S$)-He($2\,^1P$)		
$^{\infty}$He	$\Psi_{1,-}^{(0)}$	677649(3)	696503(2)	677649(3)
	$\Psi_{2,-}^{(0)}$	2052935(3)	706714(2)	2052935(3)
	$\Psi_{3,-}^{(0)}$	1182611(2)	2509977(5)	1182611(2)
^{4}He	$\Psi_{1,-}^{(0)}$	678086(3)	696908(3)	678086(3)
	$\Psi_{2,-}^{(0)}$	2054147(4)	707118(2)	2054147(4)
	$\Psi_{3,-}^{(0)}$	1183287(2)	2511492(5)	1183287(2)
^{3}He	$\Psi_{1,-}^{(0)}$	678229(3)	697041(3)	678229(3)
	$\Psi_{2,-}^{(0)}$	2054544(4)	707250(2)	2054544(4)
	$\Psi_{3,-}^{(0)}$	1183508(2)	2511988(5)	1183508(2)
		He($2\,^3S$)-He($2\,^3S$)-He($2\,^3P$)		
$^{\infty}$He	$\Psi_{1,-}^{(0)}$	242087.18(2)	226143.71(2)	242087.18(2)
	$\Psi_{2,-}^{(0)}$	660377.03(2)	224826.36(1)	660377.03(2)
	$\Psi_{3,-}^{(0)}$	371010.24(1)	822504.39(2)	371010.24(1)
^{4}He	$\Psi_{1,-}^{(0)}$	242141.77(1)	226210.21(2)	242141.77(1)
	$\Psi_{2,-}^{(0)}$	660542.33(2)	224895.80(1)	660542.33(2)
	$\Psi_{3,-}^{(0)}$	371117.31(2)	822695.40(2)	371117.31(2)
^{3}He	$\Psi_{1,-}^{(0)}$	242159.65(2)	226231.97(2)	242159.65(2)
	$\Psi_{2,-}^{(0)}$	660596.40(1)	224918.54(2)	660596.40(1)
	$\Psi_{3,-}^{(0)}$	371152.34(2)	822757.90(2)	371152.34(2)

Table 4.33: The additive and nonadditive dispersion coefficients $C_8^{(IJ,JK)}(1,M=\pm1)$ of the He($1\,^1S$)-He($1\,^1S$)-He($2\,^1P$) system for three different types of the zeroth-order wave functions, where the three atoms form a straight line, in atomic units. The numbers in parentheses represent the computational uncertainties.

Atom	State	$C_8^{(12,23)}(1,M=\pm1)$	$C_8^{(23,31)}(1,M=\pm1)$	$C_8^{(31,12)}(1,M=\pm1)$
		He($1\,^1S$)-He($1\,^1S$)-He($2\,^1P$)		
$^\infty$He	$\Psi_{1,-}^{(0)}$	4.269968371(4)	4.269968371(4)	−3.155707222(3)
	$\Psi_{2,-}^{(0)}$	−4.269968371(4)	−4.269968371(4)	−2.888834199(3)
	$\Psi_{3,-}^{(0)}$	0	0	6.044541421(6)
^{4}He	$\Psi_{1,-}^{(0)}$	4.271694335(4)	4.271694335(4)	−3.156982791(3)
	$\Psi_{2,-}^{(0)}$	−4.271694335(4)	−4.271694335(4)	−2.890001895(3)
	$\Psi_{3,-}^{(0)}$	0	0	6.046984686(6)
^{3}He	$\Psi_{1,-}^{(0)}$	4.272259249(4)	4.272259249(4)	−3.157400290(4)
	$\Psi_{2,-}^{(0)}$	−4.272259249(4)	−4.272259249(4)	−2.890384086(3)
	$\Psi_{3,-}^{(0)}$	0	0	6.047784375(6)
		He($2\,^1S$)-He($2\,^1S$)-He($2\,^1P$)		
$^\infty$He	$\Psi_{1,-}^{(0)}$	271971.4176(4)	271971.4176(4)	−200999.6545(4)
	$\Psi_{2,-}^{(0)}$	−271971.4176(4)	−271971.4176(4)	−184001.46(2)
	$\Psi_{3,-}^{(0)}$	0	0	385001.0952(6)
^{4}He	$\Psi_{1,-}^{(0)}$	272127.4354(4)	272127.4354(4)	−201114.9590(4)
	$\Psi_{2,-}^{(0)}$	−272127.4354(4)	−272127.4354(4)	−184106.9942(3)
	$\Psi_{3,-}^{(0)}$	0	0	385221.9532(7)
^{3}He	$\Psi_{1,-}^{(0)}$	272178.4910(5)	272178.4910(5)	−201152.6912(3)
	$\Psi_{2,-}^{(0)}$	−272178.4910(5)	−272178.4910(5)	−184141.5356(3)
	$\Psi_{3,-}^{(0)}$	0	0	385294.2270(7)
		He($2\,^3S$)-He($2\,^3S$)-He($2\,^3P$)		
$^\infty$He	$\Psi_{1,-}^{(0)}$	83146.60083(2)	83146.60083(2)	−61449.24409(1)
	$\Psi_{2,-}^{(0)}$	−83146.60083(2)	−83146.60083(2)	−56252.58154(1)
	$\Psi_{3,-}^{(0)}$	0	0	117701.82562(2)
^{4}He	$\Psi_{1,-}^{(0)}$	83173.14325(2)	83173.14325(2)	−61468.86023(5)
	$\Psi_{2,-}^{(0)}$	−83173.14325(2)	−83173.14325(2)	−56270.53874(1)
	$\Psi_{3,-}^{(0)}$	0	0	117739.39893(2)
^{3}He	$\Psi_{1,-}^{(0)}$	83181.82859(2)	83181.82859(2)	−61475.27906(1)
	$\Psi_{2,-}^{(0)}$	−83181.82859(2)	−83181.82859(2)	−56276.41479(2)
	$\Psi_{3,-}^{(0)}$	0	0	117751.69384(2)

(4.30) and $a = 0$ and $b = -c$ in Eq. (4.31), the dispersion coefficients have similar characteristics as the case of the isosceles right triangle. The only differences are the values of the three interior angles: $\beta = \gamma = 0$ and $\alpha = 2\pi$, leading to the relatively large nonzero dispersion coefficients $C_8^{(31,12)}(1, M = 0)$ and $C_8^{(31,12)}(1, M = \pm 1)$. Figs. 4.8-4.10 are the potential energy curves due to $\Delta E^{(1)}$ and $\Delta E^{(2)}$ for the systems of He($1\,^1S$)-He($1\,^1S$)-He($2\,^1P$), He($2\,^1S$)-He($2\,^1S$)-He($2\,^1P$), and He($2\,^3S$)-He($2\,^3S$)-He($2\,^3P$).

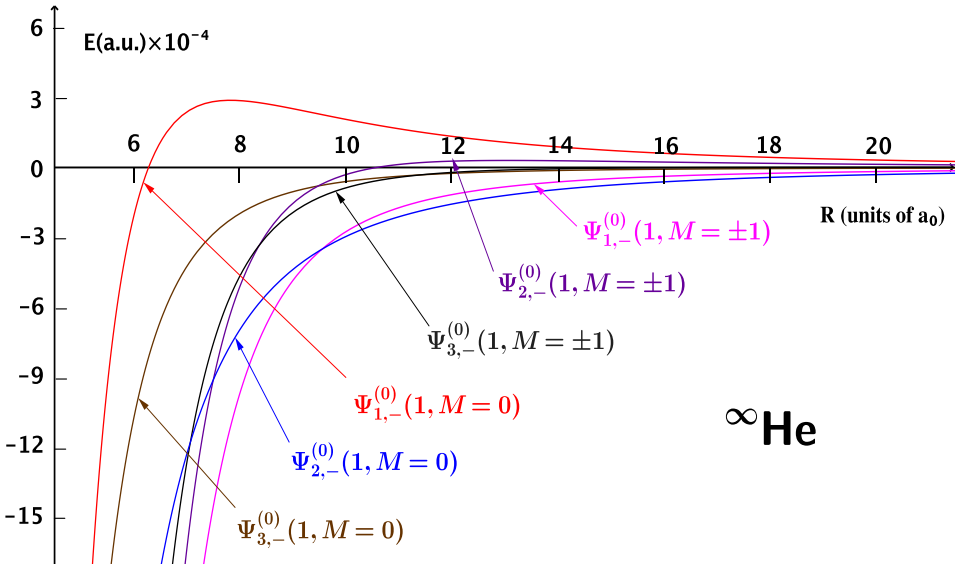

Figure 4.8: Long-range potentials for the He($1\,^1S$)-He($1\,^1S$)-He($2\,^1P$) system for three different types of the zeroth-order wave functions, where the three atoms form a straight line, in atomic units. For each curve labeled by a wave function, the plotted curve is the sum of $\Delta E^{(1)}$ and $\Delta E^{(2)}$.

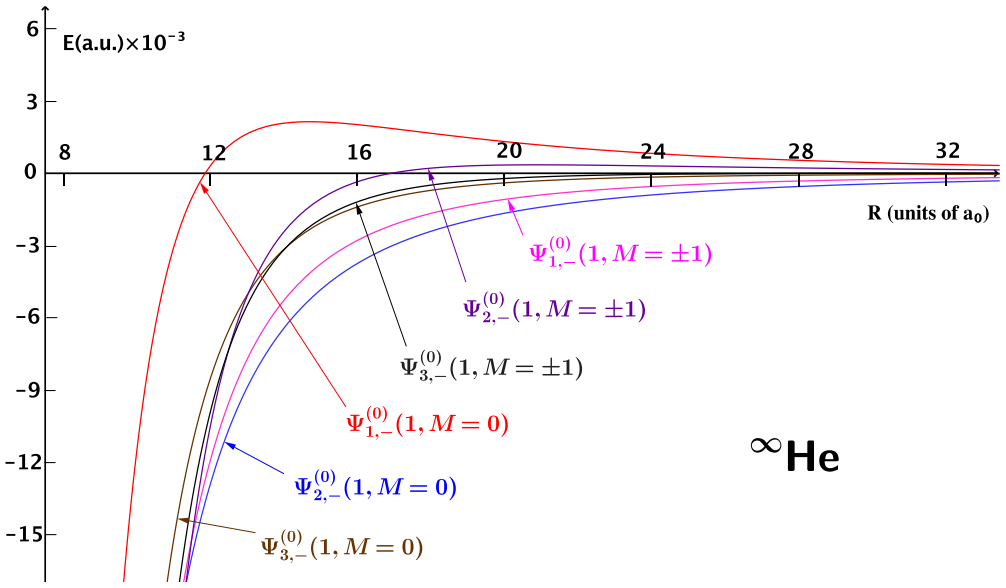

Figure 4.9: Long-range potentials for the He($2\,^1S$)-He($2\,^1S$)-He($2\,^1P$) system for three different types of the zeroth-order wave functions, where the three atoms form a straight line, in atomic units. For each curve labeled by a wave function, the plotted curve is the sum of $\Delta E^{(1)}$ and $\Delta E^{(2)}$.

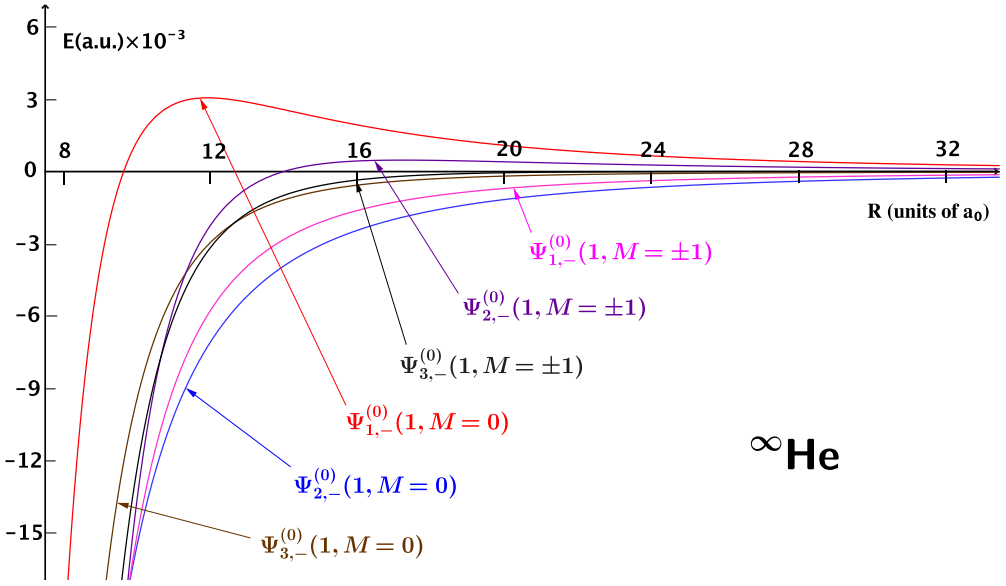

Figure 4.10: Long-range potentials for the He($2\,^3S$)-He($2\,^3S$)-He($2\,^3P$) system for three different types of the zeroth-order wave functions, where the three atoms form a straight line, in atomic units. For each curve labeled by a wave function, the plotted curve is the sum of $\Delta E^{(1)}$ and $\Delta E^{(2)}$.

Chapter 5

Calculations of Long-Range Three-Body Interactions for Li($2\,^2S$)-Li($2\,^2S$)-Li$^+$($1\,^1S$)

5.1 Theoretical Formulation

5.1.1 The Zeroth-Order Wave Functions

The Hamiltonian for the well-separated Li($2\,^2S$)-Li($2\,^2S$)-Li$^+$($1\,^1S$) system can be written as

$$H = H^{(0)} + H' \,, \tag{5.1}$$

where

$$H^{(0)} = H_1^{(0)} + H_2^{(0)} + H_3^{+(0)} \,, \tag{5.2}$$

$$H' \equiv V_{123} = V_{12} + V_{23} + V_{31} \,, \tag{5.3}$$

with $H_1^{(0)}$ and $H_2^{(0)}$ the unperturbed Hamiltonians of, atom 1 and 2 respectively, $H_3^{+(0)}$ the unperturbed Hamiltonian of the ion 3, and V_{12}, V_{23}, and V_{31} their mu-

tual electrostatic interactions. We label the particles by I, J, and K with the corresponding internal coordinates $\boldsymbol{\sigma}$, $\boldsymbol{\rho}$, and $\boldsymbol{\varsigma}$. For the nondegenerate Li($n_0\,^2S$)-Li($n_0\,^2S$)-Li$^+$($n_0'\,^1S$) system, the zeroth-order wavefunction is simple,

$$|\Psi^{(0)}\rangle = |\varphi_{n_0}(0;\boldsymbol{\sigma})\varphi_{n_0}(0;\boldsymbol{\rho})\psi_{n_0'}(0;\boldsymbol{\varsigma})\rangle\,. \tag{5.4}$$

where $\varphi_{n_0}(0;\boldsymbol{\sigma})$ or $\varphi_{n_0}(0;\boldsymbol{\rho})$ represents the wave function of the ground state lithium atom, and $\psi_{n_0'}(0;\boldsymbol{\varsigma})$ represents the wave function of the ground state lithium ion. In this work, we set the coordinates for the Li($2\,^2S$)-Li($2\,^2S$)-Li$^+$($1\,^1S$) system as shown in Fig. 3.1, which has been demonstrated in Section 3.1.2 of Chapter 3.

5.1.2 The Second-Order Energy

According to perturbation theory, the first-order correction for the Li($2\,^2S$)-Li($2\,^2S$)-Li$^+$($1\,^1S$) system is zero. The nonzero contribution starts from second-order correction,

$$\Delta E^{(2)} = -\sum_{n\geq 3,n'\geq 2}\left(\frac{C_{2n}^{(12)}}{R_{12}^{2n}}+\frac{C_{2n'}^{(23)}}{R_{23}^{2n'}}+\frac{C_{2n'}^{(31)}}{R_{31}^{2n'}}\right), \tag{5.5}$$

where $C_{2n}^{(IJ)}(L,M)$ are the long-range additive interaction coefficients. The derivation of these coefficients is given in Appendix C. In this work we only consider the cases of $n=3,4$ and $n'=2,3,4$ in Eq. (5.5). The corresponding interaction coefficients are

$$C_6^{(12)} = \sum_{n_s n_t} F_1(n_s,n_t,1,1)\,, \tag{5.6}$$

$$C_8^{(12)} = \sum_{n_s n_t}\Big\{F_1(n_s,n_t,2,1)+F_1(n_s,n_t,1,2)\Big\}, \tag{5.7}$$

$$C_4^{(23)} = C_4^{(31)} = \sum_{n_{t(s)} n_u} F_2(n_{t(s)}, n_u, 1, 0)\,, \tag{5.8}$$

$$C_6^{(23)} = C_6^{(31)} = \sum_{n_{t(s)} n_u} \Big\{ F_2(n_{t(s)}, n_u, 2, 0) + F_2(n_{t(s)}, n_u, 1, 1) \Big\}\,, \tag{5.9}$$

$$\begin{aligned} & C_8^{(23)} = C_8^{(31)} \\ = & \sum_{n_{t(s)} n_u} \Big\{ F_2(n_{t(s)}, n_u, 3, 0) + F_2(n_{t(s)}, n_u, 2, 1) + F_2(n_{t(s)}, n_u, 1, 2) \Big\}\,, \end{aligned} \tag{5.10}$$

where the F_i-functions are defined by Eqs. (C.15) and (C.16) in Appendix C.

5.1.3 The Third-Order Energy

The third-order energy correction for the Li($2\,^2S$)-Li($2\,^2S$)-Li$^+$($1\,^1S$) system can be written as

$$\begin{aligned} \Delta E^{(3)} = & - \sum_{n_4 \geq 4, n_2 \geq 2} \left(\frac{C_{2n_4+3}^{(12)}}{R_{12}^{2n_4+3}} + \frac{C_{2n_2+3}^{(23)}}{R_{23}^{2n_2+3}} + \frac{C_{2n_2+3}^{(31)}}{R_{31}^{2n_2+3}} \right) \\ & - \sum_{\substack{n_4 \geq 4, n_3 \geq 3, n_1 \geq 1 \\ n_4 + n_1 = 2n_3}} \left(\frac{C_{2n_3+3}^{(12,23)}(L_s, L_t, L_t', \ell_2', L_t'', \ell_2'')}{R_{12}^{n_4+2} R_{23}^{n_1+1}} + \frac{C_{2n_3+3}^{(31,12)}(L_t, L_s, L_s', \ell_1', L_s'', \ell_1'')}{R_{31}^{n_1+1} R_{12}^{n_4+2}} \right) \\ & - \sum_{\substack{n_2 \geq 2, n_2' \geq 2, n_1 \geq 1, n_1' \geq 1 \\ n_2' + n_1 + n_1' = 2n_2}} \left(\frac{C_{2n_2+3}^{(12,23,31)}(L_s, L_t, L_u)}{R_{12}^{n_2'+1} R_{23}^{n_1+1} R_{31}^{n_1'+1}} \right), \end{aligned} \tag{5.11}$$

where $C_{2n_i+3}^{(IJ)}$ are the long-range additive interaction coefficients, and $C_{2n_i+3}^{(IJ,JK)}$ and $C_{2n_i+3}^{(IJ,JK,KI)}$ are the long-range nonadditive interaction coefficients. The derivation of these coefficients is given in Appendix C. In this work, we only consider C_7 and C_9.

The corresponding interaction coefficients are

$$
\begin{aligned}
C_7^{(23)} = C_7^{(31)} = \sum_{n_t n_u n_t' n_u'} \Bigg\{ & \quad F_4(n_t, n_u, n_t', n_u', 1, 0, 1, 0, 2, 0) \\
& + \quad F_4(n_t, n_u, n_t', n_u', 1, 0, 2, 0, 1, 0) \\
& + \quad F_4(n_t, n_u, n_t', n_u', 2, 0, 1, 0, 1, 0) \Bigg\}, \qquad (5.12)
\end{aligned}
$$

$$
\begin{aligned}
C_9^{(23)} = C_9^{(31)} = \sum_{n_t n_u n_t' n_u'} \Bigg\{ & \quad F_4(n_t, n_u, n_t', n_u', 1, 0, 2, 0, 3, 0) \\
& + \quad F_4(n_t, n_u, n_t', n_u', 1, 0, 3, 0, 2, 0) \\
& + \quad F_4(n_t, n_u, n_t', n_u', 2, 0, 3, 0, 1, 0) \\
& + \quad F_4(n_t, n_u, n_t', n_u', 2, 0, 1, 0, 3, 0) \\
& + \quad F_4(n_t, n_u, n_t', n_u', 3, 0, 1, 0, 2, 0) \\
& + \quad F_4(n_t, n_u, n_t', n_u', 3, 0, 2, 0, 1, 0) \\
& + \quad F_4(n_t, n_u, n_t', n_u', 1, 1, 1, 1, 2, 0) \\
& + \quad F_4(n_t, n_u, n_t', n_u', 1, 1, 2, 1, 1, 0) \\
& + \quad F_4(n_t, n_u, n_t', n_u', 2, 1, 1, 1, 1, 0) \\
& + \quad F_4(n_t, n_u, n_t', n_u', 1, 0, 1, 1, 2, 1) \\
& + \quad F_4(n_t, n_u, n_t', n_u', 1, 0, 2, 1, 1, 1) \\
& + \quad F_4(n_t, n_u, n_t', n_u', 2, 0, 1, 1, 1, 1) \\
& + \quad F_4(n_t, n_u, n_t', n_u', 1, 1, 1, 0, 2, 1) \\
& + \quad F_4(n_t, n_u, n_t', n_u', 1, 1, 2, 0, 1, 1) \\
& + \quad F_4(n_t, n_u, n_t', n_u', 2, 1, 1, 0, 1, 1) \\
& + \quad F_4(n_t, n_u, n_t', n_u', 2, 0, 2, 0, 2, 0) \Bigg\}, \qquad (5.13)
\end{aligned}
$$

$$
\begin{aligned}
& C_9^{(12,23)}(1,1,1,2,2,1) \\
= & \sum_{\substack{n_s n_t n_t' \\ M_s M_t M_t' m_2'}} F_5(n_s, n_t, n_t', 1, 1, 1, 2, M_s, M_t, m_2', M_t') \cos[M_t' \beta] \\
+ & \sum_{\substack{n_s n_t n_t'' \\ M_s M_t M_t'' m_2''}} F_6(n_s, n_t, n_t'', 1, 1, 2, 1, M_s, M_t, M_t'', m_2'') \exp[-i m_2'' \beta] \,,
\end{aligned}
\tag{5.14}
$$

$$
\begin{aligned}
& C_9^{(12,23)}(1,1,2,1,1,2) \\
= & \sum_{\substack{n_s n_t n_t' \\ M_s M_t M_t' m_2'}} F_5(n_s, n_t, n_t', 1, 1, 2, 1, M_s, M_t, m_2', M_t') \cos[M_t' \beta] \\
+ & \sum_{\substack{n_s n_t n_t'' \\ M_s M_t M_t'' m_2''}} F_6(n_s, n_t, n_t'', 1, 1, 1, 2, M_s, M_t, M_t'', m_2'') \exp[-i m_2'' \beta] \,,
\end{aligned}
\tag{5.15}
$$

$$
\begin{aligned}
& C_9^{(12,23)}(1,2,1,1,1,1) \\
= & \sum_{\substack{n_s n_t n_t' \\ M_s M_t M_t' m_2'}} F_5(n_s, n_t, n_t', 1, 2, 1, 1, M_s, M_t, m_2', M_t') \cos[M_t' \beta] \\
+ & \sum_{\substack{n_s n_t n_t'' \\ M_s M_t M_t'' m_2''}} F_6(n_s, n_t, n_t'', 1, 2, 1, 1, M_s, M_t, M_t'', m_2'') \exp[-i m_2'' \beta] \,,
\end{aligned}
\tag{5.16}
$$

$$
\begin{aligned}
& C_9^{(31,12)}(1,1,1,2,2,1) \\
= & \sum_{\substack{n_s n_s' n_t \\ M_t M_s m_1' M_s'}} F_5(n_t, n_s, n_s', 1, 1, 1, 2, M_t, M_s, m_1', M_s') \cos[M_s' \alpha] \\
+ & \sum_{\substack{n_s n_s'' n_t \\ M_s M_s'' M_t m_1''}} F_6(n_t, n_s, n_s'', 1, 1, 2, 1, M_t, M_s, M_s'', m_1'') \exp[i m_1'' \alpha] \,,
\end{aligned}
\tag{5.17}
$$

$$
\begin{aligned}
& C_9^{(31,12)}(1,1,2,1,1,2) \\
= & \sum_{\substack{n_s n_s' n_t \\ M_t M_s m_1' M_s'}} F_5(n_t, n_s, n_s', 1, 1, 2, 1, M_t, M_s, m_1', M_s') \cos[M_s' \alpha] \\
+ & \sum_{\substack{n_s n_s'' n_t \\ M_s M_s'' M_t m_1''}} F_6(n_t, n_s, n_s'', 1, 1, 1, 2, M_t, M_s, M_s'', m_1'') \exp[i m_1'' \alpha] \,,
\end{aligned}
\tag{5.18}
$$

$$
\begin{aligned}
& C_9^{(31,12)}(1,2,1,1,1,1) \\
= & \sum_{\substack{n_s n_s' n_t \\ M_t M_s m_1' M_s'}} F_5(n_t, n_s, n_s', 1, 2, 1, 1, M_t, M_s, m_1', M_s') \cos[M_s' \alpha] \\
+ & \sum_{\substack{n_s n_s'' n_t \\ M_s M_s'' M_t m_1''}} F_6(n_t, n_s, n_s'', 1, 2, 1, 1, M_t, M_s, M_s'', m_1'') \exp[i m_1'' \alpha] \,,
\end{aligned}
\tag{5.19}
$$

$$
\begin{aligned}
& C_7^{(12,23,31)}(1,1,0) \\
= & \sum_{n_s n_t n_u; M_s M_t} F_7(n_s, n_t, n_u, 1, 1, 0, M_s, M_t, 0) \exp[-i M_s \alpha - i M_t \beta] \,,
\end{aligned}
\tag{5.20}
$$

$$
\begin{aligned}
& C_9^{(12,23,31)}(1,2,0) \\
= & \sum_{n_s n_t n_u; M_s M_t} F_7(n_s, n_t, n_u, 1, 2, 0, M_s, M_t, 0) \exp[-iM_s\alpha - iM_t\beta] \,,
\end{aligned}
\tag{5.21}
$$

$$
\begin{aligned}
& C_9^{(12,23,31)}(2,1,0) \\
= & \sum_{n_s n_t n_u; M_s M_t} F_7(n_s, n_t, n_u, 2, 1, 0, M_s, M_t, 0) \exp[-iM_s\alpha - iM_t\beta] \,,
\end{aligned}
\tag{5.22}
$$

$$
\begin{aligned}
& C_9^{(12,23,31)}(1,1,1) \\
= & \sum_{\substack{n_s n_t n_u \\ M_s M_t M_u}} F_7(n_s, n_t, n_u, 1, 1, 1, M_s, M_t, M_u) \exp[-iM_s\alpha - iM_t\beta - iM_u\gamma] \,,
\end{aligned}
\tag{5.23}
$$

where the F_i-functions are defined by Eqs. (C.18), (C.19), (C.20), and (C.21) in Appendix C.

5.2 Results and Discussion

Using the accurate Hylleraas variational wave functions for lithium atom and lithium ion, we calculate the second-order additive and third-order additive and nonadditive interaction coefficients for the Li($2\,^2S$)-Li($2\,^2S$)-Li$^+$($1\,^1S$) system.

5.2.1 Additive Interaction Coefficients

Table 5.1 lists the values of the second-order interaction coefficients $C_4^{(23)}$, $C_4^{(31)}$, $C_6^{(IJ)}$, and $C_8^{(IJ)}$ and the third-order additive interaction coefficients $C_7^{(23)}$, $C_7^{(31)}$, $C_9^{(23)}$, and $C_9^{(31)}$ for the Li($2\,^2S$)-Li($2\,^2S$)-Li$^+$($1\,^1S$) system. The $C_4^{(IJ)}$ term is the

Table 5.1: The Second-order additive interaction coefficients of the Li($2\,^2S$)-Li($2\,^2S$)-Li^+($1\,^1S$) system in atomic units. The numbers in parentheses represent the computational uncertainties.

Coefficient	$^{\infty}$Li	^{7}Li	^{6}Li
$C_4^{(23)}$	82.0563(6)	82.0807(7)	82.0847(7)
$C_4^{(31)}$	82.0563(6)	82.0807(7)	82.0847(7)
$C_6^{(12)}$	1393.42(5)	1394.05(5)	1394.16(5)
$C_6^{(23)}$	714.951(1)	715.028(1)	715.041(1)
$C_6^{(31)}$	714.951(1)	715.028(1)	715.041(1)
$C_8^{(12)}$	83429(1)	83456(5)	83460(5)
$C_8^{(23)}$	19977.52(1)	19979.80(1)	19980.18(1)
$C_8^{(31)}$	19977.52(1)	19979.80(1)	19980.18(1)
$C_7^{(23)}$	27143.23(6)	27153.87(6)	27155.70(6)
$C_7^{(31)}$	27143.23(6)	27153.87(6)	27155.70(6)
$C_9^{(23)}$	1080780(4)	1081089(4)	1081123(9)
$C_9^{(31)}$	1080780(4)	1081089(4)	1081123(9)

leading long-range interaction between an atom and an ion, which is equal to $\alpha/2$ with α being the dipole polarizability of the lithium atom.

5.2.2 Nonadditive interaction Coefficients

Similar to the triple-dipole (Axilrod-Muto-Teller) interaction terms [25, 26, 43], the nonadditive interaction coefficients depend on the geometrical structure of these three particles, and their numerical values are given for four geometrical configurations: equilateral triangle, isosceles right triangle, isosceles triangle with 120 degree angle, and equally-spaced collinear configuration. In addition, we find that, for each configuration, these nonadditive interaction coefficients may also depend on the different positions of the ion. Thus, for each configuration, three different situations are considered in this thesis due to the different ion positions.

5.2.2.1 Coefficients for an Equilateral Triangle

In this thesis, nonadditive interaction coefficient will be given for three different ion positions for each configuration. Three different type equilateral triangles are labeled as E1, E2 and E3, which are shown in Fig. 5.1.

Table 5.2 lists the nonadditive interaction coefficients $C_7^{(12,23,31)}(1,1,0)$ of the Li($2\,^2S$)-Li($2\,^2S$)-Li$^+$($1\,^1S$) system, where the three particles form an equilateral triangle. We note that there is only one value for each interaction coefficients for E1, E2 and E3. This is because the three interior angles are $\alpha = \beta = \gamma = \pi/3$. These three positions can be taken as equivalent.

Table 5.3 lists the nonadditive interaction coefficients $C_9^{(12,23,31)}(1,\ 1,\ 1)$, $C_9^{(12,23,31)}(1,\ 2,\ 0)$ and $C_9^{(12,23,31)}(2,\ 1,\ 0)$ of the Li($2\,^2S$)-Li($2\,^2S$)-Li$^+$($1\,^1S$) system, where three particles form an equilateral triangle. Similar to $C_7^{(12,23,31)}(1,\ 1,\ 0)$, there is only one value for $C_9^{(12,23,31)}(1,1,1)$, $C_9^{(12,23,31)}(1,2,0)$, and $C_9^{(12,23,31)}(2,1,0)$ for E1, E2 and E3 due to the same interior angles $\alpha = \beta = \gamma = \pi/3$.

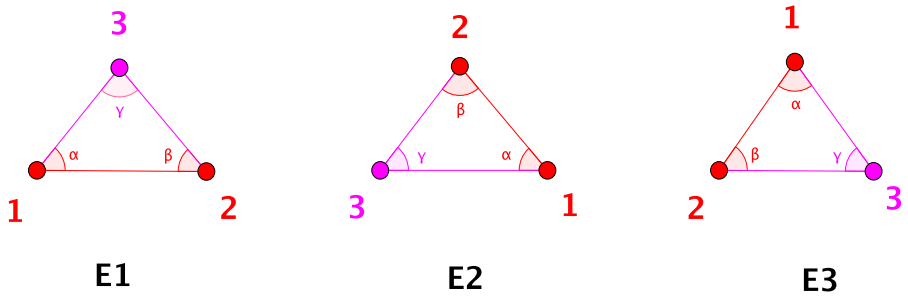

Figure 5.1: Three different type equilateral triangles E1, E2 and E3 with different ion positions, for the Li($2\,^2S$)-Li($2\,^2S$)-Li$^+$($1\,^1S$) system.

Table 5.2: The nonadditive interaction coefficients $C_7^{(12,23,31)}(1,\,1,\,0)$ of the Li($2\,^2S$)-Li($2\,^2S$)-Li$^+$($1\,^1S$) system, where the three nuclei form three equilateral triangles E1, E2 and E3 due to different ion positions, in atomic units. The numbers in parentheses represent the computational uncertainties.

Coefficient	Configuration	$^{\infty}$Li	^{7}Li	^{6}Li
$C_7^{(12,23,31)}(1,1,0)$	E1/E2/E3	$-33666.2(5)$	$-33686.1(5)$	$-33689.4(5)$

Table 5.3: The third-order nonadditive interaction coefficients $C_9^{(12,23,31)}(1,\ 1,\ 1)$, $C_9^{(12,23,31)}(1,\ 2,\ 0)$ and $C_9^{(12,23,31)}(2,\ 1,\ 0)$ of the Li($2\,^2S$)-Li($2\,^2S$)-Li$^+$($1\,^1S$) system, where the three nuclei form three equilateral triangles E1, E2 and E3 due to different ion positions, in atomic units. The numbers in parentheses represent the computational uncertainties.

Coefficient	Configuration	$^{\infty}$Li	^{7}Li	^{6}Li
$C_9^{(12,23,31)}(1,1,1)$	E1/E2/E3	$-368.45(2)$	$-368.77(2)$	$-368.82(2)$
$C_9^{(12,23,31)}(1,2,0)$	E1/E2/E3	$-218977(2)$	$-219064(2)$	$-219079(2)$
$C_9^{(12,23,31)}(2,1,0)$	E1/E2/E3	$-218977(2)$	$-219064(2)$	$-219079(2)$

Table 5.4: The nonadditive interaction coefficients $C_9^{(12,23)}(L_s,L_t,L_t',\ell_2',L_t'',\ell_2'')$ and $C_9^{(31,12)}(L_t,L_s,L_s',\ell_1',L_s'',\ell_1'')$ of the Li($2\,^2S$)-Li($2\,^2S$)-Li$^+$($1\,^1S$) system, where the three nuclei form three type equilateral triangles E1, E2 and E3 due to different ion positions, in atomic units. The numbers in parentheses represent the computational uncertainties.

Coefficient	Configuration	$^{\infty}$Li	^{7}Li	^{6}Li
$C_9^{(12,23)}(1,1,1,2,2,1)$	E1/E2/E3	417562(5)	417800(5)	417840(5)
$C_9^{(12,23)}(1,1,2,1,1,2)$	E1/E2/E3	$-21613.97(6)$	$-21625.91(6)$	$-21627.99(4)$
$C_9^{(12,23)}(1,2,1,1,1,1)$	E1/E2/E3	288502(2)	288661(2)	288687(2)
$C_9^{(31,12)}(1,1,1,2,2,1)$	E1/E2/E3	417562(5)	417800(5)	417840(5)
$C_9^{(31,12)}(1,1,2,1,1,2)$	E1/E2/E3	$-21613.97(6)$	$-21625.91(6)$	$-21627.99(4)$
$C_9^{(31,12)}(1,2,1,1,1,1)$	E1/E2/E3	288502(2)	288661(2)	288687(2)

Table 5.4 lists the values of third-order nonadditive interaction coefficients $C_9^{(12,23)}$ (L_s,L_t,L'_t,ℓ'_2,L''_t,ℓ''_2) and $C_9^{(31,12)}$ (L_t, L_s, L'_s, ℓ'_1, L''_s, ℓ''_1) of the Li($2\,^2S$)-Li($2\,^2S$)-Li$^+$($1\,^1S$) system, where three particles form an equilateral triangle. We note that $C_9^{(12,23)}$ ($L_s, L_t, L'_t, \ell'_2, L''_t, \ell''_2$) = $C_9^{(31,12)}$($L_t, L_s, L'_s, \ell'_1, L''_s, \ell''_1$), which is because the interior angles α, β are equal, i.e., $\alpha = \beta = \pi/3$. There is only one value for each coefficient for E1, E2 and E3, which means, for an equilateral triangle, these nonadditive interaction coefficients do not depend on the different positions of the ion. This is because the three positions are equivalent to each other (or the interior angles at these three positions are all equal to $\pi/3$).

5.2.2.2 Coefficients for an Isosceles Right Triangle

In this section, nonadditive interaction coefficients will be given for three different types of isosceles right triangles labeled as R1, R2 and R3 that are shown in Fig. 5.2.

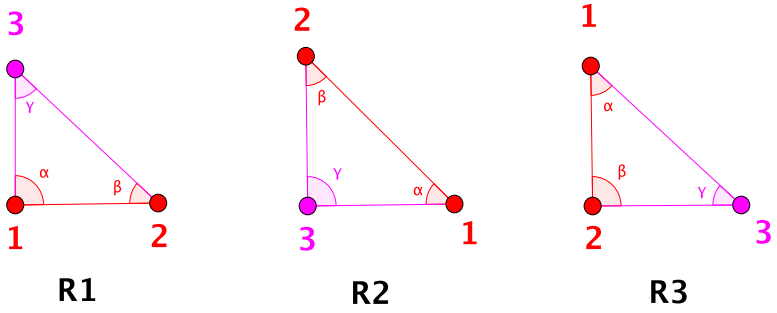

Figure 5.2: Three different type isosceles right triangles R1, R2 and R3 with different ion positions, for the Li($2\,^2S$)-Li($2\,^2S$)-Li$^+$($1\,^1S$) system.

Table 5.5: The nonadditive interaction coefficients $C_7^{(12,23,31)}(1,\,1,\,0)$ of the Li($2\,^2S$)-Li($2\,^2S$)-Li$^+$($1\,^1S$) system, where the three nuclei form three types of isosceles right triangles R1, R2, and R3 due to different ion positions, in atomic units. The numbers in parentheses represent the computational uncertainties.

Configuration	$^{\infty}$Li	^{7}Li	^{6}Li
	$C_7^{(12,23,31)}(1,1,0)$		
R1/R3	−19044.5(3)	−19055.7(3)	−19057.6(3)
R2	−40399.4(6)	−40423.3(6)	−40427.4(7)

Table 5.6: The third-order nonadditive long-range coefficients $C_9^{(12,23,31)}(1,\,2,\,0)$ and $C_9^{(12,23,31)}(2,\,1,\,0)$ of the Li($2\,^2S$)-Li($2\,^2S$)-Li$^+$($1\,^1S$) system, where the three nuclei form three types of isosceles right triangles R1, R2 and R3 due to different ion positions, in atomic units. The numbers in parentheses represent the computational uncertainties.

Configuration	$^{\infty}$Li	^{7}Li	^{6}Li
	$C_9^{(12,23,31)}(1,1,1)$		
R1/R2/R3	−267.96(1)	−268.19(1)	−268.23(1)
	$C_9^{(12,23,31)}(1,2,0)$		
R1	−350363(3)	−350503(3)	−350527(3)
R2	−371617(4)	−371766(4)	−371791(4)
R3	247745(3)	247844(3)	247861(3)
	$C_9^{(12,23,31)}(2,1,0)$		
R1	247745(3)	247844(3)	247861(3)
R2	−371617(4)	−371766(4)	−371791(4)
R3	−350363(3)	−350503(3)	−350528(4)

Table 5.5 lists the nonadditive interaction coefficients $C_7^{(12,23,31)}(1,1,0)$ of the Li($2\,^2S$)-Li($2\,^2S$)-Li$^+$($1\,^1S$) system, where the three particles form an isosceles right triangle. We note that the numerical values of $C_7^{(12,23,31)}(1,1,0)$ for R1 are the same as those for R3, because of the mathematical symmetry of the expression for $C_7^{(12,23,31)}(1,1,0)$ (see Eq. (5.20)), which only contains two interior angles α and β with $\alpha = \pi/2$, $\beta = \pi/4$ for R1, and $\alpha = \pi/4$, $\beta = \pi/2$ for R3. The exchange of α and β would not affect the values of $C_7^{(12,23,31)}(1,1,0)$. For R2, $\alpha = \pi/4$, $\beta = \pi/4$, which is why the numerical values of $C_7^{(12,23,31)}(1,1,0)$ for R2 are different from those of R1 and R3.

Tables 5.6 lists the nonadditive long-range coefficients $C_9^{(12,23,31)}(1,\,1,\,1)$, $C_9^{(12,23,31)}(1,\,2,\,0)$ and $C_9^{(12,23,31)}(2,\,1,\,0)$ of the Li($2\,^2S$)-Li($2\,^2S$)-Li$^+$($1\,^1S$) for the R1, R2 and R3. We note that the numerical values of the coefficient $C_9^{(12,23,31)}(1,\,1,\,1)$ are the same for R1, R2 and R3, whereas the numerical values of the coefficient $C_9^{(12,23,31)}(1,2,0)$ are different from each other for R1, R2 or R3, due to the mathematical symmetry of Eqs. (5.21) and (5.22). So any exchange of the interior angles would lead to a different value. We also find that the numerical values of $C_9^{(12,23,31)}(1,2,0)$ for R1 (or R2, or R3) are the same as the values of $C_9^{(12,23,31)}(2,1,0)$ for R3 (or R2, or R1), due to the symmetry under the simultaneous exchanges of values for the intermediate states L_s, L_t and the interior angles α, β. For example, the values of $C_9^{(12,23,31)}(1,2,0)$ for R1 (with the intermediate states and the interior angles $L_s = 1$, $\alpha = \pi/2$, $L_t = 2$, $\beta = \pi/4$) are same as the values of $C_9^{(12,23,31)}(2,1,0)$ for R3 (with the intermediate states and the interior angles $L_s = 2$, $\alpha = \pi/4$, $L_t = 1$, $\beta = \pi/2$) because of the exchanges of values for the intermediate states L_s, L_t and the interior angles α, β.

Table 5.7 lists the values of third-order nonadditive interaction coefficients $C_9^{(12,23)}(L_s, L_t, L_t', \ell_2', L_t'',$ and $C_9^{(31,12)}(L_t, L_s, L_s', \ell_1', L_s'', \ell_1'')$ of the Li($2\,^2S$)-Li($2\,^2S$)-Li$^+$($1\,^1S$) system, where the three particles form an isosceles right triangle. We note that $C_9^{(12,23)}(1,1,1,2,2,1) = C_9^{(12,23)}(1,2,1,1,1,1) = 0$ for the configuration of R3; $C_9^{(31,12)}(1,1,1,2,2,1) = C_9^{(12,23)}(1,2,1,1,1,1)$ 0 for the configuration of R1, because of $\beta = \pi/2$ and the odd values of M_t' and m_2''

Table 5.7: The nonadditive interaction coefficients $C_9^{(12,23)}(L_s,L_t,L_t',\ell_2',L_t'',\ell_2'')$ and $C_9^{(31,12)}(L_t,L_s,L_s',\ell_1',L_s'',\ell_1'')$ of the Li($2\,^2S$)-Li($2\,^2S$)-Li$^+$($1\,^1S$) system, where the three nuclei form three types of isosceles right triangles R1, R2 and R3 due to different ion positions, in atomic units. The numbers in parentheses represent the computational uncertainties.

Configuration	$^\infty$Li	^{7}Li	^{6}Li
	$C_9^{(12,23)}(1,1,1,2,2,1)$		
R1	590521(6)	590857(6)	590912(6)
R2	590521(6)	590857(6)	590912(6)
R3	0	0	0
	$C_9^{(12,23)}(1,1,2,1,1,2)$		
R1	43227.9(1)	43251.8(1)	43255.8(1)
R2	43227.9(1)	43251.8(1)	43255.8(1)
R3	−86455.9(2)	−86503.6(2)	−86511.6(2)
	$C_9^{(12,23)}(1,2,1,1,1,1)$		
R1	408004(4)	408230(4)	408268(4)
R2	408004(4)	408230(4)	408268(4)
R3	0	0	0
	$C_9^{(31,12)}(1,1,1,2,2,1)$		
R1	0	0	0
R2	590521(6)	590857(6)	590912(6)
R3	590521(6)	590857(6)	590912(6)
	$C_9^{(31,12)}(1,1,2,1,1,2)$		
R1	−86455.9(2)	−86503.6(2)	−86511.6(2)
R2	43227.9(1)	43251.8(1)	43255.8(1)
R3	43227.9(1)	43251.8(1)	43255.8(1)
	$C_9^{(31,12)}(1,2,1,1,1,1)$		
R1	0	0	0
R2	408004(4)	408230(4)	408268(4)
R3	408004(4)	408230(4)	408268(4)

for R3, and $\alpha = \pi/2$ and the odd values of M'_s and m''_1 for R1. $C_9^{(12,23)}(1,1,2,1,1,2)$ is not zero because of the existence of even values for M'_t. We also find that the values of $C_9^{(12,23)}(L_s, L_t, L'_t, \ell'_2, L''_t, \ell''_2)$ for R1 are equal to those for R2; the values of $C_9^{(31,12)}(L_t, L_s, L'_s, \ell'_1, L''_s, \ell''_1)$ for R2 are equal to those for R3, because of the interior angle $\beta = \pi/4$ for both R1 and R2, and the interior angle $\alpha = \pi/4$ for both R2 and R3.

5.2.2.3 Coefficients for an Isosceles Triangle

In this section, nonadditive interaction coefficients will be given for three different types of isosceles triangles with 120 degree angle labeled as I1, I2 and I3 that are shown in Fig. 5.3.

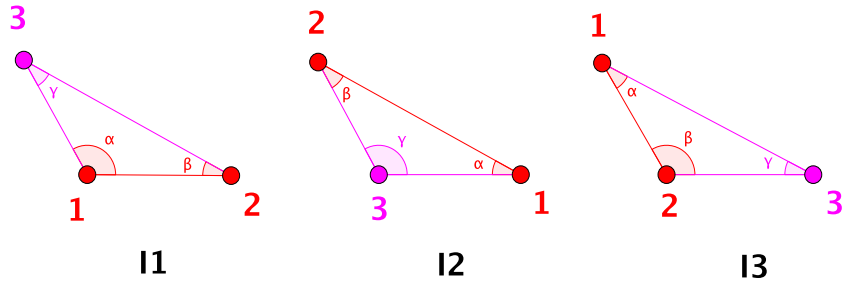

Figure 5.3: Three different types of isosceles triangles with 120 degree I1, I2 and I3 due to different ion positions, for the Li($2\,^2S$)-Li($2\,^2S$)-Li$^+$($1\,^1S$) system.

Table 5.8 lists the third-order nonadditive interaction coefficients $C_7^{(12,23,31)}(1,\ 1,\ 0)$ of the Li($2\,^2S$)-Li($2\,^2S$)-Li$^+$($1\,^1S$) system for an isosceles triangle with 120 degree angle. The numerical values of $C_7^{(12,23,31)}(1,1,0)$ for I1 are the same as that for I3,

Table 5.8: The nonadditive interaction coefficients $C_7^{(12,23,31)}(1,\,1,\,0)$ of the Li($2\,^2S$)-Li($2\,^2S$)-Li$^+$($1\,^1S$) system, where the three nuclei form three types of isosceles triangles with 120 degree angle I1, I2 and I3 due to different ion positions, in atomic units. The numbers in parentheses represent the computational uncertainties.

Configuration	$^\infty$Li	^{7}Li	^{6}Li
	$C_7^{(12,23,31)}(1,1,0)$		
I1/I3	11662.3(2)	11669.2(2)	11670.4(2)
I2	−47133(1)	−47160(1)	−47165(1)

Table 5.9: The third-order nonadditive long-range coefficients $C_9^{(12,23,31)}(1,\,2,\,0)$ and $C_9^{(12,23,31)}(2,\,1,\,0)$ of the Li($2\,^2S$)-Li($2\,^2S$)-Li$^+$($1\,^1S$) system, where the three nuclei form three types of isosceles triangles with 120 degree angle I1, I2 and I3 due to different ion positions, in atomic units. The numbers in parentheses represent the computational uncertainties.

Configuration	$^\infty$Li	^{7}Li	^{6}Li
	$C_9^{(12,23,31)}(1,1,1)$		
I1/I2/I3	33.495(1)	33.523(1)	33.528(1)
	$C_9^{(12,23,31)}(1,2,0)$		
I1	−43795.4(4)	−43812.9(4)	−43815.9(4)
I2	−530991(5)	−531204(5)	−531239(5)
I3	227567(2)	227658(2)	227674(2)
	$C_9^{(12,23,31)}(2,1,0)$		
I1	227567(2)	227658(2)	227674(2)
I2	−530991(5)	−531204(5)	−531239(5)
I3	−43795.4(4)	−43812.9(4)	−43815.9(4)

because of the interior angles $\alpha = 2\pi/3$, $\beta = \pi/6$ for I1 and $\alpha = \pi/6$, $\beta = 2\pi/3$ for I3.

Table 5.9 lists the nonadditive long-range coefficients $C_9^{(12,23,31)}(1, 2, 0)$ and $C_9^{(12,23,31)}(2, 1, 0)$ of the Li($2\,^2S$)-Li($2\,^2S$)-Li$^+$($1\,^1S$) for the isosceles triangles with 120 degree angle. We note that the coefficient $C_9^{(12,23,31)}(1, 2, 0)$ (or $C_9^{(12,23,31)}(2, 1, 0)$) has three different values for I1, I2, and I3, because of the mathematical symmetry of Eqs. (5.21) and (5.22), where the intermediate states have $L_s \neq L_t \neq L_u$. So any exchange of the interior angles would lead to a different value. We also find that the values of $C_9^{(12,23,31)}(1, 2, 0)$ for I1 (or I2, or I3) are the same as the values of $C_9^{(12,23,31)}(2, 1, 0)$ for I3 (or I2, or I1), because of the symmetry property under the simultaneous exchanges of L_s and L_t, and α and β. For example, the values of $C_9^{(12,23,31)}(1, 2, 0)$ for I1 (with the intermediate states and the interior angles $L_s = 1$, $\alpha = 2\pi/3$, $L_t = 2$, $\beta = \pi/6$) are same with the values of $C_9^{(12,23,31)}(2, 1, 0)$ for I3 (with the intermediate states and the interior angles $L_s = 2$, $\alpha = \pi/6$, $L_t = 1$, $\beta = 2\pi/3$) because of the exchanges of values for the intermediate states L_s, L_t and the interior angles α, β.

Table 5.10 lists the values of third-order nonadditive interaction coefficients $C_9^{(12,23)}(L_s, L_t, L'_t, \ell'_2, L''_t$ and $C_9^{(31,12)}(L_t, L_s, L'_s, \ell'_1, L''_s, \ell''_1)$ of the Li($2\,^2S$)-Li($2\,^2S$)-Li$^+$($1\,^1S$) system, where the three particles form an isosceles triangle with 120 degree angle. We note that the values of $C_9^{(12,23)}(L_s, L_t, L'_t, \ell'_2, L''_t, \ell''_2)$ for I1 are equal to those for I2; the values of $C_9^{(31,12)}(L_t, L_s, L'_s, \ell'_1, L''_s, \ell''_1)$ for I2 are equal to those for I3, because of the interior angle $\beta = \pi/6$ for both I1 and I2, and the interior angle $\alpha = \pi/6$ for both I2 and I3. And the negative value of $C_9^{(12,23)}(L_s, L_t, L'_t, \ell'_2, L''_t, \ell''_2)$ for I3 and $C_9^{(31,12)}(L_t, L_s, L'_s, \ell'_1, L''_s, \ell''_1)$ for I1 is due to $\beta = 2\pi/3$ and $\alpha = 2\pi/3$, respectively.

Table 5.10: The nonadditive interaction coefficients $C_9^{(12,23)}(L_s,L_t,L'_t,\ell'_2,L''_t,\ell''_2)$ and $C_9^{(31,12)}(L_t,L_s,L'_s,\ell'_1,L''_s,\ell''_1)$ of the Li($2\,^2S$)-Li($2\,^2S$)-Li$^+$($1\,^1S$) system, where the three nuclei form three types of isosceles triangles with 120 degree angle I1, I2 and I3 due to different ion positions, in atomic units. The numbers in parentheses represent the computational uncertainties.

Configuration	$^\infty$Li	^{7}Li	^{6}Li
	$C_9^{(12,23)}(1,1,1,2,2,1)$		
I1	723239(8)	723650(8)	723718(8)
I2	723239(8)	723650(8)	723718(8)
I3	−417562(5)	−417800(5)	−417840(5)
	$C_9^{(12,23)}(1,1,2,1,1,2)$		
I1	108069.8(3)	108129.5(3)	108139.4(3)
I2	108069.8(3)	108129.5(3)	108139.4(3)
I3	−21613.97(6)	−21625.91(6)	−21627.89(6)
	$C_9^{(12,23)}(1,2,1,1,1,1)$		
I1	499700(4)	499976(4)	500022(4)
I2	499700(4)	499976(4)	500022(4)
I3	−288502(2)	−288661(2)	−288688(2)
	$C_9^{(31,12)}(1,1,1,2,2,1)$		
I1	−417562(5)	−417800(5)	−417840(5)
I2	723239(8)	723650(8)	723718(8)
I3	723239(8)	723650(8)	723718(8)
	$C_9^{(31,12)}(1,1,2,1,1,2)$		
I1	−21613.97(6)	−21625.91(6)	−21627.89(6)
I2	108069.8(3)	108129.5(3)	108139.4(3)
I3	108069.8(3)	108129.5(3)	108139.4(3)
	$C_9^{(31,12)}(1,2,1,1,1,1)$		
I1	−288502(2)	−288661(2)	−288688(2)
I2	499700(4)	499976(4)	500022(4)
I3	499700(4)	499976(4)	500022(4)

5.2.2.4 Coefficients for a Straight Line

In this section, nonadditive interaction coefficients will be given for three different types of straight lines labeled as L1, L2, and L3 that are shown in Fig. 5.4.

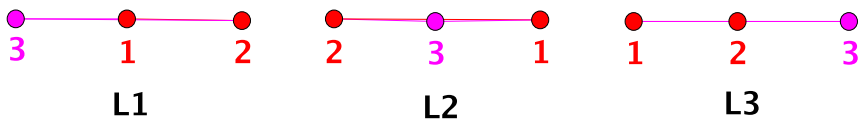

Figure 5.4: Three different types of straight lines L1, L2 and L3 with different ion positions, for the Li($2\,^2S$)-Li($2\,^2S$)-Li$^+$($1\,^1S$) system.

Table 5.11 lists the third-order nonadditive interaction coefficients $C_7^{(12,23,31)}(1,\,1,\,0)$ of the Li($2\,^2S$)-Li($2\,^2S$)-Li$^+$($1\,^1S$) system for a straight line. The numerical values of $C_7^{(12,23,31)}(1,\,1,\,0)$ for L1 are the same as that for L3, because of the interior angles $\alpha = \pi$, $\beta = 0$ for L1 and $\alpha = 0$, $\beta = \pi$ for L3.

Table 5.12 lists the nonadditive interaction coefficients $C_9^{(12,23,31)}(1,\,1,\,1)$, $C_9^{(12,23,31)}(1,\,2,\,0)$, and $C_9^{(12,23,31)}(2,\,1,\,0)$ of the Li($2\,^2S$)-Li($2\,^2S$)-Li$^+$($1\,^1S$) system, where the three nuclei form a straight line. We note that the coefficients $C_9^{(12,23,31)}(1,\,2,\,0)$ and $C_9^{(12,23,31)}(2,\,1,\,0)$ may have different signs (positive or negative), but the absolute values of them are all the same; this is because the values of interior angles α and β are 0 or π, and thus $\cos(n\alpha)$ and $\cos(m\beta)$ can only be 1 or -1, where n and m are

Table 5.11: The nonadditive interaction coefficients $C_7^{(12,23,31)}(1, 1, 0)$ of the Li($2\,^2S$)-Li($2\,^2S$)-Li$^+$($1\,^1S$) system, where the three nuclei form three type straight lines L1, L2 and L3 due to different ion positions, in atomic units. The numbers in parentheses represent the computational uncertainties.

Configuration	$^{\infty}$Li	^{7}Li	^{6}Li
	$C_7^{(12,23,31)}(1,1,0)$		
L1	53866(1)	53898(1)	53903(1)
L2	−53866(1)	−53898(1)	−53903(1)
L3	53866(1)	53898(1)	53903(1)

integers.

Table 5.13 lists the values of third-order nonadditive interaction coefficients $C_9^{(12,23)}(L_s, L_t, L_t', \ell_2', L_t''$ and $C_9^{(31,12)}(L_t, L_s, L_s', \ell_1', L_s'', \ell_1'')$ of the Li($2\,^2S$)-Li($2\,^2S$)-Li$^+$($1\,^1S$) system, where the three particles form a straight line. We note that the absolute value of nonadditive coefficients $C_9^{(12,23)}(L_s, L_t, L_t', \ell_2', L_t'', \ell_2'')$ and $C_9^{(31,12)}(L_t, L_s, L_s', \ell_1', L_s'', \ell_1'')$ for L1, L2 and L3 are all the same, where the negative signs come from the interior angle $\beta = \pi$ or $\alpha = \pi$ with odd values of M_t' and m_2'' or M_s' and m_1''.

Table 5.12: The third-order nonadditive interaction coefficients $C_9^{(12,23,31)}(1,\ 1,\ 1)$, $C_9^{(12,23,31)}(1,\ 2,\ 0)$ and $C_9^{(12,23,31)}(2,\ 1,\ 0)$ of the Li($2\,^2S$)-Li($2\,^2S$)-Li$^+$($1\,^1S$) system, where the three nuclei form three type straight lines L1, L2 and L3 due to different ion positions, in atomic units. The numbers in parentheses represent the computational uncertainties.

Configuration	$^{\infty}$Li	^{7}Li	^{6}Li
	$C_9^{(12,23,31)}(1,1,1)$		
L1/L2/L3	535.92(2)	536.38(2)	536.46(2)
	$C_9^{(12,23,31)}(1,2,0)$		
L1	700726(6)	701007(6)	701054(6)
L2	−700726(6)	−701007(6)	−701054(6)
L3	−700726(6)	−701007(6)	−701054(6)
	$C_9^{(12,23,31)}(2,1,0)$		
L1	−700726(6)	−701007(6)	−701054(6)
L2	−700726(6)	−701007(6)	−701054(6)
L3	700726(6)	701007(6)	701054(6)

Table 5.13: The nonadditive interaction coefficients $C_9^{(12,23)}(L_s,L_t,L_t',\ell_2',L_t'',\ell_2'')$ and $C_9^{(31,12)}(L_t,L_s,L_s',\ell_1',L_s'',\ell_1'')$ of the Li($2\,^2S$)-Li($2\,^2S$)-Li$^+$($1\,^1S$) system, where the three nuclei form three types of straight lines L1, L2 and L3 due to different ion positions, in atomic units. The numbers in parentheses represent the computational uncertainties.

Configuration	$^{\infty}$Li	^{7}Li	^{6}Li
	$C_9^{(12,23)}(1,1,1,2,2,1)$		
L1	835124(9)	835599(9)	835678(9)
L2	835124(9)	835599(9)	835678(9)
L3	−835124(9)	−835599(9)	−835678(9)
	$C_9^{(12,23)}(1,1,2,1,1,2)$		
L1	172911.8(5)	173007.2(5)	173023.1(5)
L2	172911.8(5)	173007.2(5)	173023.1(5)
L3	172911.8(5)	173007.2(5)	173023.1(5)
	$C_9^{(12,23)}(1,2,1,1,1,1)$		
L1	577004(4)	577322(4)	577375(4)
L2	577004(4)	577322(4)	577375(4)
L3	−577004(4)	−577322(4)	−577375(4)
	$C_9^{(31,12)}(1,1,1,2,2,1)$		
L1	−835124(9)	−835599(9)	−835678(9)
L2	835124(9)	835599(9)	835678(9)
L3	835124(9)	835599(9)	835678(9)
	$C_9^{(31,12)}(1,1,2,1,1,2)$		
L1	172911.8(5)	173007.2(5)	173023.1(5)
L2	172911.8(5)	173007.2(5)	173023.1(5)
L3	172911.8(5)	173007.2(5)	173023.2(5)
	$C_9^{(31,12)}(1,2,1,1,1,1)$		
L1	−577004(4)	−577322(4)	−577375(4)
L2	577004(4)	577322(4)	577375(4)
L3	577004(4)	577322(4)	577375(4)

Chapter 6

Summary and Future Work

6.1 Summary

In this thesis, using perturbation theory, we have investigated the long-range three-body interactions for homonuclear systems, such as Li($2\,^2S$)-Li($2\,^2S$)-Li($2\,^2P$), Li($2\,^2S$)-Li($2\,^2S$)-Li^+($1\,^1S$), He($1\,^1S$)-He($1\,^1S$)-He($2\,^1S$) and He($n_0\,^\lambda S$)-He($n_0\,^\lambda S$)-He($n_0'\,^\lambda P$), with highly accurate variationally-generated nonrelativistic wave functions in Hylleraas coordinates. The long-range additive dipolar, additive dispersion interaction, additive induced interaction, and nonadditive interaction coefficients C_3, C_4, C_6, C_7, C_8, and C_9 were obtained. General formulas for these coefficients were derived. These formulas can, in principle, be applied to geometrical configurations other than the ones used in this thesis, i.e., the equilateral triangle, the isosceles triangle, and the straight line with nuclei equally-spaced. Our calculations may be useful in constructing accurate potential energy surfaces.

These calculations may be useful in the study of Efimov molecule. Even though the interactions are short-ranged (the interaction potentials decay faster than $1/r^3$, where r is the separation between two particles), the three particles feel a long-range three-body attraction. When the interaction is just strong enough to cancel the repulsive

effect of the kinetic energy, the interaction is said to be resonant because two particles scattering at low energy are very close to binding during their collision: they spend a long time together (they resonate) before separating, which is characterised in scattering theory by an s-wave scattering length that is much larger than the range of the interactions. This seemingly counter-intuitive situation can be explained by the fact that an effective interaction is mediated between two particles by the third particle moving back and forth between the two particles. It is thus possible for the three particles to feel their influence at distances much larger than the range of interactions, typically up to distances on the order of the scattering length [74].

6.2 Future Work

Although the long-range interactions for these homonuclear system have been investigated, there are much work left to be done. An extension of this work is to study the long-range three-body interactions for other combinations, such as Li($2\,^2S$)-Li($2\,^2P$)-Li^+($1\,^1S$), Li($2\,^2S$)-Li^+($1\,^1S$)-Li^+($1\,^1S$), He($1\,^1S$)-He($2\,^1S$)-Li^+($1\,^1S$), Li($2\,^2S$)-Li($2\,^2P$)-He($1\,^1S$), Li($2\,^2S$)-Li($2\,^2P$)-He($2\,^1S$),

He($1\,^1S$)-He($2\,^1S$)-Li($2\,^2S$), and so on. Since some of these systems still need consider the symmetries due to the exchange of homonuclear atoms, new types of additive and nonadditive interactions may appear, which would give us a deeper understanding of collective effects. Van der Waals coefficients for these systems could be important for studies of cold and ultracold collision, precision measurements, and high-resolution laser spectroscopy.

There is much great interest in forming diatomic molecules or molecular ions in cold and ultracold research area, by photoassociation [75] or three-body recombination [76]. Obviously, in these processes, the systems are particularly sensitive to long-range atom-atom and atom-diatom interactions. Thus, in the future, we may

investigate the long-range interactions for the Li-Li_2 atom-dimer system and the transition between the Li-Li-Li limit and the Li-Li_2 limit using hyperspherical coordinates [77, 78], which could provide us with a better understanding of two-body dissociation, three-body dissociation, and quantum dynamics of cold collision.

As for possible applications of our work, Li($2\,^2S$)-Li($2\,^2S$)-Li($2\,^2P$) is an ideal three-body entangled system to study the superradiance phenomenon, which is a quantum radiation enhancement effect. For this indistinguishable system, there is only one atom in the excited P state (but we do not know which one it is). The decay rate of this system would be three times faster than the incoherent emission. This cooperative single-photon superradiance phenomenon has become a subject of current interest and promises to yield new tools for storing quantum information and deeper insight into quantum electrodynamics [79].

Bibliography

[1] B. Gao, *Universal Properties in Ultracold Ion-Atom Interactions*, Phys. Rev. Lett. **104** (2010), 213201.

[2] R. Côté and A. Dalgarno, *Ultracold atom-ion collisions*, Phys. Rev. A **62** (2000), 012709.

[3] R. Côté, V. Kharchenko, and M. D. Lukin, *Mesoscopic Molecular Ions in Bose-Einstein Condensates*, Phys. Rev. Lett. **89** (2002), 093001.

[4] C. Zipkes, S. Palzer, C. Sias, and M. Köhl, *A trapped single ion inside a Bose-Einstein condensate*, Nature **464** (2010), 388.

[5] P. Zhang, A. Dalgarno, and R. Côté, *Scattering of Yb and Yb^+*, Phys. Rev. A **80** (2009), 030703.

[6] M. Tomza, K. Jachymski, R. Gerritsma, A. Negretti, T. Calarco, Z. Idziaszek, and P. S. Julienne, *Cold hybrid ion-atom systems*, arXiv:1708.07832 (2017).

[7] P. Soldán, M. T. Cvitaš, J. M. Hutson, P. Honvault, and J. M. Launay, *Quantum Dynamics of Ultracold $Na+Na_2$ Collisions*, Phys. Rev. Lett. **89** (2002), 153201.

[8] P. Soldán, M. T. Cvitaš, and J. M. Hutson, *Three-body nonadditive forces between spin-polarized alkali-metal atoms*, Phys. Rev. A **67** (2003), 054702.

[9] I. C. H. Liu, J. Stanojevic, and J. M. Rost, *Ultra-Long-Range Rydberg Trimers with a Repulsive Two-Body Interaction*, Phys. Rev. Lett. **102** (2009), 173001.

[10] F. Shen, J. Gao, A. A. Senin, C. J. Zhu, J. R. Allen, Z. H. Lu, Y. Xiao, and J. G. Eden, *Many-Body Dipole-Dipole Interactions between Excited Rb Atoms Probed by Wave Packets and Parametric Four-Wave Mixing*, Phys. Rev. Lett. **99** (2007), 143201.

[11] N. Samboy and R. Côté, *Rubidium Rydberg linear macrotrimers*, Phys. Rev. A **87** (2013), 032512.

[12] Z. C. Yan and G. W. F. Drake, *Theoretical lithium $2\,^2S \rightarrow 2\,^2P$ and $2\,^2P \rightarrow 3\,^2D$ oscillator strengths*, Phys. Rev. A **52** (1995), R4316.

[13] Z. C. Yan, J. F. Babb, A. Dalgarno, and G. W. F. Drake, *Variational calculations of dispersion coefficients for interactions among H, He, and Li atoms*, Phys. Rev. A **54** (1996), 2824.

[14] Z. C. Yan, A. Dalgarno, and J. F. Babb, *Long-range interactions of lithium atoms*, Phys. Rev. A **55** (1997), 2882.

[15] J. Y. Zhang, Z. C. Yan, J. F. Babb, and H. R. Sadeghpour, *Long-range interactions between a He(2^3S) atom and a He(2^3P) for like isotopes*, Phys. Rev. A **73** (2006), 022710.

[16] J. Y. Zhang, Z. C. Yan, D. Vrinceanu, J. F. Babb, and H. R. Sadeghpour, *Long-range interactions for He(nS)-He(n′S) and He(nS)-He(n′P)*, Phys. Rev. A **74** (2006), 014704.

[17] J. Leónard, M. Walhout, A. P. Mosk, T. Müller, X. M. Leduc, and C. Cohen-Tannoudji, *Giant Helium Dimers Produced by Photoassociation of Ultracold Metastable Atoms*, Phys. Rev. Lett. **91** (2003), 073203.

[18] V. F. Lotrich, and K. Szalewicz, *Three-Body Contribution to Binding Energy of Solid Argon and Analysis of Crystal Structure*, Phys. Rev. Lett. **79** (1997), 1301.

[19] N. Gross, Z. Shotan, S. Kokkelmans, and L. Khaykovich, *Observation of Universality in Ultracold ^7Li Three-Body Recombination*, Phys. Rev. Lett. **103** (2009), 163202.

[20] S. E. Pollack, D. Dries, and R. G. Hulet, *Universality in Three- and Four-Body Bound States of Ultracold Atoms*, Science **326** (2009), 1683.

[21] A. Härter, A. Krükow, A. Brunner, W. Schnitzler, S. Schmid, and J. H. Denschlag, *Single Ion as a Three-Body Reaction Center in an Ultracold Atomic Gas*, Phys. Rev. Lett. **109** (2012), 123201.

[22] A. Saenz, *Photoabsorption and photoionization of HeH^+*, Phys. Rev. A **67** (2003), 033409.

[23] E. M. Bringa and R. E. Johnson, *Coulomb Explosion and Thermal Spikes*, Phys. Rev. Lett. **88** (2002), 165501.

[24] R. S. Fletcher, X. L. Zhang, and S. L. Rolston, *Observation of Collective Modes of Ultracold Plasmas*, Phys. Rev. Lett. **96** (2006), 105003.

[25] B. M. Axilrod and E. Teller, *Interaction of the van der Waals Type Between Three Atoms*, J. Chem. Phys. **11** (1943), 299.

[26] R. J. Bell, *Non-additive multipolar interactions in hydrogen and helium*, J. Phys. B **3** (1970), L101.

[27] D. E. Stogryn, *Higher order interaction energies for systems of asymmetric molecules*, Molec. Phys. **22** (1971), 81.

[28] S. A. C. McDowell, A. Kumar, and W. J. Meath, *On the anisotropy of the triple-dipole dispersion energy for interactions involving linear molecules*, Molec. Phys. **87** (1996), 845.

[29] B. M. Axilrod, *TripleDipole Interaction. I. Theory*, J. Chem. Phys. **19** (1951), 719.

[30] P. G. Yan, L. Y. Tang, Z. C. Yan, and Babb, J. F. *Calculations of long-range three-body interactions for Li(2 ^{2}S)-Li(2 ^{2}S)-Li(2 ^{2}P)*, Phys. Rev. A **94** (2016), 022705.

[31] R. Moszynski, P. E. S. Wormer, B. Jeziorski, and A. v. d. Avoird, *Symmetryadapted perturbation theory of nonadditive threebody interactions in van der Waals molecules. I. General theory*, J. Chem. Phys. **103** (1995), 8058.

[32] X. Li, and K. L. C. Hunt, *Nonadditive, threebody dipoles and forces on nuclei: New interrelations and an electrostatic interpretation*, J. Chem. Phys. **105** (1996), 4076.

[33] J. Pérez-Ríos, M. Lepers, and O. Dulieu, *Theory of Long-Range Ultracold Atom-Molecule Photoassociation*, Phys. Rev. Lett. **115** (2015), 073201.

[34] T. C. Thompson, G. Izmirlian Jr., S. J. Lemon, D. G. Truhlar, and C. A. Mead, *Consistent analytic representation of the two lowest potential energy surfaces for Li_3, Na_3, and K_3*, J. Chem. Phys. **82** (1985), 5597.

[35] H. G. Krämer, M. Keil, C. B. Suarez, W. Demtröder, and W. Meyer, *Vibrational structures in the A^2E" $\leftarrow$ A^2E' system of the lithium trimer: high-resolution spectroscopy and ab initio calculations*, Chem. Phys. Lett. **299** (1999), 212.

[36] W. Meyer, M. Keil, A. Kudell, M. A. Baig, J. Zhu, and W. Demtröder, *The hyperfine structure in the electronic A - X system of the pseudorotating lithium trimer*, J. Chem. Phys. **115** (2001), 2590.

[37] M. T. Cvitaš, P. Soldán, J. M. Hutson, P. Honvault, and J. M. Launay, *Ultracold Li+Li_2 Collisions: Bosonic and Fermionic Cases*, Phys. Rev. Lett. **94** (2005), 033201.

[38] J. N. Byrd, J. A. Montgomery Jr., H. H. Michels, and R. Côté, *Electronic Structure of the Li2 [X $^1\Sigma_g^+$] Li* [^{2}P] Excited ^{2}A" Surface*, Int. J. Quantum Chem. **109** (2009), 3626.

[39] J. N. Byrd, H. H. Michels, J. A. Montgomery Jr., and R. Côté, *Long-range three-body atom-diatom potential for doublet Li_3*, Chem. Phys. Lett. **529** (2012), 23.

[40] B. Paredes, T. Keilmann, and J. I. Cirac, *Pfaffian-like ground state for three-body hard-core bosons in one-dimensional lattices*, Phys. Rev. A **75** (2007), 053611.

[41] Á. Rapp, G. Zaránd, C. Honerkamp, and W. Hofstetter, *Color Superfluidity and Baryon Formation in Ultracold Fermions*, Phys. Rev. Lett. **98** (2007), 160405.

[42] K. Helfrich and H. W. Hammer, *On the Efimov effect in higher partial waves*, J. Phys. B **44** (2011), 215301.

[43] L. Y. Tang, Z. C. Yan, T. Y. Shi, J. F. Babb, and J. Mitroy, *The long-range non-additive three-body dispersion interactions for the rare gases, alkali, and alkaline-earth atoms*, J. Chem. Phys. **136** (2012), 104104.

[44] M. Marinescu and A. F. Starace, *Three-body dispersion coefficients for alkali-metal atoms*, Phys. Rev. A **55** (1997), 2067.

[45] S. Will, T. Best, U. Schneider, L. Hackermüller, D. S. Lühmann, and I. Bloch, *Time-resolved observation of coherent multi-body interactions in quantum phase revivals*, Nature **465** (2010), 197.

[46] M. J. Mark, E. Haller, K. Lauber, J. G. Danzl, A. J. Daley, and H. C. Nägerl, *Long-range three-body atom-diatom potential for doublet Li_3*, Phys. Rev. Lett. **107** (2011), 175301.

[47] K. M. Jones, E. Tiesinga, P. D. Lett, and P. S. Julienne, *Ultracold photoassociation spectroscopy: Long-range molecules and atomic scattering*, Rev. Mod. Phys. **78** (2006), 483.

[48] A. Safavi-Naini, J. von Stecher, B. Capogrosso-Sansone, and S. T. Rittenhouse, *First-Order Phase Transitions in Optical Lattices with Tunable Three-Body On-site Interaction*, Phys. Rev. Lett. **109** (2012), 135302.

[49] W. Z. Zhang, R. Li, W. X. Zhang, C. B. Duan, and T. C. Scott, *Trimer superfluid induced by photoassocation on the state-dependent optical lattice*, Phys. Rev. A **90** (2014), 033622.

[50] T. Pohl and P. R. Berman, *Breaking the Dipole Blockade: Nearly Resonant Dipole Interactions in Few-Atom Systems*, Phys. Rev. Lett. **102** (2009), 013004.

[51] D. Barredo, S. Ravets, H. Labuhn, L. Béguin, A. Vernier, F. Nogrette, T. Lahaye, and A. Browaeys, *Demonstration of a Strong Rydberg Blockade in Three-Atom Systems with Anisotropic Interactions*, Phys. Rev. Lett. **112** (2014), 183002.

[52] M. Kiffner, W. H. Li, and D. Jaksch, *Three-Body Bound States in Dipole-Dipole Interacting Rydberg Atoms*, Phys. Rev. Lett. **111** (2013), 233003.

[53] D. A. Brue, X. Li, and G. A. Parker, *Conical intersection between the lowest spin-aligned Li3(^4A) Li_3(A4) potential-energy surfaces*, J. Chem. Phys. **123** (2005), 091101.

[54] X. Li, D. A. Brue, and G. A. Parker, *Potential energy surfaces for the $1^4A'$, $2^4A'$, $1^4A''$ and $2^4A''$ states of Li_3*, J. Chem. Phys. **129** (2008), 124305.

[55] J. N. Byrd, J. A. Montgomery, H. H. Michels, and R. Côté, *Potential energy surface of the $1^2A'$ prime Li_2 + Li doublet ground state*, Int. J. Quantum Chem. **109** (2009), 3112.

[56] M. Lepers, O. Dulieu, and V. Kokoouline, *Photoassociation of a cold-atom-molecule pair: Long-range quadrupole-quadrupole interactions*, Phys. Rev. A **82** (2010), 042711.

[57] M. Lepers, R. Vexiau, N. Bouloufa, O. Dulieu, and V. Kokoouline, *Photoassociation of a cold-atom-molecule pair. II. Second-order perturbation approach*, Phys. Rev. A **83** (2011), 042707.

[58] A. J. C. Varandas and A. A. C. C. Pais, *Double many-body expansion of the two lowest potential-energy surfaces for Li_3 and dynamics of the Li + Li_2(v) reaction. Initial orientation and vibrational excitation effects*, J. Chem. Soc., Faraday Trans. **89** (1993), 1511.

[59] M. Ehara and K. Yamashita, *Theoretical studies of the potential energy surface and wavepacket dynamics of the Li_3 system*, Theor. Chem. Acc. **102** (1999), 226.

[60] E. N. Ghassemi, J. Larson, and Å. Larson, *A diabatic representation of the two lowest electronic states of Li_3*, J. Chem. Phys. **140** (2014), 154304.

[61] M. T. Cvitaš, P. Soldán, and J. M. Hutson, *Long range intermolecular forces in triatomic systems: connecting the atomdiatom and atomatomatom representations*, Mol. Phys. **104** (2006), 23.

[62] N. Herschbach, P. J. J. Tol, W. Vassen, W. Hogervorst, G. Woestenenk, J. W. Thomsen, P. van der Straten, and A. Niehaus, *Photoassociation Spectroscopy of Cold He(2^3S) Atoms*, Phys. Rev. Lett. **84** (2000), 1874.

[63] J. Weiner, V. S. Bagnato, S. Zilio, and P. S. Julienne, *Experiments and theory in cold and ultracold collisions*, Rev. Mod. Phys. **71** (1999), 1.

[64] P. J. Leo, V. Venturi, I. B. Whittingham, J. F. Babb, *Ultracold collisions of metastable helium atoms*, Phys. Rev. A **64** (2001), 042710.

[65] H. C. Mastwijk, J. W. Thomsen, P. van der Straten, and A. Niehaus, *Optical Collisions of Cold, Metastable Helium Atoms*, Phys. Rev. Lett. **80** (1998), 5516.

[66] M. Kumakura, and N. Morita, *Spinodal Decomposition in Fluids*, Phys. Rev. Lett. **82** (1999), 14.

[67] P. J. J. Tol, N. Herschbach, E. A. Hessels, W. Hogervorst, and W. Vassen, *Large numbers of cold metastable helium atoms in a magneto-optical trap*, Phys. Rev. A **60** (1999), R761.

[68] D. T. Chang, and G. I. Gellene, *An ab initio, analytically fitted, global potential energy surface for the ground electronic state of* He_3^+, J. Chem. Phys. **119** (2003), 4694.

[69] J. Y. Zhang and Z. C. Yan, *Long-range interactions for hydrogen molecular ions*, J. Phys. B **37** (2004), 723.

[70] Z. C. Yan and G. W. F. Drake, *Eigenvalues and expectation values for the* $1s^2\ 2s\ ^2S$, $1s^2\ 2p\ ^2P$, *and* $1s^2\ 3d\ ^2D$ *states of lithium* , Phys. Rev. A **52** (1995), 3711.

[71] J. K, L. MacDonald, *Successive Approximations by the Rayleigh-Ritz Variation Method*, Phys. Rev.**43** (1933), 830.

[72] Z. C. Yan and G. W. F. Drake, *Computational methods for three-electron atomic systems in Hylleraas coordinates*, J. Phys. B **30** (1997), 4723.

[73] L. Y. Tang, Z. C. Yan, T. Y. Shi, and J. F. Babb, *Non-relativistic ab initio calculations for* $2\ ^2S$, $2\ ^2P$ *and* $3\ ^2D$ *lithium isotopes: Applications to polarizabilities and dispersion interactions*, Phys. Rev. A **79** (2009), 062712.

[74] P. Naidon, and S. Endo, *Efimov Physics: a review*, arXiv:1610.09805v2 (2017).

[75] R. Wynar, R. S. Freeland, D. J. Han, C. Ryu, and D. J. Heinzen, *Molecules in a Bose-Einstein Condensate*, Science **287** (2000), 1016.

[76] S. Jochim, M. Bartenstein, A. Altmeyer, G. Hendl, S. Riedl, C. Chin, J. H. Denschlag, and R. Grimm, *Bose-Einstein Condensation of Molecules*, Science **302** (2003), 2101.

[77] C. D. Lin, *Hyperspherical coordinate approach to atomic and other coulombic three-body systems*, Phys. Rep **257** (1995), 1.

[78] B. R. Johnson, *On hyperspherical coordinates and mapping the internal configurations of a three body system*, J. Chem. Phys. **73** (1980), 5051.

[79] M. O. Scully and A. A. Svidzinsky, *The super of superradiance*, Science **325** (2009), 5947.

Appendix A

C_m Coefficients for $A(n_0S)$-$A(n_0S)$-$A(n_0'L)$

We consider three like atoms with two atoms in identical S states $|\varphi_{n_0}(0)\rangle$ and the third atom in a non-S state $|\varphi_{n_0'}(LM)\rangle$, where n_0 and n_0' are the principal quantum numbers, and L and M are the usual angular quantum numbers. In the following, we use $\boldsymbol{\sigma}$, $\boldsymbol{\rho}$, and $\boldsymbol{\varsigma}$ to represent collectively the coordinates of each atom. The three orthonormalized degenerate eigenvectors of the unperturbed Hamiltonian with the energy eigenvalue $E^{(0)}_{n_0S;n_0S;n_0'L} = 2E^{(0)}_{n_0S} + E^{(0)}_{n_0'L}$. The correct zeroth-order wavefunctions can always be expanded as a linear combination of $\{\phi_1, \phi_2, \phi_3\}$

$$|\Psi^{(0)}\rangle = a|\phi_1\rangle + b|\phi_2\rangle + c|\phi_3\rangle\,, \tag{A.1}$$

where a, b, and c are the expansion coefficients with their values depending on the geometrical configuration of the three atoms.

A.1 The First-Order Energy Correction

According to perturbation theory, the first-order energy correction is

$$
\begin{aligned}
&\Delta E^{(1)} = \langle \Psi^{(0)} | V_{123} | \Psi^{(0)} \rangle \\
&= |a|^2 \langle \phi_1 | V_{123} | \phi_1 \rangle + |b|^2 \langle \phi_2 | V_{123} | \phi_2 \rangle + |c|^2 \langle \phi_3 | V_{123} | \phi_3 \rangle \\
&+ (a^* b + b^* a) \langle \phi_1 | V_{123} | \phi_2 \rangle + (a^* c + c^* a) \langle \phi_1 | V_{123} | \phi_3 \rangle \\
&+ (b^* c + c^* b) \langle \phi_2 | V_{123} | \phi_3 \rangle \\
&= (a^* b + b^* a) \frac{4\pi}{R_{12}^{2L+1}} \frac{(-1)^{L+M}(2L)! P_{2L}(\cos\theta_{12})}{(2L+1)^2 (L-M)!(L+M)!} \\
&\times |\langle \varphi_{n_0}(0;\boldsymbol{\sigma}) \| T_L(\boldsymbol{\sigma}) \| \varphi_{n_0'}(L;\boldsymbol{\sigma}) \rangle|^2 \\
&+ (b^* c + c^* b) \frac{4\pi}{R_{23}^{2L+1}} \frac{(-1)^{L+M}(2L)! P_{2L}(\cos\theta_{23})}{(2L+1)^2 (L-M)!(L+M)!} \\
\times\ & |\langle \varphi_{n_0}(0;\boldsymbol{\rho}) \| T_L(\boldsymbol{\rho}) \| \varphi_{n_0'}(L;\boldsymbol{\rho}) \rangle|^2 \\
&+ (c^* a + a^* c) \frac{4\pi}{R_{31}^{2L+1}} \frac{(-1)^{L+M}(2L)! P_{2L}(\cos\theta_{31})}{(2L+1)^2 (L-M)!(L+M)!} \\
&\times |\langle \varphi_{n_0}(0;\boldsymbol{\varsigma}) \| T_L(\boldsymbol{\varsigma}) \| \varphi_{n_0'}(L;\boldsymbol{\varsigma}) |^2
\end{aligned}
$$

. (A.2)

A.2 The Second-Order Energy Correction

The second-order energy correction is given by

$$
\begin{aligned}
\Delta E^{(2)} &= -\sum_{\substack{n_s n_t n_u; \\ L_s L_t L_u; \\ M_s M_t M_u}} \frac{|\langle \Psi^{(0)} | V_{123} | \chi_{n_s}(L_s M_s;\boldsymbol{\sigma}) \chi_{n_t}(L_t M_t;\boldsymbol{\rho}) \chi_{n_u}(L_u M_u;\boldsymbol{\varsigma}) \rangle|^2}{E_{n_s L_s; n_t L_t; n_u L_u} - E^{(0)}_{n_0 S; n_0 S; n_0' L}} \\
&= V_{12}^{(2)} + V_{23}^{(2)} + V_{31}^{(2)} + V_{12,23}^{(2)} + V_{23,31}^{(2)} + V_{31,12}^{(2)} \,, \qquad \text{(A.3)}
\end{aligned}
$$

where $\chi_{n_s}(L_s M_s;\boldsymbol{\sigma}) \chi_{n_t}(L_t M_t;\boldsymbol{\rho}) \chi_{n_u}(L_u M_u;\boldsymbol{\varsigma})$ is an intermediate state of the system with the energy eigenvalue $E_{n_s L_s; n_t L_t; n_u L_u} = E_{n_s L_s} + E_{n_t L_t} + E_{n_u L_u}$. It is noted that the above summations should exclude terms with $E_{n_s L_s; n_t L_t; n_u L_u} = E^{(0)}_{n_0 S; n_0 S; n_0' L}$.

With $V_{123} = V_{12} + V_{23} + V_{31}$, the above expression can be expanded as

$$\Delta E^{(2)} = -\sum_{\substack{n_s n_t n_u;\\ L_s L_t L_u;\\ M_s M_t M_u}} \frac{B_1 + B_2 + B_3 + B_4 + B_5 + B_6 + B_7 + B_8 + B_9}{E_{n_s L_s; n_t L_t; n_u L_u} - E^{(0)}_{n_0 S; n_0 S; n_0' L}}\,, \tag{A.4}$$

where B_n $(n = 1 - 9)$ are

$$\begin{aligned}
B_1 &= |\langle \Psi^{(0)}|V_{12}|\chi_{n_s}(L_s M_s;\boldsymbol{\sigma})\chi_{n_t}(L_t M_t;\boldsymbol{\rho})\chi_{n_u}(L_u M_u;\boldsymbol{\varsigma})\rangle|^2 \\
&= |a|^2|\langle \phi_1|V_{12}|\chi_{n_s}(L_s M_s;\boldsymbol{\sigma})\chi_{n_t}(L_t M_t;\boldsymbol{\rho})\chi_{n_u}(L_u M_u;\boldsymbol{\varsigma})\rangle|^2 \\
&+ |b|^2|\langle \phi_2|V_{12}|\chi_{n_s}(L_s M_s;\boldsymbol{\sigma})\chi_{n_t}(L_t M_t;\boldsymbol{\rho})\chi_{n_u}(L_u M_u;\boldsymbol{\varsigma})\rangle|^2 \\
&+ |c|^2|\langle \phi_3|V_{12}|\chi_{n_s}(L_s M_s;\boldsymbol{\sigma})\chi_{n_t}(L_t M_t;\boldsymbol{\rho})\chi_{n_u}(L_u M_u;\boldsymbol{\varsigma})\rangle|^2 \\
&+ a^* b\langle \phi_1|V_{12}|\chi_{n_s}(L_s M_s;\boldsymbol{\sigma})\chi_{n_t}(L_t M_t;\boldsymbol{\rho})\chi_{n_u}(L_u M_u;\boldsymbol{\varsigma})\rangle^* \\
&\times \langle \phi_2|V_{12}|\chi_{n_s}(L_s M_s;\boldsymbol{\sigma})\chi_{n_t}(L_t M_t;\boldsymbol{\rho})\chi_{n_u}(L_u M_u;\boldsymbol{\varsigma})\rangle \\
&+ b^* a\langle \phi_2|V_{12}|\chi_{n_s}(L_s M_s;\boldsymbol{\sigma})\chi_{n_t}(L_t M_t;\boldsymbol{\rho})\chi_{n_u}(L_u M_u;\boldsymbol{\varsigma})\rangle^* \\
&\times \langle \phi_1|V_{12}|\chi_{n_s}(L_s M_s;\boldsymbol{\sigma})\chi_{n_t}(L_t M_t;\boldsymbol{\rho})\chi_{n_u}(L_u M_u;\boldsymbol{\varsigma})\rangle \\
&= |a|^2 \sum_{l_1 l_1'}\sum_{m_1} \frac{16\pi^2}{R_{12}^{2L_t+l_1+l_1'+2}} \begin{pmatrix} L & l_1 & L_s \\ -M & m_1 & M_s \end{pmatrix} \begin{pmatrix} L & l_1' & L_s \\ -M & m_1 & M_s \end{pmatrix} \\
&\times \frac{(L_t + l_1 - M_t + m_1)!(L_t + l_1' - M_t + m_1)!(l_1, l_1')^{-1/2}(L_t, L_t)^{-1}}{(L_t + M_t)!(L_t - M_t)![(l_1 + m_1)!(l_1 - m_1)!(l_1' + m_1)!(l_1' - m_1)!]^{1/2}} \\
&\times \langle \varphi_{n_0'}(L;\boldsymbol{\sigma})\|T_{l_1}(\boldsymbol{\sigma})\|\chi_{n_s}(L_s;\boldsymbol{\sigma})\rangle^* \langle \varphi_{n_0'}(L;\boldsymbol{\sigma})\|T_{l_1'}(\boldsymbol{\sigma})\|\chi_{n_s}(L_s;\boldsymbol{\sigma})\rangle \\
&\times |\langle \varphi_{n_0}(0;\boldsymbol{\rho})\|T_{L_t}(\boldsymbol{\rho})\|\chi_{n_t}(L_t;\boldsymbol{\rho})\rangle|^2 \\
&\times P_{l_1+L_t}^{M_t-m_1}(\cos\theta_{12}) P_{l_1'+L_t}^{M_t-m_1}(\cos\theta_{12}) \\
&\times \delta_{n_u,n_0}\delta_{L_u,0}\delta_{M_u,0} \\
&+ |b|^2 \sum_{l_2 l_2'}\sum_{m_2} \frac{16\pi^2}{R_{12}^{2L_s+l_2+l_2'+2}} \begin{pmatrix} L & l_2 & L_t \\ -M & m_2 & M_t \end{pmatrix} \begin{pmatrix} L & l_2' & L_t \\ -M & m_2 & M_t \end{pmatrix} \\
&\times \frac{(L_s + l_2 - M_s + m_2)!(L_s + l_2' - M_s + m_2)!(l_2, l_2')^{-1/2}(L_s, L_s)^{-1}}{(L_s + M_s)!(L_s - M_s)![(l_2 + m_2)!(l_2 - m_2)!(l_2' + m_2)!(l_2' - m_2)!]^{1/2}}
\end{aligned}$$

$$
\begin{aligned}
&\times \quad \langle\varphi_{n_0'}(L;\boldsymbol{\rho})\|T_{l_2}(\boldsymbol{\rho})\|\chi_{n_t}(L_t;\boldsymbol{\rho})\rangle^*\langle\varphi_{n_0'}(L;\boldsymbol{\rho})\|T_{l_2'}(\boldsymbol{\rho})\|\chi_{n_t}(L_t;\boldsymbol{\rho})\rangle \\
&\times \quad |\langle\varphi_{n_0}(0;\boldsymbol{\sigma})\|T_{L_s}(\boldsymbol{\sigma})\|\chi_{n_s}(L_s;\boldsymbol{\sigma})\rangle|^2 \\
&\times \quad P_{L_s+l_2}^{M_s-m_2}(\cos\theta_{12})P_{L_s+l_2'}^{M_s-m_2}(\cos\theta_{12}) \\
&\times \quad \delta_{n_u,n_0}\delta_{L_u,0}\delta_{M_u,0} \\
&+ \quad |c|^2\frac{16\pi^2}{R_{12}^{2L_s+2L_t+2}}\left\{\frac{(L_s+L_t-M_s-M_t)!(L_s,L_t)^{-1}}{[(L_s+M_s)!(L_s-M_s)!(L_t+M_t)!(L_t-M_t)!]^{1/2}}\right\}^2 \\
&\times \quad |\langle\varphi_{n_0}(0;\boldsymbol{\sigma})\|T_{L_s}(\boldsymbol{\sigma})\|\chi_{n_s}(L_s;\boldsymbol{\sigma})\rangle|^2|\langle\varphi_{n_0}(0;\boldsymbol{\rho})\|T_{L_t}(\boldsymbol{\rho})\|\chi_{n_t}(L_t;\boldsymbol{\rho})\rangle|^2 \\
&\times \quad P_{L_s+L_t}^{M_s+M_t}(\cos\theta_{12})P_{L_s+L_t}^{M_s+M_t}(\cos\theta_{12}) \\
&\times \quad \delta_{n_u,n_0'}\delta_{L_u,L}\delta_{M_u,M} \\
&+ \quad a^*b\sum_{l_1l_2'}\sum_{m_1m_2'}\frac{(-1)^{L_s+l_2'-M_s-M_t}16\pi^2}{R_{12}^{l_1+L_s+L_t+l_2'+2}} \\
&\times \quad \begin{pmatrix} L & l_1 & L_s \\ -M & -m_1 & M_s \end{pmatrix}\begin{pmatrix} L & l_2' & L_t \\ -M & m_2' & M_t \end{pmatrix} \\
&\times \quad \frac{(L_s+l_2'-M_s+m_2')!(l_1,l_2')^{-1/2}}{[(l_1+m_1)!(l_1-m_1)!(L_t+M_t)!(L_t-M_t)!]^{1/2}} \\
&\times \quad \frac{(l_1+L_t-m_1-M_t)!(L_s,L_t)^{-1}}{[(L_s+M_s)!(L_s-M_s)!(l_2'+m_2')!(l_2'-m_2')!]^{1/2}} \\
&\times \quad \langle\varphi_{n_0'}(L;\boldsymbol{\sigma})\|T_{l_1}(\boldsymbol{\sigma})\|\chi_{n_s}(L_s;\boldsymbol{\sigma})\rangle^*\langle\varphi_{n_0}(0;\boldsymbol{\rho})\|T_{L_t}(\boldsymbol{\rho})\|\chi_{n_t}(L_t;\boldsymbol{\rho})\rangle^* \\
&\times \quad \langle\varphi_{n_0}(0;\boldsymbol{\sigma})\|T_{L_s}(\boldsymbol{\sigma})\|\chi_{n_s}(L_s;\boldsymbol{\sigma})\rangle\langle\varphi_{n_0'}(L;\boldsymbol{\rho})\|T_{l_2'}(\boldsymbol{\rho})\|\chi_{n_t}(L_t;\boldsymbol{\rho})\rangle \\
&\times \quad P_{l_1+L_t}^{m_1+M_t}(\cos\theta_{12})P_{L_s+l_2'}^{M_s-m_2'}(\cos\theta_{12}) \\
&\times \quad \delta_{n_u,n_0}\delta_{L_u,0}\delta_{M_u,0} \\
&+ \quad b^*a\sum_{l_1'l_2}\sum_{m_1'}\frac{16\pi^2(-1)^{L_s+l_2-M_s-M_t}}{R_{12}^{l_1'+L_t+L_s+l_2+2}} \\
&\times \quad \begin{pmatrix} L & l_1' & L_s \\ -M & -m_1' & M_s \end{pmatrix}\begin{pmatrix} L & l_2 & L_t \\ -M & m_2 & M_t \end{pmatrix} \\
&\times \quad \frac{(l_1'+L_t-m_1'-M_t)!(L_s,L_t)^{-1}}{[(L_s+M_s)!(L_s-M_s)!(l_2+m_2)!(l_2-m_2)!]^{1/2}} \\
&\times \quad \frac{(L_s+l_2-M_s+m_2)!(l_1',l_2)^{-1/2}}{[(l_1'+m_1')!(l_1'-m_1')!(L_t+M_t)!(L_t-M_t)!]^{1/2}} \\
&\times \quad \langle\varphi_{n_0}(0;\boldsymbol{\sigma})\|T_{L_s}(\boldsymbol{\sigma})\|\chi_{n_s}(L_s;\boldsymbol{\sigma})\rangle^*\langle\varphi_{n_0'}(L;\boldsymbol{\rho})\|T_{l_2}(\boldsymbol{\rho})\|\chi_{n_t}(L_t;\boldsymbol{\rho})\rangle^*
\end{aligned}
$$

$$
\begin{aligned}
&\times \quad \langle\varphi_{n_0'}(L;\boldsymbol{\sigma})\|T_{l_1'}(\boldsymbol{\sigma})\|\chi_{n_s}(L_s;\boldsymbol{\sigma})\rangle\langle\varphi_{n_0}(0;\boldsymbol{\rho})\|T_{L_t}(\boldsymbol{\rho})\|\chi_{n_t}(L_t;\boldsymbol{\rho})\rangle \\
&\times \quad P_{L_s+l_2}^{M_s-m_2}(\cos\theta_{12})P_{l_1'+L_t}^{m_1'+M_t}(\cos\theta_{12}) \\
&\times \quad \delta_{n_u,n_0}\delta_{L_u,0}\delta_{M_u,0}\,, \qquad\qquad (A.5)
\end{aligned}
$$

$$
\begin{aligned}
B_2 \;&=\; \langle\Psi^{(0)}|V_{12}|\chi_{n_s}(L_sM_s;\boldsymbol{\sigma})\chi_{n_t}(L_tM_t;\boldsymbol{\rho})\chi_{n_u}(L_uM_u;\boldsymbol{\varsigma})\rangle^* \\
&\times \quad \langle\Psi^{(0)}|V_{23}|\chi_{n_s}(L_sM_s;\boldsymbol{\sigma})\chi_{n_t}(L_tM_t;\boldsymbol{\rho})\chi_{n_u}(L_uM_u;\boldsymbol{\varsigma})\rangle \\
&=\; a^*c\langle\phi_1|V_{12}|\chi_{n_s}(L_sM_s;\boldsymbol{\sigma})\chi_{n_t}(L_tM_t;\boldsymbol{\rho})\chi_{n_u}(L_uM_u;\boldsymbol{\varsigma})\rangle^* \\
&\times \quad \langle\phi_3|V_{23}|\chi_{n_s}(L_sM_s;\boldsymbol{\sigma})\chi_{n_t}(L_tM_t;\boldsymbol{\rho})\chi_{n_u}(L_uM_u;\boldsymbol{\varsigma})\rangle \\
&+\; c^*a\langle\phi_3|V_{12}|\chi_{n_s}(L_sM_s;\boldsymbol{\sigma})\chi_{n_t}(L_tM_t;\boldsymbol{\rho})\chi_{n_u}(L_uM_u;\boldsymbol{\varsigma})\rangle^* \\
&\times \quad \langle\phi_1|V_{23}|\chi_{n_s}(L_sM_s;\boldsymbol{\sigma})\chi_{n_t}(L_tM_t;\boldsymbol{\rho})\chi_{n_u}(L_uM_u;\boldsymbol{\varsigma})\rangle \\
&=\; a^*c\frac{16\pi^2(-1)^{L_t+L}}{R_{12}^{L_t+L+1}R_{23}^{L_t+L+1}}P_{L+L_t}^{-M+M_t}(\cos\theta_{12})P_{L_t+L}^{M_t-M}(\cos\theta_{23}) \\
&\times \quad \left\{\frac{(L_t+L-M_t+M)!(L_t,L)^{-1}}{[(L_t+M_t)!(L_t-M_t)!(L+M)!(L-M)!]^{1/2}}\right\}^2 \\
&\times \quad |\langle\varphi_{n_0'}(L;\boldsymbol{\sigma})\|T_L(\boldsymbol{\sigma})\|\chi_{n_s}(0;\boldsymbol{\sigma})\rangle|^2|\langle\varphi_{n_0}(0;\boldsymbol{\rho})\|T_{L_t}(\boldsymbol{\rho})\|\chi_{n_t}(L_t;\boldsymbol{\rho})\rangle|^2 \\
&\times \quad \exp[i(M_t-M)(\Phi_{23}-\Phi_{12})] \\
&\times \quad \delta_{n_s,n_0}\delta_{L_s,0}\delta_{M_s,0}\delta_{n_u,n_0}\delta_{L_u,0}\delta_{M_u,0} \\
&+\; c^*a\frac{16\pi^2(-1)^{L_t+L}}{R_{12}^{L_t+L+1}R_{23}^{L_t+L+1}}P_{L+L_t}^{M+M_t}(\cos\theta_{12})P_{L_t+L}^{M_t+M}(\cos\theta_{23}) \\
&\times \quad \left\{\frac{(L_t+L-M_t-M)!(L_t,L)^{-1}}{[(L_t+M_t)!(L_t-M_t)!(L+M)!(L-M)!]^{1/2}}\right\}^2 \\
&\times \quad |\langle\varphi_{n_0}(0;\boldsymbol{\sigma})\|T_L(\boldsymbol{\sigma})\|\chi_{n_s}(L;\boldsymbol{\sigma})\rangle|^2|\langle\varphi_{n_0}(0;\boldsymbol{\rho})\|T_{L_t}(\boldsymbol{\rho})\|\chi_{n_t}(L_t;\boldsymbol{\rho})\rangle|^2 \\
&\times \quad \exp[i(M_t+M)(\Phi_{23}-\Phi_{12})] \\
&\times \quad \delta_{n_s,n_0'}\delta_{L_s,L}\delta_{M_s,M}\delta_{n_u,n_0'}\delta_{L_u,L}\delta_{M_u,M}\,, \qquad\qquad (A.6)
\end{aligned}
$$

$$
\begin{aligned}
B_3 \;&=\; \langle\Psi^0|V_{12}|\chi_{n_s}(L_sM_s;\boldsymbol{\sigma})\chi_{n_t}(L_tM_t;\boldsymbol{\rho})\chi_{n_u}(L_uM_u;\boldsymbol{\varsigma})\rangle^* \\
&\times \quad \langle\Psi^{(0)}V_{31}|\chi_{n_s}(L_sM_s;\boldsymbol{\sigma})\chi_{n_t}(L_tM_t;\boldsymbol{\rho})\chi_{n_u}(L_uM_u;\boldsymbol{\varsigma})\rangle
\end{aligned}
$$

$$
\begin{aligned}
&= b^* c \langle \phi_2 | V_{12} | \chi_{n_s}(L_s M_s;\boldsymbol{\sigma}) \chi_{n_t}(L_t M_t;\boldsymbol{\rho}) \chi_{n_u}(L_u M_u;\boldsymbol{\varsigma}) \rangle^* \\
&\times \langle \phi_3 | V_{31} | \chi_{n_s}(L_s M_s;\boldsymbol{\sigma}) \chi_{n_t}(L_t M_t;\boldsymbol{\rho}) \chi_{n_u}(L_u M_u;\boldsymbol{\varsigma}) \rangle \\
&+ c^* b \langle \phi_3 | V_{12} | \chi_{n_s}(L_s M_s;\boldsymbol{\sigma}) \chi_{n_t}(L_t M_t;\boldsymbol{\rho}) \chi_{n_u}(L_u M_u;\boldsymbol{\varsigma}) \rangle^* \\
&\times \langle \phi_2 | V_{31} | \chi_{n_s}(L_s M_s;\boldsymbol{\sigma}) \chi_{n_t}(L_t M_t;\boldsymbol{\rho}) \chi_{n_u}(L_u M_u;\boldsymbol{\varsigma}) \rangle \\
&= b^* c \frac{16\pi^2 (-1)^{L_s+L}}{R_{12}^{L_s+L+1} R_{31}^{L_s+L+1}} P_{L_s+L}^{M_s-M}(\cos\theta_{12}) P_{L+L_s}^{-M+M_s}(\cos\theta_{31}) \\
&\times \left\{ \frac{(L_s+L-M_s+M)!(L_s,L)^{-1}}{[(L_s+M_s)!(L_s-M_s)!(L+M)!(L-M)!]^{1/2}} \right\}^2 \\
&\times |\langle \varphi_{n_0}(0;\boldsymbol{\sigma}) \| T_{L_s}(\boldsymbol{\sigma}) \| \chi_{n_s}(L_s;\boldsymbol{\sigma}) \rangle|^2 |\langle \varphi_{n_0'}(L;\boldsymbol{\rho}) \| T_L(\boldsymbol{\rho}) \| \chi_{n_t}(0;\boldsymbol{\rho}) \rangle|^2 \\
&\times \exp[i(M_s - M)(\Phi_{31} - \Phi_{12})] \\
&\times \delta_{n_t,n_0} \delta_{L_t,0} \delta_{M_t,0} \delta_{n_u,n_0} \delta_{L_u,0} \delta_{M_u,0} \\
&+ c^* b \frac{16\pi^2 (-1)^{L_s+L}}{R_{12}^{L_s+L+1} R_{31}^{L_s+L+1}} P_{L_s+L}^{M_s+M}(\cos\theta_{12}) P_{L+L_s}^{M+M_s}(\cos\theta_{31}) \\
&\times \left\{ \frac{(L_s+L-M_s-M)!(L_s,L)^{-1}}{[(L_s+M_s)!(L_s-M_s)!(L+M)!(L-M)!]^{1/2}} \right\}^2 \\
&\times |\langle \varphi_{n_0}(0;\boldsymbol{\sigma}) \| T_{L_s}(\boldsymbol{\sigma}) \| \chi_{n_s}(L_s;\boldsymbol{\sigma}) \rangle|^2 |\langle \varphi_{n_0}(0;\boldsymbol{\rho}) \| T_L(\boldsymbol{\rho}) \| \chi_{n_t}(L;\boldsymbol{\rho}) \rangle|^2 \\
&\times \exp[i(M_s + M)(\Phi_{31} - \Phi_{12})] \\
&\times \delta_{n_t,n_0'} \delta_{L_t,L} \delta_{M_t,M} \delta_{n_u,n_0'} \delta_{L_u,L} \delta_{M_u,M} \,, \qquad \text{(A.7)}
\end{aligned}
$$

$$
\begin{aligned}
B_4 &= \langle \Psi^{(0)} V_{23} | \chi_{n_s}(L_s M_s;\boldsymbol{\sigma}) \chi_{n_t}(L_t M_t;\boldsymbol{\rho}) \chi_{n_u}(L_u M_u;\boldsymbol{\varsigma}) \rangle^* \\
&\times \langle \Psi^{(0)} | V_{12} | \chi_{n_s}(L_s M_s;\boldsymbol{\sigma}) \chi_{n_t}(L_t M_t;\boldsymbol{\rho}) \chi_{n_u}(L_u M_u;\boldsymbol{\varsigma}) \rangle \\
&= a^* c \langle \phi_1 | V_{23} | \chi_{n_s}(L_s M_s;\boldsymbol{\sigma}) \chi_{n_t}(L_t M_t;\boldsymbol{\rho}) \chi_{n_u}(L_u M_u;\boldsymbol{\varsigma}) \rangle^* \\
&\times \langle \phi_3 | V_{12} | \chi_{n_s}(L_s M_s;\boldsymbol{\sigma}) \chi_{n_t}(L_t M_t;\boldsymbol{\rho}) \chi_{n_u}(L_u M_u;\boldsymbol{\varsigma}) \rangle \\
&+ c^* a \langle \phi_3 | V_{23} | \chi_{n_s}(L_s M_s;\boldsymbol{\sigma}) \chi_{n_t}(L_t M_t;\boldsymbol{\rho}) \chi_{n_u}(L_u M_u;\boldsymbol{\varsigma}) \rangle^* \\
&\times \langle \phi_1 | V_{12} | \chi_{n_s}(L_s M_s;\boldsymbol{\sigma}) \chi_{n_t}(L_t M_t;\boldsymbol{\rho}) \chi_{n_u}(L_u M_u;\boldsymbol{\varsigma}) \rangle \\
&= a^* c \frac{16\pi^2 (-1)^{L_t+L}}{R_{12}^{L_t+L+1} R_{23}^{L_t+L+1}} P_{L_t+L}^{M_t+M}(\cos\theta_{23}) P_{L+L_t}^{M+M_t}(\cos\theta_{12}) \\
&\times \left\{ \frac{(L_t+L-M_t-M)!(L_t,L)^{-1}}{[(L_t+M_t)!(L_t-M_t)!(L+M)!(L-M)!]^{1/2}} \right\}^2
\end{aligned}
$$

$$
\begin{aligned}
&\times \quad |\langle\varphi_{n_0}(0;\boldsymbol{\sigma})\|T_L(\boldsymbol{\sigma})\|\chi_{n_s}(L;\boldsymbol{\sigma})\rangle|^2|\langle\varphi_{n_0}(0;\boldsymbol{\rho})\|T_{L_t}(\boldsymbol{\rho})\|\chi_{n_t}(L_t;\boldsymbol{\rho})\rangle|^2 \\
&\times \quad \exp[i(M_t+M)(\Phi_{12}-\Phi_{23})] \\
&\times \quad \delta_{n_s,n_0'}\delta_{L_s,L}\delta_{M_s,M}\delta_{n_u,n_0'}\delta_{L_u,L}\delta_{M_u,M} \\
&+ \quad c^* a\frac{16\pi^2(-1)^{L_t+L}}{R_{12}^{L_t+L+1}R_{23}^{L_t+L+1}}P_{L_t+L}^{M_t-M}(\cos\theta_{23})P_{L+L_t}^{-M+M_t}(\cos\theta_{12}) \\
&\times \quad \left\{\frac{(L_t+L-M_t+M)!(L_t,L)^{-1}}{[(L_t+M_t)!(L_t-M_t)!(L+M)!(L-M)!]^{1/2}}\right\}^2 \\
&\times \quad |\langle\varphi_{n_0'}(L;\boldsymbol{\sigma})\|T_L(\boldsymbol{\sigma})\|\chi_{n_s}(0;\boldsymbol{\sigma})\rangle|^2|\langle\varphi_{n_0}(0;\boldsymbol{\rho})\|T_{L_t}(\boldsymbol{\rho})\|\chi_{n_t}(L_t;\boldsymbol{\rho})\rangle|^2 \\
&\times \quad \exp[i(M_t-M)(\Phi_{12}-\Phi_{23})] \\
&\times \quad \delta_{n_s,n_0}\delta_{L_s,0}\delta_{M_s,0}\delta_{n_u,n_0}\delta_{L_u,0}\delta_{M_u,0}\,, \qquad\qquad (A.8)
\end{aligned}
$$

$$
\begin{aligned}
B_5 \;=\;& \langle\Psi^{(0)}|V_{23}|\chi_{n_s}(L_sM_s;\boldsymbol{\sigma})\chi_{n_t}(L_tM_t;\boldsymbol{\rho})\chi_{n_u}(L_uM_u;\boldsymbol{\varsigma})\rangle^* \\
&\times \quad \langle\Psi^{(0)}|V_{23}|\chi_{n_s}(L_sM_s;\boldsymbol{\sigma})\chi_{n_t}(L_tM_t;\boldsymbol{\rho})\chi_{n_u}(L_uM_u;\boldsymbol{\varsigma})\rangle \\
&= \quad |a|^2\langle\phi_1|V_{23}|\chi_{n_s}(L_sM_s;\boldsymbol{\sigma})\chi_{n_t}(L_tM_t;\boldsymbol{\rho})\chi_{n_u}(L_uM_u;\boldsymbol{\varsigma})\rangle^* \\
&\times \quad \langle\phi_1|V_{23}|\chi_{n_s}(L_sM_s;\boldsymbol{\sigma})\chi_{n_t}(L_tM_t;\boldsymbol{\rho})\chi_{n_u}(L_uM_u;\boldsymbol{\varsigma})\rangle \\
&+ \quad |b|^2\langle\phi_2|V_{23}|\chi_{n_s}(L_sM_s;\boldsymbol{\sigma})\chi_{n_t}(L_tM_t;\boldsymbol{\rho})\chi_{n_u}(L_uM_u;\boldsymbol{\varsigma})\rangle^* \\
&\times \quad \langle\phi_2|V_{23}|\chi_{n_s}(L_sM_s;\boldsymbol{\sigma})\chi_{n_t}(L_tM_t;\boldsymbol{\rho})\chi_{n_u}(L_uM_u;\boldsymbol{\varsigma})\rangle \\
&+ \quad |c|^2\langle\phi_3|V_{12}|\chi_{n_s}(L_sM_s;\boldsymbol{\sigma})\chi_{n_t}(L_tM_t;\boldsymbol{\rho})\chi_{n_u}(L_uM_u;\boldsymbol{\varsigma})\rangle^* \\
&\times \quad \langle\phi_3|V_{12}|\chi_{n_s}(L_sM_s;\boldsymbol{\sigma})\chi_{n_t}(L_tM_t;\boldsymbol{\rho})\chi_{n_u}(L_uM_u;\boldsymbol{\varsigma})\rangle \\
&+ \quad b^*c\langle\phi_2|V_{23}|\chi_{n_s}(L_sM_s;\boldsymbol{\sigma})\chi_{n_t}(L_tM_t;\boldsymbol{\rho})\chi_{n_u}(L_uM_u;\boldsymbol{\varsigma})\rangle^* \\
&\times \quad \langle\phi_3|V_{23}|\chi_{n_s}(L_sM_s;\boldsymbol{\sigma})\chi_{n_t}(L_tM_t;\boldsymbol{\rho})\chi_{n_u}(L_uM_u;\boldsymbol{\varsigma})\rangle \\
&+ \quad c^*b\langle\phi_3|V_{23}|\chi_{n_s}(L_sM_s;\boldsymbol{\sigma})\chi_{n_t}(L_tM_t;\boldsymbol{\rho})\chi_{n_u}(L_uM_u;\boldsymbol{\varsigma})\rangle^* \\
&\times \quad \langle\phi_2|V_{23}|\chi_{n_s}(L_sM_s;\boldsymbol{\sigma})\chi_{n_t}(L_tM_t;\boldsymbol{\rho})\chi_{n_u}(L_uM_u;\boldsymbol{\varsigma})\rangle \\
&= \quad |a|^2\frac{16\pi^2}{R_{23}^{2L_t+2L_u+2}}\left\{\frac{(L_t+L_u-M_t-M_u)!(L_t,L_u)^{-1}}{[(L_t+M_t)!(L_t-M_t)!(L_u+M_u)!(L_u-M_u)!]^{1/2}}\right\}^2 \\
&\times \quad |\langle\varphi_{n_0}(0;\boldsymbol{\rho})\|T_{L_t}(\boldsymbol{\rho})\|\chi_{n_t}(L_t;\boldsymbol{\rho})\rangle|^2|\langle\varphi_{n_0}(0;\boldsymbol{\varsigma})\|T_{L_u}(\boldsymbol{\varsigma})\|\chi_{n_u}(L_u;\boldsymbol{\varsigma})\rangle|^2 \\
&\times \quad P_{L_t+L_u}^{M_t+M_u}(\cos\theta_{23})P_{L_t+L_u}^{M_t+M_u}(\cos\theta_{23})
\end{aligned}
$$

$$
\begin{aligned}
&\times \quad \delta_{n_s,n_0'}\delta_{L_s,L}\delta_{M_s,M} \\
&+ \quad |b|^2 \sum_{l_2 l_2'} \sum_{m_2} \frac{16\pi^2}{R_{23}^{2L_u+l_2+l_2'+2}} \begin{pmatrix} L & l_2 & L_t \\ -M & m_2 & M_t \end{pmatrix} \begin{pmatrix} L & l_2' & L_t \\ -M & m_2 & M_t \end{pmatrix} \\
&\times \quad \frac{(L_u+l_2-M_u+m_2)!(L_u+l_2'-M_u+m_2)!(l_2,l_2')^{-1/2}(L_u,L_u)^{-1}}{(L_u+M_u)!(L_u-M_u)![(l_2+m_2)!(l_2-m_2)!(l_2'+m_2)!(l_2'-m_2)!]^{1/2}} \\
&\times \quad \langle \varphi_{n_0'}(L;\boldsymbol{\rho}) \| T_{l_2}(\boldsymbol{\rho}) \| \chi_{n_t}(L_t;\boldsymbol{\rho}) \rangle^* \langle \varphi_{n_0'}(L;\boldsymbol{\rho}) \| T_{l_2'}(\boldsymbol{\rho}) \| \chi_{n_t}(L_t;\boldsymbol{\rho}) \rangle \\
&\times \quad |\langle \varphi_{n_0}(0;\boldsymbol{\varsigma}) \| T_{L_u}(\boldsymbol{\varsigma}) \| \chi_{n_u}(L_u;\boldsymbol{\varsigma}) \rangle|^2 \\
&\times \quad P_{l_2+L_u}^{M_u-m_2}(\cos\theta_{23}) P_{l_2'+L_u}^{M_u-m_2}(\cos\theta_{23}) \\
&\times \quad \delta_{n_s,n_0}\delta_{L_s,0}\delta_{M_s,0} \\
&+ \quad |c|^2 \sum_{l_3 l_3'} \sum_{m_3} \frac{16\pi^2}{R_{23}^{2L_t+l_3+l_3'+2}} \begin{pmatrix} L & l_3 & L_u \\ -M & m_3 & M_u \end{pmatrix} \begin{pmatrix} L & l_3' & L_u \\ -M & m_3 & M_u \end{pmatrix} \\
&\times \quad \frac{(L_t+l_3-M_t+m_3)!(L_t+l_3'-M_t+m_3)!(l_3,l_3')^{-1/2}(L_t,L_t)^{-1}}{(L_t+M_t)!(L_t-M_t)![(l_3+m_3)!(l_3-m_3)!(l_3'+m_3)!(l_3'-m_3)!]^{1/2}} \\
&\times \quad \langle \varphi_{n_0'}(L;\boldsymbol{\varsigma}) \| T_{l_3}(\boldsymbol{\varsigma}) \| \chi_{n_u}(L_u;\boldsymbol{\varsigma}) \rangle^* \langle \varphi_{n_0'}(L;\boldsymbol{\varsigma}) \| T_{l_3'}(\boldsymbol{\varsigma}) \| \chi_{n_u}(L_u;\boldsymbol{\varsigma}) \rangle \\
&\times \quad |\langle \varphi_{n_0}(0;\boldsymbol{\rho}) \| T_{L_t}(\boldsymbol{\rho}) \| \chi_{n_t}(L_t;\boldsymbol{\rho}) \rangle|^2 \\
&\times \quad P_{L_t+l_3}^{M_t-m_3}(\cos\theta_{23}) P_{L_t+l_3'}^{M_t-m_3}(\cos\theta_{23}) \\
&\times \quad \delta_{n_s,n_0}\delta_{L_s,0}\delta_{M_s,0} \\
&+ \quad b^* c \sum_{l_2 l_3'} \sum_{m_2 m_3'} \frac{16\pi^2(-1)^{L_t+l_3'-M_t-M_u}}{R_{23}^{l_2+L_u+L_t+l_3'+2}} \\
&\times \quad \begin{pmatrix} L & l_2 & L_t \\ -M & -m_2 & M_t \end{pmatrix} \begin{pmatrix} L & l_3' & L_u \\ -M & m_3' & M_u \end{pmatrix} \\
&\times \quad \frac{(l_2+L_u-m_2-M_u)!(L_t,L_u)^{-1}}{[(L_t+M_t)!(L_t-M_t)!(l_3'+m_3')!(l_3'-m_3')!]^{1/2}} \\
&\times \quad \frac{(L_t+l_3'-M_t+m_3')!(l_2,l_3')^{-1/2}}{[(l_2+m_2)!(l_2-m_2)!(L_u+M_u)!(L_u-M_u)!]^{1/2}} \\
&\times \quad \langle \varphi_{n_0'}(L;\boldsymbol{\rho}) \| T_{l_2}(\boldsymbol{\rho}) \| \chi_{n_t}(L_t;\boldsymbol{\rho}) \rangle^* \langle \varphi_{n_0}(0;\boldsymbol{\varsigma}) \| T_{L_u}(\boldsymbol{\varsigma}) \| \chi_{n_u}(L_u;\boldsymbol{\varsigma}) \rangle^* \\
&\times \quad \langle \varphi_{n_0}(0;\boldsymbol{\rho}) \| T_{L_t}(\boldsymbol{\rho}) \| \chi_{n_t}(L_t;\boldsymbol{\rho}) \rangle \langle \varphi_{n_0'}(L;\boldsymbol{\varsigma}) \| T_{l_3'}(\boldsymbol{\varsigma}) \| \chi_{n_u}(L_u;\boldsymbol{\varsigma}) \rangle \\
&\times \quad P_{l_2+L_u}^{m_2+M_u}(\cos\theta_{23}) P_{L_t+l_3'}^{M_t-m_3'}(\cos\theta_{23})
\end{aligned}
$$

$$
\begin{aligned}
&\times \quad \delta_{n_s,n_0}\delta_{L_s,0}\delta_{M_s,0} \\
&+ \quad c^* b \sum_{l_2' l_3} \sum_{m_2' m_3} \frac{16\pi^2 (-1)^{L_t+l_3-M_t-M_u}}{R_{23}^{l_2'+L_t+L_u+l_3+2}} \\
&\times \quad \begin{pmatrix} L & l_2' & L_t \\ -M & -m_2' & M_t \end{pmatrix} \begin{pmatrix} L & l_3 & L_u \\ -M & m_3 & M_u \end{pmatrix} \\
&\times \quad \frac{(l_2'+L_u-m_2'-M_u)!(L_t,L_u)^{-1}}{[(L_t+M_t)!(L_t-M_t)!(l_3+m_3)!(l_3-m_3)!]^{1/2}} \\
&\times \quad \frac{(L_t+l_3-M_t+m_3)!(l_2',l_3)^{-1/2}}{[(l_2'+m_2')!(l_2'-m_2')!(L_u+M_u)!(L_u-M_u)!]^{1/2}} \\
&\times \quad \langle \varphi_{n_0}(0;\boldsymbol{\rho}) \| T_{L_t}(\boldsymbol{\rho}) \| \chi_{n_t}(L_t;\boldsymbol{\rho}) \rangle^* \langle \varphi_{n_0'}(L;\boldsymbol{\varsigma}) \| T_{l_3}(\boldsymbol{\varsigma}) \| \chi_{n_u}(L_u;\boldsymbol{\varsigma}) \rangle^* \\
&\times \quad \langle \varphi_{n_0'}(L;\boldsymbol{\rho}) \| T_{l_2'}(\boldsymbol{\rho}) \| \chi_{n_t}(L_t;\boldsymbol{\rho}) \rangle \langle \varphi_{n_0}(0;\boldsymbol{\varsigma}) \| T_{L_u}(\boldsymbol{\varsigma}) \| \chi_{n_u}(L_u;\boldsymbol{\varsigma}) \rangle \\
&\times \quad P_{L_t+l_3}^{M_t-m_3}(\cos\theta_{23}) P_{l_2'+L_u}^{m_2'+M_u}(\cos\theta_{23}) \\
&\times \quad \delta_{n_s,n_0}\delta_{L_s,0}\delta_{M_s,0}\,, \qquad \text{(A.9)}
\end{aligned}
$$

$$
\begin{aligned}
B_6 \;&=\; \langle \Psi^{(0)} | V_{23} | \chi_{n_s}(L_s M_s;\boldsymbol{\sigma}) \chi_{n_t}(L_t M_t;\boldsymbol{\rho}) \chi_{n_u}(L_u M_u;\boldsymbol{\varsigma}) \rangle^* \\
&\times \quad \langle \Psi^{(0)} | V_{31} | \chi_{n_s}(L_s M_s;\boldsymbol{\sigma}) \chi_{n_t}(L_t M_t;\boldsymbol{\rho}) \chi_{n_u}(L_u M_u;\boldsymbol{\varsigma}) \rangle \\
&=\; a^* b \langle \phi_1 | V_{23} | \chi_{n_s}(L_s M_s;\boldsymbol{\sigma}) \chi_{n_t}(L_t M_t;\boldsymbol{\rho}) \chi_{n_u}(L_u M_u;\boldsymbol{\varsigma}) \rangle^* \\
&\times \quad \langle \phi_2 | V_{31} | \chi_{n_s}(L_s M_s;\boldsymbol{\sigma}) \chi_{n_t}(L_t M_t;\boldsymbol{\rho}) \chi_{n_u}(L_u M_u;\boldsymbol{\varsigma}) \rangle \\
&+ \quad b^* a \langle \phi_2 | V_{23} | \chi_{n_s}(L_s M_s;\boldsymbol{\sigma}) \chi_{n_t}(L_t M_t;\boldsymbol{\rho}) \chi_{n_u}(L_u M_u;\boldsymbol{\varsigma}) \rangle^* \\
&\times \quad \langle \phi_1 | V_{31} | \chi_{n_s}(L_s M_s;\boldsymbol{\sigma}) \chi_{n_t}(L_t M_t;\boldsymbol{\rho}) \chi_{n_u}(L_u M_u;\boldsymbol{\varsigma}) \rangle \\
&=\; a^* b \frac{16\pi^2 (-1)^{L_u+L}}{R_{31}^{L_u+L+1} R_{23}^{L_u+L+1}} P_{L_u+L}^{M_u+M}(\cos\theta_{23}) P_{L+L_u}^{M+M_u}(\cos\theta_{31}) \\
&\times \quad \left\{ \frac{(L_u+L-M_u-M)!(L_u,L)^{-1}}{[(L_u+M_u)!(L_u-M_u)!(L+M)!(L-M)!]^{1/2}} \right\}^2 \\
&\times \quad |\langle \varphi_{n_0}(0;\boldsymbol{\sigma}) \| T_L(\boldsymbol{\sigma}) \| \chi_{n_s}(L;\boldsymbol{\sigma}) \rangle|^2 |\langle \varphi_{n_0}(0;\boldsymbol{\varsigma}) \| T_{L_u}(\boldsymbol{\varsigma}) \| \chi_{n_u}(L_u;\boldsymbol{\varsigma}) \rangle|^2 \\
&\times \quad \exp[i(M_u+M)(\Phi_{31}-\Phi_{23})] \\
&\times \quad \delta_{n_s,n_0'}\delta_{L_s,L}\delta_{M_s,M}\delta_{n_t,n_0'}\delta_{L_t,L}\delta_{M_t,M} \\
&+ \quad b^* a \frac{16\pi^2 (-1)^{L_u+L}}{R_{31}^{L_u+L+1} R_{23}^{L_u+L+1}} P_{L+L_u}^{-M+M_u}(\cos\theta_{23}) P_{L_u+L}^{M_u-M}(\cos\theta_{31})
\end{aligned}
$$

$$
\begin{aligned}
&\times \left\{\frac{(L_u+L-M_u+M)!(L_u,L)^{-1}}{[(L_u+M_u)!(L_u-M_u)!(L+M)!(L-M)!]^{1/2}}\right\}^2 \\
&\times |\langle\varphi_{n_0'}(L;\boldsymbol{\sigma})\|T_L(\boldsymbol{\sigma})\|\chi_{n_s}(0;\boldsymbol{\sigma})\rangle|^2|\langle\varphi_{n_0}(0;\boldsymbol{\varsigma})\|T_{L_u}(\boldsymbol{\varsigma})\|\chi_{n_u}(L_u;\boldsymbol{\varsigma})\rangle|^2 \\
&\times \exp[i(M_u-M)(\Phi_{31}-\Phi_{23})] \\
&\times \delta_{n_s,n_0}\delta_{L_s,0}\delta_{M_s,0}\delta_{n_t,n_0}\delta_{L_t,0}\delta_{M_t,0}\,, \qquad \text{(A.10)}
\end{aligned}
$$

$$
\begin{aligned}
B_7 &= \langle\Psi^{(0)}|V_{31}|\chi_{n_s}(L_sM_s;\boldsymbol{\sigma})\chi_{n_t}(L_tM_t;\boldsymbol{\rho})\chi_{n_u}(L_uM_u;\boldsymbol{\varsigma})\rangle^* \\
&\times \langle\Psi^{(0)}|V_{12}|\chi_{n_s}(L_sM_s;\boldsymbol{\sigma})\chi_{n_t}(L_tM_t;\boldsymbol{\rho})\chi_{n_u}(L_uM_u;\boldsymbol{\varsigma})\rangle \\
&= b^*c\langle\phi_2|V_{31}|\chi_{n_s}(L_sM_s;\boldsymbol{\sigma})\chi_{n_t}(L_tM_t;\boldsymbol{\rho})\chi_{n_u}(L_uM_u;\boldsymbol{\varsigma})\rangle^* \\
&\times \langle\phi_3|V_{12}|\chi_{n_s}(L_sM_s;\boldsymbol{\sigma})\chi_{n_t}(L_tM_t;\boldsymbol{\rho})\chi_{n_u}(L_uM_u;\boldsymbol{\varsigma})\rangle \\
&+ c^*b\langle\phi_3|V_{31}|\chi_{n_s}(L_sM_s;\boldsymbol{\sigma})\chi_{n_t}(L_tM_t;\boldsymbol{\rho})\chi_{n_u}(L_uM_u;\boldsymbol{\varsigma})\rangle^* \\
&\times \langle\phi_2|V_{12}|\chi_{n_s}(L_sM_s;\boldsymbol{\sigma})\chi_{n_t}(L_tM_t;\boldsymbol{\rho})\chi_{n_u}(L_uM_u;\boldsymbol{\varsigma})\rangle \\
&= b^*c\frac{16\pi^2(-1)^{L_s+L}}{R_{12}^{L_s+L+1}R_{31}^{L_s+L+1}}P_{L+L_s}^{M+m_s}(\cos\theta_{31})P_{L_s+L}^{m_s+M}(\cos\theta_{12}) \\
&\times \left\{\frac{(L_s+L-m_s-M)!(L_s,L)^{-1}}{[(L_s+m_s)!(L_s-m_s)!(L+M)!(L-M)!]^{1/2}}\right\}^2 \\
&\times |\langle\varphi_{n_0}(0;\boldsymbol{\sigma})\|T_{L_s}(\boldsymbol{\sigma})\|\chi_{n_s}(L_s;\boldsymbol{\sigma})\rangle|^2|\langle\varphi_{n_0}(0;\boldsymbol{\rho})\|T_L(\boldsymbol{\rho})\|\chi_{n_t}(L;\boldsymbol{\rho})\rangle|^2 \\
&\times \exp[i(m_s+M)(\Phi_{12}-\Phi_{31})] \\
&\times \delta_{n_t,n_0'}\delta_{L_t,L}\delta_{M_t,M}\delta_{n_u,n_0'}\delta_{L_u,L}\delta_{M_u,M} \\
&+ c^*b\frac{16\pi^2(-1)^{L_s+L}}{R_{12}^{L_s+L+1}R_{31}^{L_s+L+1}}P_{L+L_s}^{-M+M_s}(\cos\theta_{31})P_{L_s+L}^{M_s-M}(\cos\theta_{12}) \\
&\times \left\{\frac{(L_s+L-M_s+M)!(L_s,L)^{-1}}{[(L_s+M_s)!(L_s-M_s)!(L+M)!(L-M)!]^{1/2}}\right\}^2 \\
&\times |\langle\varphi_{n_0}(0;\boldsymbol{\sigma})\|T_{L_s}(\boldsymbol{\sigma})\|\chi_{n_s}(L_s;\boldsymbol{\sigma})\rangle|^2|\langle\varphi_{n_0'}(L;\boldsymbol{\rho})\|T_L(\boldsymbol{\rho})\|\chi_{n_t}(0;\boldsymbol{\rho})\rangle|^2 \\
&\times \exp[i(M_s-M)(\Phi_{12}-\Phi_{31})] \\
&\times \delta_{n_t,n_0}\delta_{L_t,0}\delta_{M_t,0}\delta_{n_u,n_0}\delta_{L_u,0}\delta_{M_u,0}\,, \qquad \text{(A.11)}
\end{aligned}
$$

$$
B_8 = \langle\Psi^{(0)}|V_{31}|\chi_{n_s}(L_sM_s;\boldsymbol{\sigma})\chi_{n_t}(L_tM_t;\boldsymbol{\rho})\chi_{n_u}(L_uM_u;\boldsymbol{\varsigma})\rangle^*
$$

$$
\begin{aligned}
&\times \quad \langle\Psi_0|V_{23}|\chi_{n_s}(L_sM_s;\boldsymbol{\sigma})\chi_{n_t}(L_tM_t;\boldsymbol{\rho})\chi_{n_u}(L_uM_u;\boldsymbol{\varsigma})\rangle \\
&= \quad a^*b\langle\phi_1|V_{31}|\chi_{n_s}(L_sM_s;\boldsymbol{\sigma})\chi_{n_t}(L_tM_t;\boldsymbol{\rho})\chi_{n_u}(L_uM_u;\boldsymbol{\varsigma})\rangle^* \\
&\times \quad \langle\phi_2|V_{23}|\chi_{n_s}(L_sM_s;\boldsymbol{\sigma})\chi_{n_t}(L_tM_t;\boldsymbol{\rho})\chi_{n_u}(L_uM_u;\boldsymbol{\varsigma})\rangle \\
&+ \quad b^*a\langle\phi_2|V_{31}|\chi_{n_s}(L_sM_s;\boldsymbol{\sigma})\chi_{n_t}(L_tM_t;\boldsymbol{\rho})\chi_{n_u}(L_uM_u;\boldsymbol{\varsigma})\rangle^* \\
&\times \quad \langle\phi_1|V_{23}|\chi_{n_s}(L_sM_s;\boldsymbol{\sigma})\chi_{n_t}(L_tM_t;\boldsymbol{\rho})\chi_{n_u}(L_uM_u;\boldsymbol{\varsigma})\rangle \\
&= \quad a^*b\frac{16\pi^2(-1)^{L_u+L}}{R_{31}^{L_u+L+1}R_{23}^{L_u+L+1}}P_{L_u+L}^{M_u-M}(\cos\theta_{31})P_{L+L_u}^{-M+M_u}(\cos\theta_{23}) \\
&\times \quad \left\{\frac{(L_u+L-M_u+M)!(L_u,L)^{-1}}{[(L_u+M_u)!(L_u-M_u)!(L+M)!(L-M)!]^{1/2}}\right\}^2 \\
&\times \quad |\langle\varphi_{n_0'}(L;\boldsymbol{\sigma})\|T_L(\boldsymbol{\sigma})\|\chi_{n_s}(0;\boldsymbol{\sigma})\rangle|^2|\langle\varphi_{n_0}(0;\boldsymbol{\varsigma})\|T_{L_u}(\boldsymbol{\varsigma})\|\chi_{n_u}(L_u;\boldsymbol{\varsigma})\rangle|^2 \\
&\times \quad \exp[i(M_u-M)(\Phi_{23}-\Phi_{31})] \\
&\times \quad \delta_{n_s,n_0}\delta_{L_s,0}\delta_{M_s,0}\delta_{n_t,n_0}\delta_{L_t,0}\delta_{M_t,0} \\
&+ \quad b^*a\frac{16\pi^2(-1)^{L_u+L}}{R_{31}^{L_u+L+1}R_{23}^{L_u+L+1}}P_{L_u+L}^{M_u+M}(\cos\theta_{31})P_{L+L_u}^{M+M_u}(\cos\theta_{23}) \\
&\times \quad \left\{\frac{(L_u+L-M_u-M)!(L_u,L)^{-1}}{[(L_u+M_u)!(L_u-M_u)!(L+M)!(L-M)!]^{1/2}}\right\}^2 \\
&\times \quad |\langle\varphi_{n_0}(0;\boldsymbol{\sigma})\|T_L(\boldsymbol{\sigma})\|\chi_{n_s}(L;\boldsymbol{\sigma})\rangle|^2|\langle\varphi_{n_0}(0;\boldsymbol{\varsigma})\|T_{L_u}(\boldsymbol{\varsigma})\|\chi_{n_u}(L_u;\boldsymbol{\varsigma})\rangle|^2 \\
&\times \quad \exp[i(M_u+M)(\Phi_{23}-\Phi_{31})] \\
&\times \quad \delta_{n_s,n_0'}\delta_{L_s,L}\delta_{M_s,M}\delta_{n_t,n_0'}\delta_{L_t,L}\delta_{M_t,M}\,, \qquad \text{(A.12)}
\end{aligned}
$$

and

$$
\begin{aligned}
B_9 \quad &= \quad \langle\Psi^{(0)}|V_{31}|\chi_{n_s}(L_sM_s;\boldsymbol{\sigma})\chi_{n_t}(L_tM_t;\boldsymbol{\rho})\chi_{n_u}(L_uM_u;\boldsymbol{\varsigma})\rangle^* \\
&\times \quad \langle\Psi^{(0)}|V_{31}|\chi_{n_s}(L_sM_s;\boldsymbol{\sigma})\chi_{n_t}(L_tM_t;\boldsymbol{\rho})\chi_{n_u}(L_uM_u;\boldsymbol{\varsigma})\rangle \\
&= \quad |a|^2\langle\phi_1|V_{31}|\chi_{n_s}(L_sM_s;\boldsymbol{\sigma})\chi_{n_t}(L_tM_t;\boldsymbol{\rho})\chi_{n_u}(L_uM_u;\boldsymbol{\varsigma})\rangle^* \\
&\times \quad \langle\phi_1|V_{31}|\chi_{n_s}(L_sM_s;\boldsymbol{\sigma})\chi_{n_t}(L_tM_t;\boldsymbol{\rho})\chi_{n_u}(L_uM_u;\boldsymbol{\varsigma})\rangle \\
&+ \quad |b|^2\langle\phi_2|V_{31}|\chi_{n_s}(L_sM_s;\boldsymbol{\sigma})\chi_{n_t}(L_tM_t;\boldsymbol{\rho})\chi_{n_u}(L_uM_u;\boldsymbol{\varsigma})\rangle^* \\
&\times \quad \langle\phi_2|V_{31}|\chi_{n_s}(L_sM_s;\boldsymbol{\sigma})\chi_{n_t}(L_tM_t;\boldsymbol{\rho})\chi_{n_u}(L_uM_u;\boldsymbol{\varsigma})\rangle
\end{aligned}
$$

$$
\begin{aligned}
&+ \quad |c|^2\langle\phi_3|V_{31}|\chi_{n_s}(L_sM_s;\boldsymbol{\sigma})\chi_{n_t}(L_tM_t;\boldsymbol{\rho})\chi_{n_u}(L_uM_u;\boldsymbol{\varsigma})\rangle^* \\
&\times \quad \langle\phi_3|V_{31}|\chi_{n_s}(L_sM_s;\boldsymbol{\sigma})\chi_{n_t}(L_tM_t;\boldsymbol{\rho})\chi_{n_u}(L_uM_u;\boldsymbol{\varsigma})\rangle \\
&+ \quad a^*c\langle\phi_1|V_{31}|\chi_{n_s}(L_sM_s;\boldsymbol{\sigma})\chi_{n_t}(L_tM_t;\boldsymbol{\rho})\chi_{n_u}(L_uM_u;\boldsymbol{\varsigma})\rangle^* \\
&\times \quad \langle\phi_3|V_{31}|\chi_{n_s}(L_sM_s;\boldsymbol{\sigma})\chi_{n_t}(L_tM_t;\boldsymbol{\rho})\chi_{n_u}(L_uM_u;\boldsymbol{\varsigma})\rangle \\
&+ \quad c^*a\langle\phi_3|V_{31}|\chi_{n_s}(L_sM_s;\boldsymbol{\sigma})\chi_{n_t}(L_tM_t;\boldsymbol{\rho})\chi_{n_u}(L_uM_u;\boldsymbol{\varsigma})\rangle^* \\
&\times \quad \langle\phi_1|V_{31}|\chi_{n_s}(L_sM_s;\boldsymbol{\sigma})\chi_{n_t}(L_tM_t;\boldsymbol{\rho})\chi_{n_u}(L_uM_u;\boldsymbol{\varsigma})\rangle \\
&= \quad |a|^2\sum_{l_1l_1'}\sum_{m_1}\frac{16\pi^2}{R_{31}^{2L_u+l_1+l_1'+2}}
\begin{pmatrix} L & l_1 & L_s \\ -M & m_1 & M_s \end{pmatrix}
\begin{pmatrix} L & l_1' & L_s \\ -M & m_1 & M_s \end{pmatrix} \\
&\times \quad \frac{(L_u+l_1-M_u+m_1)!(L_u+l_1'-M_u+m_1)!(l_1,l_1')^{-1/2}(L_u,L_u)^{-1}}{(L_u+M_u)!(L_u-M_u)![(l_1+m_1)!(l_1-m_1)!(l_1'+m_1)!(l_1'-m_1)!]^{1/2}} \\
&\times \quad \langle\varphi_{n_0'}(L;\boldsymbol{\sigma})\|T_{l_1}(\boldsymbol{\sigma})\|\chi_{n_s}(L_s;\boldsymbol{\sigma})\rangle^*\langle\varphi_{n_0'}(L;\boldsymbol{\sigma})\|T_{l_1'}(\boldsymbol{\sigma})\|\chi_{n_s}(L_s;\boldsymbol{\sigma})\rangle \\
&\times \quad |\langle\varphi_{n_0}(0;\boldsymbol{\varsigma})\|T_{L_u}(\boldsymbol{\varsigma})\|\chi_{n_u}(L_u;\boldsymbol{\varsigma})\rangle|^2 \\
&\times \quad P_{L_u+l_1}^{M_u-m_1}(\cos\theta_{31})P_{L_u+l_1'}^{M_u-m_1}(\cos\theta_{31}) \\
&\times \quad \delta_{n_t,n_0}\delta_{L_t,0}\delta_{M_t,0} \\
&+ \quad |b|^2\frac{16\pi^2}{R_{31}^{2L_s+2L_u+2}}\left\{\frac{(L_u+L_s-M_u-M_s)!(L_u,L_s)^{-1}}{[(L_u+M_u)!(L_u-M_u)!(L_s+M_s)!(L_s-M_s)!]^{1/2}}\right\}^2 \\
&\times \quad |\langle\varphi_{n_0}(0;\boldsymbol{\sigma})\|T_{L_s}(\boldsymbol{\sigma})\|\chi_{n_s}(L_s;\boldsymbol{\sigma})\rangle|^2|\langle\varphi_{n_0}(0;\boldsymbol{\varsigma})\|T_{L_u}(\boldsymbol{\varsigma})\|\chi_{n_u}(L_u;\boldsymbol{\varsigma})\rangle|^2 \\
&\times \quad P_{L_u+L_s}^{M_u+M_s}(\cos\theta_{31})P_{L_u+L_s}^{M_u+M_s}(\cos\theta_{31}) \\
&\times \quad \delta_{n_t,n_0'}\delta_{L_t,L}\delta_{M_t,M} \\
&+ \quad |c|^2\sum_{l_3l_3'}\sum_{m_3}\frac{16\pi^2}{R_{31}^{2L_s+l_3+l_3'+2}}
\begin{pmatrix} L & l_3 & L_u \\ -M & m_3 & M_u \end{pmatrix}
\begin{pmatrix} L & l_3' & L_u \\ -M & m_3 & M_u \end{pmatrix} \\
&\times \quad \frac{(L_s+l_3-M_s+m_3)!(L_s+l_3'-M_s+m_3)!(l_3,l_3')^{-1/2}(L_s,L_s)^{-1}}{(L_s+M_s)!(L_s-M_s)![(l_3+m_3)!(l_3-m_3)!(l_3'+m_3)!(l_3'-m_3)!]^{1/2}} \\
&\times \quad \langle\varphi_{n_0'}(L;\boldsymbol{\varsigma})\|T_{l_3}(\boldsymbol{\varsigma})\|\chi_{n_u}(L_u\boldsymbol{\varsigma})\rangle^*\langle\varphi_{n_0'}(L;\boldsymbol{\varsigma})\|T_{l_3'}(\boldsymbol{\varsigma})\|\chi_{n_u}(L_u;\boldsymbol{\varsigma})\rangle \\
&\times \quad |\langle\varphi_{n_0}(0;\boldsymbol{\sigma})\|T_{L_s}(\boldsymbol{\sigma})\|\chi_{n_s}(L_s;\boldsymbol{\sigma})\rangle|^2 \\
&\times \quad P_{l_3+L_s}^{M_s-m_3}(\cos\theta_{31})P_{l_3'+L_s}^{M_s-m_3}(\cos\theta_{31}) \\
&\times \quad \delta_{n_t,n_0}\delta_{L_t,0}\delta_{M_t,0}
\end{aligned}
$$

$$
\begin{aligned}
&+ \quad a^* c \sum_{l_3' l_1} \sum_{m_3' m_1} \frac{16\pi^2 (-1)^{L_u + l_1 - M_u - M_s}}{R_{31}^{l_3' + L_s + L_u + l_1 + 2}} \\
&\times \quad \begin{pmatrix} L & l_3' & L_u \\ -M & -m_3' & M_u \end{pmatrix} \begin{pmatrix} L & l_1 & L_s \\ -M & m_1 & M_s \end{pmatrix} \\
&\times \quad \frac{(l_3' + L_s - m_3' - M_s)! (L_u, L_s)^{-1}}{[(l_3' + m_3')! (l_3' - m_3')! (L_s + M_s)! (L_s - M_s)!]^{1/2}} \\
&\times \quad \frac{(L_u + l_1 - M_u + m_1)! (l_3', l_1)^{-1/2}}{[(L_u + M_u)! (L_u - M_u)! (l_1 + m_1)! (l_1 - m_1)!]^{1/2}} \\
&\times \quad \langle \varphi_{n_0}(0; \boldsymbol{\varsigma}) \| T_{L_u}(\boldsymbol{\varsigma}) \| \chi_{n_u}(L_u; \boldsymbol{\varsigma}) \rangle^* \langle \varphi_{n_0'}(L; \boldsymbol{\sigma}) \| T_{l_1}(\boldsymbol{\sigma}) \| \chi_{n_s}(L_s; \boldsymbol{\sigma}) \rangle^* \\
&\times \quad \langle \varphi_{n_0'}(L; \boldsymbol{\varsigma}) \| T_{l_3'}(\boldsymbol{\varsigma}) \| \chi_{n_u}(L_u; \boldsymbol{\varsigma}) \rangle \langle \varphi_{n_0}(0; \boldsymbol{\sigma}) \| T_{L_s}(\boldsymbol{\sigma}) \| \chi_{n_s}(L_s; \boldsymbol{\sigma}) \rangle \\
&\times \quad P_{L_u + l_1}^{M_u - m_1}(\cos\theta_{31}) P_{l_3' + L_s}^{m_3' + M_s}(\cos\theta_{31}) \\
&\times \quad \delta_{n_t, n_0} \delta_{L_t, 0} \delta_{M_t, 0} \\
&+ \quad c^* a \sum_{l_3 l_1'} \sum_{m_3 m_1'} \frac{16\pi^2 (-1)^{L_u + l_1' - M_u - M_s}}{R_{31}^{l_3 + L_s + L_u + l_1' + 2}} \\
&\times \quad \begin{pmatrix} L & l_3 & L_u \\ -M & -m_3 & M_u \end{pmatrix} \begin{pmatrix} L & l_1' & L_s \\ -M & m_1' & M_s \end{pmatrix} \\
&\times \quad \frac{(L_u + l_1' - M_u + m_1')! (l_3, l_1')^{-1/2}}{[(L_u + M_u)! (L_u - M_u)! (l_1' + m_1')! (l_1' - m_1')!]^{1/2}} \\
&\times \quad \frac{(l_3 + L_s - m_3 - M_s)! (L_u, L_s)^{-1}}{[(l_3 + m_3)! (l_3 - m_3)! (L_s + M_s)! (L_s - M_s)!]^{1/2}} \\
&\times \quad \langle \varphi_{n_0'}(L; \boldsymbol{\varsigma}) \| T_{l_3}(\boldsymbol{\varsigma}) \| \chi_{n_u}(L_u; \boldsymbol{\varsigma}) \rangle^* \langle \varphi_{n_0}(0; \boldsymbol{\sigma}) \| T_{L_s}(\boldsymbol{\sigma}) \| \chi_{n_s}(L_s; \boldsymbol{\sigma}) \rangle^* \\
&\times \quad \langle \varphi_{n_0}(0; \boldsymbol{\varsigma}) \| T_{L_u}(\boldsymbol{\varsigma}) \| \chi_{n_u}(L_u; \boldsymbol{\varsigma}) \rangle \langle \varphi_{n_0'}(L; \boldsymbol{\sigma}) \| T_{l_1'}(\boldsymbol{\sigma}) \| \chi_{n_s}(L_s; \boldsymbol{\sigma}) \rangle \\
&\times \quad P_{l_3 + L_s}^{m_3 + M_s}(\cos\theta_{31}) P_{L_u + l_1'}^{M_u - m_1'}(\cos\theta_{31}) \\
&\times \quad \delta_{n_t, n_0} \delta_{L_t, 0} \delta_{M_t, 0} \,. \qquad \text{(A.13)}
\end{aligned}
$$

In this paper, we choose the coordinate system shown in Fig. 3.1. Thus in the associated Legendre functions, we have all $\cos(\theta_{IJ}) = 0$ due to $\theta_{IJ} = \pi/2$. Also in $\exp[i(m_I - m_J)\Phi_{IJ}]$ *etc.*, $\Phi_{12} = 0$, $\Phi_{23} = \pi - \beta$, and $\Phi_{31} = \pi + \alpha$. Then the three additive terms in the second-order energy correction, denoted by $V_{12}^{(2)}$, $V_{23}^{(2)}$, and $V_{31}^{(2)}$,

become respectively

$$
\begin{aligned}
V_{12}^{(2)} &= -|a|^2 \sum_{n_s n_t} \sum_{L_s L_t l_1 l_1'} \sum_{M_s M_t m_1} \frac{16\pi^2}{R_{12}^{2L_t+l_1+l_1'+2}} \\
&\times \begin{pmatrix} L & l_1 & L_s \\ -M & m_1 & M_s \end{pmatrix} \begin{pmatrix} L & l_1' & L_s \\ -M & m_1 & M_s \end{pmatrix} \\
&\times \frac{(L_t+l_1-M_t+m_1)!(L_t+l_1'-M_t+m_1)!(L_t,L_t)^{-1}(l_1,l_1')^{-1/2}}{(L_t+M_t)!(L_t-M_t)![(l_1+m_1)!(l_1-m_1)!(l_1'+m_1)!(l_1'-m_1)!]^{1/2}} \\
&\times P_{L_t+l_1}^{M_t-m_1}(0) P_{L_t+l_1'}^{M_t-m_1}(0) |\langle \varphi_{n_0}(0;\boldsymbol{\rho}) \| T_{L_t}(\boldsymbol{\rho}) \| \chi_{n_t}(L_t;\boldsymbol{\rho}) \rangle|^2 \\
&\times \frac{\langle \varphi_{n_0'}(L;\boldsymbol{\sigma}) \| T_{l_1}(\boldsymbol{\sigma}) \| \chi_{n_s}(L_s;\boldsymbol{\sigma}) \rangle^* \langle \varphi_{n_0'}(L;\boldsymbol{\sigma}) \| T_{l_1'}(\boldsymbol{\sigma}) \| \chi_{n_s}(L_s;\boldsymbol{\sigma}) \rangle}{E_{n_s L_s} + E_{n_t L_t} - E_{n_0 S}^{(0)} - E_{n_0' L}^{(0)}} \\
&- |b|^2 \sum_{n_s n_t} \sum_{L_s L_t l_2 l_2'} \sum_{M_s M_t m_2} \frac{16\pi^2}{R_{12}^{2L_s+l_2+l_2'+2}} \\
&\times \begin{pmatrix} L & l_2 & L_t \\ -M & m_2 & M_t \end{pmatrix} \begin{pmatrix} L & l_2' & L_t \\ -M & m_2 & M_t \end{pmatrix} \\
&\times \frac{(L_s+l_2-M_s+m_2)!(L_s+l_2'-M_s+m_2)!(L_s,L_s)^{-1}(l_2,l_2')^{-1/2}}{(L_s+M_s)!(L_s-M_s)![(l_2+m_2)!(l_2-m_2)!(l_2'+m_2)!(l_2'-m_2)!]^{1/2}} \\
&\times P_{L_s+l_2}^{M_s-m_2}(0) P_{L_s+l_2'}^{M_s-m_2}(0) |\langle \varphi_{n_0}(0;\boldsymbol{\sigma}) \| T_{L_s}(\boldsymbol{\sigma}) \| \chi_{n_s}(L_s;\boldsymbol{\sigma}) \rangle|^2 \\
&\times \frac{\langle \varphi_{n_0'}(L;\boldsymbol{\rho}) \| T_{l_2}(\boldsymbol{\rho}) \| \chi_{n_t}(L_t;\boldsymbol{\rho}) \rangle^* \langle \varphi_{n_0'}(L;\boldsymbol{\rho}) \| T_{l_2'}(\boldsymbol{\rho}) \| \chi_{n_t}(L_t;\boldsymbol{\rho}) \rangle}{E_{n_s L_s} + E_{n_t L_t} - E_{n_0 S}^{(0)} - E_{n_0' L}^{(0)}} \\
&- |c|^2 \sum_{n_s n_t} \sum_{L_s L_t} \sum_{M_s M_t} \frac{16\pi^2}{R_{12}^{2L_s+2L_t+2}} \\
&\times \frac{[P_{L_s+L_t}^{M_s+M_t}(0)(L_s+L_t-M_s-M_t)!]^2 (L_s,L_t)^{-2}}{(L_s+M_s)!(L_s-M_s)!(L_t+M_t)!(L_t-M_t)!} \\
&\times \frac{|\langle \varphi_n(0;\boldsymbol{\sigma}) \| T_{L_s}(\boldsymbol{\sigma}) \| \chi_{n_s}(L_s;\boldsymbol{\sigma}) \rangle|^2 |\langle \varphi_n(0;\boldsymbol{\rho}) \| T_{L_t}(\boldsymbol{\rho}) \| \chi_{n_t}(L_t;\boldsymbol{\rho}) \rangle|^2}{E_{n_s L_s} + E_{n_t L_t} - 2E_{n_0 S}^{(0)}} \\
&- a^* b \sum_{n_s n_t} \sum_{L_s L_t l_1 l_2'} \sum_{M_s M_t m_1 m_2'} \frac{16\pi^2 (-1)^{L_s+l_2'-M_s-M_t}}{R_{12}^{l_1+L_s+L_t+l_2'+2}} \\
&\times \begin{pmatrix} L & l_1 & L_s \\ -M & -m_1 & M_s \end{pmatrix} \begin{pmatrix} L & l_2' & L_t \\ -M & m_2' & M_t \end{pmatrix} \\
&\times \frac{P_{L_t+l_1}^{M_t+m_1}(0) P_{L_s+l_2'}^{M_s-m_2'}(0)(L_t+l_1-M_t-m_1)!}{[(L_s+M_s)!(L_s-M_s)!(L_t+M_t)!(L_t-M_t)!]^{1/2}}
\end{aligned}
$$

$$
\begin{aligned}
&\times \frac{(L_s+l_2'-M_s+m_2')!(L_s,L_t)^{-1}(l_1,l_2')^{-1/2}}{[(l_1+m_1)!(l_1-m_1)!(l_2'+m_2')!(l_2'-m_2')!]^{1/2}} \\
&\times \langle\varphi_{n_0'}(L;\boldsymbol{\sigma})\|T_{l_1}(\boldsymbol{\sigma})\|\chi_{n_s}(L_s;\boldsymbol{\sigma})\rangle^*\langle\varphi_{n_0}(0;\boldsymbol{\rho})\|T_{L_t}(\boldsymbol{\rho})\|\chi_{n_t}(L_t;\boldsymbol{\rho})\rangle^* \\
&\times \frac{\langle\varphi_{n_0}(0;\boldsymbol{\sigma})\|T_{L_s}(\boldsymbol{\sigma})\|\chi_{n_s}(L_s;\boldsymbol{\sigma})\rangle\langle\varphi_{n_0'}(L;\boldsymbol{\rho})\|T_{l_2'}(\boldsymbol{\rho})\|\chi_{n_t}(L_t;\boldsymbol{\rho})\rangle}{E_{n_sL_s}+E_{n_tL_t}-E^{(0)}_{n_0S}-E^{(0)}_{n_0'L}} \\
&- b^*a\sum_{n_sn_t}\sum_{L_sL_tl_1'l_2}\sum_{M_sM_tm_1'm_2}\frac{16\pi^2(-1)^{L_s+l_2-M_s-M_t}}{R_{12}^{l_1'+L_t+L_s+l_2+2}} \\
&\times \begin{pmatrix} L & l_1' & L_s \\ -M & -m_1' & M_s \end{pmatrix}\begin{pmatrix} L & l_2 & L_t \\ -M & m_2 & M_t \end{pmatrix} \\
&\times \frac{P^{M_s-m_2}_{L_s+l_2}(0)P^{M_t+m_1'}_{L_t+l_1'}(0)(L_t+l_1'-M_t-m_1')!}{[(L_s+M_s)!(L_s-M_s)!(L_t+M_t)!(L_t-M_t)!]^{1/2}} \\
&\times \frac{(L_s+l_2-M_s+m_2)!(L_s,L_t)^{-1}(l_1',l_2)^{-1/2}}{[(l_1'+m_1')!(l_1'-m_1')!(l_2+m_2)!(l_2-m_2)!]^{1/2}} \\
&\times \langle\varphi_{n_0}(0;\boldsymbol{\sigma})\|T_{L_s}(\boldsymbol{\sigma})\|\chi_{n_s}(L_s;\boldsymbol{\sigma})\rangle^*\langle\varphi_{n_0'}(L;\boldsymbol{\rho})\|T_{l_2}(\boldsymbol{\rho})\|\chi_{n_t}(L_t;\boldsymbol{\rho})\rangle^* \\
&\times \frac{\langle\varphi_{n_0'}(L;\boldsymbol{\sigma})\|T_{l_1'}(\boldsymbol{\sigma})\|\chi_{n_s}(L_s;\boldsymbol{\sigma})\rangle\langle\varphi_{n_0}(0;\boldsymbol{\rho})\|T_{L_t}(\boldsymbol{\rho})\|\chi_{n_t}(L_t;\boldsymbol{\rho})\rangle}{E_{n_sL_s}+E_{n_tL_t}-E^{(0)}_{n_0S}-E^{(0)}_{n_0'L}} \\
&= -\Bigg\{|a|^2\sum_{n_sn_t}\sum_{L_sL_tl_1l_1'}\frac{F_1(n_s,n_t,L_s,L_t;l_1,l_1';L,M)}{R_{12}^{2L_t+l_1+l_1'+2}} \\
&+ |b|^2\sum_{n_sn_t}\sum_{L_sL_tl_2l_2'}\frac{F_1(n_t,n_s,L_t,L_s;l_2,l_2';L,M)}{R_{12}^{2L_s+l_2+l_2'+2}} \\
&+ |c|^2\sum_{n_sn_t}\sum_{L_sL_t}\frac{F_2(n_s,n_t,L_s,L_t)}{R_{12}^{2L_s+2L_t+2}} \\
&+ a^*b\sum_{n_sn_t}\sum_{L_sL_tl_1l_2'}\frac{F_3(n_s,n_t,L_s,L_t;l_1,l_2';L,M)}{R_{12}^{L_s+L_t+l_1+l_2'+2}} \\
&+ b^*a\sum_{n_sn_t}\sum_{L_sL_tl_1'l_2}\frac{F_3^*(n_s,n_t,L_s,L_t;l_1',l_2;L,M)}{R_{12}^{L_s+L_t+l_1'+l_2+2}}\Bigg\},
\end{aligned}
\tag{A.14}
$$

$$
\begin{aligned}
V_{23}^{(2)} &= -|a|^2\sum_{n_tn_u}\sum_{L_tL_u}\sum_{M_tM_u}\frac{16\pi^2}{R_{23}^{2L_t+2L_u+2}} \\
&\times \frac{[P^{M_t+M_u}_{L_t+L_u}(0)(L_t+L_u-M_t-M_u)!]^2(L_t,L_u)^{-2}}{(L_t+M_t)!(L_t-M_t)!(L_u+M_u)!(L_u-M_u)!}
\end{aligned}
$$

$$
\begin{aligned}
&\times \quad \frac{|\langle\varphi_{n_0}(0;\boldsymbol{\rho})\|T_{L_t}(\boldsymbol{\rho})\|\chi_{n_t}(L_t;\boldsymbol{\rho})\rangle|^2|\langle\varphi_{n_0}(0;\boldsymbol{\varsigma})\|T_{L_u}(\boldsymbol{\varsigma})\|\chi_{n_u}(L_u;\boldsymbol{\varsigma})\rangle|^2}{E_{n_tL_t}+E_{n_uL_u}-2E^{(0)}_{n_0S}} \\
&- \quad |b|^2\sum_{n_tn_u}\sum_{L_tL_ul_2l_2'}\sum_{M_tM_um_2}\frac{16\pi^2}{R_{23}^{2L_u+l_2+l_2'+2}} \\
&\times \quad \begin{pmatrix} L & l_2 & L_t \\ -M & m_2 & M_t \end{pmatrix}\begin{pmatrix} L & l_2' & L_t \\ -M & m_2 & M_t \end{pmatrix} \\
&\times \quad \frac{(L_u+l_2-M_u+m_2)!(L_u+l_2'-M_u+m_2)!(L_u,L_u)^{-1}(l_2,l_2')^{-1/2}}{(L_u+M_u)!(L_u-M_u)![(l_2+m_2)!(l_2-m_2)!(l_2'+m_2)!(l_2'-m_2)!]^{1/2}} \\
&\times \quad P^{M_u-m_2}_{L_u+l_2}(0)P^{M_u-m_2}_{L_u+l_2'}(0)|\langle\varphi_{n_0}(0;\boldsymbol{\varsigma})\|T_{L_u}(\boldsymbol{\varsigma})\|\chi_{n_u}(L_u;\boldsymbol{\varsigma})\rangle|^2 \\
&\times \quad \frac{\langle\varphi_{n_0'}(L;\boldsymbol{\rho})\|T_{l_2}(\boldsymbol{\rho})\|\chi_{n_t}(L_t;\boldsymbol{\rho})\rangle^*\langle\varphi_{n_0'}(L;\boldsymbol{\rho})\|T_{l_2'}(\boldsymbol{\rho})\|\chi_{n_t}(L_t;\boldsymbol{\rho})\rangle}{E_{n_tL_t}+E_{n_uL_u}-E^{(0)}_{n_0S}-E^{(0)}_{n_0'L}} \\
&- \quad |c|^2\sum_{n_tn_u}\sum_{L_tL_ul_3l_3'}\sum_{M_tM_um_3}\frac{16\pi^2}{R_{23}^{2L_t+l_3+l_3'+2}} \\
&\times \quad \begin{pmatrix} L & l_3 & L_u \\ -M & m_3 & M_u \end{pmatrix}\begin{pmatrix} L & l_3' & L_u \\ -M & m_3 & M_u \end{pmatrix} \\
&\times \quad \frac{(L_t+l_3-M_t+m_3)!(L_t+l_3'-M_t+m_3)!(L_t,L_t)^{-1}(l_3,l_3')^{-1/2}}{(L_t+M_t)!(L_t-M_t)![(l_3+m_3)!(l_3-m_3)!(l_3'+m_3)!(l_3'-m_3)!]^{1/2}} \\
&\times \quad P^{M_t-m_3}_{L_t+l_3}(0)P^{M_t-m_3}_{L_t+l_3'}(0)|\langle\varphi_{n_0}(0;\boldsymbol{\rho})\|T_{L_t}(\boldsymbol{\rho})\|\chi_{n_t}(L_t;\boldsymbol{\rho})\rangle|^2 \\
&\times \quad \frac{\langle\varphi_{n_0'}(L;\boldsymbol{\varsigma})\|T_{l_3}(\boldsymbol{\varsigma})\|\chi_{n_u}(L_u;\boldsymbol{\varsigma})\rangle^*\langle\varphi_{n_0'}(L;\boldsymbol{\varsigma})\|T_{l_3'}(\boldsymbol{\varsigma})\|\chi_{n_u}(L_u;\boldsymbol{\varsigma})\rangle}{E_{n_tL_t}+E_{n_uL_u}-E^{(0)}_{n_0S}-E^{(0)}_{n_0'L}} \\
&- \quad b^*c\sum_{n_tn_u}\sum_{L_tL_ul_2l_3'}\sum_{M_tM_um_2m_3'}\frac{16\pi^2(-1)^{L_t+l_3'-M_t-M_u}}{R_{23}^{l_2+L_u+L_t+l_3'+2}} \\
&\times \quad \begin{pmatrix} L & l_2 & L_t \\ -M & -m_2 & M_t \end{pmatrix}\begin{pmatrix} L & l_3' & L_u \\ -M & m_3' & M_u \end{pmatrix} \\
&\times \quad \frac{P^{M_u+m_2}_{L_u+l_2}(0)P^{M_t-m_3'}_{L_t+l_3'}(0)(L_u+l_2-M_u-m_2)!}{[(l_2+m_2)!(l_2-m_2)!(L_u+M_u)!(L_u-M_u)!]^{1/2}} \\
&\times \quad \frac{(L_t+l_3'-M_t+m_3')!(L_t,L_u)^{-1}(l_2,l_3')^{-1/2}}{[(L_t+M_t)!(L_t-M_t)!(l_3'+m_3')!(l_3'-m_3')!]^{1/2}} \\
&\times \quad \langle\varphi_{n_0'}(L;\boldsymbol{\rho})\|T_{l_2}(\boldsymbol{\rho})\|\chi_{n_t}(L_t;\boldsymbol{\rho})\rangle^*\langle\varphi_{n_0}(0;\boldsymbol{\varsigma})\|T_{L_u}(\boldsymbol{\varsigma})\|\chi_{n_u}(L_u;\boldsymbol{\varsigma})\rangle^* \\
&\times \quad \frac{\langle\varphi_{n_0}(0;\boldsymbol{\rho})\|T_{L_t}(\boldsymbol{\rho})\|\chi_{n_t}(L_t;\boldsymbol{\rho})\rangle\langle\varphi_{n_0'}(L;\boldsymbol{\varsigma})\|T_{l_3'}(\boldsymbol{\varsigma})\|\chi_{n_u}(L_u;\boldsymbol{\varsigma})\rangle}{E_{n_tL_t}+E_{n_uL_u}-E^{(0)}_{n_0S}-E^{(0)}_{n_0'L}}
\end{aligned}
$$

$$
\begin{aligned}
&- \quad c^* b \sum_{n_t n_u} \sum_{L_t L_u l_2' l_3} \sum_{M_t M_u m_2' m_3} \frac{16\pi^2 (-1)^{L_t+l_3-M_t-M_u}}{R_{23}^{l_2'+L_t+L_u+l_3+2}} \\
&\times \quad \begin{pmatrix} L & l_2' & L_t \\ -M & -m_2' & M_t \end{pmatrix} \begin{pmatrix} L & l_3 & L_u \\ -M & m_3 & M_u \end{pmatrix} \\
&\times \quad \frac{P_{L_t+l_3}^{M_t-m_3}(0) P_{L_u+l_2'}^{M_u+m_2'}(0) (L_u+l_2'-M_u-m_2')!}{[(l_2'+m_2')!(l_2'-m_2')!(L_u+M_u)!(L_u-M_u)!]^{1/2}} \\
&\times \quad \frac{(L_t+l_3-M_t+m_3)!(L_t,L_u)^{-1}(l_2',l_3)^{-1/2}}{[(L_t+M_t)!(L_t-M_t)!(l_3+m_3)!(l_3-m_3)!]^{1/2}} \\
&\times \quad \langle \varphi_{n_0}(0;\boldsymbol{\rho}) \| T_{L_t}(\boldsymbol{\rho}) \| \chi_{n_t}(L_t;\boldsymbol{\rho}) \rangle^* \langle \varphi_{n_0'}(L;\boldsymbol{\varsigma}) \| T_{l_3}(\boldsymbol{\varsigma}) \| \chi_{n_u}(L_u;\boldsymbol{\varsigma}) \rangle^* \\
&\times \quad \frac{\langle \varphi_{n_0'}(L;\boldsymbol{\rho}) \| T_{l_2'}(\boldsymbol{\rho}) \| \chi_{n_t}(L_t;\boldsymbol{\rho}) \rangle \langle \varphi_{n_0}(0;\boldsymbol{\varsigma}) \| T_{L_u}(\boldsymbol{\varsigma}) \| \chi_{n_u}(L_u;\boldsymbol{\varsigma}) \rangle}{E_{n_t L_t} + E_{n_u L_u} - E_{n_0 S}^{(0)} - E_{n_0' L}^{(0)}} \\
&= \quad -\Bigg\{ |a|^2 \sum_{n_t n_u} \sum_{L_t L_u} \frac{F_2(n_t,n_u,L_t,L_u)}{R_{23}^{2L_t+2L_u+2}} \\
&+ \quad |b|^2 \sum_{n_t n_u} \sum_{L_t L_u l_2 l_2'} \frac{F_1(n_t,n_u,L_t,L_u;l_2,l_2';L,M)}{R_{23}^{2L_u+l_2+l_2'+2}} \\
&+ \quad |c|^2 \sum_{n_t n_u} \sum_{L_t L_u l_3 l_3'} \frac{F_1(n_u,n_t,L_u,L_t;l_3,l_3';L,M)}{R_{23}^{2L_t+l_3+l_3'+2}} \\
&+ \quad b^* c \sum_{n_t n_u} \sum_{L_t L_u l_2 l_3'} \frac{F_3(n_t,n_u,L_t,L_u;l_2,l_3';L,M)}{R_{23}^{l_2+L_u+L_t+l_3'+2}} \\
&+ \quad c^* b \sum_{n_s n_t n_u} \sum_{L_s L_t L_u l_2' l_3} \frac{F_3^*(n_t,n_u,L_t,L_u;l_2',l_3;L,M)}{R_{23}^{L_t+L_u+l_2'+l_3+2}} \Bigg\},
\end{aligned}
\tag{A.15}
$$

$$
\begin{aligned}
V_{31}^{(2)} \quad &= \quad -|a|^2 \sum_{n_s n_u} \sum_{L_s L_u l_1 l_1'} \sum_{M_s M_u m_1} \frac{16\pi^2}{R_{31}^{2L_u+l_1+l_1'+2}} \\
&\times \quad \begin{pmatrix} L & l_1 & L_s \\ -M & m_1 & M_s \end{pmatrix} \begin{pmatrix} L & l_1' & L_s \\ -M & m_1 & M_s \end{pmatrix} \\
&\times \quad \frac{(L_u+l_1-M_u+m_1)!(L_u+l_1'-M_u+m_1)!(L_u,L_u)^{-1}(l_1,l_1')^{-1/2}}{(L_u+M_u)!(L_u-M_u)![(l_1+m_1)!(l_1-m_1)!(l_1'+m_1)!(l_1'-m_1)!]^{1/2}} \\
&\times \quad P_{L_u+l_1}^{M_u-m_1}(0) P_{L_u+l_1'}^{M_u-m_1}(0) |\langle \varphi_{n_0}(0;\boldsymbol{\varsigma}) \| T_{L_u}(\boldsymbol{\varsigma}) \| \chi_{n_u}(L_u;\boldsymbol{\varsigma}) \rangle|^2
\end{aligned}
$$

$$\times \quad \frac{\langle\varphi_{n_0'}(L;\boldsymbol{\sigma})\|T_{l_1}(\boldsymbol{\sigma})\|\chi_{n_s}(L_s;\boldsymbol{\sigma})\rangle^*\langle\varphi_{n_0'}(L;\boldsymbol{\sigma})\|T_{l_1'}(\boldsymbol{\sigma})\|\chi_{n_s}(L_s;\boldsymbol{\sigma})\rangle}{E_{n_sL_s}+E_{n_uL_u}-E^{(0)}_{n_0S}-E^{(0)}_{n_0'L}}$$

$$- \quad |b|^2\sum_{n_sn_u}\sum_{L_sL_u}\sum_{M_sM_u}\frac{16\pi^2}{R_{31}^{2L_s+2L_u+2}}$$

$$\times \quad \frac{[P^{M_u+M_s}_{L_u+L_s}(0)(L_u+L_s-M_u-M_s)!]^2(L_u,L_s)^{-2}}{(L_u+M_u)!(L_u-M_u)!(L_s+M_s)!(L_s-M_s)!}$$

$$\times \quad \frac{|\langle\varphi_{n_0}(0;\boldsymbol{\sigma})\|T_{L_s}(\boldsymbol{\sigma})\|\chi_{n_s}(L_s;\boldsymbol{\sigma})\rangle|^2|\langle\varphi_{n_0}(0;\boldsymbol{\varsigma})\|T_{L_u}(\boldsymbol{\varsigma})\|\chi_{n_u}(L_u;\boldsymbol{\varsigma})\rangle|^2}{E_{n_sL_s}+E_{n_uL_u}-2E^{(0)}_{n_0S}}$$

$$- \quad |c|^2\sum_{n_sn_u}\sum_{L_sL_ul_3l_3'}\sum_{M_sM_um_3}\frac{16\pi^2}{R_{31}^{2L_s+l_3+l_3'+2}}$$

$$\times \quad \begin{pmatrix} L & l_3 & L_u \\ -M & m_3 & M_u \end{pmatrix}\begin{pmatrix} L & l_3' & L_u \\ -M & m_3 & M_u \end{pmatrix}$$

$$\times \quad \frac{(L_s+l_3-M_s+m_3)!(L_s+l_3'-M_s+m_3)!(L_s,L_s)^{-1}(l_3,l_3')^{-1/2}}{(L_s+M_s)!(L_s-M_s)![(l_3+m_3)!(l_3-m_3)!(l_3'+m_3)!(l_3'-m_3)!]^{1/2}}$$

$$\times \quad P^{M_s-m_3}_{L_s+l_3}(0)P^{M_s-m_3}_{L_s+l_3'}(0)|\langle\varphi_{n_0}(0;\boldsymbol{\sigma})\|T_{L_s}(\boldsymbol{\sigma})\|\chi_{n_s}(L_s;\boldsymbol{\sigma})\rangle|^2$$

$$\times \quad \frac{\langle\varphi_{n_0'}(L;\boldsymbol{\varsigma})\|T_{l_3}(\boldsymbol{\varsigma})\|\chi_{n_u}(L_u\boldsymbol{\varsigma})\rangle^*\langle\varphi_{n_0'}(L;\boldsymbol{\varsigma})\|T_{l_3'}(\boldsymbol{\varsigma})\|\chi_{n_u}(L_u;\boldsymbol{\varsigma})\rangle}{E_{n_sL_s}+E_{n_uL_u}-E^{(0)}_{n_0S}-E^{(0)}_{n_0'L}}$$

$$- \quad a^*c\sum_{n_sn_u}\sum_{L_sL_ul_3'l_1}\sum_{M_sM_um_3'm_1}\frac{16\pi^2(-1)^{L_u+l_1-M_u-M_s}}{R_{31}^{l_3'+L_s+L_u+l_1+2}}$$

$$\times \quad \begin{pmatrix} L & l_3' & L_u \\ -M & -m_3' & M_u \end{pmatrix}\begin{pmatrix} L & l_1 & L_s \\ -M & m_1 & M_s \end{pmatrix}$$

$$\times \quad \frac{P^{M_u-m_1}_{L_u+l_1}(0)P^{M_s+m_3'}_{L_s+l_3'}(0)(L_s+l_3'-M_s-m_3')!}{[(L_s+M_s)!(L_s-M_s)!(L_u+M_u)!(L_u-M_u)!]^{1/2}}$$

$$\times \quad \frac{(L_u+l_1-M_u+m_1)!(L_u,L_s)^{-1}(l_3',l_1)^{-1/2}}{[(l_3'+m_3')!(l_3'-m_3')!(l_1+m_1)!(l_1-m_1)!]^{1/2}}$$

$$\times \quad \langle\varphi_{n_0'}(L;\boldsymbol{\sigma})\|T_{l_1}(\boldsymbol{\sigma})\|\chi_{n_s}(L_s;\boldsymbol{\sigma})\rangle^*\langle\varphi_{n_0}(0;\boldsymbol{\varsigma})\|T_{L_u}(\boldsymbol{\varsigma})\|\chi_{n_u}(L_u;\boldsymbol{\varsigma})\rangle^*$$

$$\times \quad \frac{\langle\varphi_{n_0}(0;\boldsymbol{\sigma})\|T_{L_s}(\boldsymbol{\sigma})\|\chi_{n_s}(L_s;\boldsymbol{\sigma})\rangle\langle\varphi_{n_0'}(L;\boldsymbol{\varsigma})\|T_{l_3'}(\boldsymbol{\varsigma})\|\chi_{n_u}(L_u;\boldsymbol{\varsigma})\rangle}{E_{n_sL_s}+E_{n_uL_u}-E^{(0)}_{n_0S}-E^{(0)}_{n_0'L}}$$

$$- \quad c^*a\sum_{n_sn_u}\sum_{L_sL_ul_3l_1'}\sum_{M_sM_um_3m_1'}\frac{16\pi^2(-1)^{L_u+l_1'-M_u-M_s}}{R_{31}^{l_3+L_s+L_u+l_1'+2}}$$

$$\times \quad \begin{pmatrix} L & l_3 & L_u \\ -M & -m_3 & M_u \end{pmatrix}\begin{pmatrix} L & l_1' & L_s \\ -M & m_1' & M_s \end{pmatrix}$$

$$
\begin{aligned}
\times\ & \frac{P_{L_s+l_3}^{M_s+m_3}(0)P_{L_u+l_1'}^{M_u-m_1'}(0)(L_s+l_3-M_s-m_3)!}{[(L_s+M_s)!(L_s-M_s)!(L_u+M_u)!(L_u-M_u)!]^{1/2}} \\
\times\ & \frac{(L_u+l_1'-M_u+m_1')!(L_u,L_s)^{-1}(l_3,l_1')^{-1/2}}{[(l_3+m_3)!(l_3-m_3)!(l_1'+m_1')!(l_1'-m_1')!]^{1/2}} \\
\times\ & \langle\varphi_{n_0'}(L;\boldsymbol{\varsigma})\|T_{l_3}(\boldsymbol{\varsigma})\|\chi_{n_u}(L_u;\boldsymbol{\varsigma})\rangle^*\langle\varphi_{n_0}(0;\boldsymbol{\sigma})\|T_{L_s}(\boldsymbol{\sigma})\|\chi_{n_s}(L_s;\boldsymbol{\sigma})\rangle^* \\
\times\ & \frac{\langle\varphi_{n_0}(0;\boldsymbol{\varsigma})\|T_{L_u}(\boldsymbol{\varsigma})\|\chi_{n_u}(L_u;\boldsymbol{\varsigma})\rangle\langle\varphi_{n_0'}(L;\boldsymbol{\sigma})\|T_{l_1'}(\boldsymbol{\sigma})\|\chi_{n_s}(L_s;\boldsymbol{\sigma})\rangle}{E_{n_sL_s}+E_{n_uL_u}-E_{n_0S}^{(0)}-E_{n_0'L}^{(0)}} \\
=\ & -\Bigg\{|a|^2\sum_{n_sn_u}\sum_{L_sL_ul_1l_1'}\frac{F_1(n_s,n_u,L_s,L_u;l_1,l_1';L,M)}{R_{31}^{2L_u+l_1+l_1'+2}} \\
& +|b|^2\sum_{n_sn_u}\sum_{L_sL_u}\frac{F_2(n_s,n_u,L_s,L_u)}{R_{31}^{2L_s+2L_u+2}} \\
& +|c|^2\sum_{n_sn_u}\sum_{L_sL_ul_3l_3'}\frac{F_1(n_u,n_s,L_u,L_s;l_3,l_3';L,M)}{R_{31}^{2L_s+l_3+l_3'+2}} \\
& +(a^*c)\sum_{n_sn_u}\sum_{L_sL_ul_3'l_1}\frac{F_3(n_u,n_s,L_u,L_s;l_3',l_1;L,M)}{R_{31}^{l_3'+L_s+L_u+l_1+2}} \\
& +(c^*a)\sum_{n_sn_u}\sum_{L_sL_ul_3l_1'}\frac{F_3^*(n_u,n_s,L_u,L_s;l_3,l_1';L,M)}{R_{31}^{l_3+L_s+L_u+l_1'+2}}\Bigg\}. \qquad \text{(A.16)}
\end{aligned}
$$

Similarly, the three nonadditive terms are

$$
\begin{aligned}
V_{12,23}^{(2)} =\ & -\sum_{n_tL_tM_t}\frac{16\pi^2(-1)^{L_t+L+M_t-M}}{R_{12}^{L_t+L+1}R_{23}^{L_t+L+1}} \\
\times\ & \frac{[P_{L_t+L}^{M_t-M}(0)(L_t+L-M_t+M)!(L_t,L)^{-1}]^2}{(L_t+M_t)!(L_t-M_t)!(L+M)!(L-M)!} \\
\times\ & \{(a^*c)\exp[-i(M_t-M)\beta]+(c^*a)\exp[i(M_t-M)\beta]\} \\
\times\ & \frac{|\langle\varphi_{n_0'}(L;\boldsymbol{\sigma})\|T_L(\boldsymbol{\sigma})\|\chi_{n_0}(0;\boldsymbol{\sigma})\rangle|^2|\langle\varphi_{n_0}(0;\boldsymbol{\rho})\|T_{L_t}(\boldsymbol{\rho})\|\chi_{n_t}(L_t;\boldsymbol{\rho})\rangle|^2}{E_{n_tL_t}-E_{n_0'L}^{(0)}} \\
& -\sum_{n_tL_tM_t}\frac{16\pi^2(-1)^{L_t+L+M_t+M}}{R_{12}^{L_t+L+1}R_{23}^{L_t+L+1}} \\
\times\ & \frac{[P_{L_t+L}^{M_t+M}(0)(L_t+L-M_t-M)!(L_t,L)^{-1}]^2}{(L_t+M_t)!(L_t-M_t)!(L+M)!(L-M)!} \\
\times\ & \{(a^*c)\exp[i(M_t+M)\beta]+(c^*a)\exp[-i(M_t+M)\beta]\} \\
\times\ & \frac{|\langle\varphi_{n_0}(0;\boldsymbol{\sigma})\|T_L(\boldsymbol{\sigma})\|\chi_{n_0'}(L;\boldsymbol{\sigma})\rangle|^2|\langle\varphi_{n_0}(0;\boldsymbol{\rho})\|T_{L_t}(\boldsymbol{\rho})\|\chi_{n_t}(L_t;\boldsymbol{\rho})\rangle|^2}{E_{n_tL_t}+E_{n_0'L}-2E_{n_0S}^{(0)}}
\end{aligned}
$$

$$
\begin{aligned}
&= -\Big\{ \sum_{n_t L_t M_t} \{(a^* c)\exp[-i(M_t - M)\beta]\} \frac{F_4(n_t, L_t, M_t; L, M)}{R_{12}^{L_t+L+1} R_{23}^{L_t+L+1}} \\
&+ \sum_{n_t L_t M_t} \{(c^* a)\exp[i(M_t - M)\beta]\} \frac{F_4(n_t, L_t, M_t; L, M)}{R_{12}^{L_t+L+1} R_{23}^{L_t+L+1}} \Big\}, \qquad \text{(A.17)}
\end{aligned}
$$

$$
\begin{aligned}
V_{23,31}^{(2)} &= -\sum_{n_u L_u M_u} \frac{16\pi^2 (-1)^{L_u+L+M_u-M}}{R_{23}^{L_u+L+1} R_{31}^{L_u+L+1}} \\
&\times \frac{[P_{L_u+L}^{M_u-M}(0)(L_u + L - M_u + M)!(L_u, L)^{-1}]^2}{(L_u + M_u)!(L_u - M_u)!(L + M)!(L - M)!} \\
&\times \{(a^* b)\exp[i(M_u - M)\gamma] + (b^* a)\exp[-i(M_u - M)\gamma]\} \\
&\times \frac{|\langle \varphi_{n_0'}(L;\boldsymbol{\sigma}) \| T_L(\boldsymbol{\sigma}) \| \chi_{n_0}(0;\boldsymbol{\sigma})\rangle|^2 |\langle \varphi_{n_0}(0;\boldsymbol{\varsigma}) \| T_{L_u}(\boldsymbol{\varsigma}) \| \chi_{n_u}(L_u;\boldsymbol{\varsigma})\rangle|^2}{E_{n_u L_u} - E_{n_0' L}^{(0)}} \\
&- \sum_{n_u L_u M_u} \frac{16\pi^2 (-1)^{L_u+L+M_u+M}}{R_{23}^{L_u+L+1} R_{31}^{L_u+L+1}} \\
&\times \frac{[P_{L_u+L}^{M_u+M}(0)(L_u + L - M_u - M)!(L_u, L)^{-1}]^2}{(L_u + M_u)!(L_u - M_u)!(L + M)!(L - M)!} \\
&\times \{(a^* b)\exp[-i(M_u + M)\gamma] + (b^* a)\exp[i(M_u + M)\gamma]\} \\
&\times \frac{|\langle \varphi_{n_0}(0;\boldsymbol{\sigma}) \| T_L(\boldsymbol{\sigma}) \| \chi_{n_0'}(L;\boldsymbol{\sigma})\rangle|^2 |\langle \varphi_{n_0}(0;\boldsymbol{\varsigma}) \| T_{L_u}(\boldsymbol{\varsigma}) \| \chi_{n_u}(L_u;\boldsymbol{\varsigma})\rangle|^2}{E_{n_u L_u} + E_{n_0' L} - 2E_{n_0 S}^{(0)}} \\
&= -\Big\{ \sum_{n_u L_u M_u} \{(a^* b)\exp[i(M_u - M)\gamma]\} \frac{F_4(n_u, L_u, M_u; L, M)}{R_{23}^{L_u+L+1} R_{31}^{L_u+L+1}} \\
&+ \sum_{n_u L_u M_u} \{(b^* a)\exp[-i(M_u - M)\gamma]\} \frac{F_4(n_u, L_u, M_u; L, M)}{R_{23}^{L_u+L+1} R_{31}^{L_u+L+1}} \Big\}, \qquad \text{(A.18)}
\end{aligned}
$$

$$
\begin{aligned}
V_{31,12}^{(2)} &= -\sum_{n_s L_s M_s} \frac{16\pi^2 (-1)^{L_s+L+M_s-M}}{R_{31}^{L_s+L+1} R_{12}^{L_s+L+1}} \\
&\times \frac{[P_{L_s+L}^{M_s-M}(0)(L_s + L - M_s + M)!(L_s, L)^{-1}]^2}{(L_s + M_s)!(L_s - M_s)!(L + M)!(L - M)!} \\
&\times \{(b^* c)\exp[i(M_s - M)\alpha] + (c^* b)\exp[-i(M_s - M)\alpha]\} \\
&\times \frac{|\langle \varphi_{n_0}(0;\boldsymbol{\sigma}) \| T_{L_s}(\boldsymbol{\sigma}) \| \chi_{n_s}(L_s;\boldsymbol{\sigma})\rangle|^2 |\langle \varphi_{n_0'}(L;\boldsymbol{\rho}) \| T_L(\boldsymbol{\rho}) \| \chi_{n_0}(0;\boldsymbol{\rho})\rangle|^2}{E_{n_s L_s} - E_{n_0' L}^{(0)}} \\
&- \sum_{n_s L_s M_s} \frac{16\pi^2 (-1)^{L_s+L+M_s+M}}{R_{31}^{L_s+L+1} R_{12}^{L_s+L+1}}
\end{aligned}
$$

$$
\begin{aligned}
&\times \quad \frac{[P_{L_s+L}^{M_s+M}(0)(L_s+L-M_s-M)!(L_s,L)^{-1}]^2}{(L_s+M_s)!(L_s-M_s)!(L+M)!(L-M)!} \\
&\times \quad \{(b^*c)\exp[-i(M_s+M)(\alpha)] + (c^*b)\exp[i(M_s+M)(\alpha)]\} \\
&\times \quad \frac{|\langle\varphi_{n_0}(0;\boldsymbol{\sigma})\|T_{L_s}(\boldsymbol{\sigma})\|\chi_{n_s}(L_s;\boldsymbol{\sigma})\rangle|^2|\langle\varphi_{n_0'}(L;\boldsymbol{\rho})\|T_L(\boldsymbol{\rho})\|\chi_{n_0}(0;\boldsymbol{\rho})\rangle|^2}{E_{n_sL_s}+E^{(0)}_{n_0'L}-2E^{(0)}_{n_0S}} \\
&= \quad -\Bigg\{\sum_{n_sL_sM_s}\{(b^*c)\exp[i(M_s-M)\alpha]\}\frac{F_4(n_s,L_s,M_s;L,M)}{R_{31}^{L_s+L+1}R_{12}^{L_s+L+1}} \\
&+ \quad \sum_{n_sL_sM_s}\{(c^*b)\exp[-i(M_s-M)\alpha]\}\frac{F_4(n_s,L_s,M_s;L,M)}{R_{31}^{L_s+L+1}R_{12}^{L_s+L+1}}\Bigg\}. \qquad \text{(A.19)}
\end{aligned}
$$

In the above, the F_i functions are defined by

$$
\begin{aligned}
&F_1(n_s,n_t,L_s,L_t;l_1,l_1';L,M) \\
&= \quad G_1(L_s,L_t,l_1,l_1';L,M)\langle\varphi_{n_0'}(L;\boldsymbol{\sigma})\|T_{l_1}(\boldsymbol{\sigma})\|\chi_{n_s}(L_s;\boldsymbol{\sigma})\rangle^* \\
&\times \quad \frac{\langle\varphi_{n_0'}(L;\boldsymbol{\sigma})\|T_{l_1'}(\boldsymbol{\sigma})\|\chi_{n_s}(L_s;\boldsymbol{\sigma})\rangle|\langle\varphi_{n_0}(0;\boldsymbol{\rho})\|T_{L_t}(\boldsymbol{\rho})\|\chi_{n_t}(L_t;\boldsymbol{\rho})\rangle|^2}{E_{n_sL_s}+E_{n_tL_t}-E^{(0)}_{n_0S}-E^{(0)}_{n_0'L}}, \qquad \text{(A.20)}
\end{aligned}
$$

$$
\begin{aligned}
&F_2(n_s,n_t,L_s,L_t) = G_2(L_s,L_t) \\
&\times \quad \frac{|\langle\varphi_{n_0}(0;\boldsymbol{\sigma})\|T_{L_s}(\boldsymbol{\sigma})\|\chi_{n_s}(L_s;\boldsymbol{\sigma})\rangle|^2|\langle\varphi_{n_0}(0;\boldsymbol{\rho})\|T_{L_t}(\boldsymbol{\rho})\|\chi_{n_t}(L_t;\boldsymbol{\rho})\rangle|^2}{E_{n_sL_s}+E_{n_tL_t}-2E^{(0)}_{n_0S}}, \qquad \text{(A.21)}
\end{aligned}
$$

$$
\begin{aligned}
&F_3(n_s,n_t,L_s,L_t;l_1,l_2';L,M) \\
&= \quad (-1)^{L_s+l_2'}G_3(L_s,L_t,l_1,l_2';L,M) \\
&\times \quad \langle\varphi_{n_0}(0;\boldsymbol{\sigma})\|T_{L_s}(\boldsymbol{\sigma})\|\chi_{n_s}(L_s;\boldsymbol{\sigma})\rangle^*\langle\varphi_{n_0'}(L;\boldsymbol{\rho})\|T_{l_2'}(\boldsymbol{\rho})\|\chi_{n_t}(L_t;\boldsymbol{\rho})\rangle^* \\
&\times \quad \frac{\langle\varphi_{n_0'}(L;\boldsymbol{\sigma})\|T_{l_1}(\boldsymbol{\sigma})\|\chi_{n_s}(L_s;\boldsymbol{\sigma})\rangle\langle\varphi_{n_0}(0;\boldsymbol{\rho})\|T_{L_t}(\boldsymbol{\rho})\|\chi_{n_t}(L_t;\boldsymbol{\rho})\rangle}{E_{n_sL_s}+E_{n_tL_t}-E^{(0)}_{n_0S}-E^{(0)}_{n_0'L}}. \qquad \text{(A.22)}
\end{aligned}
$$

$$
\begin{aligned}
& F_4(n_t, L_t, M_t; L, M) \\
= \; & (-1)^{L_t+L+M_t+M} G_4(L_t, M_t; L, M) \\
\times \; & \Bigg[\frac{|\langle \varphi_{n_0'}(L;\boldsymbol{\sigma}) \| T_L(\boldsymbol{\sigma}) \| \chi_{n_0}(0;\boldsymbol{\sigma}) \rangle|^2 |\langle \varphi_{n_0}(0;\boldsymbol{\rho}) \| T_{L_t}(\boldsymbol{\rho}) \| \chi_{n_t}(L_t;\boldsymbol{\rho}) \rangle|^2}{E_{n_t L_t} - E^{(0)}_{n_0' L}} \\
+ \; & \frac{|\langle \varphi_{n_0'}(L;\boldsymbol{\sigma}) \| T_L(\boldsymbol{\sigma}) \| \chi_{n_0}(0;\boldsymbol{\sigma}) \rangle|^2 |\langle \varphi_{n_0}(0;\boldsymbol{\rho}) \| T_{L_t}(\boldsymbol{\rho}) \| \chi_{n_t}(L_t;\boldsymbol{\rho}) \rangle|^2}{E_{n_t L_t} + E^{(0)}_{n_0' L} - 2E^{(0)}_{n_0 S}} \Bigg] ,
\end{aligned}
\tag{A.23}
$$

where $G_1(L_i, L_j, \ell_k, \ell_k'; L, M)$, $G_2(L_i, L_j)$, $G_3(L_i, L_j, \ell_{k_1}, \ell_{k_2}'; L, M)$, and $G_4(L_i, M_i; L, M)$ are further defined by:

$$
\begin{aligned}
& G_1(L_i, L_j, \ell_k, \ell_k'; L, M) \\
= \; & \frac{16\pi^2 (\ell_k, \ell_k')^{-1/2}}{(2L_j+1)^2} \sum_{M_i M_j m_k} \begin{pmatrix} L & \ell_k & L_i \\ -M & m_k & M_i \end{pmatrix} \begin{pmatrix} L & \ell_k' & L_i \\ -M & m_k & M_i \end{pmatrix} \\
\times \; & \frac{(L_j + \ell_k - M_j + m_k)! (L_j + \ell_k' - M_j + m_k)! P^{M_j - m_k}_{L_j + \ell_k}(0) P^{M_j - m_k}_{L_j + \ell_k'}(0)}{(L_j + M_j)! (L_j - M_j)! [(\ell_k + m_k)! (\ell_k - m_k)! (\ell_k' + m_k)! (\ell_k' - m_k)!]^{1/2}} ,
\end{aligned}
\tag{A.24}
$$

$$
\begin{aligned}
& G_2(L_i, L_j) = 16\pi^2 (L_i, L_j)^{-2} \\
\times \; & \sum_{M_i M_j} \frac{[P^{M_i + M_j}_{L_i + L_j}(0) (L_i + L_j - M_i - M_j)!]^2}{(L_i + M_i)! (L_i - M_i)! (L_j + M_j)! (L_j - M_j)!} ,
\end{aligned}
\tag{A.25}
$$

$$
\begin{aligned}
& G_3(L_i, L_j, \ell_{k_1}, \ell_{k_2}'; L, M) \\
= \; & \frac{16\pi^2 (\ell_{k_1}, \ell_{k_2}')^{-1/2}}{(2L_i+1)(2L_j+1)} \sum_{M_i M_j m_{k_1} m_{k_2}'}
\end{aligned}
$$

$$
\begin{aligned}
\times & \begin{pmatrix} L & \ell_{k_1} & L_i \\ -M & -m_{k_1} & M_i \end{pmatrix} \begin{pmatrix} L & \ell'_{k_2} & L_j \\ -M & m'_{k_2} & M_j \end{pmatrix} \\
\times & \frac{(-1)^{M_i+M_j} P_{L_j+\ell_{k_1}}^{M_j+m_{k_1}}(0) P_{L_i+\ell'_{k_2}}^{M_i-m'_{k_2}}(0)}{[(L_i+M_i)!(L_i-M_i)!(L_j+M_j)!(L_j-M_j)!]^{1/2}} \\
\times & \frac{(L_j+\ell_{k_1}-M_j-m_{k_1})!(L_i+\ell'_{k_2}-M_i+m'_{k_2})!}{[(\ell_{k_1}+m_{k_1})!(\ell_{k_1}-m_{k_1})!(\ell'_{k_2}+m'_2)!(\ell'_{k_2}-m'_2)!]^{1/2}} ,
\end{aligned}
\tag{A.26}
$$

$$
G_4(L_i, M_i; L, M) = 16\pi^2 \frac{[P_{L_i+L}^{M_i-M}(0)(L_i+L-M_i+M)!(L_i,L)^{-1}]^2}{(L_i+M_i)!(L_i-M_i)!(L+M)!(L-M)!} .
\tag{A.27}
$$

Then the second-order energy correction is simplified as,

$$
\begin{aligned}
\Delta E^{(2)} &= -\sum_{n\geq 3} \left(\frac{C_{2n}^{(12)}(L,M)}{R_{12}^{2n}} + \frac{C_{2n}^{(23)}(L,M)}{R_{23}^{2n}} + \frac{C_{2n}^{(31)}(L,M)}{R_{31}^{2n}} \right. \\
&+ \left. \frac{C_{2n}^{(12,23)}(L,M)}{R_{12}^{n}R_{23}^{n}} + \frac{C_{2n}^{(23,31)}(L,M)}{R_{23}^{n}R_{31}^{n}} + \frac{C_{2n}^{(31,12)}(L,M)}{R_{31}^{n}R_{12}^{n}} \right)
\end{aligned}
\tag{A.28}
$$

where $C_{2n}^{(IJ)}(L,M)$ and $C_{2n}^{(IJ,JK)}(L,M)$ are, respectively, the additive and nonadditive dispersion coefficients. These coefficients can be expressed as

$$
\begin{aligned}
C_{2n}^{(12)}(L,M) &= |a|^2 \sum_{n_s n_t} \sum_{\substack{L_s L_t l_1 l'_1 \\ 2L_t+l_1+l'_1+2=2n}} F_1(n_s, n_t, L_s, L_t; l_1, l'_1; L, M) \\
&+ |b|^2 \sum_{n_s n_t} \sum_{\substack{L_s L_t l_2 l'_2 \\ 2L_s+l_2+l'_2+2=2n}} F_1(n_t, n_s, L_t, L_s; l_2, l'_2; L, M) \\
&+ |c|^2 \sum_{n_s n_t} \sum_{\substack{L_s L_t \\ 2L_s+2L_t+2=2n}} F_2(n_s, n_t, L_s, L_t)
\end{aligned}
$$

$$
\begin{aligned}
&+ \quad a^* b \sum_{n_s n_t} \sum_{\substack{L_s L_t l_1 l_2' \\ L_s+L_t+l_1+l_2'+2=2n}} F_3(n_s, n_t, L_s, L_t; l_1, l_2'; L, M) \\
&+ \quad b^* a \sum_{n_s n_t} \sum_{\substack{L_s L_t l_1' l_2 \\ L_s+L_t+l_1'+l_2+2=2n}} F_3^*(n_s, n_t, L_s, L_t; l_1', l_2; L, M)\,,
\end{aligned}
\tag{A.29}
$$

$$
\begin{aligned}
C_{2n}^{(23)}(L, M) \;=\;& |a|^2 \sum_{n_t n_u} \sum_{\substack{L_t L_u \\ 2L_t+2L_u+2=2n}} F_2(n_t, n_u, L_t, L_u) \\
&+ \quad |b|^2 \sum_{n_t n_u} \sum_{\substack{L_t L_u l_2 l_2' \\ 2L_u+l_2+l_2'+2=2n}} F_1(n_t, n_u, L_t, L_u; l_2, l_2'; L, M) \\
&+ \quad |c|^2 \sum_{n_t n_u} \sum_{\substack{L_t L_u l_3 l_3' \\ 2L_t+l_3+l_3'+2=2n}} F_1(n_u, n_t, L_u, L_t; l_3, l_3'; L, M) \\
&+ \quad b^* c \sum_{n_t n_u} \sum_{\substack{L_t L_u l_2 l_3' \\ L_u+L_t+l_2+l_3'+2=2n}} F_3(n_t, n_u, L_t, L_u; l_2, l_3'; L, M) \\
&+ \quad c^* b \sum_{n_t n_u} \sum_{\substack{L_s L_t L_u l_2' l_3 \\ L_t+L_u+l_2'+l_3+2=2n}} F_3^*(n_t, n_u, L_t, L_u; l_2', l_3; L, M)\,,
\end{aligned}
\tag{A.30}
$$

$$
\begin{aligned}
C_{2n}^{(31)}(L, M) \;=\;& |a|^2 \sum_{n_s n_u} \sum_{\substack{L_s L_u l_1 l_1' \\ 2L_u+l_1+l_1'+2=2n}} F_1(n_s, n_u, L_s, L_u; l_1, l_1'; L, M) \\
&+ \quad |b|^2 \sum_{n_s n_u} \sum_{\substack{L_s L_u \\ 2L_s+2L_u+2=2n}} F_2(n_s, n_u, L_s, L_u) \\
&+ \quad |c|^2 \sum_{n_s n_u} \sum_{\substack{L_s L_u l_3 l_3' \\ 2L_s+l_3+l_3'+2=2n}} F_1(n_u, n_s, L_u, L_s; l_3, l_3'; L, M) \\
&+ \quad (a^* c) \sum_{n_s n_u} \sum_{\substack{L L_s L_u l_3' l_1 \\ L_s+L_u+l_1+l_3'+2=2n}} F_3^*(n_u, n_s, L_u, L_s; l_3', l_1; L, M) \\
&+ \quad (c^* a) \sum_{n_s n_u} \sum_{\substack{L_s L_u l_3 l_1' \\ L_s+L_u+l_1'+l_3+2=2n}} F_3(n_u, n_s, L_u, L_s; l_3, l_1'; L, M)\,,
\end{aligned}
$$

(A.31)

$$C_{2n}^{(12,23)}(L,M) = \sum_{\substack{n_t L_t M_t \\ L_t+L+1=n}} \{(a^*c)\exp[-i(M_t-M)\beta]\}F_4(n_t,L_t,M_t;L,M) + \sum_{\substack{n_t L_t M_t \\ L_t+L+1=n}} \{(c^*a)\exp[i(M_t-M)\beta]\}F_4(n_t,L_t,M_t;L,M)\,, \tag{A.32}$$

$$C_{2n}^{(23,31)}(L,M) = \sum_{\substack{n_u L_u M_u \\ L_u+L+1=n}} \{(a^*b)\exp[i(M_u-M)\gamma]\}F_4(n_u,L_u,M_u;L,M) + \sum_{\substack{n_u L_u M_u \\ L_u+L+1=n}} \{(b^*a)\exp[-i(M_u-M)\gamma]\}F_4(n_u,L_u,M_u;L,M)\,, \tag{A.33}$$

$$C_{2n}^{(31,12)}(L,M) = \sum_{\substack{n_s L_s M_s \\ L_s+L+1=n}} \{(b^*c)\exp[i(M_s-M)\alpha]\}F_4(n_s,L_s,M_s;L,M) + \sum_{\substack{n_s L_s M_s \\ L_s+L+1=n}} \{(c^*b)\exp[-i(M_s-M)\alpha]\}F_4(n_s,L_s,M_s;L,M)\,. \tag{A.34}$$

Appendix B

C_m Coefficients for $He(1\,^1S)$-$He(1\,^1S)$-$He(2\,^1S)$

In the present work, we take the mutual electrostatic interactions V_{IJ} between pairs of atoms for the He($n_0\,^\lambda S$)-He($n_0\,^\lambda S$)-He($n_0'\,^\lambda S$) system as a perturbation. According to degenerate perturbation theory, the zero-order wave function of the unperturbed system can be written as,

$$|\Psi^{(0)}\rangle = a|\phi_1\rangle + b|\phi_2\rangle + c|\phi_3\rangle\,. \tag{B.1}$$

where ϕ_1, ϕ_2, ϕ_3 are three orthogonal eigenvectors corresponding to the same energy eigenvalue $E^{(0)}_{n_0 n_0 n_0'} = 2E^{(0)}_{n_0 S} + E^{(0)}_{n_0' S}$. With the zero-order wavefunction of Eq. (B.1), we can derive a general formulas of the dispersion coefficients for the He($1\,^1S$)-He($1\,^1S$)-He($2\,^1L$) system. The values of coefficients a, b and c can be obtained by the degenerate perturbation theory.

B.1 The Zeroth-Order Wave Function

According to degenerate perturbation theory, the zero-order energy correction is obtained by the perturbation matrix with respect to $\{\phi_1, \phi_2, \phi_3\}$ thus becomes

$$H' = \begin{pmatrix} \Delta_{11} & \Delta_{12} & \Delta_{13} \\ \Delta_{21} & \Delta_{22} & \Delta_{23} \\ \Delta_{31} & \Delta_{32} & \Delta_{33} \end{pmatrix}, \tag{B.2}$$

where

$$\begin{aligned}
\Delta_{11} &= -\sum_{n_s n_t n_u} \sum_{L_s L_t L_u} \sum_{M_s M_t M_u} \frac{|\langle\phi_1|V_{123}|\chi_{n_s}(L_s M_s;\boldsymbol{\sigma})\chi_{n_t}(L_t M_t;\boldsymbol{\rho})\chi_{n_u}(L_u M_u;\boldsymbol{\varsigma})\rangle|^2}{E_{n_s L_s;n_t L_t;n_u L_u} - E^{(0)}_{n_0 S;n_0 S;n'_0 S}} \\
&= -\sum_{n_s n_t} \sum_{L_s L_t} \sum_{M_s M_t} \frac{16\pi^2}{R_{12}^{2L_s+2L_t+2}} \frac{[P^{M_s+M_t}_{L_s+L_t}(0)(L_s+L_t-M_s-M_t)!]^2 (L_s,L_t)^{-2}}{(L_s+M_s)!(L_s-M_s)!(L_t+M_t)!(L_t-M_t)!} \\
&\quad \frac{|\langle\varphi_{n'_0}(0;\boldsymbol{\sigma})\|T_{L_s}(\boldsymbol{\sigma})\|\chi_{n_s}(L_s;\boldsymbol{\sigma})\rangle|^2 |\langle\varphi_{n_0}(0;\boldsymbol{\rho})\|T_{L_t}(\boldsymbol{\rho})\|\chi_{n_t}(L_t;\boldsymbol{\rho})\rangle|^2}{E_{n_s L_s} + E_{n_t L_t} - E^{(0)}_{n_0 S} - E^{(0)}_{n'_0 S}} \\
&\quad - \sum_{n_t n_u} \sum_{L_t L_u} \sum_{M_t M_u} \frac{16\pi^2}{R_{23}^{2L_t+2L_u+2}} \frac{[P^{M_t+M_u}_{L_t+L_u}(0)(L_t+L_u-M_t-M_u)!]^2 (L_t,L_u)^{-2}}{(L_t+M_t)!(L_t-M_t)!(L_u+M_u)!(L_u-M_u)!} \\
&\quad \frac{|\langle\varphi_{n_0}(0;\boldsymbol{\rho})\|T_{L_t}(\boldsymbol{\rho})\|\chi_{n_t}(L_t;\boldsymbol{\rho})\rangle|^2 |\langle\varphi_{n_0}(0;\boldsymbol{\varsigma})\|T_{L_u}(\boldsymbol{\varsigma})\|\chi_{n_u}(L_u;\boldsymbol{\varsigma})\rangle|^2}{E_{n_t L_t} + E_{n_u L_u} - 2E^{(0)}_{n_0 S}} \\
&\quad - \sum_{n_s n_u} \sum_{L_s L_u} \sum_{M_s M_u} \frac{16\pi^2}{R_{31}^{2L_s+2L_u+2}} \frac{[P^{M_u+M_s}_{L_u+L_s}(0)(L_u+L_s-M_u-M_s)!]^2 (L_u,L_s)^{-2}}{(L_u+M_u)!(L_u-M_u)!(L_s+M_s)!(L_s-M_s)!} \\
&\quad \frac{|\langle\varphi_{n'_0}(0;\boldsymbol{\sigma})\|T_{L_s}(\boldsymbol{\sigma})\|\chi_{n_s}(L_s;\boldsymbol{\sigma})\rangle|^2 |\langle\varphi_{n_0}(0;\boldsymbol{\varsigma})\|T_{L_u}(\boldsymbol{\varsigma})\|\chi_{n_u}(L_u;\boldsymbol{\varsigma})\rangle|^2}{E_{n_s L_s} + E_{n_u L_u} - E_{n_0 S} - E_{n'_0 S}},
\end{aligned} \tag{B.3}$$

$$\begin{aligned}
\Delta_{22} &= -\sum_{n_s n_t n_u} \sum_{L_s L_t L_u} \sum_{M_s M_t M_u} \frac{|\langle\phi_2|V_{123}|\chi_{n_s}(L_s M_s;\boldsymbol{\sigma})\chi_{n_t}(L_t M_t;\boldsymbol{\rho})\chi_{n_u}(L_u M_u;\boldsymbol{\varsigma})\rangle|^2}{E_{n_s L_s;n_t L_t;n_u L_u} - E^{(0)}_{n_0 S;n_0 S;n'_0 S}} \\
&= -\sum_{n_s n_t} \sum_{L_s L_t} \sum_{M_s M_t} \frac{16\pi^2}{R_{12}^{2L_s+2L_t+2}} \frac{[P^{M_s+M_t}_{L_s+L_t}(0)(L_s+L_t-M_s-M_t)!]^2 (L_s,L_t)^{-2}}{(L_s+M_s)!(L_s-M_s)!(L_t+M_t)!(L_t-M_t)!}
\end{aligned}$$

$$
\frac{|\langle\varphi_{n_0}(0;\boldsymbol{\sigma})\|T_{L_s}(\boldsymbol{\sigma})\|\chi_{n_s}(L_s;\boldsymbol{\sigma})\rangle|^2|\langle\varphi_{n_0'}(0;\boldsymbol{\rho})\|T_{L_t}(\boldsymbol{\rho})\|\chi_{n_t}(L_t;\boldsymbol{\rho})\rangle|^2}{E_{n_sL_s}+E_{n_tL_t}-E^{(0)}_{n_0S}-E^{(0)}_{n_0'S}}
$$

$$
- \sum_{n_tn_u}\sum_{L_tL_u}\sum_{M_tM_u}\frac{16\pi^2}{R_{23}^{2L_t+2L_u+2}}\frac{[P^{M_t+M_u}_{L_t+L_u}(0)(L_t+L_u-M_t-M_u)!]^2(L_t,L_u)^{-2}}{(L_t+M_t)!(L_t-M_t)!(L_u+M_u)!(L_u-M_u)!}
$$

$$
\frac{|\langle\varphi_{n_0'}(0;\boldsymbol{\rho})\|T_{L_t}(\boldsymbol{\rho})\|\chi_{n_t}(L_t;\boldsymbol{\rho})\rangle|^2|\langle\varphi_{n_0}(0;\boldsymbol{\varsigma})\|T_{L_u}(\boldsymbol{\varsigma})\|\chi_{n_u}(L_u;\boldsymbol{\varsigma})\rangle|^2}{E_{n_tL_t}+E_{n_uL_u}-E^{(0)}_{n_0S}-E^{(0)}_{n_0'S}}
$$

$$
- \sum_{n_sn_u}\sum_{L_sL_u}\sum_{M_sM_u}\frac{16\pi^2}{R_{31}^{2L_s+2L_u+2}}\frac{[P^{M_u+M_s}_{L_u+L_s}(0)(L_u+L_s-M_u-M_s)!]^2(L_u,L_s)^{-2}}{(L_u+M_u)!(L_u-M_u)!(L_s+M_s)!(L_s-M_s)!}
$$

$$
\frac{|\langle\varphi_{n_0}(0;\boldsymbol{\sigma})\|T_{L_s}(\boldsymbol{\sigma})\|\chi_{n_s}(L_s;\boldsymbol{\sigma})\rangle|^2|\langle\varphi_{n_0}(0;\boldsymbol{\varsigma})\|T_{L_u}(\boldsymbol{\varsigma})\|\chi_{n_u}(L_u;\boldsymbol{\varsigma})\rangle|^2}{E_{n_sL_s}+E_{n_uL_u}-2E_{n_0S}}\,, \tag{B.4}
$$

$$
\begin{aligned}
\Delta_{33} &= -\sum_{n_sn_tn_u}\sum_{L_sL_tL_u}\sum_{M_sM_tM_u}\frac{|\langle\phi_3|V_{123}|\chi_{n_s}(L_sM_s;\boldsymbol{\sigma})\chi_{n_t}(L_tM_t;\boldsymbol{\rho})\chi_{n_u}(L_uM_u;\boldsymbol{\varsigma})\rangle|^2}{E_{n_sL_s;n_tL_t;n_uL_u}-E^{(0)}_{n_0S;n_0S;n_0'S}} \\
&= -\sum_{n_sn_t}\sum_{L_sL_t}\sum_{M_sM_t}\frac{16\pi^2}{R_{12}^{2L_s+2L_t+2}}\frac{[P^{M_s+M_t}_{L_s+L_t}(0)(L_s+L_t-M_s-M_t)!]^2(L_s,L_t)^{-2}}{(L_s+M_s)!(L_s-M_s)!(L_t+M_t)!(L_t-M_t)!} \\
&\quad \frac{|\langle\varphi_{n_0}(0;\boldsymbol{\sigma})\|T_{L_s}(\boldsymbol{\sigma})\|\chi_{n_s}(L_s;\boldsymbol{\sigma})\rangle|^2|\langle\varphi_{n_0}(0;\boldsymbol{\rho})\|T_{L_t}(\boldsymbol{\rho})\|\chi_{n_t}(L_t;\boldsymbol{\rho})\rangle|^2}{E_{n_sL_s}+E_{n_tL_t}-2E^{(0)}_{n_0S}} \\
&\quad - \sum_{n_tn_u}\sum_{L_tL_u}\sum_{M_tM_u}\frac{16\pi^2}{R_{23}^{2L_t+2L_u+2}}\frac{[P^{M_t+M_u}_{L_t+L_u}(0)(L_t+L_u-M_t-M_u)!]^2(L_t,L_u)^{-2}}{(L_t+M_t)!(L_t-M_t)!(L_u+M_u)!(L_u-M_u)!} \\
&\quad \frac{|\langle\varphi_{n_0}(0;\boldsymbol{\rho})\|T_{L_t}(\boldsymbol{\rho})\|\chi_{n_t}(L_t;\boldsymbol{\rho})\rangle|^2|\langle\varphi_{n_0'}(0;\boldsymbol{\varsigma})\|T_{L_u}(\boldsymbol{\varsigma})\|\chi_{n_u}(L_u;\boldsymbol{\varsigma})\rangle|^2}{E_{n_tL_t}+E_{n_uL_u}-E^{(0)}_{n_0S}-E^{(0)}_{n_0'S}} \\
&\quad - \sum_{n_sn_u}\sum_{L_sL_u}\sum_{M_sM_u}\frac{16\pi^2}{R_{31}^{2L_s+2L_u+2}}\frac{[P^{M_u+M_s}_{L_u+L_s}(0)(L_u+L_s-M_u-M_s)!]^2(L_u,L_s)^{-2}}{(L_u+M_u)!(L_u-M_u)!(L_s+M_s)!(L_s-M_s)!} \\
&\quad \frac{|\langle\varphi_{n_0}(0;\boldsymbol{\sigma})\|T_{L_s}(\boldsymbol{\sigma})\|\chi_{n_s}(L_s;\boldsymbol{\sigma})\rangle|^2|\langle\varphi_{n_0}(0;\boldsymbol{\varsigma})\|T_{L_u}(\boldsymbol{\varsigma})\|\chi_{n_u}(L_u;\boldsymbol{\varsigma})\rangle|^2}{E_{n_sL_s}+E_{n_uL_u}-E_{n_0S}-E_{n_0'S}}\,,
\end{aligned} \tag{B.5}
$$

$$
\begin{aligned}
\Delta_{12} &= -\sum_{n_sn_tn_u}\sum_{L_sL_tL_u}\sum_{M_sM_tM_u}\langle\phi_1|V_{123}|\chi_{n_s}(L_sM_s;\boldsymbol{\sigma})\chi_{n_t}(L_tM_t;\boldsymbol{\rho})\chi_{n_u}(L_uM_u;\boldsymbol{\varsigma})\rangle^* \\
&\quad \frac{\langle\phi_2|V_{123}|\chi_{n_s}(L_sM_s;\boldsymbol{\sigma})\chi_{n_t}(L_tM_t;\boldsymbol{\rho})\chi_{n_u}(L_uM_u;\boldsymbol{\varsigma})\rangle}{E_{n_sL_s;n_tL_t;n_uL_u}-E^{(0)}_{n_0S;n_0S;n_0'S}}
\end{aligned}
$$

$$
\begin{aligned}
&= -\sum_{n_s n_t}\sum_{L_s L_t}\sum_{M_s M_t}\frac{16\pi^2}{R_{12}^{2L_s+2L_t+2}}\frac{[P_{L_s+L_t}^{M_s+M_t}(0)(L_s+L_t-M_s-M_t)!]^2(L_s,L_t)^{-2}}{(L_s+M_s)!(L_s-M_s)!(L_t+M_t)!(L_t-M_t)!}\\
&\langle\varphi_{n_0'}(0;\boldsymbol{\sigma})\|T_{L_s}(\boldsymbol{\sigma})\|\chi_{n_s}(L_s;\boldsymbol{\sigma})\rangle^*\langle\varphi_{n_0}(0;\boldsymbol{\rho})\|T_{L_t}(\boldsymbol{\rho})\|\chi_{n_t}(L_t;\boldsymbol{\rho})\rangle^*\\
&\frac{\langle\varphi_{n_0}(0;\boldsymbol{\sigma})\|T_{L_s}(\boldsymbol{\sigma})\|\chi_{n_s}(L_s;\boldsymbol{\sigma})\rangle\langle\varphi_{n_0'}(0;\boldsymbol{\rho})\|T_{L_t}(\boldsymbol{\rho})\|\chi_{n_t}(L_t;\boldsymbol{\rho})\rangle}{E_{n_sL_s}+E_{n_tL_t}-E_{n_0S}^{(0)}-E_{n_0'S}^{(0)}},
\end{aligned}
\tag{B.6}
$$

$$
\begin{aligned}
\Delta_{13} &= -\sum_{n_s n_t n_u}\sum_{L_s L_t L_u}\sum_{M_s M_t M_u}\langle\phi_1|V_{123}|\chi_{n_s}(L_sM_s;\boldsymbol{\sigma})\chi_{n_t}(L_tM_t;\boldsymbol{\rho})\chi_{n_u}(L_uM_u;\boldsymbol{\varsigma})\rangle^*\\
&\frac{\langle\phi_3|V_{123}|\chi_{n_s}(L_sM_s;\boldsymbol{\sigma})\chi_{n_t}(L_tM_t;\boldsymbol{\rho})\chi_{n_u}(L_uM_u;\boldsymbol{\varsigma})\rangle}{E_{n_sL_s;n_tL_t;n_uL_u}-E_{n_0S;n_0S;n_0'S}^{(0)}}\\
&= -\sum_{n_s n_u}\sum_{L_s L_u}\sum_{M_s M_u}\frac{16\pi^2}{R_{31}^{2L_s+2L_u+2}}\frac{[P_{L_u+L_s}^{M_u+M_s}(0)(L_u+L_s-M_u-M_s)!]^2(L_u,L_s)^{-2}}{(L_u+M_u)!(L_u-M_u)!(L_s+M_s)!(L_s-M_s)!}\\
&\langle\varphi_{n_0'}(0;\boldsymbol{\sigma})\|T_{L_s}(\boldsymbol{\sigma})\|\chi_{n_s}(L_s;\boldsymbol{\sigma})\rangle^*\langle\varphi_{n_0}(0;\boldsymbol{\varsigma})\|T_{L_u}(\boldsymbol{\varsigma})\|\chi_{n_u}(L_u;\boldsymbol{\varsigma})\rangle^*\\
&\frac{\langle\varphi_{n_0}(0;\boldsymbol{\sigma})\|T_{L_s}(\boldsymbol{\sigma})\|\chi_{n_s}(L_s;\boldsymbol{\sigma})\rangle\langle\varphi_{n_0'}(0;\boldsymbol{\varsigma})\|T_{L_u}(\boldsymbol{\varsigma})\|\chi_{n_u}(L_u;\boldsymbol{\varsigma})\rangle}{E_{n_sL_s}+E_{n_uL_u}-E_{n_0S}-E_{n_0'S}},
\end{aligned}
\tag{B.7}
$$

$$
\begin{aligned}
\Delta_{21} &= -\sum_{n_s n_t n_u}\sum_{L_s L_t L_u}\sum_{M_s M_t M_u}\langle\phi_2|V_{123}|\chi_{n_s}(L_sM_s;\boldsymbol{\sigma})\chi_{n_t}(L_tM_t;\boldsymbol{\rho})\chi_{n_u}(L_uM_u;\boldsymbol{\varsigma})\rangle^*\\
&\frac{\langle\phi_1|V_{123}|\chi_{n_s}(L_sM_s;\boldsymbol{\sigma})\chi_{n_t}(L_tM_t;\boldsymbol{\rho})\chi_{n_u}(L_uM_u;\boldsymbol{\varsigma})\rangle}{E_{n_sL_s;n_tL_t;n_uL_u}-E_{n_0S;n_0S;n_0'S}^{(0)}}\\
&= -\sum_{n_s n_t}\sum_{L_s L_t}\sum_{M_s M_t}\frac{16\pi^2}{R_{12}^{2L_s+2L_t+2}}\frac{[P_{L_s+L_t}^{M_s+M_t}(0)(L_s+L_t-M_s-M_t)!]^2(L_s,L_t)^{-2}}{(L_s+M_s)!(L_s-M_s)!(L_t+M_t)!(L_t-M_t)!}\\
&\langle\varphi_{n_0}(0;\boldsymbol{\sigma})\|T_{L_s}(\boldsymbol{\sigma})\|\chi_{n_s}(L_s;\boldsymbol{\sigma})\rangle^*\langle\varphi_{n_0'}(0;\boldsymbol{\rho})\|T_{L_t}(\boldsymbol{\rho})\|\chi_{n_t}(L_t;\boldsymbol{\rho})\rangle^*\\
&\frac{\langle\varphi_{n_0'}(0;\boldsymbol{\sigma})\|T_{L_s}(\boldsymbol{\sigma})\|\chi_{n_s}(L_s;\boldsymbol{\sigma})\rangle\langle\varphi_{n_0}(0;\boldsymbol{\rho})\|T_{L_t}(\boldsymbol{\rho})\|\chi_{n_t}(L_t;\boldsymbol{\rho})\rangle}{E_{n_sL_s}+E_{n_tL_t}-E_{n_0S}^{(0)}-E_{n_0'S}^{(0)}},
\end{aligned}
\tag{B.8}
$$

$$
\Delta_{23} = -\sum_{n_s n_t n_u}\sum_{L_s L_t L_u}\sum_{M_s M_t M_u}\langle\phi_2|V_{123}|\chi_{n_s}(L_sM_s;\boldsymbol{\sigma})\chi_{n_t}(L_tM_t;\boldsymbol{\rho})\chi_{n_u}(L_uM_u;\boldsymbol{\varsigma})\rangle^*
$$

$$
\begin{aligned}
&\frac{\langle\phi_3|V_{123}|\chi_{n_s}(L_sM_s;\boldsymbol{\sigma})\chi_{n_t}(L_tM_t;\boldsymbol{\rho})\chi_{n_u}(L_uM_u;\boldsymbol{\varsigma})\rangle}{E_{n_sL_s;n_tL_t;n_uL_u}-E^{(0)}_{n_0S;n_0S;n_0'S}}\\
=\;&-\sum_{n_tn_u}\sum_{L_tL_u}\sum_{M_tM_u}\frac{16\pi^2}{R_{23}^{2L_t+2L_u+2}}\frac{[P^{M_t+M_u}_{L_t+L_u}(0)(L_t+L_u-M_t-M_u)!]^2(L_t,L_u)^{-2}}{(L_t+M_t)!(L_t-M_t)!(L_u+M_u)!(L_u-M_u)!}\\
&\langle\varphi_{n_0'}(0;\boldsymbol{\rho})\|T_{L_t}(\boldsymbol{\rho})\|\chi_{n_t}(L_t;\boldsymbol{\rho})\rangle^*\langle\varphi_{n_0}(0;\boldsymbol{\varsigma})\|T_{L_u}(\boldsymbol{\varsigma})\|\chi_{n_u}(L_u;\boldsymbol{\varsigma})\rangle^*\\
&\frac{\langle\varphi_{n_0}(0;\boldsymbol{\rho})\|T_{L_t}(\boldsymbol{\rho})\|\chi_{n_t}(L_t;\boldsymbol{\rho})\rangle\langle\varphi_{n_0'}(0;\boldsymbol{\varsigma})\|T_{L_u}(\boldsymbol{\varsigma})\|\chi_{n_u}(L_u;\boldsymbol{\varsigma})\rangle}{E_{n_tL_t}+E_{n_uL_u}-E^{(0)}_{n_0S}-E^{(0)}_{n_0'S}},
\end{aligned}
\tag{B.9}
$$

$$
\begin{aligned}
\Delta_{31}\;=\;&-\sum_{n_sn_tn_u}\sum_{L_sL_tL_u}\sum_{M_sM_tM_u}\langle\phi_3|V_{123}|\chi_{n_s}(L_sM_s;\boldsymbol{\sigma})\chi_{n_t}(L_tM_t;\boldsymbol{\rho})\chi_{n_u}(L_uM_u;\boldsymbol{\varsigma})\rangle^*\\
&\frac{\langle\phi_1|V_{123}|\chi_{n_s}(L_sM_s;\boldsymbol{\sigma})\chi_{n_t}(L_tM_t;\boldsymbol{\rho})\chi_{n_u}(L_uM_u;\boldsymbol{\varsigma})\rangle}{E_{n_sL_s;n_tL_t;n_uL_u}-E^{(0)}_{n_0S;n_0S;n_0'S}}\\
=\;&-\sum_{n_sn_u}\sum_{L_sL_u}\sum_{M_sM_u}\frac{16\pi^2}{R_{31}^{2L_s+2L_u+2}}\frac{[P^{M_u+M_s}_{L_u+L_s}(0)(L_u+L_s-M_u-M_s)!]^2(L_u,L_s)^{-2}}{(L_u+M_u)!(L_u-M_u)!(L_s+M_s)!(L_s-M_s)!}\\
&\langle\varphi_{n_0'}(0;\boldsymbol{\varsigma})\|T_{L_u}(\boldsymbol{\varsigma})\|\chi_{n_u}(L_u;\boldsymbol{\varsigma})\rangle^*\langle\varphi_{n_0}(0;\boldsymbol{\sigma})\|T_{L_s}(\boldsymbol{\sigma})\|\chi_{n_s}(L_s;\boldsymbol{\sigma})\rangle^*\\
&\frac{\langle\varphi_{n_0}(0;\boldsymbol{\varsigma})\|T_{L_u}(\boldsymbol{\varsigma})\|\chi_{n_u}(L_u;\boldsymbol{\varsigma})\rangle\langle\varphi_{n_0'}(0;\boldsymbol{\sigma})\|T_{L_s}(\boldsymbol{\sigma})\|\chi_{n_s}(L_s;\boldsymbol{\sigma})\rangle}{E_{n_sL_s}+E_{n_uL_u}-E_{n_0S}-E_{n_0'S}},
\end{aligned}
\tag{B.10}
$$

$$
\begin{aligned}
\Delta_{32}\;=\;&-\sum_{n_sn_tn_u}\sum_{L_sL_tL_u}\sum_{M_sM_tM_u}\langle\phi_3|V_{123}|\chi_{n_s}(L_sM_s;\boldsymbol{\sigma})\chi_{n_t}(L_tM_t;\boldsymbol{\rho})\chi_{n_u}(L_uM_u;\boldsymbol{\varsigma})\rangle^*\\
&\frac{\langle\phi_2|V_{123}|\chi_{n_s}(L_sM_s;\boldsymbol{\sigma})\chi_{n_t}(L_tM_t;\boldsymbol{\rho})\chi_{n_u}(L_uM_u;\boldsymbol{\varsigma})\rangle}{E_{n_sL_s;n_tL_t;n_uL_u}-E^{(0)}_{n_0S;n_0S;n_0'S}}\\
=\;&-\sum_{n_tn_u}\sum_{L_tL_u}\sum_{M_tM_u}\frac{16\pi^2}{R_{23}^{2L_t+2L_u+2}}\frac{[P^{M_t+M_u}_{L_t+L_u}(0)(L_t+L_u-M_t-M_u)!]^2(L_t,L_u)^{-2}}{(L_t+M_t)!(L_t-M_t)!(L_u+M_u)!(L_u-M_u)!}\\
&\langle\varphi_{n_0}(0;\boldsymbol{\rho})\|T_{L_t}(\boldsymbol{\rho})\|\chi_{n_t}(L_t;\boldsymbol{\rho})\rangle^*\langle\varphi_{n_0'}(0;\boldsymbol{\varsigma})\|T_{L_u}(\boldsymbol{\varsigma})\|\chi_{n_u}(L_u;\boldsymbol{\varsigma})\rangle^*\\
&\frac{\langle\varphi_{n_0'}(0;\boldsymbol{\rho})\|T_{L_t}(\boldsymbol{\rho})\|\chi_{n_t}(L_t;\boldsymbol{\rho})\rangle\langle\varphi_{n_0}(0;\boldsymbol{\varsigma})\|T_{L_u}(\boldsymbol{\varsigma})\|\chi_{n_u}(L_u;\boldsymbol{\varsigma})\rangle}{E_{n_tL_t}+E_{n_uL_u}-E^{(0)}_{n_0S}-E^{(0)}_{n_0'S}},
\end{aligned}
\tag{B.11}
$$

Then solve this eigenvalue problem to get the eigenvalues and corresponding zero-

order wave functions.

B.2 The Second-Order Energy Correction

The second-order energy correction is given by

$$\begin{aligned}\Delta E^{(2)} &= -\sum_{n_s n_t n_u}\sum_{L_s L_t L_u}\sum_{M_s M_t M_u}\frac{|\langle\Psi^{(0)}|V_{123}|\chi_{n_s}(L_s M_s;\boldsymbol{\sigma})\chi_{n_t}(L_t M_t;\boldsymbol{\rho})\chi_{n_u}(L_u M_u;\boldsymbol{\varsigma})\rangle|^2}{E_{n_s L_s;n_t L_t;n_u L_u}-E^{(0)}_{n_0 S;n_0 S;n_0' S}}\\ &= V_{12}^{(2)}+V_{23}^{(2)}+V_{31}^{(2)}, \end{aligned}\tag{B.12}$$

where $\chi_{n_s}(L_s M_s;\boldsymbol{\sigma})\chi_{n_t}(L_t M_t;\boldsymbol{\rho})\chi_{n_u}(L_u M_u;\boldsymbol{\varsigma})$ is an intermediate state of the system with the energy eigenvalue $E_{n_s L_s;n_t L_t;n_u L_u} = E_{n_s L_s}+E_{n_t L_t}+E_{n_u L_u}$. It is noted that the above summations should exclude terms with $E_{n_s L_s;n_t L_t;n_u L_u} = E^{(0)}_{n_0 S;n_0 S;n_0' S}$. Then the three additive terms in the second-order energy correction, denoted by $V_{12}^{(2)}$, $V_{23}^{(2)}$, and $V_{31}^{(2)}$, become respectively

$$\begin{aligned}V_{12}^{(2)} &= -|a|^2\sum_{n_s n_t}\sum_{L_s L_t}\sum_{M_s M_t}\frac{16\pi^2}{R_{12}^{2L_s+2L_t+2}}\frac{[P^{M_s+M_t}_{L_s+L_t}(0)(L_s+L_t-M_s-M_t)!]^2(L_s,L_t)^{-2}}{(L_s+M_s)!(L_s-M_s)!(L_t+M_t)!(L_t-M_t)!}\\ &\quad\frac{|\langle\varphi_{n_0'}(0;\boldsymbol{\sigma})\|T_{L_s}(\boldsymbol{\sigma})\|\chi_{n_s}(L_s;\boldsymbol{\sigma})\rangle|^2|\langle\varphi_{n_0}(0;\boldsymbol{\rho})\|T_{L_t}(\boldsymbol{\rho})\|\chi_{n_t}(L_t;\boldsymbol{\rho})\rangle|^2}{E_{n_s L_s}+E_{n_t L_t}-E^{(0)}_{n_0 S}-E^{(0)}_{n_0' S}}\\ &\quad -|b|^2\sum_{n_s n_t}\sum_{L_s L_t}\sum_{M_s M_t}\frac{16\pi^2}{R_{12}^{2L_s+2L_t+2}}\frac{[P^{M_s+M_t}_{L_s+L_t}(0)(L_s+L_t-M_s-M_t)!]^2(L_s,L_t)^{-2}}{(L_s+M_s)!(L_s-M_s)!(L_t+M_t)!(L_t-M_t)!}\\ &\quad\frac{|\langle\varphi_{n_0}(0;\boldsymbol{\sigma})\|T_{L_s}(\boldsymbol{\sigma})\|\chi_{n_s}(L_s;\boldsymbol{\sigma})\rangle|^2|\langle\varphi_{n_0'}(0;\boldsymbol{\rho})\|T_{L_t}(\boldsymbol{\rho})\|\chi_{n_t}(L_t;\boldsymbol{\rho})\rangle|^2}{E_{n_s L_s}+E_{n_t L_t}-E^{(0)}_{n_0 S}-E^{(0)}_{n_0' S}}\\ &\quad -|c|^2\sum_{n_s n_t}\sum_{L_s L_t}\sum_{M_s M_t}\frac{16\pi^2}{R_{12}^{2L_s+2L_t+2}}\frac{[P^{M_s+M_t}_{L_s+L_t}(0)(L_s+L_t-M_s-M_t)!]^2(L_s,L_t)^{-2}}{(L_s+M_s)!(L_s-M_s)!(L_t+M_t)!(L_t-M_t)!}\\ &\quad\frac{|\langle\varphi_{n_0}(0;\boldsymbol{\sigma})\|T_{L_s}(\boldsymbol{\sigma})\|\chi_{n_s}(L_s;\boldsymbol{\sigma})\rangle|^2|\langle\varphi_{n_0}(0;\boldsymbol{\rho})\|T_{L_t}(\boldsymbol{\rho})\|\chi_{n_t}(L_t;\boldsymbol{\rho})\rangle|^2}{E_{n_s L_s}+E_{n_t L_t}-2E^{(0)}_{n_0 S}}\\ &\quad -a^* b\sum_{n_s n_t}\sum_{L_s L_t}\sum_{M_s M_t}\frac{16\pi^2}{R_{12}^{2L_s+2L_t+2}}\frac{[P^{M_s+M_t}_{L_s+L_t}(0)(L_s+L_t-M_s-M_t)!]^2(L_s,L_t)^{-2}}{(L_s+M_s)!(L_s-M_s)!(L_t+M_t)!(L_t-M_t)!}\\ &\quad\langle\varphi_{n_0'}(0;\boldsymbol{\sigma})\|T_{L_s}(\boldsymbol{\sigma})\|\chi_{n_s}(L_s;\boldsymbol{\sigma})\rangle^*\langle\varphi_{n_0}(0;\boldsymbol{\rho})\|T_{L_t}(\boldsymbol{\rho})\|\chi_{n_t}(L_t;\boldsymbol{\rho})\rangle^*\end{aligned}$$

$$
\begin{aligned}
& \frac{\langle\varphi_{n_0}(0;\boldsymbol{\sigma})\|T_{L_s}(\boldsymbol{\sigma})\|\chi_{n_s}(L_s;\boldsymbol{\sigma})\rangle\langle\varphi_{n_0'}(0;\boldsymbol{\rho})\|T_{L_t}(\boldsymbol{\rho})\|\chi_{n_t}(L_t;\boldsymbol{\rho})\rangle}{E_{n_sL_s}+E_{n_tL_t}-E^{(0)}_{n_0S}-E^{(0)}_{n_0'S}} \\
- \quad & b^*a\sum_{n_sn_t}\sum_{L_sL_t}\sum_{M_sM_t}\frac{16\pi^2}{R_{12}^{2L_s+2L_t+2}}\frac{[P^{M_s+M_t}_{L_s+L_t}(0)(L_s+L_t-M_s-M_t)!]^2(L_s,L_t)^{-2}}{(L_s+M_s)!(L_s-M_s)!(L_t+M_t)!(L_t-M_t)!} \\
& \langle\varphi_{n_0}(0;\boldsymbol{\sigma})\|T_{L_s}(\boldsymbol{\sigma})\|\chi_{n_s}(L_s;\boldsymbol{\sigma})\rangle^*\langle\varphi_{n_0'}(0;\boldsymbol{\rho})\|T_{L_t}(\boldsymbol{\rho})\|\chi_{n_t}(L_t;\boldsymbol{\rho})\rangle^* \\
& \frac{\langle\varphi_{n_0'}(0;\boldsymbol{\sigma})\|T_{L_s}(\boldsymbol{\sigma})\|\chi_{n_s}(L_s;\boldsymbol{\sigma})\rangle\langle\varphi_{n_0}(0;\boldsymbol{\rho})\|T_{L_t}(\boldsymbol{\rho})\|\chi_{n_t}(L_t;\boldsymbol{\rho})\rangle}{E_{n_sL_s}+E_{n_tL_t}-E^{(0)}_{n_0S}-E^{(0)}_{n_0'S}} \\
= \quad & -\Bigg\{|a|^2\sum_{n_sn_t}\sum_{L_sL_t}\frac{K_1(n_s,n_t,L_s,L_t)}{R_{12}^{2L_s+2L_t+2}}+|b|^2\sum_{n_sn_t}\sum_{L_sL_t}\frac{K_1(n_t,n_s,L_t,L_s)}{R_{12}^{2L_s+2L_t+2}} \\
+ \quad & |c|^2\sum_{n_sn_t}\sum_{L_sL_t}\frac{K_2(n_s,n_t,L_s,L_t)}{R_{12}^{2L_s+2L_t+2}}+a^*b\sum_{n_sn_t}\sum_{L_sL_t}\frac{K_3(n_s,n_t,L_s,L_t)}{R_{12}^{2L_s+2L_t+2}} \\
+ \quad & b^*a\sum_{n_sn_t}\sum_{L_sL_t}\frac{K_3^*(n_s,n_t,L_s,L_t)}{R_{12}^{2L_s+2L_t+2}}\Bigg\}, \qquad \text{(B.13)}
\end{aligned}
$$

$$
\begin{aligned}
V_{23}^{(2)} \quad = \quad & -|a|^2\sum_{n_tn_u}\sum_{L_tL_u}\sum_{M_tM_u}\frac{16\pi^2}{R_{23}^{2L_t+2L_u+2}}\frac{[P^{M_t+M_u}_{L_t+L_u}(0)(L_t+L_u-M_t-M_u)!]^2(L_t,L_u)^{-2}}{(L_t+M_t)!(L_t-M_t)!(L_u+M_u)!(L_u-M_u)!} \\
& \frac{|\langle\varphi_{n_0}(0;\boldsymbol{\rho})\|T_{L_t}(\boldsymbol{\rho})\|\chi_{n_t}(L_t;\boldsymbol{\rho})\rangle|^2|\langle\varphi_{n_0}(0;\boldsymbol{\varsigma})\|T_{L_u}(\boldsymbol{\varsigma})\|\chi_{n_u}(L_u;\boldsymbol{\varsigma})\rangle|^2}{E_{n_tL_t}+E_{n_uL_u}-2E^{(0)}_{n_0S}} \\
- \quad & |b|^2\sum_{n_tn_u}\sum_{L_tL_u}\sum_{M_tM_u}\frac{16\pi^2}{R_{23}^{2L_t+2L_u+2}}\frac{[P^{M_t+M_u}_{L_t+L_u}(0)(L_t+L_u-M_t-M_u)!]^2(L_t,L_u)^{-2}}{(L_t+M_t)!(L_t-M_t)!(L_u+M_u)!(L_u-M_u)!} \\
& \frac{|\langle\varphi_{n_0'}(0;\boldsymbol{\rho})\|T_{L_t}(\boldsymbol{\rho})\|\chi_{n_t}(L_t;\boldsymbol{\rho})\rangle|^2|\langle\varphi_{n_0}(0;\boldsymbol{\varsigma})\|T_{L_u}(\boldsymbol{\varsigma})\|\chi_{n_u}(L_u;\boldsymbol{\varsigma})\rangle|^2}{E_{n_tL_t}+E_{n_uL_u}-E^{(0)}_{n_0S}-E^{(0)}_{n_0'S}} \\
- \quad & |c|^2\sum_{n_tn_u}\sum_{L_tL_u}\sum_{M_tM_u}\frac{16\pi^2}{R_{23}^{2L_t+2L_u+2}}\frac{[P^{M_t+M_u}_{L_t+L_u}(0)(L_t+L_u-M_t-M_u)!]^2(L_t,L_u)^{-2}}{(L_t+M_t)!(L_t-M_t)!(L_u+M_u)!(L_u-M_u)!} \\
& \frac{|\langle\varphi_{n_0}(0;\boldsymbol{\rho})\|T_{L_t}(\boldsymbol{\rho})\|\chi_{n_t}(L_t;\boldsymbol{\rho})\rangle|^2|\langle\varphi_{n_0'}(0;\boldsymbol{\varsigma})\|T_{L_u}(\boldsymbol{\varsigma})\|\chi_{n_u}(L_u;\boldsymbol{\varsigma})\rangle|^2}{E_{n_tL_t}+E_{n_uL_u}-E^{(0)}_{n_0S}-E^{(0)}_{n_0'S}} \\
- \quad & b^*c\sum_{n_tn_u}\sum_{L_tL_u}\sum_{M_tM_u}\frac{16\pi^2}{R_{23}^{2L_t+2L_u+2}}\frac{[P^{M_t+M_u}_{L_t+L_u}(0)(L_t+L_u-M_t-M_u)!]^2(L_t,L_u)^{-2}}{(L_t+M_t)!(L_t-M_t)!(L_u+M_u)!(L_u-M_u)!} \\
& \langle\varphi_{n_0'}(0;\boldsymbol{\rho})\|T_{L_t}(\boldsymbol{\rho})\|\chi_{n_t}(L_t;\boldsymbol{\rho})\rangle^*\langle\varphi_{n_0}(0;\boldsymbol{\varsigma})\|T_{L_u}(\boldsymbol{\varsigma})\|\chi_{n_u}(L_u;\boldsymbol{\varsigma})\rangle^* \\
& \frac{\langle\varphi_{n_0}(0;\boldsymbol{\rho})\|T_{L_t}(\boldsymbol{\rho})\|\chi_{n_t}(L_t;\boldsymbol{\rho})\rangle\langle\varphi_{n_0'}(0;\boldsymbol{\varsigma})\|T_{L_u}(\boldsymbol{\varsigma})\|\chi_{n_u}(L_u;\boldsymbol{\varsigma})\rangle}{E_{n_tL_t}+E_{n_uL_u}-E^{(0)}_{n_0S}-E^{(0)}_{n_0'S}} \\
- \quad & c^*b\sum_{n_tn_u}\sum_{L_tL_u}\sum_{M_tM_u}\frac{16\pi^2}{R_{23}^{2L_t+2L_u+2}}\frac{[P^{M_t+M_u}_{L_t+L_u}(0)(L_t+L_u-M_t-M_u)!]^2(L_t,L_u)^{-2}}{(L_t+M_t)!(L_t-M_t)!(L_u+M_u)!(L_u-M_u)!}
\end{aligned}
$$

$$
\begin{aligned}
&\langle\varphi_{n_0}(0;\boldsymbol{\rho})\|T_{L_t}(\boldsymbol{\rho})\|\chi_{n_t}(L_t;\boldsymbol{\rho})\rangle^*\langle\varphi_{n_0'}(0;\boldsymbol{\varsigma})\|T_{L_u}(\boldsymbol{\varsigma})\|\chi_{n_u}(L_u;\boldsymbol{\varsigma})\rangle^*\\
&\frac{\langle\varphi_{n_0'}(0;\boldsymbol{\rho})\|T_{L_t}(\boldsymbol{\rho})\|\chi_{n_t}(L_t;\boldsymbol{\rho})\rangle\langle\varphi_{n_0}(0;\boldsymbol{\varsigma})\|T_{L_u}(\boldsymbol{\varsigma})\|\chi_{n_u}(L_u;\boldsymbol{\varsigma})\rangle}{E_{n_tL_t}+E_{n_uL_u}-E^{(0)}_{n_0S}-E^{(0)}_{n_0'S}}\\
=\;&-\Bigg\{|a|^2\sum_{n_tn_u}\sum_{L_tL_u}\frac{K_2(n_t,n_u,L_t,L_u)}{R_{23}^{2L_t+2L_u+2}}+|b|^2\sum_{n_tn_u}\sum_{L_tL_u}\frac{K_1(n_t,n_u,L_t,L_u)}{R_{23}^{2L_t+2L_u+2}}\\
+\;&|c|^2\sum_{n_tn_u}\sum_{L_tL_u}\frac{K_1(n_u,n_t,L_u,L_t)}{R_{23}^{2L_t+2L_u+2}}+b^*c\sum_{n_tn_u}\sum_{L_tL_u}\frac{K_3(n_t,n_u,L_t,L_u)}{R_{23}^{2L_u+2L_t+2}}\\
+\;&c^*b\sum_{n_tn_u}\sum_{L_tL_u}\frac{K_3^*(n_t,n_u,L_t,L_u)}{R_{23}^{2L_t+2L_u+2}}\Bigg\},
\end{aligned}
\tag{B.14}
$$

$$
\begin{aligned}
V_{31}^{(2)}\;=\;&-|a|^2\sum_{n_sn_u}\sum_{L_sL_u}\sum_{M_sM_u}\frac{16\pi^2}{R_{31}^{2L_s+2L_u+2}}\frac{[P_{L_u+L_s}^{M_u+M_s}(0)(L_u+L_s-M_u-M_s)!]^2(L_u,L_s)^{-2}}{(L_u+M_u)!(L_u-M_u)!(L_s+M_s)!(L_s-M_s)!}\\
&\frac{|\langle\varphi_{n_0'}(0;\boldsymbol{\sigma})\|T_{L_s}(\boldsymbol{\sigma})\|\chi_{n_s}(L_s;\boldsymbol{\sigma})\rangle|^2|\langle\varphi_{n_0}(0;\boldsymbol{\varsigma})\|T_{L_u}(\boldsymbol{\varsigma})\|\chi_{n_u}(L_u;\boldsymbol{\varsigma})\rangle|^2}{E_{n_sL_s}+E_{n_uL_u}-E_{n_0S}-E_{n_0'S}}\\
-\;&|b|^2\sum_{n_sn_u}\sum_{L_sL_u}\sum_{M_sM_u}\frac{16\pi^2}{R_{31}^{2L_s+2L_u+2}}\frac{[P_{L_u+L_s}^{M_u+M_s}(0)(L_u+L_s-M_u-M_s)!]^2(L_u,L_s)^{-2}}{(L_u+M_u)!(L_u-M_u)!(L_s+M_s)!(L_s-M_s)!}\\
&\frac{|\langle\varphi_{n_0}(0;\boldsymbol{\sigma})\|T_{L_s}(\boldsymbol{\sigma})\|\chi_{n_s}(L_s;\boldsymbol{\sigma})\rangle|^2|\langle\varphi_{n_0}(0;\boldsymbol{\varsigma})\|T_{L_u}(\boldsymbol{\varsigma})\|\chi_{n_u}(L_u;\boldsymbol{\varsigma})\rangle|^2}{E_{n_sL_s}+E_{n_uL_u}-2E_{n_0S}}\\
-\;&|c|^2\sum_{n_sn_u}\sum_{L_sL_u}\sum_{M_sM_u}\frac{16\pi^2}{R_{31}^{2L_s+2L_u+2}}\frac{[P_{L_u+L_s}^{M_u+M_s}(0)(L_u+L_s-M_u-M_s)!]^2(L_u,L_s)^{-2}}{(L_u+M_u)!(L_u-M_u)!(L_s+M_s)!(L_s-M_s)!}\\
&\frac{|\langle\varphi_{n_0}(0;\boldsymbol{\sigma})\|T_{L_s}(\boldsymbol{\sigma})\|\chi_{n_s}(L_s;\boldsymbol{\sigma})\rangle|^2|\langle\varphi_{n_0}(0;\boldsymbol{\varsigma})\|T_{L_u}(\boldsymbol{\varsigma})\|\chi_{n_u}(L_u;\boldsymbol{\varsigma})\rangle|^2}{E_{n_sL_s}+E_{n_uL_u}-E_{n_0S}-E_{n_0'S}}\\
-\;&c^*a\sum_{n_sn_u}\sum_{L_sL_u}\sum_{M_sM_u}\frac{16\pi^2}{R_{31}^{2L_s+2L_u+2}}\frac{[P_{L_u+L_s}^{M_u+M_s}(0)(L_u+L_s-M_u-M_s)!]^2(L_u,L_s)^{-2}}{(L_u+M_u)!(L_u-M_u)!(L_s+M_s)!(L_s-M_s)!}\\
&\langle\varphi_{n_0'}(0;\boldsymbol{\varsigma})\|T_{L_u}(\boldsymbol{\varsigma})\|\chi_{n_u}(L_u;\boldsymbol{\varsigma})\rangle^*\langle\varphi_{n_0}(0;\boldsymbol{\sigma})\|T_{L_s}(\boldsymbol{\sigma})\|\chi_{n_s}(L_s;\boldsymbol{\sigma})\rangle^*\\
&\frac{\langle\varphi_{n_0}(0;\boldsymbol{\varsigma})\|T_{L_u}(\boldsymbol{\varsigma})\|\chi_{n_u}(L_u;\boldsymbol{\varsigma})\rangle\langle\varphi_{n_0'}(0;\boldsymbol{\sigma})\|T_{L_s}(\boldsymbol{\sigma})\|\chi_{n_s}(L_s;\boldsymbol{\sigma})\rangle}{E_{n_sL_s}+E_{n_uL_u}-E_{n_0S}-E_{n_0'S}}\\
-\;&a^*c\sum_{n_sn_u}\sum_{L_sL_u}\sum_{M_sM_u}\frac{16\pi^2}{R_{31}^{2L_s+2L_u+2}}\frac{[P_{L_u+L_s}^{M_u+M_s}(0)(L_u+L_s-M_u-M_s)!]^2(L_u,L_s)^{-2}}{(L_u+M_u)!(L_u-M_u)!(L_s+M_s)!(L_s-M_s)!}\\
&\langle\varphi_{n_0'}(0;\boldsymbol{\sigma})\|T_{L_s}(\boldsymbol{\sigma})\|\chi_{n_s}(L_s;\boldsymbol{\sigma})\rangle^*\langle\varphi_{n_0}(0;\boldsymbol{\varsigma})\|T_{L_u}(\boldsymbol{\varsigma})\|\chi_{n_u}(L_u;\boldsymbol{\varsigma})\rangle^*\\
&\frac{\langle\varphi_{n_0}(0;\boldsymbol{\sigma})\|T_{L_s}(\boldsymbol{\sigma})\|\chi_{n_s}(L_s;\boldsymbol{\sigma})\rangle\langle\varphi_{n_0'}(0;\boldsymbol{\varsigma})\|T_{L_u}(\boldsymbol{\varsigma})\|\chi_{n_u}(L_u;\boldsymbol{\varsigma})\rangle}{E_{n_sL_s}+E_{n_uL_u}-E_{n_0S}-E_{n_0'S}}\\
=\;&-\Bigg\{|a|^2\sum_{n_sn_u}\sum_{L_sL_u}\frac{K_1(n_s,n_u,L_s,L_u)}{R_{31}^{2L_u+2L_s+2}}+|b|^2\sum_{n_sn_u}\sum_{L_sL_u}\frac{K_2(n_s,n_u,L_s,L_u)}{R_{31}^{2L_s+2L_u+2}}
\end{aligned}
$$

$$+ \quad |c|^2 \sum_{n_s n_u} \sum_{L_s L_u} \frac{K_1(n_u, n_s, L_u, L_s)}{R_{31}^{2L_s+2L_u+2}} + a^* c \sum_{n_s n_u} \sum_{L_s L_u} \frac{K_3(n_u, n_s, L_u, L_s)}{R_{31}^{2L_s+2L_u+2}}$$
$$+ \quad c^* a \sum_{n_s n_u} \sum_{L_s L_u} \frac{K_3^*(n_u, n_s, L_u, L_s)}{R_{31}^{2L_s+2L_u+2}} \Bigg\}, \tag{B.15}$$

In the above, the K_i functions are defined by

$$K_1(n_s, n_t, L_s, L_t) = G_1(L_s, L_t) \times \frac{|\langle \varphi_{n_0'}(0;\boldsymbol{\sigma}) \| T_{L_s}(\boldsymbol{\sigma}) \| \chi_{n_s}(L_s;\boldsymbol{\sigma}) \rangle|^2 |\langle \varphi_{n_0}(0;\boldsymbol{\rho}) \| T_{L_t}(\boldsymbol{\rho}) \| \chi_{n_t}(L_t;\boldsymbol{\rho}) \rangle|^2}{E_{n_s L_s} + E_{n_t L_t} - E_{n_0 S}^{(0)} - E_{n_0' S}^{(0)}}, \tag{B.16}$$

$$K_2(n_s, n_t, L_s, L_t) = G_1(L_s, L_t) \times \frac{|\langle \varphi_{n_0}(0;\boldsymbol{\sigma}) \| T_{L_s}(\boldsymbol{\sigma}) \| \chi_{n_s}(L_s;\boldsymbol{\sigma}) \rangle|^2 |\langle \varphi_{n_0}(0;\boldsymbol{\rho}) \| T_{L_t}(\boldsymbol{\rho}) \| \chi_{n_t}(L_t;\boldsymbol{\rho}) \rangle|^2}{E_{n_s L_s} + E_{n_t L_t} - 2E_{n_0 S}^{(0)}}, \tag{B.17}$$

$$K_3(n_s, n_t, L_s, L_t) = G_1(L_s, L_t) \langle \varphi_{n_0}(0;\boldsymbol{\sigma}) \| T_{L_s}(\boldsymbol{\sigma}) \| \chi_{n_s}(L_s;\boldsymbol{\sigma}) \rangle^* \langle \varphi_{n_0'}(0;\boldsymbol{\rho}) \| T_{l_2'}(\boldsymbol{\rho}) \| \chi_{n_t}(L_t;\boldsymbol{\rho}) \rangle^* \times \frac{\langle \varphi_{n_0'}(0;\boldsymbol{\sigma}) \| T_{l_1}(\boldsymbol{\sigma}) \| \chi_{n_s}(L_s;\boldsymbol{\sigma}) \rangle \langle \varphi_{n_0}(0;\boldsymbol{\rho}) \| T_{L_t}(\boldsymbol{\rho}) \| \chi_{n_t}(L_t;\boldsymbol{\rho}) \rangle}{E_{n_s L_s} + E_{n_t L_t} - E_{n_0 S}^{(0)} - E_{n_0' S}^{(0)}}. \tag{B.18}$$

where $G_1(L_i, L_j)$ is further defined by:

$$G_1(L_i, L_j) = 16\pi^2 (L_i, L_j)^{-2} \sum_{M_i M_j} \frac{[P_{L_i+L_j}^{M_i+M_j}(0)(L_i + L_j - M_i - M_j)!]^2}{(L_i + M_i)!(L_i - M_i)!(L_j + M_j)!(L_j - M_j)!}. \tag{B.19}$$

Then the second-order energy correction is simplified as,

$$\Delta E^{(2)} = -\sum_{n\geq 3}\left(\frac{C_{2n}^{(12)}}{R_{12}^{2n}}+\frac{C_{2n}^{(23)}}{R_{23}^{2n}}+\frac{C_{2n}^{(31)}}{R_{31}^{2n}}\right). \tag{B.20}$$

where $C_{2n}^{(IJ)}$ are the additive dispersion coefficients. These coefficients can be expressed as

$$\begin{aligned} C_{2n}^{(12)} &= |a|^2\sum_{n_sn_t}\sum_{L_sL_t}K_1(n_s,n_t,L_s,L_t)+|b|^2\sum_{n_sn_t}\sum_{L_sL_t}K_1(n_t,n_s,L_t,L_s) \\ &+ |c|^2\sum_{n_sn_t}\sum_{L_sL_t}K_2(n_s,n_t,L_s,L_t)+a^*b\sum_{n_sn_t}\sum_{L_sL_t}K_3(n_s,n_t,L_s,L_t) \\ &+ b^*a\sum_{n_sn_t}\sum_{L_sL_t}K_3^*(n_s,n_t,L_s,L_t), \end{aligned} \tag{B.21}$$

$$\begin{aligned} C_{2n}^{(23)} &= |a|^2\sum_{n_tn_u}\sum_{L_tL_u}K_2(n_t,n_u,L_t,L_u)+|b|^2\sum_{n_tn_u}\sum_{L_tL_u}K_1(n_t,n_u,L_t,L_u) \\ &+ |c|^2\sum_{n_tn_u}\sum_{L_tL_u}K_1(n_u,n_t,L_u,L_t)+b^*c\sum_{n_tn_u}\sum_{L_tL_u}K_3(n_t,n_u,L_t,L_u) \\ &+ c^*b\sum_{n_tn_u}\sum_{L_tL_u}K_3^*(n_t,n_u,L_t,L_u), \end{aligned} \tag{B.22}$$

$$\begin{aligned} C_{2n}^{(31)} &= |a|^2\sum_{n_sn_u}\sum_{L_sL_u}K_1(n_s,n_u,L_s,L_u)+|b|^2\sum_{n_sn_u}\sum_{L_sL_u}K_2(n_s,n_u,L_s,L_u) \\ &+ |c|^2\sum_{n_sn_u}\sum_{L_sL_u}K_1(n_u,n_s,L_u,L_s)+a^*c\sum_{n_sn_u}\sum_{L_sL_u}K_3^*(n_u,n_s,L_u,L_s) \\ &+ c^*a\sum_{n_sn_u}\sum_{L_sL_u}K_3(n_u,n_s,L_u,L_s), \end{aligned} \tag{B.23}$$

Appendix C

C_m Coefficients for

$A(n_0S)$-$A(n_0S)$-$A^+(n_0'S)$

The non-degenerate ground state of the unperturbed system may be written as,

$$|\Psi^{(0)}\rangle = |\varphi_{n_0}(0;\boldsymbol{\sigma})\varphi_{n_0}(0;\boldsymbol{\rho})\psi_{n_0'}(0;\boldsymbol{\varsigma})\rangle\,. \tag{C.1}$$

Where $\boldsymbol{\sigma}$, $\boldsymbol{\rho}$, and $\boldsymbol{\varsigma}$ represent collectively the coordinates of each particle.

C.1 The Second-Order Energy Correction

The second-order energy correction is given by

$$\begin{aligned}\Delta E^{(2)} &= -\sum_{\substack{n_s n_t n_u;\\ L_s L_t L_u;\\ M_s M_t M_u}} \frac{|\langle\Psi^{(0)}|V_{123}|\chi_{n_s}(L_sM_s;\boldsymbol{\sigma})\chi_{n_t}(L_tM_t;\boldsymbol{\rho})\phi_{n_u}(L_uM_u;\boldsymbol{\varsigma})\rangle|^2}{E_{n_sL_s;n_tL_t;n_uL_u} - E^{(0)}_{n_0S;n_0S;n_0'S}} \\ &= V_{12}^{(2)} + V_{23}^{(2)} + V_{31}^{(2)}\,,\end{aligned} \tag{C.2}$$

where $\chi_{n_s}(L_sM_s;\boldsymbol{\sigma})\chi_{n_t}(L_tM_t;\boldsymbol{\rho})\phi_{n_u}(L_uM_u;\boldsymbol{\varsigma})$ is an intermediate state of the system with the energy eigenvalue $E_{n_sL_s;n_tL_t;n_uL_u} = E_{n_sL_s} + E_{n_tL_t} + E_{n_uL_u}$. It is noted that

the above summations should exclude terms with $E_{n_sL_s;n_tL_t;n_uL_u} = E^{(0)}_{n_0S;n_0S;n_0'S}$. The three additive interaction terms, denoted by $V^{(2)}_{12}$, $V^{(2)}_{23}$, $V^{(2)}_{31}$, become, respectively,

$$\begin{aligned} V^{(2)}_{12} &= -\sum_{n_sn_t}\sum_{L_sL_t}\sum_{M_sM_t}\frac{16\pi^2}{R_{12}^{2L_s+2L_t+2}} \\ &\times \frac{[P^{M_s+M_t}_{L_s+L_t}(\cos\theta_{12})(L_s+L_t-M_s-M_t)!]^2(L_s,L_t)^{-2}}{(L_s+M_s)!(L_s-M_s)!(L_t+M_t)!(L_t-M_t)!} \\ &\times \frac{|\langle\varphi_{n_0}(0;\boldsymbol{\sigma})\|T_{L_s}(\boldsymbol{\sigma})\|\chi_{n_s}(L_s;\boldsymbol{\sigma})\rangle|^2|\langle\varphi_{n_0}(0;\boldsymbol{\rho})\|T_{L_t}(\boldsymbol{\rho})\|\chi_{n_t}(L_t;\boldsymbol{\rho})\rangle|^2}{E_{n_sL_s}+E_{n_tL_t}-2E^{(0)}_{n_0S}} \\ &= -\sum_{n_sn_t}\sum_{L_sL_t}\frac{F_1(n_s,n_t,L_s,L_t)}{R_{12}^{2L_s+2L_t+2}}\,, \end{aligned} \tag{C.3}$$

$$\begin{aligned} V^{(2)}_{23} &= -\sum_{n_tn_u}\sum_{L_tL_u}\sum_{M_tM_u}\frac{16\pi^2}{R_{23}^{2L_t+2L_u+2}} \\ &\times \frac{[P^{M_t+M_u}_{L_t+L_u}(\cos\theta_{23})(L_t+L_u-M_t-M_u)!]^2(L_t,L_u)^{-2}}{(L_t+M_t)!(L_t-M_t)!(L_u+M_u)!(L_u-M_u)!} \\ &\times \frac{|\langle\varphi_{n_0}(0;\boldsymbol{\rho})\|T_{L_t}(\boldsymbol{\rho})\|\chi_{n_t}(L_t;\boldsymbol{\rho})\rangle|^2|\langle\psi_{n_0'}(0;\boldsymbol{\varsigma})\|T_{L_u}(\boldsymbol{\varsigma})\|\phi_{n_u}(L_u;\boldsymbol{\varsigma})\rangle|^2}{E_{n_tL_t}+E_{n_uL_u}-E^{(0)}_{n_0S}-E^{(0)}_{n_0'S}} \\ &= -\sum_{n_tn_u}\sum_{L_tL_u}\frac{F_2(n_t,n_u,L_t,L_u)}{R_{23}^{2L_t+2L_u+2}}\,, \end{aligned} \tag{C.4}$$

$$\begin{aligned} V^{(2)}_{31} &= -\sum_{n_sn_u}\sum_{L_sL_u}\sum_{M_sM_u}\frac{16\pi^2}{R_{31}^{2L_s+2L_u+2}} \\ &\times \frac{[P^{M_u+M_s}_{L_u+L_s}(\cos\theta_{31})(L_u+L_s-M_u-M_s)!]^2(L_u,L_s)^{-2}}{(L_u+M_u)!(L_u-M_u)!(L_s+M_s)!(L_s-M_s)!} \\ &\times \frac{|\langle\varphi_{n_0}(0;\boldsymbol{\sigma})\|T_{L_s}(\boldsymbol{\sigma})\|\chi_{n_s}(L_s;\boldsymbol{\sigma})\rangle|^2|\langle\psi_{n_0'}(0;\boldsymbol{\varsigma})\|T_{L_u}(\boldsymbol{\varsigma})\|\phi_{n_u}(L_u;\boldsymbol{\varsigma})\rangle|^2}{E_{n_sL_s}+E_{n_uL_u}-E^{(0)}_{n_0S}-E^{(0)}_{n_0'S}} \\ &= -\sum_{n_sn_u}\sum_{L_sL_u}\frac{F_2(n_s,n_u,L_s,L_u)}{R_{31}^{2L_s+2L_u+2}}\,, \end{aligned}$$

. (C.5)

C.2 The Third-Order Energy Correction

The third-order energy correction is given by

$$\begin{aligned}\Delta E^{(3)} &= \sum_{n_s n_t n_u} \sum_{L_s L_t L_u} \sum_{M_s M_t M_u} \sum_{n'_s n'_t n'_u} \sum_{L'_s L'_t L'_u} \sum_{M'_s M'_t M'_u} \frac{B}{D} \\ &= V_{12}^{(3)} + V_{23}^{(3)} + V_{31}^{(3)} + V_{23,31}^{(3)} + V_{31,12}^{(3)} + V_{12,23,31}^{(3)} \,, \end{aligned} \tag{C.6}$$

where B and D are

$$\begin{aligned} B &= \langle \Psi^{(0)} | V_{123} | \chi_{n_s}(L_s M_s; \boldsymbol{\sigma}) \chi_{n_t}(L_t M_t; \boldsymbol{\rho}) \phi_{n_u}(L_u M_u; \boldsymbol{\varsigma}) \rangle \\ &\times \langle \chi_{n_s}(L_s M_s; \boldsymbol{\sigma}) \chi_{n_t}(L_t M_t; \boldsymbol{\rho}) \phi_{n_u}(L_u M_u; \boldsymbol{\varsigma}) | V_{123} | \chi_{n'_s}(L'_s M'_s; \boldsymbol{\sigma}) \chi_{n'_t}(L'_t M'_t; \boldsymbol{\rho}) \phi_{n'_u}(L'_u M'_u; \boldsymbol{\varsigma}) \rangle \\ &\times \langle \chi_{n'_s}(L'_s M'_s; \boldsymbol{\sigma}) \chi_{n'_t}(L'_t M'_t; \boldsymbol{\rho}) \phi_{n'_u}(L'_u M'_u; \boldsymbol{\varsigma}) | V_{123} | \Psi^{(0)} \rangle \,, \end{aligned} \tag{C.7}$$

$$D = (E_{n_s L_s; n_t L_t; n_u L_u} - E^{(0)}_{n_0 S; n_0 S; n'_0 S})(E_{n'_s L'_s; n'_t L'_t; n'_u L'_u} - E^{(0)}_{n_0 S; n_0 S; n'_0 S}) \,, \tag{C.8}$$

where $\chi_{n_s}(L_s M_s; \boldsymbol{\sigma}) \chi_{n_t}(L_t M_t; \boldsymbol{\rho}) \phi_{n_u}(L_u M_u; \boldsymbol{\varsigma})$ and $\chi_{n'_s}(L'_s M'_s; \boldsymbol{\sigma}) \chi_{n'_t}(L'_t M'_t; \boldsymbol{\rho}) \phi_{n'_u}(L'_u M'_u; \boldsymbol{\varsigma})$ are intermediate states of the system with the energy eigenvalues $E_{n_s L_s; n_t L_t; n_u L_u} = E_{n_s L_s} + E_{n_t L_t} + E_{n_u L_u}$ and $E_{n'_s L'_s; n'_t L'_t; n'_u L'_u} = E_{n'_s L'_s} + E_{n'_t L'_t} + E_{n'_u L'_u}$, respectively. It is noted that the above summations should exclude terms with $E_{n_s L_s; n_t L_t; n_u L_u} = E^{(0)}_{n_0 S; n_0 S; n'_0 S}$ and $E_{n'_s L'_s; n'_t L'_t; n'_u L'_u} = E^{(0)}_{n_0 S; n_0 S; n'_0 S}$. The three additive interaction terms, denoted by $V_{12}^{(3)}$, $V_{23}^{(3)}$, $V_{31}^{(3)}$, become, respectively,

$$\begin{aligned} V_{12}^{(3)} &= \sum_{n_s n_t n'_s n'_t} \sum_{L_s L_t L'_s L'_t \ell'_1 \ell'_2} \sum_{M_s M_t M'_s M'_t m'_1 m'_2} \frac{64\pi^3}{R_{12}^{L_s+L_t+L'_s+L'_t+\ell'_1+\ell'_2+3}} \\ &\times \frac{P_{L_s+L_t}^{M_s+M_t}(\cos\theta_{12})(L_s+L_t-M_s-M_t)!(L_s,L_t)^{-1}}{[(L_s+M_s)!(L_s-M_s)!(L_t+M_t)!(L_t-M_t)!]^{1/2}} \\ &\times \frac{P_{L'_s+L'_t}^{M'_s+M'_t}(\cos\theta_{12})(L'_s+L'_t-M'_s-M'_t)!(L'_s,L'_t)^{-1}}{[(L'_s+M'_s)!(L'_s-M'_s)!(L'_t+M'_t)!(L'_t-M'_t)!]^{1/2}} \end{aligned}$$

$$
\begin{aligned}
&\times \quad \frac{P^{m_1'+m_2'}_{\ell_1'+\ell_2'}(\cos\theta_{12})(\ell_1'+\ell_2'-m_1'-m_2')!(\ell_1',\ell_2')^{-1/2}}{[(\ell_1'+m_1')!(\ell_1'-m_1')!(\ell_2'+m_2')!(\ell_2'-m_2')!]^{1/2}} \\
&\times \quad \langle\chi_{n_s}(L_s;\boldsymbol{\sigma})\|T_{\ell_1'}(\boldsymbol{\sigma})\|\chi_{n_s'}(L_s';\boldsymbol{\sigma})\rangle\langle\chi_{n_t}(L_t;\boldsymbol{\rho})\|T_{\ell_2'}(\boldsymbol{\rho})\|\chi_{n_t'}(L_t';\boldsymbol{\rho})\rangle \\
&\times \quad \frac{\langle\varphi_{n_0}(0;\boldsymbol{\sigma})\|T_{L_s}(\boldsymbol{\sigma})\|\chi_{n_s}(L_s;\boldsymbol{\sigma})\rangle\langle\varphi_{n_0}(0;\boldsymbol{\rho})\|T_{L_t}(\boldsymbol{\rho})\|\chi_{n_t}(L_t;\boldsymbol{\rho})\rangle}{E_{n_sL_s}+E_{n_tL_t}-2E^{(0)}_{n_0S}} \\
&\times \quad \frac{\langle\chi_{n_s'}(L_s';\boldsymbol{\sigma})\|T_{L_s'}(\boldsymbol{\sigma})\|\varphi_{n_0}(0;\boldsymbol{\sigma})\rangle\langle\chi_{n_t'}(L_t';\boldsymbol{\rho})\|T_{L_t'}(\boldsymbol{\rho})\|\varphi_{n_0}(0;\boldsymbol{\rho})\rangle}{E_{n_s'L_s'}+E_{n_t'L_t'}-2E^{(0)}_{n_0S}} \\
&\times \quad \begin{pmatrix} L_s & \ell_1' & L_s' \\ -M_s & -m_1' & -M_s' \end{pmatrix}\begin{pmatrix} L_t & \ell_2' & L_t' \\ -M_t & -m_2' & -M_t' \end{pmatrix} \\
&= \quad \sum_{n_sn_tn_s'n_t'}\sum_{L_sL_tL_s'L_t'\ell_1'\ell_2'}\frac{F_3(n_s,n_t,n_s',n_t',L_s,L_t,L_s',L_t',\ell_1',\ell_2')}{R_{12}^{L_s+L_t+L_s'+L_t'+\ell_1'+\ell_2'+3}},
\end{aligned}
\tag{C.9}
$$

$$
\begin{aligned}
V^{(3)}_{23} \quad &= \quad \sum_{n_tn_un_t'n_u'}\sum_{L_tL_uL_t'L_u'\ell_2'\ell_3'}\sum_{M_tM_uM_t'M_u'm_2'm_3'}\frac{64\pi^3}{R_{23}^{L_t+L_u+L_t'+L_u'+\ell_2'+\ell_3'+3}} \\
&\times \quad \frac{P^{M_t+M_u}_{L_t+L_u}(\cos\theta_{23})(L_t+L_u-M_t-M_u)!(L_t,L_u)^{-1}}{[(L_t+M_t)!(L_t-M_t)!(L_u+M_u)!(L_u-M_u)!]^{1/2}} \\
&\times \quad \frac{P^{M_t'+M_u'}_{L_t'+L_u'}(\cos\theta_{23})(L_t'+L_u'-M_t'-M_u')!(L_t',L_u')^{-1}}{[(L_t'+M_t')!(L_t'-M_t')!(L_u'+M_u')!(L_u'-M_u')!]^{1/2}} \\
&\times \quad \frac{P^{m_2'+m_3'}_{\ell_2'+\ell_3'}(\cos\theta_{23})(\ell_2'+\ell_3'-m_2'-m_3')!(\ell_2',\ell_3')^{-1/2}}{[(\ell_2'+m_2')!(\ell_2'-m_2')!(\ell_3'+m_3')!(\ell_3'-m_3')!]^{1/2}} \\
&\times \quad \langle\chi_{n_t}(L_t;\boldsymbol{\rho})\|T_{\ell_2'}(\boldsymbol{\rho})\|\chi_{n_t'}(L_t';\boldsymbol{\rho})\rangle\langle\phi_{n_u}(L_u;\boldsymbol{\varsigma})\|T_{\ell_3'}(\boldsymbol{\varsigma})\|\phi_{n_u'}(L_u';\boldsymbol{\varsigma})\rangle \\
&\times \quad \frac{\langle\varphi_{n_0}(0;\boldsymbol{\rho})\|T_{L_t}(\boldsymbol{\rho})\|\chi_{n_t}(L_t;\boldsymbol{\rho})\rangle\langle\psi_{n_0'}(0;\boldsymbol{\varsigma})\|T_{L_u}(\boldsymbol{\varsigma})\|\phi_{n_u}(L_u;\boldsymbol{\varsigma})\rangle}{E_{n_tL_t}+E_{n_uL_u}-E^{(0)}_{n_0S}-E^{(0)}_{n_0'S}} \\
&\times \quad \frac{\langle\chi_{n_t'}(L_t';\boldsymbol{\rho})\|T_{L_t'}(\boldsymbol{\rho})\|\varphi_{n_0}(0;\boldsymbol{\rho})\rangle\langle\phi_{n_u'}(L_u';\boldsymbol{\varsigma})\|T_{L_u'}(\boldsymbol{\varsigma})\|\psi_{n_0'}(0;\boldsymbol{\varsigma})\rangle}{E_{n_t'L_t'}+E_{n_u'L_u'}-E^{(0)}_{n_0S}-E^{(0)}_{n_0'S}} \\
&\times \quad \begin{pmatrix} L_t & \ell_2' & L_t' \\ -M_t & -m_2' & -M_t' \end{pmatrix}\begin{pmatrix} L_u & \ell_3' & L_u' \\ -M_u & -m_3' & -M_u' \end{pmatrix} \\
&= \quad \sum_{n_tn_un_t'n_u'}\sum_{L_tL_uL_t'L_u'\ell_2'\ell_3'}\frac{F_4(n_t,n_u,n_t',n_u',L_t,L_u,L_t',L_u',\ell_2',\ell_3')}{R_{23}^{L_t+L_u+L_t'+L_u'+\ell_2'+\ell_3'+3}},
\end{aligned}
\tag{C.10}
$$

$$
\begin{aligned}
V_{31}^{(3)} &= \sum_{n_s n_u n_s' n_u'} \sum_{L_s L_u L_s' L_u' \ell_3' \ell_1'} \sum_{M_s M_u M_s' M_u' m_3' m_1'} \frac{64\pi^3}{R_{31}^{L_s+L_u+L_s'+L_u'+\ell_3'+\ell_1'+3}} \\
&\times \frac{P_{L_u+L_s}^{M_u+M_s}(\cos\theta_{31})(L_u+L_s-M_u-M_s)!(L_u,L_s)^{-1}}{[(L_u+M_u)!(L_u-M_u)!(L_s+M_s)!(L_s-M_s)!]^{1/2}} \\
&\times \frac{P_{L_u'+L_s'}^{M_u'+M_s'}(\cos\theta_{31})(L_u'+L_s'-M_u'-M_s')!(L_u',L_s')^{-1}}{[(L_u'+M_u')!(L_u'-M_u')!(L_s'+M_s')!(L_s'-M_s')!]^{1/2}} \\
&\times \frac{P_{\ell_3'+\ell_1'}^{m_3'+m_1'}(\cos\theta_{31})(\ell_3'+\ell_1'-m_3'-m_1')!(\ell_3',\ell_1')^{-1/2}}{[(\ell_3'+m_3')!(\ell_3'-m_3')!(\ell_1'+m_1')!(\ell_1'-m_1')!]^{1/2}} \\
&\times \langle\chi_{n_s}(L_s;\boldsymbol{\sigma})\|T_{\ell_1'}(\boldsymbol{\sigma})\|\chi_{n_s'}(L_s';\boldsymbol{\sigma})\rangle|\langle\phi_{n_u}(L_u;\boldsymbol{\varsigma})\|T_{\ell_3'}(\boldsymbol{\varsigma})\|\phi_{n_u'}(L_u';\boldsymbol{\varsigma})\rangle \\
&\times \frac{\langle\varphi_{n_0}(0;\boldsymbol{\sigma})\|T_{L_s}(\boldsymbol{\sigma})\|\chi_{n_s}(L_s;\boldsymbol{\sigma})\rangle\langle\psi_{n_0'}(0;\boldsymbol{\varsigma})\|T_{L_u}(\boldsymbol{\varsigma})\|\phi_{n_u}(L_u;\boldsymbol{\varsigma})\rangle}{E_{n_sL_s}+E_{n_uL_u}-E_{n_0S}^{(0)}-E_{n_0'S}^{(0)}} \\
&\times \frac{\langle\chi_{n_s'}(L_s';\boldsymbol{\sigma})\|T_{L_s'}(\boldsymbol{\sigma})\|\varphi_{n_0}(0;\boldsymbol{\sigma})\rangle\langle\phi_{n_u'}(L_u';\boldsymbol{\varsigma})\|T_{L_u'}(\boldsymbol{\varsigma})\|\psi_{n_0'}(0;\boldsymbol{\varsigma})\rangle}{E_{n_s'L_s'}+E_{n_u'L_u'}-E_{n_0S}^{(0)}-E_{n_0'S}^{(0)}} \\
&\times \begin{pmatrix} L_u & \ell_3' & L_u' \\ -M_u & -m_3' & -M_u' \end{pmatrix} \begin{pmatrix} L_s & \ell_1' & L_s' \\ -M_s & -m_1' & -M_s' \end{pmatrix} \\
&= \sum_{n_s n_u n_s' n_u'} \sum_{L_s L_u L_s' L_u' \ell_1' \ell_3'} \frac{F_4(n_s,n_u,n_s',n_u',L_s,L_u,L_s',L_u',\ell_1',\ell_3')}{R_{31}^{L_s+L_u+L_s'+L_u'+\ell_1'+\ell_3'+3}},
\end{aligned}
$$

. (C.11)

Similarly, the three nonadditive terms are

$$
\begin{aligned}
V_{12,23}^{(3)} &= \sum_{n_s n_t n_t'} \sum_{L_s L_t L_t' \ell_2'} \sum_{M_s M_t M_t' m_2'} \frac{64\pi^3}{\sqrt{\pi}} \frac{(-1)^{L_t'-M_t}}{R_{12}^{2L_s+L_t+\ell_2'+2} R_{23}^{L_t'+1}} \\
&\times \frac{P_{L_s+L_t}^{M_s+M_t}(\cos\theta_{12})(L_s+L_t-M_s-M_t)!(L_s,L_t)^{-1}}{[(L_s+M_s)!(L_s-M_s)!(L_t+M_t)!(L_t-M_t)!]^{1/2}} \\
&\times \frac{P_{L_s+\ell_2'}^{M_s+m_2'}(\cos\theta_{12})(L_s+\ell_2'-M_s-m_2')!(L_s,L_s,\ell_2')^{-1/2}}{[(L_s+M_s)!(L_s-M_s)!(\ell_2'+m_2')!(\ell_2'-m_2')!]^{1/2}} \\
&\times \frac{P_{L_t'}^{M_t'}(\cos\theta_{23})(L_t'-M_t')!(L_t')^{-1}}{[(L_t'+M_t')!(L_t'-M_t')!]^{1/2}} \begin{pmatrix} L_t & \ell_2' & L_t' \\ -M_t & m_2' & -M_t' \end{pmatrix} \cos[M_t'\beta] \\
&\times \frac{|\langle\varphi_{n_0}(0;\boldsymbol{\sigma})\|T_{L_s}(\boldsymbol{\sigma})\|\chi_{n_s}(L_s;\boldsymbol{\sigma})\rangle|^2\langle\varphi_{n_0}(0;\boldsymbol{\rho})\|T_{L_t}(\boldsymbol{\rho})\|\chi_{n_t}(L_t;\boldsymbol{\rho})\rangle}{E_{n_sL_s}+E_{n_tL_t}-2E_{n_0S}^{(0)}}
\end{aligned}
$$

$$\times \quad \frac{\langle\chi_{n_t}(L_t;\boldsymbol{\rho})\|T_{\ell_2'}(\boldsymbol{\rho})\|\chi_{n_t'}(L_t';\boldsymbol{\rho})\rangle\langle\chi_{n_t'}(L_t';\boldsymbol{\rho})\|T_{L_t'}(\boldsymbol{\rho})\|\varphi_{n_0}(0;\boldsymbol{\rho})\rangle}{E_{n_t'L_t'}-E^{(0)}_{n_0S}}$$

$$\begin{aligned}
&+ \sum_{n_sn_tn_t'}\sum_{L_sL_tL_t'\ell_2'}\sum_{M_sM_tM_t'm_2'}\frac{32\pi^3}{\sqrt{\pi}}\frac{(-1)^{\ell_2'-M_t}}{R_{12}^{2L_s+L_t+L_t'+2}R_{23}^{\ell_2'+1}}\\
&\times \frac{P_{L_s+L_t}^{M_s+M_t}(\cos\theta_{12})(L_s+L_t-M_s-M_t)!(L_s,L_t)^{-1}}{[(L_s+M_s)!(L_s-M_s)!(L_t+M_t)!(L_t-M_t)!]^{1/2}}\\
&\times \frac{P_{L_s+L_t'}^{M_s+M_t'}(\cos\theta_{12})(L_s+L_t'-M_s-M_t')!(L_s,L_t')^{-1}}{[(L_s+M_s)!(L_s-M_s)!(L_t'+M_t')!(L_t'-M_t')!]^{1/2}}\\
&\times \frac{P_{\ell_2'}^{m_2'}(\cos\theta_{23})(\ell_2'-m_2')!(\ell_2')^{-1/2}}{[(\ell_2'+m_2')!(\ell_2'-m_2')!]^{1/2}}\begin{pmatrix} L_t & \ell_2' & L_t'\\ -M_t & -m_2' & M_t'\end{pmatrix}\exp[-im_2'\beta]\\
&\times \frac{|\langle\varphi_{n_0}(0;\boldsymbol{\sigma})\|T_{L_s}(\boldsymbol{\sigma})\|\chi_{n_s}(L_s;\boldsymbol{\sigma})\rangle|^2\langle\varphi_{n_0}(0;\boldsymbol{\rho})\|T_{L_t}(\boldsymbol{\rho})\|\chi_{n_t}(L_t;\boldsymbol{\rho})\rangle}{E_{n_sL_s}+E_{n_tL_t}-2E^{(0)}_{n_0S}}\\
&\times \frac{\langle\chi_{n_t}(L_t;\boldsymbol{\rho})\|T_{\ell_2'}(\boldsymbol{\rho})\|\chi_{n_t'}(L_t';\boldsymbol{\rho})\rangle\langle\chi_{n_t'}(L_t';\boldsymbol{\rho})\|T_{L_t'}(\boldsymbol{\rho})\|\varphi_{n_0}(0;\boldsymbol{\rho})\rangle}{E_{n_sL_s}+E_{n_t'L_t'}-2E^{(0)}_{n_0S}}\\
&= \sum_{\substack{n_sn_tn_t'\\L_sL_tL_t'\ell_2'\\M_sM_tM_t'm_2'}}\frac{F_5(n_s,n_t,n_t',L_s,L_t,L_t',\ell_2',M_s,M_t,M_t',m_2')\cos[M_t'\beta]}{R_{12}^{2L_s+L_t+\ell_2'+2}R_{23}^{L_t'+1}}\\
&+ \sum_{\substack{n_sn_tn_t'\\L_sL_tL_t'\ell_2'\\M_sM_tM_t'm_2'}}\frac{F_6(n_s,n_t,n_t',L_s,L_t,L_t',\ell_2',M_s,M_t,M_t',m_2')\exp[-im_2'\beta]}{R_{12}^{2L_s+L_t+L_t'+2}R_{23}^{\ell_2'+1}},
\end{aligned} \tag{C.12}$$

$$\begin{aligned}
V^{(3)}_{31,12} &= \sum_{n_sn_s'n_t}\sum_{L_sL_s'L_t\ell_1'}\sum_{M_sM_s'M_tm_1'}\frac{64\pi^3}{\sqrt{\pi}}\frac{(-1)^{L_s'-M_s}}{R_{12}^{2L_t+L_s+\ell_1'+2}R_{31}^{L_s'+1}}\\
&\times \frac{P_{L_s+L_t}^{M_s+M_t}(\cos\theta_{12})(L_s+L_t-M_s-M_t)!(L_s,L_t)^{-1}}{[(L_s+M_s)!(L_s-M_s)!(L_t+M_t)!(L_t-M_t)!]^{1/2}}\\
&\times \frac{P_{\ell_1'+L_t}^{m_1'+M_t}(\cos\theta_{12})(\ell_1'+L_t-m_1'-M_t)!(\ell_1',L_t,L_t)^{-1/2}}{[(\ell_1'+m_1')!(\ell_1'-m_1')!(L_t+M_t)!(L_t-M_t)!]^{1/2}}
\end{aligned}$$

$$
\begin{aligned}
&\times \quad \frac{P_{L'_s}^{M'_s}(\cos\theta_{31})(L'_s-M'_s)!(L'_s)^{-1}}{[(L'_s+M'_s)!(L'_s-M'_s)!]^{1/2}} \begin{pmatrix} L_s & \ell'_1 & L'_s \\ -M_s & m'_1 & -M'_s \end{pmatrix} \cos[M'_s\alpha] \\
&\times \quad \frac{|\langle\varphi_{n_0}(0;\boldsymbol{\rho})\|T_{L_t}(\boldsymbol{\rho})\|\chi_{n_t}(L_t;\boldsymbol{\rho})\rangle|^2\langle\varphi_{n_0}(0;\boldsymbol{\sigma})\|T_{L_s}(\boldsymbol{\sigma})\|\chi_{n_s}(L_s;\boldsymbol{\sigma})\rangle}{E_{n_sL_s}+E_{n_tL_t}-2E^{(0)}_{n_0S}} \\
&\times \quad \frac{\langle\chi_{n_s}(L_s;\boldsymbol{\sigma})\|T_{\ell'_1}(\boldsymbol{\sigma})\|\chi_{n'_s}(L'_s;\boldsymbol{\sigma})\rangle\langle\chi_{n'_s}(L'_s;\boldsymbol{\sigma})\|T_{L'_s}(\boldsymbol{\sigma})\|\varphi_{n_0}(0;\boldsymbol{\sigma})\rangle}{E_{n'_sL'_s}-E^{(0)}_{n_0S}}
\end{aligned}
$$

$$
\begin{aligned}
&+ \quad \sum_{n_sn'_sn_t}\sum_{L_sL'_sL_t\ell'_1}\sum_{M_sM'_sM_tm'_1} \frac{32\pi^3}{\sqrt{\pi}} \frac{(-1)^{\ell'_1-M_s}}{R_{12}^{2L_t+L_s+L'_s+2}R_{31}^{\ell'_1+1}} \\
&\times \quad \frac{P_{L_s+L_t}^{M_s+M_t}(\cos\theta_{12})(L_s+L_t-M_s-M_t)!(L_s,L_t)^{-1}}{[(L_s+M_s)!(L_s-M_s)!(L_t+M_t)!(L_t-M_t)!]^{1/2}} \\
&\times \quad \frac{P_{L'_s+L_t}^{M'_s+M_t}(\cos\theta_{12})(L'_s+L_t-M'_s-M_t)!(L'_s,L_t)^{-1}}{[(L'_s+M'_s)!(L'_s-M'_s)!(L_t+M_t)!(L_t-M_t)!]^{1/2}} \\
&\times \quad \frac{P_{\ell'_1}^{m'_1}(\cos\theta_{31})(\ell'_1-m'_1)!(\ell'_1)^{-1/2}}{[(\ell'_1+m'_1)!(\ell'_1-m'_1)!]^{1/2}} \begin{pmatrix} L_s & \ell'_1 & L'_s \\ -M_s & -m'_1 & M'_s \end{pmatrix} \exp[im'_1\alpha] \\
&\times \quad \frac{|\langle\varphi_{n_0}(0;\boldsymbol{\rho})\|T_{L_t}(\boldsymbol{\rho})\|\chi_{n_t}(L_t;\boldsymbol{\rho})\rangle|^2\langle\varphi_{n_0}(0;\boldsymbol{\sigma})\|T_{L_s}(\boldsymbol{\sigma})\|\chi_{n_s}(L_s;\boldsymbol{\sigma})\rangle}{E_{n_sL_s}+E_{n_tL_t}-2E^{(0)}_{n_0S}} \\
&\times \quad \frac{\langle\chi_{n_s}(L_s;\boldsymbol{\sigma})\|T_{\ell'_1}(\boldsymbol{\sigma})\|\chi_{n'_s}(L'_s;\boldsymbol{\sigma})\rangle\langle\chi_{n'_s}(L'_s;\boldsymbol{\sigma})\|T_{L'_s}(\boldsymbol{\sigma})\|\varphi_{n_0}(0;\boldsymbol{\sigma})\rangle}{E_{n'_sL'_s}+E_{n_tL_t}-2E^{(0)}_{n_0S}} \\
&= \quad \sum_{\substack{n_sn'_sn_t\\L_sL'_sL_t\ell'_1\\M_tM_sm'_1M'_s}} \frac{F_5(n_t,n_s,n'_s,L_t,L_s,L'_s,\ell'_1,M_t,M_s,M'_s,m'_1)\cos[M'_s\alpha]}{R_{12}^{2L_t+L_s+\ell'_1+2}R_{31}^{L'_s+1}} \\
&+ \quad \sum_{\substack{n_sn'_sn_t\\L_sL'_sL_t\ell'_1\\M_tM_sm'_1M'_s}} \frac{F_6(n_t,n_s,n'_s,L_t,L_s,L'_s,\ell'_1,M_t,M_s,M'_s,m'_1)\exp[im'_1\alpha]}{R_{12}^{2L_t+L_s+L'_s+2}R_{31}^{\ell'_1+1}}\,,
\end{aligned}
\tag{C.13}
$$

$V^{(3)}_{12,23,31}$

$$
\begin{aligned}
&= \sum_{n_s n_t n_u} \sum_{L_s L_t L_u} \sum_{M_s M_t M_u} \frac{256\pi^3 (-1)^{L_s+L_t+L_u}}{R_{12}^{L_s+L_t+1} R_{23}^{L_t+L_u+1} R_{31}^{L_u+L_s+1}} \\
&\times \frac{(L_s+L_t-M_s+M_t)!(L_t+L_u-M_t+M_u)!(L_u+L_s-M_u+M_s)!}{(L_s+M_s)!(L_s-M_s)!(L_t+M_t)!(L_t-M_t)!(L_u+M_u)!(L_u-M_u)!} \\
&\times (L_s, L_t, L_u)^{-2} P_{L_s+L_t}^{M_s-M_t}(\cos\theta_{12}) P_{L_t+L_u}^{M_t-M_u}(\cos\theta_{23}) P_{L_u+L_s}^{M_u-M_s}(\cos\theta_{31}) \\
&\times |\langle \varphi_{n_0}(0;\boldsymbol{\sigma}) \| T_{L_s}(\boldsymbol{\sigma}) \| \chi_{n_s}(L_s;\boldsymbol{\sigma})\rangle|^2 |\langle \varphi_{n_0}(0;\boldsymbol{\rho}) \| T_{L_t}(\boldsymbol{\rho}) \| \chi_{n_t}(L_t;\boldsymbol{\rho})\rangle|^2 \\
&\times \frac{|\langle \phi_{n_0'}(0;\boldsymbol{\varsigma}) \| T_{L_u}(\boldsymbol{\varsigma}) \| \psi_{n_u}(L_u;\boldsymbol{\varsigma})\rangle|^2 \exp[-iM_s\alpha - iM_t\beta - iM_u\gamma]}{(E_{n_s L_s} + E_{n_u L_u} - E_{n_0 S}^{(0)} - E_{n_0' S}^{(0)})} \\
&\times \frac{E_{n_s L_s} + E_{n_t L_t} + E_{n_u L_u} - 2E_{n_0 S}^{(0)} - E_{n_0' S}^{(0)}}{(E_{n_s L_s} + E_{n_t L_t} - 2E_{n_0 S}^{(0)})(E_{n_t L_t} + E_{n_u L_u} - E_{n_0 S}^{(0)} - E_{n_0' S}^{(0)})} \\
&= \sum_{n_s n_t n_u} \sum_{L_s L_t L_u} \sum_{M_s M_t M_u} \frac{F_7(n_s, n_t, n_u, L_s, L_t, L_u, M_s, M_t, M_u)}{R_{12}^{L_s+L_t+1} R_{23}^{L_t+L_u+1} R_{31}^{L_u+L_s+1}} \\
&\times \exp[-iM_s\alpha - iM_t\beta - iM_u\gamma]\,.
\end{aligned}
\tag{C.14}
$$

In the above, the F_i functions are defined by

$$
\begin{aligned}
&F_1(n_s, n_t, L_s, L_t) = G_1(L_s, L_t) \\
&\times \frac{|\langle \varphi_{n_0}(0;\boldsymbol{\sigma}) \| T_{L_s}(\boldsymbol{\sigma}) \| \chi_{n_s}(L_s;\boldsymbol{\sigma})\rangle|^2 |\langle \varphi_{n_0}(0;\boldsymbol{\rho}) \| T_{L_t}(\boldsymbol{\rho}) \| \chi_{n_t}(L_t;\boldsymbol{\rho})\rangle|^2}{E_{n_s L_s} + E_{n_t L_t} - 2E_{n_0 S}^{(0)}}\,,
\end{aligned}
\tag{C.15}
$$

$$
\begin{aligned}
&F_2(n_s, n_u, L_s, L_u) = G_1(L_s, L_u) \\
&\times \frac{|\langle \varphi_{n_0}(0;\boldsymbol{\sigma}) \| T_{L_s}(\boldsymbol{\sigma}) \| \chi_{n_s}(L_s;\boldsymbol{\sigma})\rangle|^2 |\langle \psi_{n_0}(0;\boldsymbol{\rho}) \| T_{L_t}(\boldsymbol{\rho}) \| \phi_{n_t}(L_t;\boldsymbol{\rho})\rangle|^2}{E_{n_s L_s} + E_{n_t L_t} - E_{n_0 S}^{(0)} - E_{n_0' S}^{(0)}}\,,
\end{aligned}
\tag{C.16}
$$

$$
\begin{aligned}
&F_3(n_s, n_t, n_s', n_t', L_s, L_t, L_s', L_t', \ell_1', \ell_2') \\
&= G_2(L_s, L_t, L_s', L_t', \ell_1', \ell_2')
\end{aligned}
$$

$$
\begin{aligned}
&\times \quad \langle \chi_{n_s}(L_s;\boldsymbol{\sigma}) \| T_{\ell_1'}(\boldsymbol{\sigma}) \| \chi_{n_s'}(L_s';\boldsymbol{\sigma}) \rangle \langle \chi_{n_t}(L_t;\boldsymbol{\rho}) \| T_{\ell_2'}(\boldsymbol{\rho}) \| \chi_{n_t'}(L_t';\boldsymbol{\rho}) \rangle \\
&\times \quad \frac{\langle \varphi_{n_0}(0;\boldsymbol{\sigma}) \| T_{L_s}(\boldsymbol{\sigma}) \| \chi_{n_s}(L_s;\boldsymbol{\sigma}) \rangle \langle \varphi_{n_0}(0;\boldsymbol{\rho}) \| T_{L_t}(\boldsymbol{\rho}) \| \chi_{n_t}(L_t;\boldsymbol{\rho}) \rangle}{E_{n_s L_s} + E_{n_t L_t} - 2E_{n_0 S}^{(0)}} \\
&\times \quad \frac{\langle \chi_{n_s'}(L_s';\boldsymbol{\sigma}) \| T_{L_s'}(\boldsymbol{\sigma}) \| \varphi_{n_0}(0;\boldsymbol{\sigma}) \rangle \langle \chi_{n_t'}(L_t';\boldsymbol{\rho}) \| T_{L_t'}(\boldsymbol{\rho}) \| \varphi_{n_0}(0;\boldsymbol{\rho}) \rangle}{E_{n_s' L_s'} + E_{n_t' L_t'} - 2E_{n_0 S}^{(0)}},
\end{aligned}
\tag{C.17}
$$

$$
\begin{aligned}
&F_4(n_s, n_t, n_s', n_u', L_s, L_u, L_s', L_u', \ell_1', \ell_3') \\
=\ & G_2(L_s, L_u, L_s', L_u', \ell_1', \ell_3') \\
\times\ & \langle \chi_{n_s}(L_s;\boldsymbol{\sigma}) \| T_{\ell_1'}(\boldsymbol{\sigma}) \| \chi_{n_s'}(L_s';\boldsymbol{\sigma}) \rangle | \langle \phi_{n_u}(L_u;\boldsymbol{\varsigma}) \| T_{\ell_3'}(\boldsymbol{\varsigma}) \| \phi_{n_u'}(L_u';\boldsymbol{\varsigma}) \rangle \\
\times\ & \frac{\langle \varphi_{n_0}(0;\boldsymbol{\sigma}) \| T_{L_s}(\boldsymbol{\sigma}) \| \chi_{n_s}(L_s;\boldsymbol{\sigma}) \rangle \langle \psi_{n_0'}(0;\boldsymbol{\varsigma}) \| T_{L_u}(\boldsymbol{\varsigma}) \| \phi_{n_u}(L_u;\boldsymbol{\varsigma}) \rangle}{E_{n_s L_s} + E_{n_u L_u} - E_{n_0 S}^{(0)} - E_{n_0' S}^{(0)}} \\
\times\ & \frac{\langle \chi_{n_s'}(L_s';\boldsymbol{\sigma}) \| T_{L_s'}(\boldsymbol{\sigma}) \| \varphi_{n_0}(0;\boldsymbol{\sigma}) \rangle \langle \phi_{n_u'}(L_u';\boldsymbol{\varsigma}) \| T_{L_u'}(\boldsymbol{\varsigma}) \| \psi_{n_0'}(0;\boldsymbol{\varsigma}) \rangle}{E_{n_s' L_s'} + E_{n_u' L_u'} - E_{n_0 S}^{(0)} - E_{n_0' S}^{(0)}},
\end{aligned}
\tag{C.18}
$$

$$
\begin{aligned}
&F_5(n_s, n_t, n_t', L_s, L_t, L_t', \ell_2', M_s, M_t, M_t', m_2',) \\
=\ & G_3(L_s, L_t, L_t', \ell_2', M_s, M_t, M_t', m_2') \\
\times\ & \frac{|\langle \varphi_{n_0}(0;\boldsymbol{\sigma}) \| T_{L_s}(\boldsymbol{\sigma}) \| \chi_{n_s}(L_s;\boldsymbol{\sigma}) \rangle|^2 \langle \varphi_{n_0}(0;\boldsymbol{\rho}) \| T_{L_t}(\boldsymbol{\rho}) \| \chi_{n_t}(L_t;\boldsymbol{\rho}) \rangle}{E_{n_s L_s} + E_{n_t L_t} - 2E_{n_0 S}^{(0)}} \\
\times\ & \frac{\langle \chi_{n_t}(L_t;\boldsymbol{\rho}) \| T_{\ell_2'}(\boldsymbol{\rho}) \| \chi_{n_t'}(L_t';\boldsymbol{\rho}) \rangle \langle \chi_{n_t'}(L_t';\boldsymbol{\rho}) \| T_{L_t'}(\boldsymbol{\rho}) \| \varphi_{n_0}(0;\boldsymbol{\rho}) \rangle}{E_{n_t' L_t'} - E_{n_0 S}^{(0)}},
\end{aligned}
\tag{C.19}
$$

$$
\begin{aligned}
&F_6(n_s, n_t, n_t', L_s, L_t, L_t', \ell_2', M_s, M_t, M_t', m_2') \\
=\ & G_4(L_s, L_t, L_t', \ell_2', M_s, M_t, M_t', m_2') \\
\times\ & \frac{|\langle \varphi_{n_0}(0;\boldsymbol{\sigma}) \| T_{L_s}(\boldsymbol{\sigma}) \| \chi_{n_s}(L_s;\boldsymbol{\sigma}) \rangle|^2 \langle \varphi_{n_0}(0;\boldsymbol{\rho}) \| T_{L_t}(\boldsymbol{\rho}) \| \chi_{n_t}(L_t;\boldsymbol{\rho}) \rangle}{E_{n_s L_s} + E_{n_t L_t} - 2E_{n_0 S}^{(0)}}
\end{aligned}
$$

$$\times \quad \frac{\langle \chi_{n_t}(L_t;\boldsymbol{\rho}) \| T_{\ell_2'}(\boldsymbol{\rho}) \| \chi_{n_t'}(L_t';\boldsymbol{\rho}) \rangle \langle \chi_{n_t'}(L_t';\boldsymbol{\rho}) \| T_{L_t'}(\boldsymbol{\rho}) \| \varphi_{n_0}(0;\boldsymbol{\rho}) \rangle}{E_{n_s L_s} + E_{n_t' L_t'} - 2E_{n_0 S}^{(0)}}\,, \tag{C.20}$$

$$\begin{aligned}
& F_7(n_s, n_t, n_u, L_s, L_t, L_u, M_s, M_t, M_u) \\
= \quad & G_5(L_s, L_t, L_u, M_s, M_t, M_u) \\
\times \quad & |\langle \varphi_{n_0}(0;\boldsymbol{\sigma}) \| T_{L_s}(\boldsymbol{\sigma}) \| \chi_{n_s}(L_s;\boldsymbol{\sigma}) \rangle|^2 |\langle \varphi_{n_0}(0;\boldsymbol{\rho}) \| T_{L_t}(\boldsymbol{\rho}) \| \chi_{n_t}(L_t;\boldsymbol{\rho}) \rangle|^2 \\
\times \quad & \frac{|\langle \phi_{n_0'}(0;\boldsymbol{\varsigma}) \| T_{L_u}(\boldsymbol{\varsigma}) \| \psi_{n_u}(L_u;\boldsymbol{\varsigma}) \rangle|^2}{(E_{n_s L_s} + E_{n_u L_u} - E_{n_0 S}^{(0)} - E_{n_0' S}^{(0)})} \\
\times \quad & \frac{E_{n_s L_s} + E_{n_t L_t} + E_{n_u L_u} - 2E_{n_0 S}^{(0)} - E_{n_0' S}^{(0)}}{(E_{n_s L_s} + E_{n_t L_t} - 2E_{n_0 S}^{(0)})(E_{n_t L_t} + E_{n_u L_u} - E_{n_0 S}^{(0)} - E_{n_0' S}^{(0)})}\,,
\end{aligned} \tag{C.21}$$

where $G_1(L_i, L_j)$, $G_2(L_i, L_j, \ell_{k_1}, \ell_{k_2}'; L, M)$, and $G_3(L_i, M_i; L, M)$ are further defined by:

$$\begin{aligned}
& G_1(L_i, L_j) = 16\pi^2 (L_i, L_j)^{-2} \\
\times \quad & \sum_{M_i M_j} \frac{[P_{L_i+L_j}^{M_i+M_j}(0)(L_i + L_j - M_i - M_j)!]^2}{(L_i + M_i)!(L_i - M_i)!(L_j + M_j)!(L_j - M_j)!}\,,
\end{aligned} \tag{C.22}$$

$$\begin{aligned}
& G_2(L_i, L_j, L_i', L_j', \ell_{k_1}, \ell_{k_2}') \\
= \quad & \sum_{M_i M_j M_i' M_j'} \sum_{m_{k_1}' m_{k_2}'} -64\pi^3 \\
\times \quad & \begin{pmatrix} L_i & \ell_{k_1}' & L_i' \\ -M_i & -m_{k_1}' & -M_i' \end{pmatrix} \begin{pmatrix} L_j & \ell_{k_2}' & L_j' \\ -M_j & -m_{k_2}' & -M_j' \end{pmatrix}
\end{aligned}$$

$$
\begin{aligned}
&\times \quad \frac{P_{L_i+L_j}^{M_i+M_j}(0)(L_i+L_j-M_i-M_j)!(L_i,L_j)^{-1}}{[(L_i+M_i)!(L_i-M_i)!(L_j+M_j)!(L_j-M_j)!]^{1/2}} \\
&\times \quad \frac{P_{L'_i+L'_j}^{M'_i+M'_j}(0)(L'_i+L'_j-M'_i-M'_j)!(L'_i,L'_j)^{-1}}{[(L'_i+M'_i)!(L'_i-M'_i)!(L'_j+M'_j)!(L'_j-M'_j)!]^{1/2}} \\
&\times \quad \frac{P_{\ell'_{k_1}+\ell'_{k_2}}^{m'_{k_1}+m'_{k_2}}(0)(\ell'_{k_1}+\ell'_{k_2}-m'_{k_1}-m'_{k_2})!(\ell'_{k_1},\ell'_{k_2})^{-1/2}}{[(\ell'_{k_1}+m'_{k_1})!(\ell'_{k_1}-m'_{k_1})!(\ell'_{k_2}+m'_{k_2})!(\ell'_{k_2}-m'_{k_2})!]^{1/2}},
\end{aligned}
\tag{C.23}
$$

$$
\begin{aligned}
&G_3(L_i,L_j,L'_j,\ell'_{k_2},M_i,M_j,M'_j,m'_{k_2}) \\
&= \quad \frac{64\pi^3}{\sqrt{\pi}}(-1)^{1+L'_j-M_j} \\
&\times \quad \frac{P_{L_i+L_j}^{M_i+M_j}(0)(L_i+L_j-M_i-M_j)!(L_i,L_j)^{-1}}{[(L_i+M_i)!(L_i-M_i)!(L_j+M_j)!(L_j-M_j)!]^{1/2}} \\
&\times \quad \frac{P_{L_i+\ell'_{k_2}}^{M_i+m'_{k_2}}(0)(L_i+\ell'_{k_2}-M_i-m'_{k_2})!(L_i,L_i,\ell'_{k_2})^{-1/2}}{[(L_i+M_i)!(L_i-M_i)!(\ell'_{k_2}+m'_{k_2})!(\ell'_{k_2}-m'_{k_2})!]^{1/2}} \\
&\times \quad \frac{P_{L'_j}^{M'_j}(0)(L'_j-M'_j)!(L'_j)^{-1}}{[(L'_j+M'_j)!(L'_j-M'_j)!]^{1/2}} \begin{pmatrix} L_j & \ell'_{k_2} & L'_j \\ -M_j & m'_{k_2} & -M'_j \end{pmatrix},
\end{aligned}
\tag{C.24}
$$

$$
\begin{aligned}
&G_4(L_i,L_j,L'_j,\ell'_{k_2},M_i,M_j,M'_j,m'_{k_2}) \\
&= \quad \frac{32\pi^3}{\sqrt{\pi}}(-1)^{1+\ell'_{k_2}-M_j} \\
&\times \quad \frac{P_{L_i+L_j}^{M_i+M_j}(0)(L_i+L_j-M_i-M_j)!(L_i,L_j)^{-1}}{[(L_i+M_i)!(L_i-M_i)!(L_j+M_j)!(L_j-M_j)!]^{1/2}} \\
&\times \quad \frac{P_{L_i+L'_j}^{M_i+M'_j}(0)(L_i+L'_j-M_i-M'_j)!(L_i,L'_j)^{-1}}{[(L_i+M_i)!(L_i-M_i)!(L'_j+M'_j)!(L'_j-M'_j)!]^{1/2}} \\
&\times \quad \frac{P_{\ell'_{k_2}}^{m'_{k_2}}(0)(\ell'_{k_2}-m'_{k_2})!(\ell'_{k_2})^{-1/2}}{[(\ell'_{k_2}+m'_{k_2})!(\ell'_{k_2}-m'_{k_2})!]^{1/2}} \begin{pmatrix} L_j & L'_j & \ell'_{k_2} \\ -M_j & M'_j & -m'_{k_2} \end{pmatrix},
\end{aligned}
$$

(C.25)

$$
\begin{aligned}
& G_5(L_i, L_j, L_k, M_i, M_j, M_k) \\
= \; & 256\pi^3(-1)^{1+L_i+L_j+L_k}(L_i, L_j, L_k)^{-2} P^{M_i-M_j}_{L_i+L_j}(0) P^{M_j-M_k}_{L_j+L_k}(0) P^{M_k-M_i}_{L_k+L_i}(0) \\
\times \; & \frac{(L_i+L_j-M_i+M_j)!}{(L_i+M_i)!(L_i-M_i)!} \frac{(L_j+L_k-M_j+M_k)!}{(L_j+M_j)!(L_j-M_j)!} \frac{(L_k+L_i-M_k+M_i)!}{(L_k+M_k)!(L_k-M_k)!} ,
\end{aligned}
\tag{C.26}
$$

Then the second-order energy correction is simplified as,

$$
\Delta E^{(2)} = - \sum_{n \geq 3, n' \geq 2} \left(\frac{C^{(12)}_{2n}}{R^{2n}_{12}} + \frac{C^{(23)}_{2n'}}{R^{2n'}_{23}} + \frac{C^{(31)}_{2n'}}{R^{2n'}_{31}} \right) ,
\tag{C.27}
$$

where $C^{(IJ)}_{2n}(L, M)$ are the additive dispersion coefficients. These coefficients can be expressed as

$$
C^{(12)}_{2n} = \sum_{\substack{n_s n_t; L_s L_t \\ 2L_s+2L_t+2=2n}} F_1(n_s, n_t, L_s, L_t) ,
\tag{C.28}
$$

$$
C^{(23)}_{2n'} = \sum_{\substack{n_t n_u; L_t L_u \\ 2L_t+2L_u+2=2n'}} F_2(n_t, n_u, L_t, L_u) ,
\tag{C.29}
$$

$$
C^{(31)}_{2n'} = \sum_{\substack{n_s n_u; L_s L_u \\ 2L_s+2L_u+2=2n'}} F_2(n_s, n_u, L_s, L_u) .
\tag{C.30}
$$

Then the third-order energy correction is simplified as,

$$
\Delta E^{(3)} = - \sum_{n_4 \geq 4, n_2 \geq 2} \left(\frac{C^{(12)}_{2n_4+3}}{R^{2n_4+3}_{12}} + \frac{C^{(23)}_{2n_2+3}}{R^{2n_2+3}_{23}} + \frac{C^{(31)}_{2n_2+3}}{R^{2n_2+3}_{31}} \right)
$$

$$
- \sum_{\substack{n_4\geq 4, n_3\geq 3, n_1\geq 1 \\ n_4+n_1=2n_3}} \left(\frac{C^{(12,23)}_{2n_3+3}(L_s, L_t, L'_t, \ell'_2, L''_t, \ell''_2)}{R_{12}^{n_4+2} R_{23}^{n_1+1}} + \frac{C^{(31,12)}_{2n_3+3}(L_t, L_s, L'_s, \ell'_1, L''_s, \ell''_1)}{R_{31}^{n_1+1} R_{12}^{n_4+2}} \right),
$$

$$
- \sum_{\substack{n_2\geq 2, n'_2\geq 2, n_1\geq 1, n'_1\geq 1 \\ n'_2+n_1+n'_1=2n_2}} \left(\frac{C^{(12,23,31)}_{2n_2+3}(L_s, L_t, L_u)}{R_{12}^{n'_2+1} R_{23}^{n_1+1} R_{31}^{n'_1+1}} \right), \tag{C.31}
$$

where $C^{(IJ)}_{2n_i+3}$ are the additive dispersion coefficients, and $C^{(IJ,JK)}_{2n_i+3}$, $C^{(IJ,JK,KI)}_{2n_i+3}$ are the nonadditive dispersion coefficients. These coefficients can be expressed as

$$
C^{(12)}_{2n_4+3} = \sum_{\substack{n_s n_t n'_s n'_t; L_s L_t L'_s L'_t \ell'_1 \ell'_2 \\ L_s+L_t+L'_s+L'_t+\ell'_1+\ell'_2=2n_4}} F_3(n_s, n_t, n'_s, n'_t, L_s, L_t, L'_s, L'_t, \ell'_1, \ell'_2)\,, \tag{C.32}
$$

$$
C^{(23)}_{2n_2+3} = \sum_{\substack{n_t n_u n'_t n'_u; L_t L_u L'_t L'_u \ell'_2 \ell'_3 \\ L_t+L_u+L'_t+L'_u+\ell'_2+\ell'_3=2n_2}} F_4(n_t, n_u, n'_t, n'_u, L_t, L_u, L'_t, L'_u, \ell'_2, \ell'_3)\,, \tag{C.33}
$$

$$
C^{(31)}_{2n_2+3} = \sum_{\substack{n_s n_u n'_s n'_u; L_s L_u L'_s L'_u \ell'_1 \ell'_3 \\ L_s+L_u+L'_s+L'_u+\ell'_1+\ell'_3=2n_2}} F_4(n_s, n_u, n'_s, n'_u, L_s, L_u, L'_s, L'_u, \ell'_1, \ell'_3)\,, \tag{C.34}
$$

$$
\begin{aligned}
& C^{(12,23)}_{2n_3+3}(L_s, L_t, L'_t, \ell'_2, L''_t, \ell''_2) \\
= & \sum_{\substack{n_s n_t n'_t; M_s M_t M'_t m'_2 \\ 2L_s+L_t+L'_t+\ell'_2=2n_3}} F_5(n_s, n_t, n'_t, L_s, L_t, L'_t, \ell'_2, M_s, M_t, m'_2, M'_t) \cos[M'_t \beta] \\
+ & \sum_{\substack{n_s n_t n''_t; M_s M_t M''_t m''_2 \\ 2L_s+L_t+L''_t+\ell''_2=2n_3}} F_6(n_s, n_t, n''_t, L_s, L_t, L''_t, \ell''_2, M_s, M_t, M''_t, m''_2) \exp[-i m''_2 \beta]\,,
\end{aligned} \tag{C.35}
$$

$$
\begin{aligned}
& C^{(31,12)}_{2n_3+3}(L_t, L_s, L'_s, \ell'_1, L''_s, \ell''_1) \\
= & \sum_{\substack{n_s n'_s n_t; M_t M_s m'_1 M'_s \\ 2L_t+L_s+L'_s+\ell'_1=2n_3}} F_5(n_t, n_s, n'_s, L_t, L_s, L'_s, \ell'_1, M_t, M_s, M'_s, m'_1) \cos[M'_s \alpha] \\
+ & \sum_{\substack{n_s n''_s n_t; M_s M''_s M_t m''_1 \\ 2L_t+L_s+L''_s+\ell''_1=2n_3}} F_6(n_t, n_s, n''_s, L_t, L_s, L''_s, \ell''_1, M_t, M_s, M''_s, m''_1) \exp[i m''_1 \alpha] \,,
\end{aligned}
\tag{C.36}
$$

$$
\begin{aligned}
& C^{(12,23,31)}_{2n_2+3}(L_s, L_t, L_u) \\
= & \sum_{\substack{n_s n_t n_u; M_s M_t M_u \\ 2L_s+2L_t+2L_u=2n_2}} F_7(n_s, n_t, n_u, L_s, L_t, L_u, M_s, M_t, M_u) \exp[-i M_s \alpha - i M_t \beta - i M_u \gamma] \,,
\end{aligned}
\tag{C.37}
$$

Curriculum Vitae

Candidate's full name: Pei-Gen Yan

Universities attended:

Jilin University, China, 2010.9-2013.7, Master of Science

Ludong University, China, 2006.9-2010.7, Bachelor of Science

Publications:

Pei-Gen Yan, Li-Yan Tang, Zong-Chao Yan, James F. Babb, Calculations of long-range three-body interactions for Li(2^2S)-Li(2^2P)-Li^+(1^1S) (In Process).

Pei-Gen Yan, Li-Yan Tang, Zong-Chao Yan, James F. Babb, Calculations of long-range three-body interactions for Li(2^2S)-Li(2^2S)-Li^+(1^1S) (In Process).

Pei-Gen Yan, Li-Yan Tang, Zong-Chao Yan, James F. Babb, Calculations of long-range three-body interactions for He($n_0\,^\lambda S$)-He($n_0\,^\lambda S$)-He($n_0'\,^\lambda L$), Phys. Rev. A **97**, 042710 (2018)..

Pei-Gen Yan, Li-Yan Tang, Zong-Chao Yan, James F. Babb, Calculations of long-range three-body interactions for Li(2^2S)-Li(2^2S)-Li(2^2P), Phys. Rev. A **94**, 022705 (2016).

Conference Presentations:

Pei-Gen Yan, Li-Yan Tang, Zong-Chao Yan, James F. Babb, "Universal study of long-range three-body interaction for $S-S-P$ system", AMO Physics Summer School, National Tsinghua University, August 25-28, 2015, Taiwan.

ITAMP/B2 Institute Winter Graduate School on "Ultrafast and Ultrastrong", January 4-12, 2016, Tucson, Arizona, USA.

Pei-Gen Yan, Li-Yan Tang, Zong-Chao Yan, James F. Babb, "Calculations of long-range three-body interactions for Li(2^2S)-Li(2^2S)-Li(2^2P)", Division of Atomic, Molecular and Optical Physics, May 23-27, 2016, Providence, Rhode Island, USA.

Pei-Gen Yan, Li-Yan Tang, Zong-Chao Yan, James F. Babb, "Calculations of long-range three-body interactions for Li(2^2S)-Li(2^2S)-Li(2^2P)", International Conference on Atomic Physics, July 24-29, 2016, Seoul, South Korea.

Pei-Gen Yan, Li-Yan Tang, Zong-Chao Yan, James F. Babb, "Calculations of long-range three-body interactions for Li(2^2S)-Li(2^2S)-Li^+(1^1S)", Division of Atomic, Molecular and Optical Physics, June 5-9, 2017, Sacramento, California, USA.

Pei-Gen Yan, Li-Yan Tang, Zong-Chao Yan, James F. Babb, "Calculations of long-range three-body interactions for He($n_0\,^\lambda S$)-He($n_0\,^\lambda S$)-He($n_0'\,^\lambda L$)", International Conference on Photonic, Electronic and Atomic Collisions, July 26 - August 1, 2017, Cairns, Queensland, Australia.

Pei-Gen Yan, Li-Yan Tang, Zong-Chao Yan, James F. Babb, "Calculations of long-range three-body interactions for Li(2^2S)-Li(2^2S)-Li(2^2P)", The TAMU Physics of Quantum Electronics Follow-on Workshop, January 16-17, 2018, Texas A&M, College Station, Texas, USA.